



# **The Role of RL13 in Human Cytomegalovirus Pathogenesis**

A thesis submitted in candidature for the degree of

DOCTOR OF PHILOSOPHY (PhD)

by

**Carmen Grace Bedford**

December 2018

Division of Infection and Immunity,

School of Medicine,

Cardiff University



## Declaration

This work has not been submitted in substance for any other degree or award at this or any other university or place of learning, nor is being submitted concurrently in candidature for any degree or other award.

Signed ..... Date .....

### STATEMENT 1

This thesis is being submitted in partial fulfilment of the requirements for the degree of PhD.

Signed ..... Date .....

### STATEMENT 2

This thesis is the result of my own independent work/investigation, except where otherwise stated, and the thesis has not been edited by a third party beyond what is permitted by Cardiff University's Policy on the Use of Third-Party Editors by Research Degree Students. Other sources are acknowledged by explicit references. The views expressed are my own.

Signed ..... Date .....

### STATEMENT 3

I hereby give consent for my thesis, if accepted, to be available online in the University's Open Access repository and for inter-library loan, and for the title and summary to be made available to outside organisations.

Signed ..... Date .....

### STATEMENT 4: PREVIOUSLY APPROVED BAR ON ACCESS

I hereby give consent for my thesis, if accepted, to be available online in the University's Open Access repository and for inter-library loans after expiry of a bar on access previously approved by the Academic Standards & Quality Committee.

Signed ..... Date .....



## Acknowledgements

I would first like to express my sincerest gratitude to my supervisors for the opportunity to undertake this PhD project. In particular to Dr Richard Stanton, whose support, guidance and patience with me throughout made this possible. Thank you for challenging me and allowing me to develop professionally and personally. I am always amazed at your capacity to multitask and your ability to appraise and return a piece of work so quickly! I am also very grateful to Prof Gavin Wilkinson for his guidance and valuable insight and to Dr Peter Tomasec who sadly is no longer with us but is fondly remembered.

I would like to thank Health and Care Research Wales who have funded this thesis. I am very appreciative to Prof Robin Antrobus, Dr Mike Weekes and Dr Paul Lehner who performed the mass-spectrometry analysis of virions used in this work.

I am indebted to all members of the HCMV and Adenovirus Research groups for their friendship, assistance and encouragement without which I would have struggled. Thank you, Dawn Roberts, for your help and answering my “stupid questions”, Dr Evelina Statkute for your guidance and Dr Isa Murrell for your constant enthusiasm in what RL13 does. Thank you, Dr Mihil Patel, for your company during Bake-Off season, Dr Simone Forbes for all the caffeine-fuelled laughs, and Dr Hester Nichols for your continued friendship and for maintaining my sanity with endless cups of tea and a great taste in films!

Thank you to my parents, Mike and Linda, and the rest of the Bedford clan for their love, kindness, generosity and constant support. Tori, thank you for all the weekends and evenings away from the lab winning pots in the double – to this day *no one knew who they were or what they were doing*.

Finally, to my fiancé Nathan, thank you for believing in me even when I didn't believe in myself. Without you keeping me together I would never have made it here. I look forward to our next adventure together.

**“You miss 100% of the shots you don't take.**

- Wayne Gretzky”

- Michael Scott



## Summary

Human cytomegalovirus (HCMV) is the leading infectious cause of congenital malformation. *In vitro* propagation of HCMV strains that authentically represent clinical virus are required to facilitate effective research. However, this is problematic, since efficient replication of clinical HCMV strains *in vitro* is achieved only after mutations have been selected. The first gene to mutate is consistently RL13. RL13 encodes a virion envelope protein that suppresses release of infectious virus from cells. Despite mutation in cell culture it is conserved in clinical strains, indicating that it is important *in vivo*. However, it is unclear how RL13 inhibits virus *in vitro*, or what advantage it provides *in vivo*.

RL13 expression did not affect genome replication or virion protein production, however it reduced the infectivity of released virions. Mass spectrometry revealed that RL13 expression altered the composition of released virions, however there was no obvious reason for these changes to effect infectivity. During virus spread, RL13 promoted cell-cell transfer of virus, reducing the ability of neutralising antibodies to inhibit virus spread in fibroblasts, however this effect was masked by UL128L expression in other cell types. Genetic analysis of RL13 from clinical strains revealed that RL13 sequences clustered into 9 distinct clades, with sequences from different clades retaining the ability to inhibit the release of infectious virus. A RL13 homologue from Rhesus CMV also restricted the release of infectious virus. This conservation of function suggests that the phenotype is not an artefact of *in vitro* culture conditions. RL13 on the cell surface bound human IgG, however it did not inhibit antibody-dependent cellular cytotoxicity during infection.

This thesis has delivered insights into the role of RL13 during infection, has demonstrated the importance of using more clinically relevant RL13+ HCMV strains and will aid future research using such HCMV strains.





# Table of Contents

Declaration .....	I
Acknowledgements .....	III
Summary.....	V
Table of Contents .....	VII
List of Figures.....	XII
List of Tables .....	XIV
CHAPTER 1. INTRODUCTION .....	1
1.1 Human Cytomegalovirus (HCMV).....	2
1.1.1 The Herpesvirus Family .....	2
1.1.2 Discovery and Isolation .....	4
1.2 Clinical Importance and manifestations of HCMV infection .....	5
1.2.1 Epidemiology .....	5
1.2.2 Transmission and Primary Infection.....	5
1.2.3 Infection in the Immunocompetent Host.....	6
1.2.4 Congenital and Perinatal Infection .....	6
1.2.5 Infection in at-risk groups.....	7
1.2.6 Treatments and Vaccination .....	8
1.3 Viral Particles .....	10
1.3.1 Components of Infectious virions.....	10
1.3.2 Non-infectious Viral Particles .....	12
1.4 Viral Lifecycle.....	16
1.4.1 Virus Entry .....	16
1.4.2 Viral DNA Replication and Gene Expression Regulation during Infection.....	16
1.4.3 Viral Particle Maturation and Egress.....	20
1.4.4 Latency and Reactivation .....	23
1.5 HCMV Infection .....	24

1.5.1	Intra-host Dissemination and Tropism .....	24
1.5.2	Lessons from HCMV Infection <i>in vitro</i> .....	25
1.5.3	The Immune Response and Immunomodulation .....	26
1.6	The Genetics of HCMV .....	31
1.6.1	Genome Organisation and Coding Potential .....	31
1.6.2	Natural Genetic Variation Between Strains .....	34
1.6.3	Mutations Associated with Adaptation to Cell Culture .....	34
1.7	Current Methods in HCMV Research .....	36
1.7.1	Viral Propagation <i>in vitro</i> .....	36
1.8	RL13.....	38
1.8.1	The RL11 Family .....	38
1.8.2	Limitations of Working with Functional RL13 .....	38
1.8.3	Rh13.1 – an RL13 Homolog .....	39
1.9	Thesis Aims.....	42
CHAPTER 2.	MATERIALS AND METHODS .....	43
2.1	Reagents.....	44
2.1.1	Buffers and Solutions .....	44
2.1.2	Bacterial Culture Media and Reagents .....	45
2.1.3	Tissue Culture Media and Reagents.....	46
2.2	Cell Culture.....	47
2.2.2	Cell Culture.....	47
2.2.2	Peripheral Blood Monocyte cell culture .....	48
2.3	Viruses and Infections.....	50
2.3.1	Generation of HCMV Stocks.....	50
2.3.2	Quantification of HCMV Infectivity .....	51
2.3.3	Infection of Cells with HCMV .....	52
2.3.4	Viral Timecourses.....	52

2.3.5	Isolation of DNA and Protein .....	52
2.3.6	Purification of Virions .....	54
2.4	Molecular Biology Techniques .....	56
2.4.1	In-silico Analysis and Oligonucleotide Design .....	56
2.4.2	Polymerase Chain Reaction (PCR) .....	56
2.4.3	DNA Gel Electrophoresis .....	57
2.4.4	DNA Gel Extraction and Purification .....	57
2.4.5	Measuring DNA Concentration .....	58
2.4.6	Recombineering.....	58
2.5	Functional Assays .....	63
2.5.1	Co-Cultures .....	63
2.5.2	Flowcytometry.....	64
2.5.3	Antibody-Dependent Cellular Cytotoxicity (ADCC) Assay .....	65
2.5.4	SiRNA Knockdown of Cellular Proteins.....	65
2.5.5	Western Blotting .....	67
2.5.6	Quantitative PCR (qPCR).....	68
2.5.7	Infectivity vs Particle Numbers.....	69
2.6	Microscopy .....	70
2.6.1	Zeiss Microscope for Immunofluorescence .....	70
2.6.2	Transmission Electron Microscopy (TEM) .....	70
2.7	Statistical Analysis .....	71
CHAPTER 3.	GENETIC MANIPULATION AND ANALYSIS OF RL13 .....	72
3.1	Generation of HCMV Reporter Viruses to Aid Investigation into RL13 Function.....	75
3.1.1	Generation of Novel Reporter Viruses by Recombineering .....	75
3.1.2	Growth characterisation of modified virus by Plaque Assay.....	79
3.1.3	Brighter GFP Expression Observed from IE2-P2A-GFP Virus by Flow Cytometry Assessment .....	79
3.2	Genetic Analysis of RL13 .....	82

3.2.1	RL13 is a Hypervariable Gene .....	82
3.2.2	Insertion of TR RL13 into the Merlin BAC .....	87
3.2.3	Insertion of Rhesus CMV RL13.1 into the Merlin BAC .....	92
3.3	Chapter Summary .....	95
CHAPTER 4.	THE EFFECTS OF RL13 ON THE VIRAL LIFECYCLE .....	97
4.1	Replication .....	99
4.1.1	RL13 Expression has no Effect on Viral Genome Replication .....	99
4.1.2	RL13 Expression has no Effect on Viral Protein Expression .....	101
4.2	Maturation .....	105
4.2.1	Particle Formation Analysis.....	105
4.3	Virion Release .....	110
4.3.1	Supernatant Virion Particle Numbers VS Infectivity .....	110
4.4	Chapter Summary .....	116
CHAPTER 5.	THE FUNCTIONAL EFFECTS OF RL13.....	118
5.1	Effects of RL13 on the Virus .....	120
5.1.1	Analysis of Viral Infection Spread by Co-Culture .....	120
5.1.2	Analysis of RL13 Expression Effect on Virion Composition .....	126
5.1.3	HCMV Virion Stability.....	132
5.2	Effects of RL13 on the Host Cell .....	136
5.2.1	Cell Surface Glycoprotein Expression .....	136
5.2.2	Identifying Functionally Relevant RL13: Protein Interactions.....	138
5.3	Effects of RL13 on the Host Immune System.....	146
5.3.1	RL13 is an Fc-Binding Protein.....	146
5.3.2	NK Cell Degranulation .....	149
5.4	Chapter Summary .....	152
CHAPTER 6.	DISCUSSION.....	158
6.1	The Importance of RL13.....	160
6.2	Is RL13 Hypervariable?.....	166

6.3	Investigating the Restrictive Phenotype of RL13 in <i>in vitro</i> HCMV infection .....	169
6.4	Future Directions and Concluding Remarks .....	174
CHAPTER 7.	APPENDIX.....	176
CHAPTER 8.	REFERENCES.....	181

## List of Figures

- Figure 1. Phylogenetic tree showing the evolution of the Betaherpesvirinae family
- Figure 2. The Formation of A, B and C capsids with the hypothetical Bt capsid
- Figure 3. The lifecycle of HCMV
- Figure 4. Viral particle formation and maturation start in the nucleus and continues in the AC found in the cytoplasm
- Figure 5. The AC structure and virion maturation and egress pathway
- Figure 6. The genome organisation of WT HCMV (Merlin)
- Figure 7. Schematic representation of the WT Merlin RL13 and the truncated RL13 sequence in Merlin  $\Delta$ RL13/ $\Delta$ UL128 and  $\Delta$ RL13.
- Figure 8. IE2-GFP fusion virus shows altered growth properties
- Figure 9. Recombineering of a Novel reporter virus
- Figure 10. Comparison of plaque sizes of current and novel reporter viruses
- Figure 11. Novel reporter viruses show brighter GFP expression than IE2-GFP fusion counter parts
- Figure 12. Conservation of RL13 Nucleotide and Protein sequences
- Figure 13. RL13 ORFs cluster into distinct clades
- Figure 14. Consensus sequences between clades display variation
- Figure 15. Recombineering plan to create TR RL13 Merlin BAC
- Figure 16. TR RL13 displays the same phenotype as Merlin RL13 as similar sized plaques
- Figure 17. Recombineering plan to create Rh13.1 in Merlin
- Figure 18. The effect of Rh13.1 in the Merlin BAC on plaque size
- Figure 19. RL13 expression does not affect viral genome replication
- Figure 20. Western blots showing temporal viral protein expression
- Figure 21. Early detection of viral proteins attributable to input virions
- Figure 22. TEM images of the nucleus and the AC of cells infected with  $\Delta$ RL13/ $\Delta$ UL128
- Figure 23. Expression of RL13 shows no significant difference in the proportions of developing viral particles within either the nucleus or AC
- Figure 24.  $\Delta$ UL128 infection produced the greatest total number of C-capsids in the nucleus, however this did not affect the number of virions that mature
- Figure 25. RL13 expression does not affect genome copy numbers but does affect titre over a timecourse of 10 days
- Figure 26. Particle size distribution of viruses between 100-350 nm

Figure 27. RL13 expression results in a relatively low genome/PFU ratio despite reducing particle numbers and viral titre

Figure 28. Cell-cell spread is dependent on UL128 expression, however RL13 expression provides no advantage to cell-cell spread

Figure 29. Cell-cell spread of virus expressing RL13 shows resistance to neutralising antibodies in HFFF Terts

Figure 30. Cell-cell spread of virus expressing RL13 shows resistance to neutralising antibodies in ARPE19s

Figure 31. RL13 expression results in significant loss of proteins within the virion

Figure 32. Second virion composition comparison to verify first analysis

Figure 33. Virus expressing RL13 and UL128 display virion degradation resistance

Figure 34. Virion degradation over 144 hrs in different temperature conditions

Figure 35. RL13 expression does not affect gB cell-surface expression on infected cells

Figure 36. The V5-tag does not affect RL13 expression

Figure 37. Selection of siRNA to target proteins

Figure 38. Optimisation of chosen siRNA to target proteins

Figure 39. An example siRNA Co-culture assay at 48 hr and 72 hr

Figure 40. RL13 binds Fc.

Figure 41. RL13 expression does not affect NK cell degranulation against infected target cells

Figure 42. ADCC varies with different donor's serum

Figure S1. RL13 recruits some host cell proteins to the AC

Figure S2. RL13 recruits some host cell proteins to the AC.

## List of Tables

- Table 1.* Viral particles produced in productive HCMV infection
- Table 2.* Buffers and solutions
- Table 3.* Bacterial culture media and reagents
- Table 4.* Bacterial culture media supplements
- Table 5.* Tissue culture media and reagents
- Table 6.* Cell lines used
- Table 7.* Antibodies used to check for correct differentiation
- Table 8.* LONG PCR programme
- Table 9.* HIFI PCR programme
- Table 10.* Stains and antibodies used for flow cytometry
- Table 11.* siRNAs used in this study
- Table 12.* Antibodies used in Western Blotting
- Table 13.* qPCR Thermocycling program
- Table 14.* Viruses used and created for this study
- Table 15.* TR RL13 sequence similarity search
- Table 16.* Viral Particles to analyse within the Nucleus and Assembly compartment
- Table 17.* Proteins identified that were highly significantly reduced in the virion when RL13 was expressed
- Table 18.* Host cell proteins identified to bind RL13 during infection
- Supplementary Table 1. Primers used in this project







# **CHAPTER 1. INTRODUCTION**

## 1.1 Human Cytomegalovirus (HCMV)

Human Cytomegalovirus (HCMV), also known as Human Herpes virus 5 (HHV-5), infects people worldwide and is the leading infectious cause of congenital malformation. Infections are lifelong and although typically asymptomatic, HCMV infection poses a serious risk of disease in the immunocompromised or immunosuppressed. The management of complications caused by this virus is very costly and a burden on health care. As currently there is no licensed HCMV vaccine, the development of a successful vaccine is a high priority target (8).

### 1.1.1 The Herpesvirus Family

The family *Herpesviridae* under the order *Herpesvirales* includes a large collection of DNA viruses that infect a range of hosts that include fish, reptiles, birds as well as mammals (9). Herpes viruses are very successful pathogens as proved by their wide distribution in nature with most animal species playing host to at least one herpesvirus (10). Herpes viruses are defined based on their general structure (9, 10). The large linear double stranded DNA genome is encased in an icosahedral capsid which is coated by a proteinaceous layer termed the tegument. This entire structure is then further surrounded by the glycoprotein studded lipid bi-layer envelope. Members are assigned to subfamilies based on criteria such as growth kinetics, host range, tropism and genetic homology (11). The family *Herpesviridae* contains three subfamilies: the *Alphaherpesvirinae*, *Betaherpesvirinae* and *Gammapherpesvirinae* (10). HCMV is a member of the subfamily *Betaherpesvirinae* and the genus Cytomegalovirus. *Betaherpesvirinae* generally are highly host specific, exhibit cell-associated methods of infection and have relatively long replication cycles (11). This subfamily currently includes five genera: Cytomegaloviruses, Muromegaloviruses, Roseoloviruses, Probosciviruses and a genus for unassigned (Figure 1). So far 20 different species of viruses have been assigned within these genera, with 8 occupying the *Cytomegalovirus* genus (4).

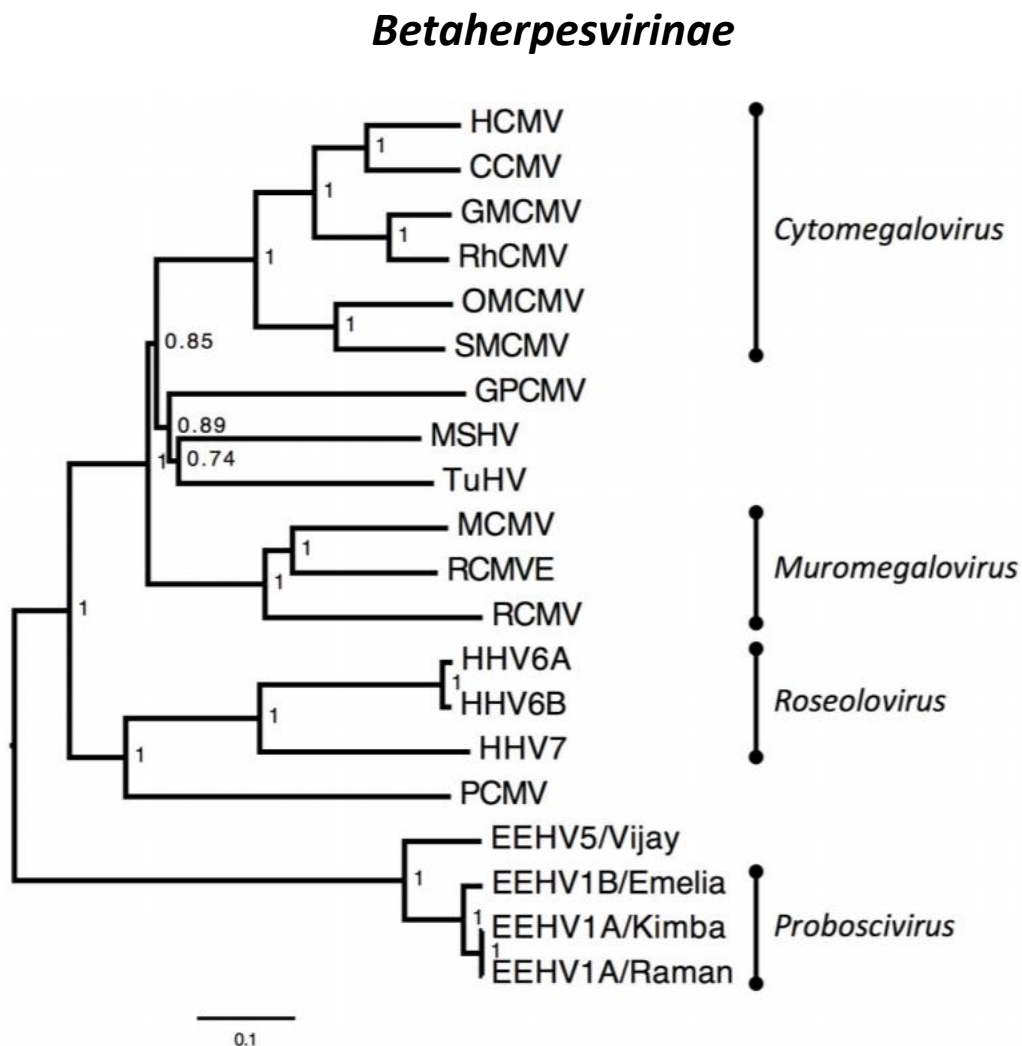


Figure 1 – Phylogenetic tree showing the evolution of the *Betaherpesvirinae* family (adapted from (4)). The concatenated amino acid sequences of the essential genes (U38, U39, U40, U41, U57, U60, U77, and U81) were used to create this phylogenetic neighbour-joining tree. The scale bar shown at the bottom displays nucleotide differences/nucleotide and the confidence values are shown as fractions. The 20 betaherpesviruses are; HCMV, human cytomegalovirus; CCMV, chimpanzee cytomegalovirus; GMCMV, green monkey cytomegalovirus; RhCMV, rhesus cytomegalovirus; OMCMV, owl monkey cytomegalovirus; SMCMV, squirrel monkey cytomegalovirus; GPCMV, guinea pig cytomegalovirus; MSHV, *Miniopterus schreibersii* herpesvirus; TuHV, *tupaia* herpesvirus 1; MCMV, murine cytomegalovirus; RCMVE, rat cytomegalovirus England; RCMV, rat cytomegalovirus; HHV6A, human herpesvirus 6A; HHV6B, human herpesvirus 6B; HHV7, human herpesvirus 7; and PCMV, porcine cytomegalovirus.

### **1.1.2 Discovery and Isolation**

HCMV infection was first noted by Pathologist Dr. Ribbert. His case study, presented in a meeting of the *Natural History Society of Prussian Rhineland and Westphalia* in Germany 1881, detailed enlarged 'cytomegalic' cells with intranuclear inclusions observed in kidney secretions from a stillborn presenting with interstitial nephritis and Lues-like symptoms (12, 13). Similar giant cells were described again in 1904 by Jesionek and Kiolemenoglou (14) prompting Dr Ribbert to reinterpret the cytomegalic cells as protozoa (15). von Glahn and Pappenheimer and co-workers were the first to suggest that the intranuclear inclusions were a result of virally infected cells (16), however this aetiology would not be confirmed until the electron microscopy analysis of cytomegalic pancreatic cells in 1953 which found 199-nm particles thought to be the virus responsible (17). The name "Cytomegalic inclusion disease (CID)" was suggested after noting the presentation of cytomegalic cells correlated with the clinical manifestations of congenital infection in both humans and other animals (18).

Early attempts to isolate and propagate HCMV were frustrated by an inability to culture human cells routinely and the host-specificity of the virus. Successful isolation and propagation of the infectious agent was reported almost simultaneously by three independent research groups (19-21). During Margaret Smith's early attempts to isolate virus from human salivary gland, she noted that the clinical agent was only able to be propagated in human tissues and not in murine cells indicating the host specificity of the virus (20, 22). Weller was responsible for the serological testing that identified the distinct strain differences within the viral species and propose the name cytomegalovirus (22, 23).

## **1.2 Clinical Importance and manifestations of HCMV infection**

### **1.2.1 Epidemiology**

HCMV is a ubiquitous pathogen with a worldwide distribution. For example, seroprevalence rates of adults of reproductive age in the United States are around 60%, and these rates increase with age to around 90% in adults over 80 years. HCMV seroprevalence is significantly influenced by socioeconomic status, age and geography old (24, 25). Generally, people in developing countries are at more risk of contact during the early years of life, likely due to overcrowding, large families or unsanitary living conditions. However, this does mean that in more developed countries likely exposure to the virus increases with age, and so developed countries have a higher risk of primary infection during pregnancy (24, 26). Lower seroprevalence is seen in Western Europe and the United States, whilst the highest seroprevalence is seen in South American, African and Asian countries (27). Some studies show a tendency of higher infection rates in females than in males (24) however in most of these cases the differences are small.

### **1.2.2 Transmission and Primary Infection**

The main method of dissemination is through contact with bodily fluids containing the infectious agent from individuals with symptomatic or asymptomatic infection. This can be via saliva, breast milk, blood transfusion, solid-organ transplant, hematopoietic stem cell transplantation, placental transfer or sexual contact (5, 28, 29). A study found that HCMV was viable for as long as 6 hours if the surface it was applied to was wet (30). This demonstrates the necessity of good hygiene practices such as handwashing in limiting transmission of HCMV.

Most frequently initial acquisition of HCMV (primary infection) occurs in mucosal tissues after direct contact with the infectious secretions of another seropositive individual. This primary acute infection typically lasts weeks to a few months and is characterised by persistently shedding virus from restricted cellular sites from within the host. HCMV persists for the lifetime of the host following primary infection and, in the immune-competent individual, infection is generally asymptomatic and constantly under immune surveillance (5, 31). After primary infection there are two potential routes the infection

can follow, chronic infection characterised by dissemination of the virus to form restricted infection foci, lytic replication and low titre shedding (31) or latent infection characterised by epigenetic repression of the viral genome allowing for the maintenance of the viral genomes in the absence of virion production (32). Primary infection appears to be associated with more clinical problems than exogenous reinfection or endogenous reactivation (33, 34), however seropositive stem cell transplant recipients are also at great risk when receiving seronegative stem cells naïve to HCMV infection (35).

### **1.2.3 Infection in the Immunocompetent Host**

Infection in the immunologically competent host can very occasionally result in mild febrile mononucleosis-like illness characterised by prolonged fever, fatigue and cervical lymphadenopathy. HCMV infection has also been reported to cause gastrointestinal disease or even pneumonia (36). Only rarely do more serious clinical complications involving specific organ systems occur (1).

### **1.2.4 Congenital and Perinatal Infection**

While transplacental transmission is rare with other herpes viruses, HCMV is the leading infectious cause of congenital malformation and the prognosis can include sensorineural hearing loss, mental retardation and loss of or compromised vision (1, 5, 34, 37). A small percentage of infected neonates develop severe systemic, life-threatening cytomegalic inclusion disease. These problems can occur due to primary infection, reactivation or reinfection with a different strain. The birth prevalence of congenital HCMV infections varies amongst populations from 0.2-2.2% of live births (25, 38). Although the medical complications that coincide with congenital HCMV infection can be severe, the majority of infected infants are asymptomatic at birth with only around 13.5% displaying symptoms immediately and a further 12.7% displaying symptoms on follow-up (38, 39). Mothers who experience primary infection during pregnancy are at higher risk from congenital infection than seropositive mothers undergoing reinfection or reactivation. A study found that of the children born to mothers experiencing primary HCMV infection during pregnancy, 32.3% suffered from congenital HCMV infection. This was significantly higher than the 1.4% of children with congenital HCMV born to mothers with reactivated HCMV infection (25). Children with congenital HCMV infection from a



mother experiencing primary infection during pregnancy are more likely to have at least one sequela and are likely to be more severely affected (40). Although infection can occur during all trimesters, if primary infection to a seronegative mother occurs during the first trimester the risk and severity of disease are greatest (41). Transplacental transmission of HCMV is the most medically significant route of maternal transmission however, the most frequent method of transmission between mother and child is through breastfeeding. It is thought that around 69% of infants contract HCMV from breastfeeding by shedding seropositive mothers. In fact, virus is most prevalent in breast milk from day 9 to 3 months postpartum after which it declines (42). Clinical disease is more uncommon in cases where transmission to infants occurs after birth (1).

### **1.2.5 Infection in at-risk groups**

HCMV is a clinically important opportunistic pathogen and lytic viral replication can cause serious medical complications for those who do not have a fully functioning immune system. These at-risk groups include neonates (covered in section 1.2.4), the immunocompromised and the immunosuppressed. What makes these populations at-risk is their inability to respond effectively to primary infection or recurrent infection.

Individuals in these groups include Acquired Immunodeficiency Syndrome (AIDS) patients, solid organ transplant (SOT) recipients, haematopoietic stem cell transplantation (HSCT) patients and other allograft recipients. Symptoms are similar to those that the immunocompetent experience but typically more severe and usually HCMV viraemia is seen. For unknown reasons, HCMV disease can vary between patient groups (43). The most common pathology observed in AIDS patients is retinitis, usually starting with one eye but eventually leading to both and can lead to complete loss of vision. The introduction of Highly Active Antiretroviral Therapy (HAART) has had a dramatic effect on the incidence of end organ disease caused by HCMV infection (44, 45). New cases of HCMV retinitis have declined by roughly 80% following HAART and the survival rate of those already suffering with this end organ disease has increased by 93% (46). High levels of HCMV viraemia are common in HIV-infected individuals, and is strongly associated with progression to AIDS and mortality (44).

HCMV infection is often associated with allograft rejection as a result of the pro-inflammatory environment resulting from persistent and chronic infection (47). However, the cause and effect relationship is considered controversial. One study found evidence of a bidirectional relationship between the two post-transplant complications. They found that the immunosuppressive effect of graft-versus-host disease and its therapy can induce HCMV infection, but also that patients experiencing active HCMV replication were at a greater risk of allograft rejection than those without active HCMV replication (48). Liver transplant patients are often diagnosed with HCMV hepatitis, whereas HCMV pneumonitis is a major complication for bone marrow transplant patients (43).

HCMV infection has also been reported to cause serious complications in settings not traditionally known to have been a risk for HCMV disease. It is not known whether HCMV is a causative agent in these diseases or whether it is just an opportunistic bystander, but it has been suggested that HCMV can be associated with glioblastomas (49, 50), new-onset post-transplant diabetes (51), inflammatory bowel disease (52), atherosclerosis (53) and immunosenescence (54).

### **1.2.6 Treatments and Vaccination**

As there is currently no licensed HCMV vaccine, an anti-HCMV vaccine that successfully treats and clears infection is still a highest priority target (8). However, five HCMV antivirals are currently available: Ganciclovir (GCV) and its orally administered prodrug Valganciclovir, Foscarnet (FOS), Cidofovir (CDV) and Fomivirsen (FMV) (55). However these therapies only provide disease management and have some substantial limitations (56). The commonly used HCMV antivirals can cause significant toxicity (57) and HCMV can become resistant through prolonged treatments (58).

GCV was the first antiviral therapy approved for HCMV disease and remains the most commonly used (55). It is a synthetic analogue of 2'-deoxyguanosine which is phosphorylated by the viral protein kinase encoded by HCMV UL97, and subsequently converted into GCV triphosphate. Viral DNA synthesis catalysed by the HCMV DNA polymerase (HCMV UL54) is targeted by GCV triphosphate (59). It is rare for HCMV to develop resistance to GCV, however, when it does it is likely to be the result of a

mutation in the HCMV gene UL97 or UL54 (60). In fact, mutations in UL54 have also been reported to lead to HCMV resistance to FOS and CDV (55).

The first live-attenuated vaccine to be trialled on humans was derived from the laboratory-adapted strain AD169. Shortly after vaccine candidates were based on the strain Towne (61). The live-attenuated Towne vaccine was trialled in seronegative renal transplant patients and although the HCMV pathologies seen in the treatment group were not as severe as the control, the vaccine did not protect patients from acquisition of the virus or development of acute infection (62).

Recently a recombinant HCMV vaccine based on the envelope glycoprotein B has had significant success in clinical trials. This subunit vaccine was developed in the 1980s and is comprised of soluble gB in an oil-in-water adjuvant (MF59) (63). In phase 1 clinical trials the vaccine was found to be immunogenic and safe (64). The recipients of the vaccine reported to elicit potent anti-gB responses (65). In phase 2 clinical trials the vaccine proved to reduce the HCMV infection rate in young mothers by 50% (66) and in adolescents girls by 43% (67). In another study conducted in SOT patients, the gB subunit vaccine was found to not only reduce CMV disease but also to decrease the duration that patients required pre-emptive anti-CMV antivirals after transplant (68). It was presumed that the efficacy of the gB subunit vaccine was due to induction of a neutralising antibody response, however this has since been proved false (69, 70).

The T-cell target pp65 (ppUL83) and IE1 have also undergone evaluation as potential vectored or subunit vaccines (56). A bivalent plasmid DNA vaccine has also been evaluated in phase 2 clinical trials. This vaccine encoding HCMV pp65 and gB was reported to cause fewer cases of viraemia in seropositive HSCT patients compared to the control group (71). gB and pp65 have also been the focus in another type of vaccine that has reached phase 2 of clinical trials and delivers the HCMV antigens via an attenuated canarypox vector (72, 73).

## 1.3 Viral Particles

### 1.3.1 Components of Infectious virions

Like other Herpesvirus virions, mature HCMV virions are large and are reported to range from 150-200nm (45, 74) to 200-300 nm (1) in diameter. HCMV virions follow the same basic structure of four concentric layers found in all herpesviruses. These four layers consist of a double stranded genome core, an icosahedral capsid to protect the DNA, a thick proteinaceous layer and finally a membrane derived from the host cell studded with envelope glycoproteins (11, 75, 76).

#### *Nucleocapsid*

The nucleocapsid, otherwise known as the C capsid is a sturdy icosahedral lattice with T=16 symmetry measuring 100–110 nm in diameter. What differentiates the nucleocapsid from the other capsids (A and B, described in section 1.3.2.1) is the efficient packaging of the large double stranded HCMV genome inside (77).

Many HCMV proteins structure the capsid making up 162 capsomeres (capsid subunits) and 320 hetero-trimeric triplexes. Capsomeres are either hexamers or pentamers of the UL86 encoding major capsid protein (MCP) located within either the 20 triangular faces or the 12 vertices respectively. The triplexes are composed of two copies of the UL85 encoding minor capsid protein (mCP), and one copy of the mCP-binding protein (pUL46) (76-78). One vertex is specialised in that it is made of 12 copies of the portal protein (PORT, pUL104) forming a symmetrical portal complex enabling the viral DNA to pass through during encapsidation and viral DNA release (2, 79). The smallest protein UL48.5 (SCP) is found tightly bound exterior faces of capsomeres. Six copies are attached to each hexon and it is essential for the production of infectious HCMV virions (2, 80).

#### *Tegument*

The tegument is an intricate layer of proteins that associate with the capsid and lie beneath the outer viral envelope. It is formed of 59 viral proteins and also contains cellular proteins, many of which are phosphorylated (75). However only 39 of the viral tegument proteins are incorporated into the virion at significant levels (74, 75). The tegument is thought to be amorphous and relatively unstructured in nature, however

some tegument proteins are bound to the capsid giving some structure (81). This proteinaceous layer is approximately 50 nm thick and predominated by pp150 (UL32), pp71 (UL82), pp65 (UL83) (2, 82).

As tegument proteins are components of virions and are delivered to the host cell during initial infection, they can have significant impact on viral replication even before the viral genome has been transcribed. These important roles include delivery of preformed protein necessary for the commencement of infection, providing structural stability to nucleocapsids and regulating signalling required for final envelopment and egress of virions (7). They are also reported to contribute to immune evasion, regulation of cellular processes and the release of viral DNA from the capsid into the nucleus (83).

### *Envelope*

HCMV virions, dense bodies and non-infectious enveloped particles are all enclosed in a lipid bilayer envelope derived from the host cell. The virion envelope is ~10 nm thick and like all herpesviruses is studded with an array of envelope glycoproteins (82). Five of these envelope glycoproteins (gB, gH, gL, gM and gN) are considered essential for replication, whilst loss of gO (UL74) results in moderately defective viral growth (84). During infection these glycoproteins accumulate on the plasma and internal membranes of infected cells and are targets of neutralising antibodies (85).

Virion envelope proteins can be potential targets for neutralising antibodies but could also be involved in modulating the host cell response to infection or could aid in attachment/entry or even tropism. The envelope glycoproteins encoded by RL11 and UL119-UL118 (gp34 and gp68 respectively) are Fc receptors that bind IgG (86). A trimer of gB (UL55) assists membrane fusion during entry. Another glycoprotein complex of gH:gL (UL75 and UL115 respectively) can modify the tropism of the virus. gH:gL functions to stimulate attachment and when used with gB-mediated fusion it is more efficient than gB alone (87). The gH:gL complex can be found in two forms, firstly as a trimer consisting of gH:gL:gO, which is necessary for entry into fibroblasts by binding to PDGFR $\alpha$  (88) and secondly as the pentameric complex. The pentameric complex consists of gH:gL and the three gene products of the UL128 locus (UL128L:UL128, UL130 and UL131A) giving gH:gL:pUL128:pUL130:pUL131A. This complex binds to neuropilin-2 and allows for the expansion of viral tropism into epithelial and endothelial cells (89-91) as

well as for viral interactions with other cell types including neutrophils and DCs (92). Attachment and endocytosis without the pentameric complex is possible in epithelial and endothelial cells, however the virus is unable to enter the cytosol (89, 90).

### **1.3.2 Non-infectious Viral Particles**

During productive HCMV infection many non-infectious particles are generated and some are even released along with infectious virions. Five types of viral particle excluding virions have been recovered and characterised from HCMV infections (77) (table 1).

#### *A, B and C capsids*

Similarly to other herpesviruses, three stable and distinct nuclear capsids are formed: A, B and C (also termed Nucleocapsids) and their fate is determined by the success or failure of DNA packaging (93). Their lack of viral DNA and/or scaffold proteins is what distinguishes these similar capsid forms (77). It is thought that the three capsid structures plus the additional transient procapsid are linked by their maturation pathway in the nucleus by a hypothetical transition B capsid ( $B_t$ -capsid) (figure 2) (2). The  $B_t$  capsid has the potential to mature fully into a mature C capsid packaged with viral DNA and lacking scaffold proteins. If the viral DNA packaging is aborted during C capsid formation or the scaffold protein is prematurely lost from a B capsid without subsequent DNA packaging an A capsid could form. B capsids still contain an inner array of scaffold protein with no DNA packaged inside. It is though that C capsids can still mature from B capsids (94).

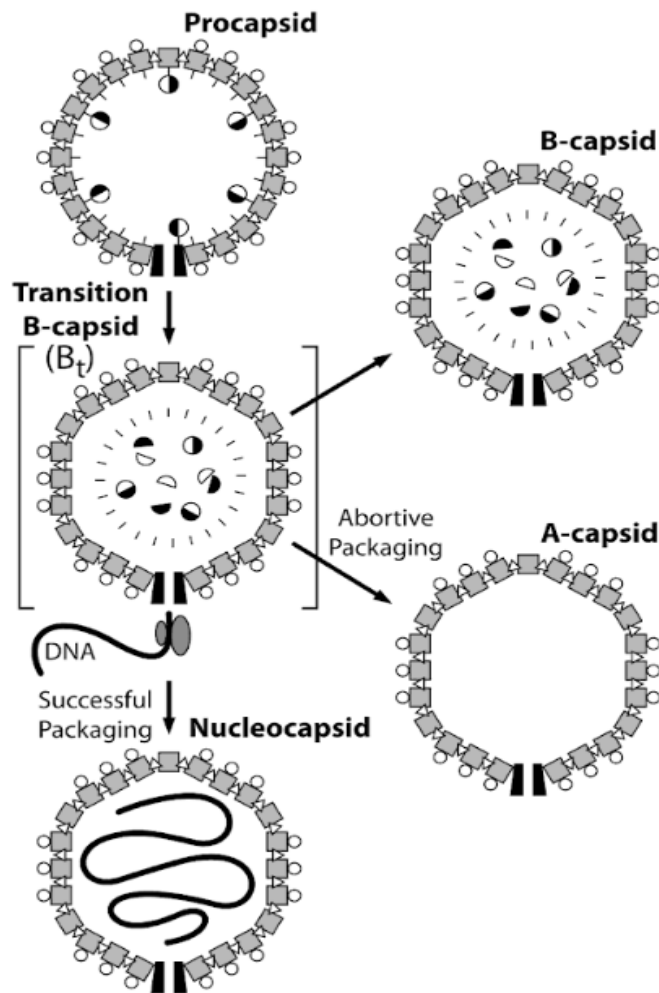


Figure 2 – The Formation of A, B and C capsids with the hypothetical Bt capsid. A-capsids represent empty capsid shells that contain neither viral DNA nor any other discernible internal structure. B-capsids are capsid shells containing an inner array of scaffolding protein. C-capsids are mature capsid shells that are packaged with viral DNA and do not contain the scaffolding proteins. The Bt capsid is thought to be an intermediate showing how the fate of each capsid's formation is reliant on the successful packaging of the viral genome and the abortion of the scaffold proteins. Reproduced from (2).

### *Non-infectious Enveloped Particles (NIEPs)*




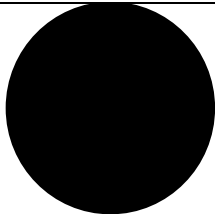
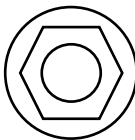
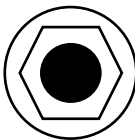
Structurally and biochemically similar to virions, NIEPs differ in that they lack infectious viral DNA and keep some scaffold proteins. It is thought that NIEPs are a result of matured B capsids that have progressed into the cytoplasmic assembly compartment (AC) (2, 82). As they contain an immature capsid lacking DNA (B capsid) they lack an electron dense core compared to virions making them distinguishable from one another in Electron microscopy. NIEPs are often found released into the culture medium of infected cells in great excess along with dense bodies (DBs) (95).

### *Dense bodies (DBs)*

DBs have a simple structure and composition compared to virions and NIEPs. They are much larger with a diameter range of ~250-600 nm. They are composed of mainly pUL83 aggregates enveloped in a lipid envelope in the same manner as virions and NIEPs. They lack any viral DNA or any capsid proteins (82). gB is also a major constituent of DBs (77, 82). Similarly to NIEPs, their exact purpose during HCMV infection was unknown for some time. It was hypothesised that these aberrant viral particles could aid HCMV survival by saturating or overwhelming the hosts viral immune surveillance (95). In fact, these large non-infectious particles composed of antigenic determinants induced the humoral and the cellular immune response in the absence of infectious virus. It was therefore proposed that DBs could be a promising recombinant non-replicating vaccine (96).



Table 1 - Viral particles produced in productive HCMV infection. Adapted from (7)

Location	Nucleus			Assembly Compartment		
Particle	A-capsids	B-capsids	C-capsids	Dense bodies	NIEPs	Virions
Description	Thought to be the result of failed viral DNA encapsidation and lacking both viral DNA and a scaffold.	Likely to have resulted from failed capsid formation as they contain a scaffold but lack viral DNA.	Likely nucleocapsids during maturation, containing viral DNA.	Non-infectious particles lacking capsids and composed mainly of pp65.	Non-infectious enveloped particles (NIEPs) resulting from envelopment of B-capsids.	The only infectious particle containing viral DNA resulting from envelopment of C-capsids.
Particle appearance in TEM						

## **1.4 Viral Lifecycle**

The main mechanisms present at each of the stages of the HCMV lytic lifecycle are shared between the Herpesvirus family. These are attachment, entry, uncoating, replication, assembly, maturation and finally egress (figure 2). Herpes viruses have further distinct consecutive stages during replication; immediate early (IE), early (E), and late (L) cascades of gene expression.

### **1.4.1 Virus Entry**

First contact of cell free HCMV virions with a viable host cell is mediated by the glycoproteins found on the HCMV virion envelope. Viral glycoproteins such as gB, gH/gL and gM interact with a series of cellular receptors on the host cell membrane (87). In fact, through studies with mutants it has been noted that several glycoproteins are essential for HCMV infection. Thus, the glycoproteins gB (UL55), gL (UL115), gM (UL100), gH (UL75), and gN (UL73) are highly conserved (97, 98).

The method of HCMV entry into a viable host cell depends on the cell type. HCMV infects many different human cell types despite the narrow tropism observed of laboratory strains *in vitro* (99). Entry into fibroblasts is pH-neutral and occurs by direct fusion of the plasma membrane with the viral envelope (100). However, a low-pH is required for receptor mediated endocytosis into epithelial and endothelial cells (101). Entry into DCs is via clathrin-independent endocytosis which resembles macropinocytosis and is pH-independent (102).

Clinical HCMV is mostly found cell-associated (103, 104) and this equates with direct cell-cell transmission. The mechanism behind this has been postulated to be through transitory microfusion events after direct contact between the plasma membranes of the uninfected and infected cells expressing the viral glycoproteins involved in cell-free entry (105, 106).

### **1.4.2 Viral DNA Replication and Gene Expression Regulation during Infection**

Viral transcription, genome replication and finally encapsulation of the newly synthesised viral genomes occur in the cell nucleus. The HCMV lytic genes are transcribed in a temporal cascade. This cascade consists of three kinetic classes of HCMV

genes; Immediate early (IE), Delayed early (DE) and Late (L) which can be further categorised into leaky late and true late and are sequentially expressed over the course of a 72 hour lytic replication cycle (1).

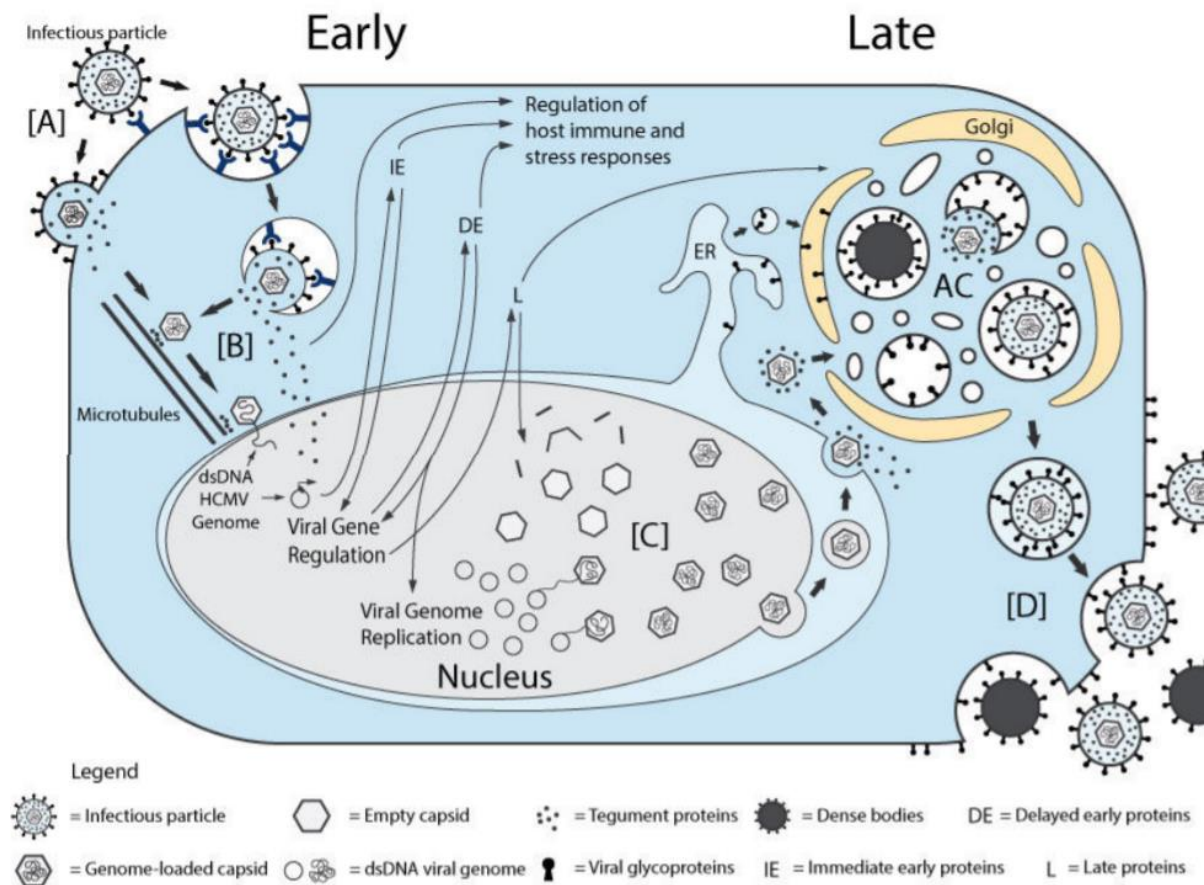
After entry into the host cell, cytoplasmic microtubules assist the nucleocapsid to the nuclear pores (78). The viral tegument proteins found surrounding the capsid are thought to diffuse into the cell and facilitate entry into the nucleus pores by interacting with the host's microtubule machinery. Some tegument proteins track to specific sites and modify cellular metabolism (107) or cellular signalling pathways (108) in order to promote both intrinsic and innate cellular immune evasion as well as viral replication (109). The tegument protein ppUL48 and a binding protein, ppUL47, initiate viral uncoating and release of viral DNA (110).

Once inside the nucleus, the virus is subjected to the intrinsic antiviral defence, promyelocytic leukaemia nuclear bodies (PML-NBs). The death-domain associated protein (Daxx) is a prominent PML-NB which localise with the viral genome by associating with DNA-binding transcription factors. Daxx silences IE gene expression by recruiting histone deacetylases (HDAC) to viral gene promoters (111, 112). IE gene transcription is mapped to five loci distributed across the genome: UL36 and UL37, TRS1, IRS1, US3, and IE1/IE2 (UL123 and UL122). Expression of the major IE gene (MIE or IE1/IE2) is controlled by the MIE promoter (MIEP) and the transcribed product is alternatively spliced into either IE1 or IE2 (113, 114).

The temporal cascade of HCMV lytic gene expression initiates as tegument protein pp71 (UL82) degrades Daxx, which in turn relieves the Daxx and HDAC-mediated transcriptional suppression on IE1 (112). The viral genome then circularises and IE genes can be transcribed. Further PML-NBs are disrupted by newly synthesised IE1 and replication is initiated (115). ppUL84 is a transcriptional transactivator which binds IE2 and mediates the successive association of viral proteins with the viral genome in order to promote viral gene transcription and the formation of replication centres (116). Viral DNA is replicated via the rolling circle mode by which concatemers are produced. The enzyme complex terminase (composed of pUL56 and pUL89) feeds the head-to-tail linked genomes into newly synthesised scaffold-containing procapsid until a single genome has entered and then cleaves the DNA at precise locations (117, 118). The two

*cis*-acting DNA packaging motifs, *pac1* and *pac2*, are found at the ends of the genomes and are thought to aid in cleavage of concatemeric DNA (119). pUL56 of the terminase complex is responsible for binding to the *pac* sequences and for packaging the DNA into the procapsids whilst pUL89 is required to cleave the DNA at the specific locations (120).

IE2 is a potent transactivator of DE and L viral genes, cellular genes and negatively autoregulates its own expression (121). The cascade continues as the expression of the DE genes is required for expression of L genes, which encode virion components necessary for virion formation, maturation and release. IE gene expression is independent of de novo HCMV replication as it relies on host and preformed viral machinery whereas translation requires host cell ribosomes (1).



*Figure 3 -The lifecycle of HCMV. (A) HCMV fuses to the plasma membrane or utilises the endocytic pathway to gain entry into the host cell. (B) After entry and uncoating of the virion, the nucleocapsid is directed to the nucleus where expression of IE genes occurs initiating viral DNA replication. (C) The viral DNA is packaged into capsids which gain an envelope as they egress from the nucleus. (D) A secondary envelope is gained prior to the infectious virion leaving the cell by exocytosis. Figure reproduced from (5).*

### **1.4.3 Viral Particle Maturation and Egress**

The newly formed capsids mature to become virions in a two-stage envelopment and egress process. The new capsids are transported to the cytoplasm by a herpesvirus-conserved nuclear egress complex (NEC). The NEC enables the capsid to migrate through to the cytoplasm by binding and dissolving the nuclear lamina and mediating initial envelopment in the peri-nuclear space shortly followed by de-envelopment of the capsids at the outer nuclear membrane (1, 7, 85, 122). It is thought that the NEC could play a part in quality control by preferentially binding and transporting the DNA-filled C capsids over the non-infectious A and B capsids (123). The nascent capsids actually begin to acquire some of their tegument proteins during this time prior to reaching the cytoplasm. The translocated nucleocapsids then congregate in the viral assembly compartment (AC), a structure unique to beta herpesvirus-infected that forms in the cytoplasm 72-96 hours p.i. It is composed of hijacked and relocated cellular secretory compartments including the Golgi body (GB), trans-Golgi network (TGN), and early endosomes. This structure is described as concentric circles as Golgi and TGN vesicles encircle the AC, ER is distributed throughout the cytoplasm but also in a ring at the AC periphery and early endosomes make up the AC interior (6) (see figure 4). Viral tegument and envelope proteins accumulate along with the nucleocapsids in the AC. The tegument proteins associated with and offer stability to the maturing nucleocapsids, and also signal for the final envelopment process to begin. The final envelopment is influenced by HCMV envelope glycoproteins as well as viral proteins pUL71, ppUL35 and pUL103 (7). pUL71 promotes envelopment (83), ppUL35 affects virion egress (124) whilst pUL103 coordinates virion and dense body egress (125). The tegumented nucleocapsids acquire their final envelope in a vesicle thought to be either a vesicle in transit between the TGN and endosomes or a hybrid compartment expressing markers for the two vesicles. The matured virions leave the AC vertically to the cell surface where they merge with the plasma membrane and egress by exocytosis (6, 126).

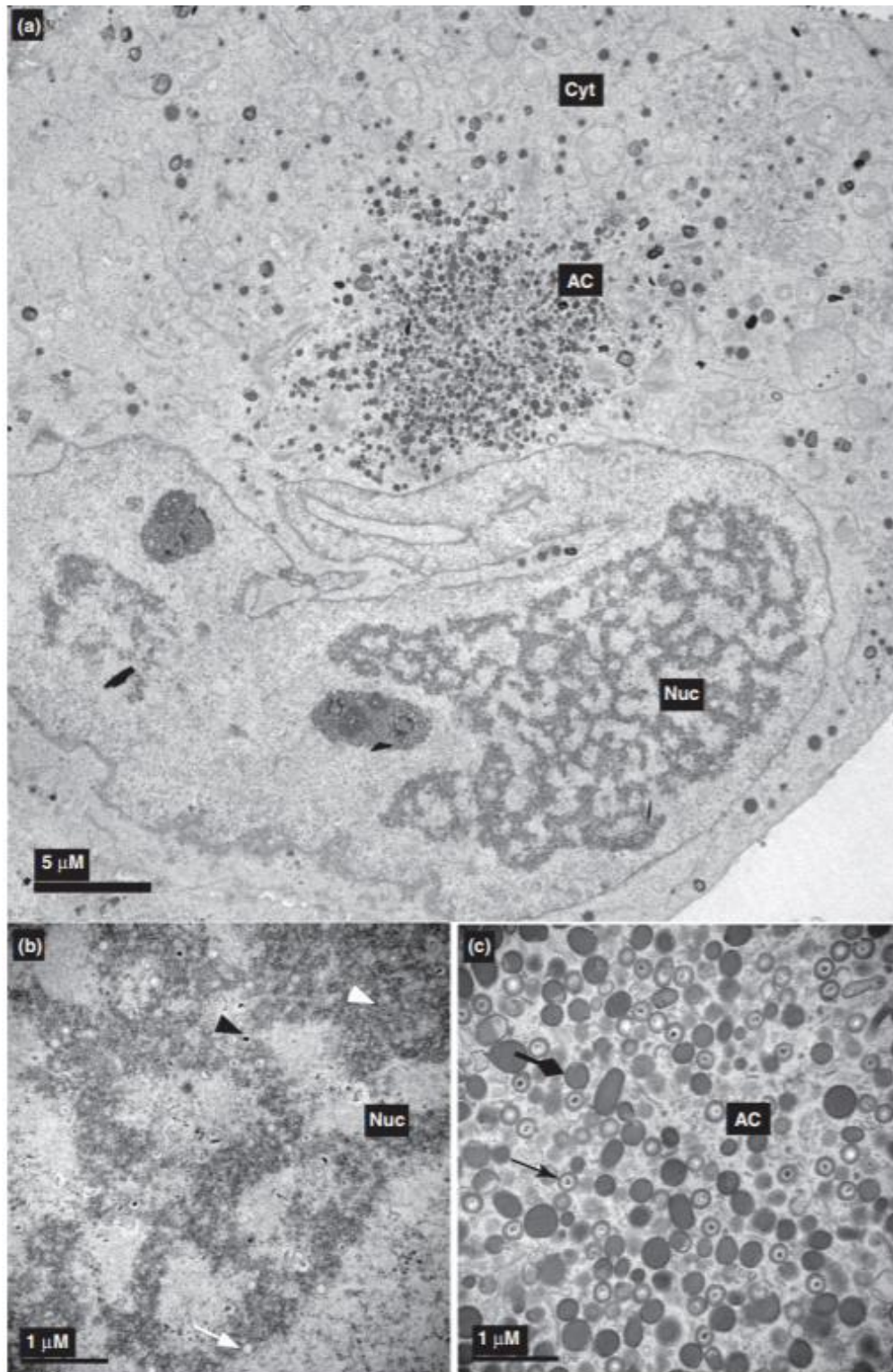
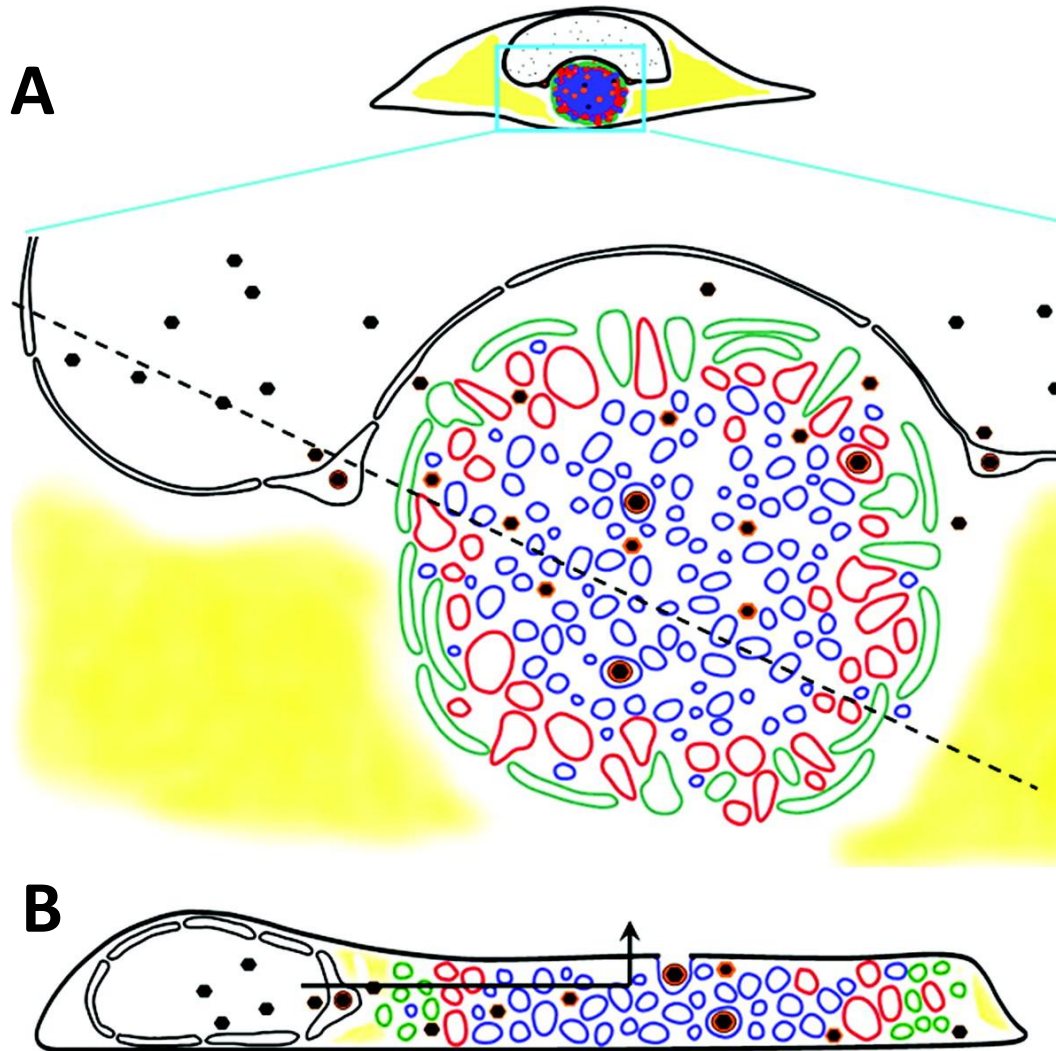


Figure 4 -Viral particle formation and maturation start in the nucleus and continues in the AC found in the cytoplasm. HCMV-infected fibroblast shown by Transmission electron microscopy (TEM). The many types of viral particle formed during infection can be seen in: (a) The whole cell showing the nucleus and the AC formed next to it, (b) the nucleus and (c) the AC found in the cytoplasm. Symbols: white arrowheads, B capsids; black arrowheads, C capsids; white arrows, A capsids; black arrows, mature virus particles; black diamond heads, dense bodies. Abbreviations: Nuc, nucleus; Cyt, cytoplasm; AC, assembly compartment. Scale bars represented: (a) 5 mm and (b,c) 1 mm. Reproduced from (7).





ER, Golgi, trans-Golgi, early endosomes

Figure 5 – The AC structure and virion maturation and egress pathway. Reproduced from (6). (A) AC structure. The AC is a large structure of concentric rings of the Golgi, TGN and early endosomes. The ER is found throughout the cytoplasm and encircles the AC. (B) Virion maturation and egress pathway. Nucleocapsids leave the nucleus and mature through the AC until finally egressing vertically to the extracellular space.



#### **1.4.4 Latency and Reactivation**

Latency is defined by the retention of the HCMV genome without the production of infectious virion progeny but with the potential to reactivate (127). This feature appears to be shared among all herpesviruses and allows for the virus to reside within specific sites within the host for prolonged periods of time whilst not actively replicating or producing any viral progeny. Expression of the IE genes can be initiated and the virus is reactivated into its lytic lifecycle in response to certain stimuli (128). In immune-competent individuals reactivation events are usually controlled by cell-mediated immunosurveillance and HCMV can remain in its latent state for the lifetime of the host. Unlike the lytic lifecycle of HCMV which is permitted in multiple cell-types, the HCMV latent lifecycle is only permissible in restricted cell types (129). HCMV persists in a latent state in bone marrow-derived CD34+ progenitor cells (precursors of monocytes, macrophages and dendritic cells (DCs)) and CD14+ monocytes (127-129).

In order to enable this transcriptionally inactive state within CD34+ progenitor cells, a repressive chromatin structure is required. This is possible through a number of processes such as the recruitment of histone proteins to the MIEP which are then trimethylated at H3K9 and H3K27, the presence of HP1 a repressive chromatin marker and HDAC activity (32). Not only is the MIEP regulated by chromatin structure but many repressive or activating transcription factors have binding sites within the MIEP (130). To name a few, repressive transcriptional factors Ying Yang-1 (YY1) and Ets-2 Repressor Factor (ERF) bind to repeated sequences within the MIEP. HDAC1 is recruited to the MIEP by ERF which acts to silence gene expression (131). The chromatin organiser KAP1 along with the SETDB1 histone methyltransferase and HP1, associates with distal sites of the HCMV genome to mediate repression (132). Additionally, latency-associated viral factors help to the suppression of the MIEP and the viral transactivator protein pp71 which acts to initiate the temporal cascade of HCMV lytic gene expression (see section 1.4.2) is excluded from the nucleus and remains in the cytoplasm (133).

Myeloid cell differentiation has been shown to initiate chromatin remodelling of the MIEP, acetylation of the heavily methylated histones bound to the MIEP and the dissociation with HP1 likely allowing for the reactivation of the HCMV lytic lifecycle by allowing IE gene expression (32, 134, 135).

## **1.5 HCMV Infection**

HCMV infection in humans most often initiates at mucosal sites. Although infection typically causes no overt pathology, an acute productive viral replication phase occurs and lasts from a few weeks to months, during which high titres of virus are shed. Once an immune response has been mounted against the pathogen the viral replication and shedding is heavily restricted. HCMV infection will result in systemic dissemination to ensure transmission to future hosts and the establishment of latency (136).

### **1.5.1 Intra-host Dissemination and Tropism**

CMV exhibits a strict species specificity. However, within a host the virus spreads throughout the majority of organ tissues. HCMV spreads to multiple organs including the heart, brain, lungs, kidney, liver, spleen, retina, oesophagus, colon salivary glands, and inner ear (137). The broad tropism of cell types and organs is likely responsible for the wide variety of sequelae observed in HCMV infection. The cell range of HCMV infection is remarkably broad with targets of natural infection including connective tissue cells of various organs, parenchyma tissues, and various hematopoietic cell types (60, 138).

The initial stage of viral dissemination, often termed primary dissemination, is likely to occur in mucosal tissues of the pharynx or the genital tract (137, 139). The initial cellular targets of HCMV after acquisition are likely epithelial cells which are thought to not only be an important primary infection site but for shedding of virus as well. The virus undergoes its lytic replication cycle and subsequently infects other permissible cell types such as fibroblasts, endothelial cells, dendritic cells, and other innate immune cells including alveolar macrophages most likely via cell-cell transmission of virus. Infection in polymorphonuclear leukocytes is not productive and instead it's thought that these cells take up and transport virus particles to initiate infection in other tissues (137). Once innate immune cells with the potential to circulate in the bloodstream are infected, it is thought that the second stage of viral dissemination occurs (systemic spread) (136). HCMV viremia tends to be cell-associated as HCMV can travel through the body via circulating cells as well as haematogenous spread. Vascular endothelial tissues that form the interface between the blood circulation and solid tissues play a critical role in the dissemination of HCMV. These endothelial cells when infected with HCMV, can infect

neighbouring cells including non-endothelial cells of the underlying submucosa (29), but they can also swell and enter the bloodstream by detaching from the blood vessel wall (140). The majority of these infected cells lyse but some initiate organ infection as they accumulate in capillary beds (141). Data from HCMV studies suggests the importance of patrolling monocytes in the dissemination of HCMV as well. It is thought that these CX3CR1<sup>hi</sup> monocytes but not inflammatory monocytes aid in HCMV dissemination to distal organs most likely due to their immune-privileged phenotype post differentiation (142).

The virus establishes latency in bone marrow-derived hematopoietic cells (e.g. CD34+ progenitors and CD14+ monocytes) and even endothelial cells from within the arterial walls (127-129) (see section 1.4.3). These monocytes do not support lytic replication of HCMV (127, 143).

### **1.5.2 Lessons from HCMV Infection *in vitro***

Some nonessential genes of HCMV encode cell type-specific functions for virus-growth, functioning as either tropism factors or replication temperance factors. UL24 and UL64 proved to be important in Human Dermal Microvascular Endothelial Cells (HMVEC) and Retinal pigment epithelium (RPE) infection respectively. UL10 and UL16 are considered some of HCMVs temperance factors as UL10 mutants and UL16 mutants were shown to propagate exceptionally well in RPE and HMVEC cells respectively (84). The discovery of pathogen-encoded temperance factors in a herpesvirus is relatively new (84), but temperance factors that suppress virulence have been seen in *Mycobacterium tuberculosis* (144) and *Leishmania major* (145) before. Temperance factors are a prevalent survival strategy to allow the pathogen to suppress productive lytic replication in order to achieve co-existence with the host.

Differences in the tropism of HCMV strains or variants is usually due to receptor recognition by virion envelope glycoprotein complexes (see section 1.4.1). Interestingly, the cell type the virus is produced in can also be important. The two gH/gL complexes (see section 1.3.1.3), the trimeric and pentameric complexes, dictate receptor recognition and when both are present the virus can infect a wider range of cell types. *In vitro* HCMV virions can exhibit different tropisms by manipulating the amount of

pentameric complex present on their viral envelope. Virions derived from fibroblasts produced cell-free progeny tropic for fibroblasts and endothelial cells whilst endothelial cells retained endothelial cell tropic virus on its cell membrane which in turn infected other endothelial cells in foci likely through cell-cell methods, and released fibroblast-tropic virus (146). The role for this tropism switch *in vivo* has not yet been determined.

### **1.5.3 The Immune Response and Immunomodulation**

HCMV infection is targeted by both the innate and adaptive responses. Engaging both cellular and humoral immunity, it generates a robust immune response in humans (147). The complex virus/host relationship begins with an acute infection that is normally controlled by a combination of innate defences and a specific adaptive response, but neither appears capable of eradicating the virus completely.

#### *Innate Immunity*

Briefly, the Innate immune system is a non-specific pathogen detection system that is always present. It is the first line of defence which responds within hours to a threat. It includes physical barriers (skin), immune cells such as NK cells, monocytes, macrophages and DCs, and processes such as phagocytosis and inflammation (148). Antigen presenting cells (APCs) such as DCs and macrophages bridge the gap between the innate and the adaptive immune system. Foreign material is processed by these APCs and the peptides are presented to the adaptive immune system. Foreign material degraded by the lysosome is presented on major histocompatibility complex (MHC) class II molecules to CD4+ T cells whereas peptides produced from proteasomal degradation are then presented on MHC class I molecules to CD8+ T cells (149). HCMV infection results in the reduction of MHC-I cell surface expression. The gene products of US2, US3, US6, US8, US10 and US11 all act to prevent MHC-I cell surface presentation allowing escape from CD8+ T cell lysis. The UL18 MHC-I homologue is not affected by the expression of these viral genes and so acts as an inhibitory ligand for NK cells (150).

Another component of the innate immune system is Complement. Complement is an immunological defence consisting of > 20 distinct plasma proteins that react with each other upon activation in a sequential reaction which can result in the formation of the membrane attack complex (MAC), opsonisation of the pathogen, direct killing of the

pathogen and inflammatory cell recruitment. Virus and virally infected cells can be eliminated through antibody-activated complement-mediated virolysis and cytolysis respectively (reviewed in (151)). Complement can be activated in three ways: the classical pathway, which is triggered by antigen-antibody immune complexes or even direct binding of one of the plasma proteins C1q to the surface of the pathogen; the Lectin pathway which is initiated by mannose-binding lectins that binds carbohydrate ligands found on many microorganisms; and the alternative pathway, which is activated directly on pathogen surfaces but is also constitutively active at low levels (reviewed in (151)). The neutralising ability of human serum is enhanced 2-3 fold by complement in the presence of specific anti-CMV antibodies (152). HCMV infection has been shown to downregulate the complement receptors CR3 and CR4 affecting the complement cascade (153). HCMV virions have also found to incorporate the complement regulatory proteins CD55, CD59 and CD46 which could represent another way that HCMV evades the host immune response (152).

The receptors of innate immunity are called Pattern Recognition Receptors (PRRs) which are germline-encoded host sensors that bind to conserved molecular signatures that are shared by groups of pathogens. PRRs are expressed mainly on cells of the innate immune system and can respond to cellular proteins or DNA as a result of damage, microbial or viral proteins and nucleic acids (154). These are referred to as pathogen-, microbe- or damage-associated molecular patterns (PAMPs/MAMPs/DAMPs). PRRs have several classes including nucleotide-binding oligomerization domain (NOD)-like receptors (NLRs), Toll-like receptors (TLRs) and RIG-I-like receptors (RLR) and once activated can induce downstream inflammatory signalling leading to the production of inflammatory cytokines and activation of the interferon pathway (148, 154).

In both the immunocompetent and the immunocompromised, HCMV induces inflammatory cytokine production and the Interferon (IFN) pathway. These innate immune responses can be activated through the interaction of viral envelope glycoproteins with host cell attachment and entry receptors as well as TLRs. Inflammatory cytokine release can be triggered by gB or gH binding TLR2. In fact, it was proposed that a TLR2/TLR1 heterodimer functions as a sensor for the virus (155). This rapid innate immune detection of HCMV may provide the host cell a temporal

advantage; the induction of an immune response prior to the virus becoming transcriptionally active. TLR signalling leads to the production of IFN-alpha/beta by macrophages and DCs which in turn activate NK cells (5).

NK cells are a critical part of the innate immune response to HCMV; individuals with genetic defects in their NK-cell response are exceptionally vulnerable to HCMV disease. NK cells are vital in host-rejection of virally infected cells. NK cells receive both activating and inhibitory signals from a wide array of cell surface receptors. The ratio of these inhibitory to stimulating signals is what directs the NK cell to kill the target cell or not (156). In addition to direct killing of HCMV-infected cells by NK cells, viral replication may be restricted due to NK cell release of IFN-gamma. NK cells also stimulate NF- $\kappa$ B-dependent IFN-beta production from infected cells *in vitro* (157). Several HCMV genes function as NK-cell evasion genes: UL16, UL18, UL40, miR112, UL135, UL141, UL142, UL148, US18 and US20. These characterised evasion genes act by a variety of mechanisms that are informing us on how human NK cell function, namely: direct stimulation of an inhibitory receptor (the MHC class I homologue UL18), rescue expression of an endogenous inhibitor (UL40 donates a peptide that stabilises HLA-E), inhibition formation of the immunological synapse (UL135) and downregulation of activating ligands (e.g. UL16, miR-UL112, UL141, US18, US20) or an adhesion molecule (UL148) (158-160).

### *Adaptive immunity*

The adaptive immune response takes longer to initiate and take effect but can provide a more robust response due to its pathogen-specificity and can also lead to the development of immunological memory that provides a faster response to subsequent repeat infections. The adaptive immune system comprises of T cells and B cells and can be divided into two broad classes of responses; cellular and humoral responses respectively both of which are involved in the HCMV adaptive immune response (161).

The adaptive cellular immune response to HCMV is dominated by T cells with HCMV disease occurring almost exclusively, with the exception of congenital disease, in cellular immunodeficient individuals (5). T cells can be classified into different subsets; cytotoxic T cells (CD8+ T cells), T helper cells (CD4+ T cells), regulatory T cells (TRegs, a CD4+ T cell subset), natural killer T (NKT) cells and  $\gamma\delta$  T cells. T cells function to restrict viral

replication, but do not eliminate the virus nor prevent transmission. They do this by binding and reacting through their T cell receptor (TCR) to foreign antigens that are presented to them by APCs on MHC molecules, however this process is more complex as additional signals are needed for T cell activation (162). Activation of CD4+ T cells results in enhanced antibody responses and production from B cells whereas CD8+ T cells once activated result in the development of cell-mediated immune mechanisms such as the lysing of HCMV-infected cells through the use of perforin and granzyme B (161). An astounding 10-25 % of all peripheral CD8+ T cells can be specific for HCMV (5, 163). CD8+ T cells also take on a protective role against latent virus reactivation by targeting both immediate-early genes and early genes. However, the most commonly targeted antigens of these cells are pp65 as well as IE-1. Pp65, although expressed late is found in the viral tegument and so is presented to APCs immediately upon initial infection of the cell (163).

Around 9% of all periphery CD4+ T cells are HCMV specific and recognise at least 59% of HCMV ORFs. CD4+ T cells also target pp65 along with other HCMV antigens such as gB, pp28, and IE-2. The importance of CD4+ T cells is apparent in transplant patients. HCMV-specific CD4+ T cell low lung transplant recipients experienced difficulty clearing infection and increased frequency of viral reactivation (164). CD4+ T cells are said to be necessary for memory T cell induction, replication, and preservation.

B cells are fundamental to the humoral immune response. B cells express antibodies as a secreted form but also retain them bound to their membranes. Once differentiated, B cells become Plasma cells which secrete antibodies once activated. These antibodies can inactivate virus by obstructing their ability to bind cell surface receptors for entry, but also can mark them for destruction through ADCC or complement (161). Animal models show the importance of B cells in HCMV immunity. Neutralising antibodies are shown to protect mice from primary infection (165) and also restricting dissemination of reactivated of MCMV (166). Another study showed that adoptive transfer of memory B cells from immune mice to B cell and T cell immunodeficient mice was able to induce an IgG response, significantly reduce viral load and protect long term against the lethal course of infection after infection with MCMV (167). In fact, HCMV infection has been

shown to mobilise and induce the expansion of activated memory B cells (168). This shows the importance of B cells and the humoral immune response to HCMV.

HCMV-specific antibodies also play an important role in controlling HCMV dissemination and viral load. HCMV antibodies are detectable in human serum 2-4 weeks after primary infection. These antibodies are raised to an array of viral proteins, including tegument proteins pp65 and pp150, transcriptional protein IE-1 and viral glycoproteins (163, 169). In fact, gB, the gH-gL-gO complex, and the gM-gN complex, are all major antigens for neutralizing antibodies (169-171) however the majority of neutralising activity stems from antibodies directed against the pentamer (172). The genes RL11, RL12, RL13 and UL118-UL119 encode Fc binding proteins that are thought to circumvent the humoral immune response through protecting against antibody-dependent cellular cytotoxicity (ADCC) (86, 173, 174).



## **1.6 The Genetics of HCMV**

In HCMV research the terms clinical and laboratory strains are used frequently. Clinical HCMV is a term that is widely used to mean several different things. In this thesis Clinical refers to strains either found circulating within patients or isolates that have been passaged only minimally, whereas laboratory strains are considered to be passaged extensively in cell culture and usually adapted to fibroblasts.

### **1.6.1 Genome Organisation and Coding Potential**

The HCMV genome is the largest (~236 kbp) of all human herpesviruses (37, 175). The class E HCMV genome consists of unique short (US) and unique long (UL) segments flanked by internal (IRL and IRS) and terminal (TRL and TRS) inverted repeating segments (11), and at each terminus of the linear genome are 3'-unpaired nucleotide overhangs (176). The inverted repeat sequences contain cis-acting signals (pac1 and pac2) which are essential for genome cleavage and encapsidation (119) but also promote genome isomerisation by sequence inversion (176). This potential for genome isomerisation yields four genomic isomers in equal amounts (11).

Originally, based on the sequencing of a highly passaged laboratory strain, AD169, it was originally predicted that HCMV possessed 189 protein coding open reading frames (ORFs) (177). However, many of these ORFs were later discounted due to the fact that they were unlikely to encode functional proteins and further ORFs that were missed in the first genome analysis were added after comparative genome analysis of the closest relative of HCMV, CCMV (178). Since then, the low-passage strain Merlin has been analysed and 165 functional protein coding genes have been mapped (175). However, a study using ribosome profiling and transcript analysis of Merlin infected fibroblasts identified 751 potentially protein-coding ORFs, 604 of which were previously unidentified. Many of the ORFs were very short (<20 codons) and found upstream of longer ORFs, and could possibly be non-functional polypeptides that are rapidly degraded (179). Yet, a recent study could only identify stable expression of 4 of these 604 non-canonical ORFs (180). Current estimates of the coding potential of HCMV are 170 canonical protein coding ORFs, 4 abundantly produced long non-coding RNAs (RNA2.7, RNA1.2, RNA4.9, and RNA5.0), at least 23 microRNAs of which some regulate

cellular gene expression and 2 oriLyt RNA (1, 181-186). The origin of lytic replication (oriLyt) is conserved for betaherpesviruses and is found between UL57 and UL69. The core genes, found in the central portion of the U<sub>L</sub> region, are also conserved between herpesviruses and are mostly essential for viral replication. The vast majority of the remaining genes are non-essential for lytic replication and instead have functions such as immune evasion and tropism. Many of these genes are grouped into the 15 multigene families found to cluster together in the extremities of the U<sub>L</sub> and U<sub>S</sub> regions of the HCMV genome (175, 177, 178)

Although some genes also have names describing their function, conventionally HCMV gene nomenclature is determined by the position of the gene within the genome (37). As seen in figure 6, the genes UL148-UL133 which make up the U<sub>L</sub>/b' sequence are inverted in reference to the rest of the genome. The U<sub>L</sub>/b' sequence was first characterised in the strain Toledo. Due to genetic rearrangement in early passage, the U<sub>L</sub>/b' sequence of Toledo is in an inverted orientation relative to other strains (187).

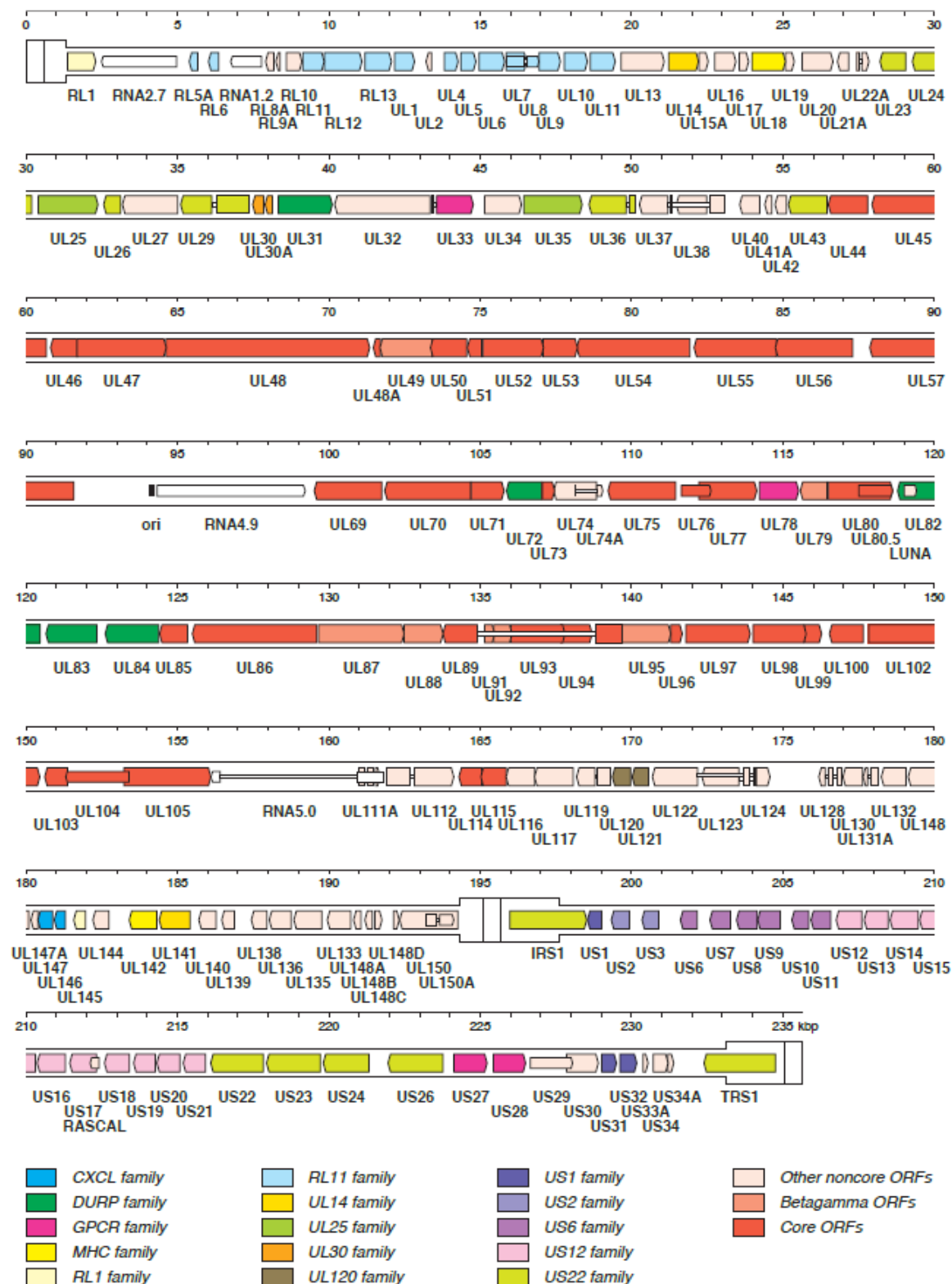


Figure 6 - The genome organisation of WT HCMV (Merlin). Reproduced from (1). The genome organisation can be seen as TRL-UL-IRL-IRS-US-TRS. Protein coding regions are depicted as arrows with the repeated regions shown as broader arrows compared to unique regions. The gene families are colour coded with herpesvirus core genes shown as red and introns as narrow white bars.

### **1.6.2 Natural Genetic Variation Between Strains**

In *in vivo* infections it is commonly accepted that multiple strains circulate within the population and so an individual can be infected with multiple strains. Whilst natural selection gives rise to genetic diversity, inter-strain recombination can contribute (188, 189). Sequence comparisons of whole HCMV genomes has identified a subset of genes that display a high level of variability: RL6, RL12, RL13, US9, US28, UL4, UL11, UL18, UL37, UL55 (gB), UL73 (gN), UL75 (gN), UL74 (gO), UL139, UL144, UL146 and UL115 (gL) (175, 190-192). The UL55 gene encodes the glycoprotein gB and was one of the first examples of natural sequence variation in clinical and laboratory HCMV strains (189).

In a high-throughput analysis of clinical isolate genomes 15% of genes were found to have a mutated ORF in at least one clinical HCMV isolate, and only 23% of the isolate's sequences had the full set of intact HCMV genes. Thus, only approximately one quarter of clinical isolates can be considered genetically intact (3). Sequence variability in ORFs creates distinct genotypes and depending on the ORF the consensus nucleotide sequences can vary by up to 50% or even more between genotypes (190).

### **1.6.3 Mutations Associated with Adaptation to Cell Culture**

Propagation of HCMV *in vitro* is associated with the accumulation of mutations during serial passaging and adaptation to cell culture. As a result, this eliminates the broad tropism seen in the clinical virus but allows for efficient viral replication in fibroblasts and the production of high titre (reaching  $10^7$  pfu/mL) cell-free virus for experimentation (193). Since its discovery and isolation, many laboratory-adapted strains have been used in HCMV research. The most widely used and distributed laboratory adapted strains include Towne (61) and AD169 (19). These strains have been invaluable tools over years of research and served as candidate vaccines. Due to extensive and serial cell culture passaging of the strains, both have undergone substantial genetic alterations resulting in the loss of virulence (193). Large deletions in the  $U_L/b'$  region have been acquired resulting in a 15 kbp loss in AD169 and a 13 kbp loss in Towne (178, 194, 195). The  $U_L/b'$  region (UL148-UL133) contains many genes with the potential to contribute to the virus's virulence in many ways. Found within the  $U_L/b'$  region, the gene UL46 encodes a

viral CXCL chemokine (196), UL144 encodes a tumour necrosis factor receptor homolog (197), and UL142 encodes an MHC class I-like molecule that inhibits NK cell lysis (198).

One region that is commonly affected in many laboratory strains is the UL128L which results in restricted tropism. The strain Toledo is considered to be low passage, however the gene UL128 is disrupted by a substantial sequence inversion. Many other laboratory strains including AD169, TB40F and Towne have acquired mutations in at least one of the three genes in the UL128L resulting in a virus that only expresses the trimeric complex (see section 1.3.1.3)(175, 178, 187, 199-202). Much research to date has been performed using human fibroblasts, despite the virus's wide tropism *in vivo*, and so using these laboratory strains with restricted tropism is not problematic (138). Another ORF commonly affected by adaptation to cell culture is the RL13 ORF and is usually one of the first mutations observed when passaging clinical virus in cell culture. A mutation in RL13 results in more efficient *in vitro* viral growth in fibroblasts (193, 203).

As well as mutations that plague laboratory adapted strains, the presence of multiple variants within and between stocks can also be a challenge for HCMV research. It has become apparent that laboratory adapted strains that are in common use worldwide differ markedly from one another despite originating from the same stock (194, 195, 204). Inter-strain variation is also reported within stocks. The Towne strain (VR977) distributed by the American Type Culture Collection (ATCC) was shown by sequence analysis to contain two variants, one containing an inverted duplication of part of the left extremity of the genome replacing the  $U_L/b'$  region (varS), and the other containing an intact  $U_L/b'$  region (varL) (194, 205).

## 1.7 Current Methods in HCMV Research

In order for HCMV research to be relevant, it is vital we can work with a virus *in vitro* that is an accurate representation of the virus found in clinical samples. Adaptive mutations observed in passaging laboratory strains *in vitro* are mainly associated with the gene RL13 and the UL128L (193). Genome stability was an issue for *in vitro* research until the cloning of low-passage strains into bacterial artificial chromosomes (BAC) such as FIX, TR, TB40/E and TB40-BAC4 (206, 207). These BACs however were created from stocks that had not been sequenced prior to their creation and therefore run the risk that they harbour mutations from the initial passaging, potentially affecting viral biology (208). For example, substitution mutations have been found in the UL128L of TB40-BAC4 and FIX, which reduced (but did not eliminate) the efficiency of epithelial cell infection (208). The RL13 ORF in most HCMV BACs is mutated by deletions, substitutions or frameshifts resulting in the introduction of premature stop codons (175).

Merlin was the first full length HCMV genome to be cloned into a BAC, it was developed to provide a genetically intact source of clinical HCMV and has been designated as the first World Health Organization reference sequence for HCMV. Merlin was BAC cloned after minimal passage (p5) in fibroblasts. Genome comparison of the BAC with the clinical isolate revealed mutations in the UL128L and RL13. Repair of these genes drastically impeded the virus's *in vitro* growth properties and limited cell-free virus secretion (203). As a result of expression of these 2 genes, clinical HCMV is heavily cell-associated (103, 104).

### 1.7.1 Viral Propagation *in vitro*

To address the issue of rapidly arising mutations, a system has been developed to work with Merlin *in vitro* that provides for conditional expression of RL13 and UL128 (203). Transcription of the two unstable genes, RL13 and UL128, is repressed by inserting a Tet-operator upstream of the gene promoters. This strain Merlin variant is propagated in a special cell-line expressing a Tet-repressor to allow for viral growth without expression of RL13 or UL128, and thus without selection of mutants (203). Using this construct, it is now possible to study genetically intact, phenotypically wild type HCMV by simply

infecting cells that lack the Tet repressor. More specifically, it allows the function of RL13 to be investigated in the context of a productive HCMV infection.

## **1.8 RL13**

RL13 encodes a highly glycosylated type 1 transmembrane protein (203) expressed in the late expression phase (209, 210). As gpRL13 is expressed on the virion envelope it therefore has the potential to modulate tropism (203). RL13 is conserved *in vivo*, suggesting that the gene is essential for the survival of HCMV *in vivo* even though it suppresses *in vitro* propagation (37, 193).

### **1.8.1 The RL11 Family**

RL13 is a member of the RL11 gene family which all encode a characteristic domain termed RL11D. The RL11 gene family has 14 members located at the left terminus of the genome. Eleven of the members are conserved in HCMV as well as CCMV (RL11, RL12, RL13, UL4, UL5, UL6, UL7, UL8, UL9, UL10, and UL11), and the remaining three are HCMV-specific (UL1, RL5A, and RL6) which are thought to have originated in the last 6-5 million years when the CMV species separated through gene duplication (177, 191, 211). The RL11 family consists of genes that are nonessential for viral growth (98) and among the most variable HCMV genes (175, 212). In fact, RL5A and UL9 along with RL13 are part of a restricted group of HCMV hypervariable genes (175).

Many of the genes in the RL11 family are predicted to encode membrane glycoproteins and function in viral entry. RL13 and UL10 are termed temperance genes that repress viral replication on a cell type-specific basis (see section 1.5.2) (84, 203). Similarly to gpRL13, gpUL4 and gpUL1 were found to be incorporated into the virion envelope (203, 213, 214).

### **1.8.2 Limitations of Working with Functional RL13**

*In vitro* propagation of HCMV clinical isolates is consistently inefficient until mutations are selected, generally growing through first for RL13 and subsequently in the UL128L (193, 203). During creation of the Merlin BAC the mutations observed in RL13 was a single adenine insertion causing a frameshift at nucleotide 11363 (Accession number NC\_006273.2). When an additional 10 BAC clones from the same series of experiment were sequenced, each Merlin BAC had acquired RL13 disruptive mutations predicted to result in a truncated protein, but not all mutations were identical (203). Research into



the function of RL13 now will use a natural truncated RL13 mutant Merlin BAC ( $\Delta$ RL13) as well as the WT Merlin BAC (WT) which was repaired by the deletion of the additional nucleotide (Fig. 7).

Since RL13 and the UL128 ORF are conditionally repressed, propagation of virus is performed utilising the Tet-repression system which allows for genetic preservation of the ORFs. However, in order for research to be performed the full genetic content of Merlin needs to be expressed and so experimentation is performed in a non-Tet-repressing cell line allowing for the production of virions containing the wildtype HCMV protein content.

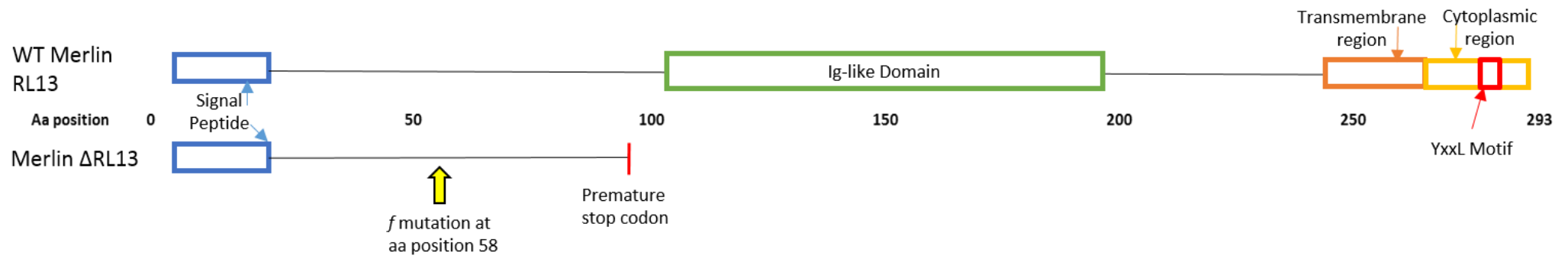
### **1.8.3 Rh13.1 – an RL13 Homolog**

Sequence alignments of CMVs determined that the closest evolutionary relative to HCMV is Chimpanzee CMV (CCMV), followed by Rhesus CMV (RhCMV) and green monkey cytomegalovirus (GMCMV) (1) (see figure 1).

The RL11 family is dispensable for viral growth and in fact Rat and Mouse CMVs lack the RL11 family (215). Although MCMV lacks the RL11 family it does possess the m138 gene that encodes a Fc receptor for murine IgG (216), and so it is possible that some of the immunological advantages of the RL11 family are replicated by genes elsewhere in the murine and rat CMV genomes. The lack of mouse or rat models does not make *in vivo* experimentation with this gene family easy and so the closest model available that has homologues to members of the RL11 gene family is with CMVs that infect nonhuman primate species such as rhesus CMV (RhCMV) (217). Sequences of different RhCMV strains have been fully sequenced and published and the strain RhCMV strain 68-1 is available as a BAC (218). Unlike HCMV, RhCMV has a class F genome with no identified terminal repeat sequences. Due to this, the RhCMV genome lacks the potential to isomerise (11). The prototypical wild-type RhCMV genome is slightly larger than HCMV and contains 135 ORFs homologous to known HCMV proteins (217).

Similarly to HCMV, RhCMV was found to acquire and select for multiple mutations including in Rh13.1 during adaptation to fibroblasts. The mutation resulted in a premature stop codon, which resulted in a protein sequence almost a third of the WT sequence length. Once repaired, the RhCMV 68-1 BAC encoded a gene with striking

homology to HCMV RL13 in both sequence and length (218). Despite this homology, the RhCMV RL11 gene family has diverged substantially from HCMV (218).



*Figure 7 – Schematic representation of the WT Merlin RL13 and the truncated RL13 sequence in Merlin  $\Delta$ RL13/ $\Delta$ UL128 and  $\Delta$ RL13. An extra Adenine at nucleotide position 11363 results in a frameshift mutation at aa position 58. This frameshift mutation causes a premature truncation of the protein (95aa long) leaving a protein roughly a third of the size of the wild type.*

## 1.9 Thesis Aims

RL13 expression is strongly inhibitory to viral replication in cell culture with sequence analysis detecting disruptive mutations in RL13 rapidly upon viral propagation in fibroblasts (203). Yet RL13 is clearly retained in many clinical isolates suggesting that RL13 is necessary for the success of the virus in the human host.

The vast majority of laboratory based HCMV research has been performed using RL13 mutant viruses. RL13 is not only conserved in clinical isolates but is a viral envelope glycoprotein that has the potential to modulate tropism and/or immune responses.

As UL128L mutations have also been shown to restrict efficient viral growth in cell culture (203), this project will utilise a Merlin BAC RL13 mutant ( $\Delta$ RL13), UL128 mutant ( $\Delta$ UL128), a double mutant ( $\Delta$ RL13/  $\Delta$ UL128) and the WT Merlin BAC.

The aims of this thesis are to explore the function of RL13 by investigating its effect on the efficiency of viral infection at the different stages of the viral lifecycle. We will also attempt to identify how and why RL13 inhibits virus growth so drastically *in vitro* through genetic and growth analysis of HCMV variants alongside the Merlin BACs, and through analysis of the effects of RL13 on the virion and viral infection. To determine what advantage RL13 provides the virus we will explore the effects of RL13 expression on the virus, the host cell and host immune system. A minor aim of this thesis will be to generate novel reporter viruses to assist in this and future projects.

Determining the function of RL13 could assist in the development of systems for the propagation of a virus containing the complete intact HCMV genome which could in turn would greatly facilitate HCMV research.

## **CHAPTER 2. MATERIALS AND METHODS**

## 2.1 Reagents

### 2.1.1 Buffers and Solutions

All solutions, buffers and media were prepared with double-distilled ultra-pure water (ddH<sub>2</sub>O) delivered from a Purelab Ultra water system.

*Table 2 – Buffers and solutions.*

Wash Buffer (PBS-Tween20)	Phosphate Buffered Saline (PBS), 0.05 % (v/v) Tween20 (Merck, 9005-64-5)
TE buffer (pH 8.0)	10 mM Tris, 1 mM EDTA in ddH <sub>2</sub> O
6x DNA loading buffer	ddH <sub>2</sub> O, 10 mM Tris-HCl, 0.03% bromophenol blue, 60% glycerol, 60 mM EDTA
1x TAE	50x TAE buffer (National Diagnostics, EC-872) diluted in ddH <sub>2</sub> O 1:50
Fluorescence activated cell sorting (FACS) buffer	PBS containing 1 % (v/v) Foetal bovine serum (FBS) (Gibco, Life technologies, 10500) and 2 mM EDTA
4% Paraformaldehyde (PFA)	4% (w/v) paraformaldehyde (Acros Organics) dissolved in PBS.
NaPh buffer	0.0076 M sodium di-hydrogen phosphate, 0.0324 M disodium hydrogen phosphate, in ddH <sub>2</sub> O
Gradient 'Light' solution	NaPh buffer, 15% (w/w) sodium tartrate, 30% (w/w) glycerol
Gradient 'Heavy' solution	NaPh buffer, 35% (w/w) sodium tartrate
PBST	0.1% (v/v) Tween20 (Merck, 9005-64-5) dissolved in PBS
Immunoblotting block/stain buffer	PBST with either 5% (w/v) fat-free milk proteins (dry milk powder) or 5% (w/v) BSA (Sigma-Aldrich, A7906)
Transfer buffer	10% (v/v) NuPage transfer buffer (20X, Novel, life technologies, NP0006-1), 10% (v/v) methanol, 400ml ddH <sub>2</sub> O
Reducing buffer	10% DTT (Sigma), 25% NU-Page buffer (Life technologies), 65% ddH <sub>2</sub> O
Running buffer	50ml 20X NuPage MOPS SDS running buffer (Invitrogen, 1936381) in 1L ddH <sub>2</sub> O
Stripping buffer	Restore stripping buffer (Thermo, 21063)

### 2.1.2 Bacterial Culture Media and Reagents

All bacterial culture reagents and analytical grade chemicals were sourced from either Sigma or ThermoFisher unless otherwise stated. Autoclaving was used to sterilise all bacterial culture media which was allowed to cool to around 50°C prior to the addition of antibiotics and/or supplements.

*Table 3 - Bacterial culture media and reagents*

Luria-Bertani (LB) broth	2% (w/v) LB powder (Melford Biolaboratories Ltd, L1703) in ddH <sub>2</sub> O
LB Agar	LB broth, 15% (w/v) agar.
LB Agar + Sucrose	ddH <sub>2</sub> O, 1% (w/v) tryptone, 0.5% (w/v) yeast extract, 15% (w/v) agar, 5% (w/v) sucrose

*Table 4 - Bacterial culture media supplements*

Antibiotic or Chemical	Stock concentration	Dilution
Chloramphenicol	12.5 mg/mL chloramphenicol (Doehringer), in 100% ethanol	1:1000
Ampicillin	100 mg/mL Ampicillin (Duchefa Biochemie) in ddH <sub>2</sub> O, 0.22 µm filter sterilised	1:2000
Kanamycin	15mg/ml Kanamycin monosulphate (Melford) in ddH <sub>2</sub> O, 0.22 µm filter sterilised	1:1000
Streptomycin	200 mg/ml Streptomycin sulphate (Melford) in ddH <sub>2</sub> O, 0.22 µm filter sterilised	1:500
Isopropyl β-D-1-thiogalactopyranoside (IPTG) stock	100 mM IPTG (Melford), in ddH <sub>2</sub> O	1:500
5-bromo-4-chloro-indolyl-β-D-galactopyranoside (X-gal)	40 mg/mL X-gal (Melford) in Dimethyl sulfoxide (DMSO) (Sigma-Aldrich, 41647)	1:500

### 2.1.3 Tissue Culture Media and Reagents

All tissue culture media was sourced from Gibco or Invitrogen/Life Technologies unless otherwise stated.

*Table 5 - Tissue culture media and reagents*

DMEM 10%	Dulbecco's Modified Eagle Medium (DMEM, Sigma, D5796), 5% (v/v) Penicillin and streptomycin, 10% (v/v) FBS
DMEM 0%	DMEM, 5% (v/v) Penicillin/Streptomycin sulphate (pen/strep, Gibco, Life technologies, 15070-063), 0% (v/v) FBS
2X DMEM	50% (v/v) ddH <sub>2</sub> O, 20% (v/v) 10X MEM (Life Technologies), 20% (v/v) FBS, 6% (v/v) sodium bicarbonate (Life Technologies), 1000 U.L <sup>-1</sup> penicillin (Life Technologies), 1000 µg.L <sup>-1</sup> streptomycin (Life Technologies), 4 mM L <sup>-1</sup> glutamine (Life Technologies)
Freezing Medium	90% (v/v) FBS and 10 % (v/v) DMSO
RPMI 10%	RPMI-1640 (Life Technologies) 10% (v/v) FBS



## 2.2 Cell Culture

Table 6 - Cell lines used

Name	Organism	Cell type	Immortalised	Notes
HFFF Tert	Human	Fibroblast	Yes	Immortalised by constitutive expression of telomerase
HFFF Tet	Human	Fibroblast	Yes	tetracycline repressor expressing HF Terts used for growing up viral stocks
Primary HF	Human	Foetal Foreskin Fibroblasts	No	Obtained from Frank Graham (Porton Down).
ARPE19	Human	Adult Retinal pigment epithelials	Yes	ATCC #: CRL-2302
CARs	Human	fibroblast	Yes	HFFF Tert overexpressing CAR receptor

### 2.2.2 Cell Culture

All tissue culture work was performed with aseptic techniques in a Class II biological safety cabinet. The inside of the Class II biological safety cabinet and all equipment and reagent bottles to go inside were sprayed with a solution of 70% (v/v) IMS before any work commenced. Any tissue culture reagents to be used were first warmed to 37°C in a water bath.

#### *Cell Maintenance*

All cells were incubated at standard tissue culture conditions: 37°C at 5% CO<sub>2</sub>. Cells were propagated in DMEM 10% unless otherwise stated. Cells were passaged when confluency reached 90-100%, the monolayer was first washed with PBS. Cells were then dissociated from the flask by adding 0.05% Trypsin/EDTA (x1, Thermo Fisher, 25300-054) for 3 min in a rocking incubator at 37°C. Monolayers could be disrupted by gentle tapping of the flask before the addition of DMEM 10% to neutralise residual trypsin. Once harvested the cells were either used for experiments or for sub-culturing by splitting 1:4 – 1:6 depending on cell type every 3-4 days.

#### *Cell Counting*

Cells were counted prior to plating using disposable counting chambers (Sigma, Z35962). Once cells were harvested as previously described, the cell suspension was pipetted to

ensure a single cell suspension, before 10  $\mu$ l was loaded into a counting chamber. At least four grids within the counting chamber were counted to give an average cells/ml. The average cells/ml could be calculated by multiplying the average cell count by a factor of  $10^4$ . The appropriate number of cells were either plated in DMEM 10% or centrifuged at 1500rpm for 3 min to eliminate any FBS if to be plated in DMEM 0%.

#### *Long Term Storage and Recovery of Cells*

Cells were grown to confluency, washed with PBS and harvested with the addition of 0.05% trypsin-EDTA as previously described. The cell suspension was then pelleted at 1500rpm for 3 min, supernatant discarded and resuspended in an appropriate volume of freezing medium. Cells were aliquoted into 1.5 mL cryovials (ThermoFisher Scientific) and stored at  $-196^{\circ}\text{C}$  in liquid nitrogen. Cells were initially cooled at a rate of  $-1^{\circ}\text{C}$  per min using an isopropanol-based freezing vessel (Nalgene) to  $-80^{\circ}\text{C}$  before transfer to liquid nitrogen. When recovering cells, vials were retrieved from liquid nitrogen and immediately put on dry ice. Vials were then transferred to a  $37^{\circ}\text{C}$  water bath to ensure rapid defrosting. After 3-5min thawing, cells were transferred to an appropriately sized flask in DMEM 10% and incubated for 24 hr. Cells were monitored by phase-contrast microscopy after 24 hr and DMEM 10% replaced if necessary.

### **2.2.2 Peripheral Blood Monocyte cell culture**

Blood collection was approved by the school of medicine research ethics committee under the project 'The Pathogenesis of Human Cytomegalovirus, ref 16/52'. Seropositivity of cell samples were determined using a CMV IgG ELISA as per manufacturers guideline (Sigma, SE120034).

#### *Isolation of PBMC from Whole Blood*

50 ml of donor blood was collected with heparin (1  $\mu$ l/ml blood). Peripheral blood monocyte cells (PBMCs) were isolated by layering 2/3 human blood on top of 1/3 Histopaque (Sigma) and centrifuged at 2000 rpm for 20 min without using a brake in a Beckman coulter centrifuge. PBMCs were extracted from the interface between the plasma and Histopaque, then washed with PBS three times, first by centrifugation at 2000 rpm for 7 min and then centrifugation at 1000 rpm for 5 min twice.

### *Monocyte Differentiation*

Monocytes were isolated from PBMCs by magnetic separation with CD14 microbeads (Miltenyi). This was checked by staining with anti-human CD14 antibody. Monocytes were then differentiated into Dendritic cells (DCs) and Langerhans cells (LCs) by incubating in RPMI 10% in non-treated tissue culture dishes (Corning Costar, Sigma, CLS3738-100EA) with the appropriate cytokines (DCs: IL-4 100ng/ml and GM-CSF 100ng/ml every 2 days. LCs: GM-CSF 100ng/ml and TGF- $\beta$ 1 20ng/ml every 2 days and IL-4 10ng/ml for the first 2 days only.) DCs and LCs, were phenotyped by Flow cytometry using a BD Accuri C6 cytometer to check for correct differentiation (see table 6). Correct differentiation was assumed when DCs presented as CD1a +ve, DC-SIGN +ve, CD14 low and LCs presented as CD1a +ve, DC-SIGN +ve, CD14 low, Langerin +ve.

*Table 7 – Antibodies used to check for correct differentiation*

Immunogen	Company	Catalogue number	Dilution	Conjugate
CD14 (clone 61D3)	eBioscience Dx	9025-0149-120	1:50	Pe/Cy 7
CD1a	BD Pharmingen	555806	1:50	FITC
DC Sign	BD Pharmingen	551265	1:50	PE
Langerin (CD207)	Miltenyi Biotec	130-098-364	1:50	APC

### *Non-adherent Cell Culture*

Non-adherent cells including PBMCs, DCs and LCs were cultured in upright T25s (25 cm<sup>2</sup>, Corning, Sigma-Aldrich, 430639) at standard tissue culture conditions. Cell culture medium for non-adherent cells consisted of RPMI 10% with the addition of IFN $\alpha$  when required at 1:6000.

## **2.3 Viruses and Infections**

With the exception of TB40/E kindly supplied from Jay Nelson (OHSU, Portland Oregon, USA), and Rhesus CMV kindly supplied from Klaus Früh (OHSU, Portland Oregon, USA), all viruses used were HCMV strain Merlin and were either provided by or generated from HCMV provided by Dr Richard Stanton (203). All Merlin virus had either mutated or wildtype RL13 and/or UL128L. Tet-operators were located upstream of the wildtype ORFs to prevent acquired mutations during viral propagation under conditional expression (219). GFP variants of these viruses were also used, some containing a P2A self-cleaving peptide upstream of an eGFP ORF to increase efficiency of GFP expression. Viruses used can be found in Results chapter 3.

### **2.3.1 Generation of HCMV Stocks**

Viral stocks were either grown up from existing stocks or transfected from viral BAC DNA. When growing virus from existing stocks, ten T150s (150 cm<sup>2</sup>, Corning, Sigma-Aldrich, 430825) of HFFF Tets were grown to 75-90% confluency and then infected at a multiplicity of infection (MOI) of 0.03. When transfecting, 2ug of viral BAC DNA (generated from section 2.4.6.7) was transfected into HFFF using the AMAXA nucleofactor kit to the manufacturer's guidelines (Amaya Biosystems, Lonza). The transfected cells were then seeded in a T25 in DMEM 10% and once viral plaques appeared cells were trypsinised and reseeded to encourage viral spread. When the entire T25 monolayer was infected, bleeds were taken and frozen down at -80C. One bleed would usually be sufficient to infect ten T150s. The T150s were fed until the monolayer was sufficiently infected and CPE visible for 75-95% of cells. Bleeds were taken every two days and frozen at -80C until the monolayer was exhausted. Once finished, all bleeds were defrosted quickly at 37°C in a water bath before centrifugation at 1500rpm for 3 min to remove cells. Once pooled, the bleeds were centrifuged in a Beckman coulter Highspeed centrifuge at 14000rpm for 2 hr at 21°C. Once the supernatant was discarded the pellets were resuspended in a total volume of 6-8 ml 10% DMEM, aspirated with a 25-gauge needle to break up aggregates, and aliquoted as 300ul aliquots.

### 2.3.2 Quantification of HCMV Infectivity

Infectivity or titration of viral stocks and experimental supernatants were quantified by either plaque assay or by IE1 titration assay (both outlined below). Both methods were performed in HF Primary cells and viruses were diluted in a 10-fold dilution series. The dilution range was chosen per sample so that a predicted quantifiable number of plaques/infected cells could be easily counted per well. After plaques or infected cells were counted, titrations were calculated and expressed as total plaque forming units per mL (PFU mL<sup>-1</sup>). The following calculation was used to calculate PFU mL<sup>-1</sup>:

$$\text{Plaques/infected cells (in 100 } \mu\text{L)} \times 10 \times \text{dilution factor}$$

#### *Plaque Assay*

Primary HFs were seeded into a 6 well plate in DMEM 10% 24 hrs prior to infection. The virus to be titred was thawed quickly in a water bath at 37°C before a serial dilution added to cells in duplicate. Infections were performed under the conditions described below and after 2hr inoculum replaced with 1:1 2x DMEM and Avicel; sodium carboxymethylcellulose, microcrystalline cellulose mixture previously described by Matrosovich (220) which limits cell-free viral spread allowing for the accurate titre of viral stock to be calculated. After 10-21 days, depending on virus background and proximity of plaques, plaques were counted in the duplicate serial dilution condition which was most appropriate.

#### *Experimental Titration by IE1 Immuno-fluorescence*

Cells were seeded the day before in clear-bottomed 96-well plates, culture media was removed and 100 µl of appropriate serial dilutions of viral supernatant added directly to the wells in duplicate. After 24 hrs, viral supernatant was removed and the monolayer washed with PBS. Cells were fixed and permeabilised by incubation with 50 µl Acetone/Methanol at -20 °C for 15 mins. The Acetone/Methanol was removed and the monolayers washed with excess PBS three times, before incubation with IE1 primary antibody diluted in PBS for 1 hr at 37 °C in a rocking incubator. Primary antibody was removed, monolayers washed in excess PBS three times. Anti-Mouse IgG was used as a secondary antibody diluted in PBS and incubated with monolayers for 1 hr at 37°C in a rocking incubator. Secondary antibody was removed and the stained monolayers were

washed with PBS in excess three times. The Zeiss Fluorescent microscope was used as described in section 2.6.1 and Viral titre was calculated by counting fluorescently stained nuclei in the dilution that was most appropriate.

### **2.3.3 Infection of Cells with HCMV**

Standard tissue culture conditions were used when for all infections. Unless otherwise stated, cells were plated in DMEM 0% 24 hr before infections. Virus was added to cells with enough DMEM 0% to sufficiently cover cells whilst incubating on a rocking platform. After 2 hrs the inoculum was removed and replaced with fresh DMEM 0%. Infections were monitored 24 hr after by phase-contrast microscopy for cytopathic effects (CPE) and media changed and replaced with DMEM 10%.

### **2.3.4 Viral Timecourses**

Viral infections were set up as previously described in section 2.3.3 in a tissue culture plate (Thermo Fisher).

#### *Harvesting Cells from a Viral Timecourse*

One well would be harvested per day by addition of Trypsin-EDTA, so sufficient replicate wells for the duration of the timecourse had to be infected per sample. Cells would then be processed for DNA extraction or lysed for western blotting.

#### *Harvesting Supernatant from a Viral Timecourse*

When harvesting the supernatant, the same well/flask would be used each day and replaced with fresh DMEM 10%. The supernatant would then either be frozen at -80 °C or processed immediately for DNA extraction.

### **2.3.5 Isolation of DNA and Protein**

#### *DNA Extraction*

Samples were defrosted quickly at 37°C if necessary. Samples were first centrifuged to remove cellular debris. Samples were then DNase treated by the addition of 2% DNase buffer and 1% DNase (RQ1 RNase-free DNase, Promega) for 1 hr at 37°C until the reaction was stopped by the addition of 10% DNase Stop buffer (RQ1 RNase-free DNase, Promega) incubated at 65°C for 10 min. DNA was then extracted from samples

using a QIAamp MinElute Virus Spin Kit (Qiagen) as per manufacturers protocol and eluted as a volume of 100 µl Viral DNA.

### *Large Scale DNA Extraction from Supernatants*

Large quantities of viral DNA from supernatants were prepared a little differently with the following method. Supernatant samples were defrosted quickly in a 37°C water bath and centrifuged at 1500 rpm for 3 min to remove any cellular contamination. Samples were then centrifuged at 23,000 rpm for 1 hr at 21°C in a Beckman coulter Ultracentrifuge to pellet virions. Once pelleted the supernatant was discarded and the pellet resuspended in 500 µl ddH<sub>2</sub>O. The resuspended virions were then incubated with DNase as described previously in section 2.3.5.1. NP40 was then added to a final concentration of 1% to break open capsids and membranes and expose the viral DNA and samples were vortexed briefly. DNA was released from DNA binding proteins and histones by the addition of SDS to a final concentration of 0.5%. Samples were then incubated at 37°C overnight with 200ug/ml proteinase K. Equal volumes of phenol:chloroform:isoamylalcohol were then added and samples shaken gently to allow for the precipitation of proteins. Proteins were removed by the subsequent centrifugation of samples at 13,000 rpm for 5 min and the removal of the DNA layer found above the phenol and protein layers. This step is repeated with phenol:chloroform:isoamylalcohol again and then a third time using just chloroform:isoamylalcohol ensuring samples are mixed before centrifugation. DNA was then precipitated by the addition of 10% sodium acetate, 1 µl glycogen, and 250% absolute ethanol and kept at -20°C for 1 hr. DNA was then pelleted by centrifugation at 13,000 rpm for 30 mins at 4°C, washed in 70% ethanol and then centrifuged again. DNA pellets were left to air dry before resuspension in 10 mM Tris pH8.

### *Protein Extraction*

Cell samples were first washed with PBS before incubation with reducing buffer on a rocking incubator for 3 mins. Once samples were fully lysed, cell scrapers (Greiner Bio-one, 541 070) were used to ensure all sample had dissociated from the plate or flask before collection and storage at -20°C. Before loading for a western blot, samples needed boiling at 100°C for 10 mins to ensure complete reduction.

### **2.3.6 Purification of Virions**

Virions were purified on a Glycerol-Tartrate gradient which enabled the removal of NIEPs, Dense bodies and other cellular contamination.

#### *Sample Preparation and Concentration*

Once the timecourse was completed, samples were defrosted and all timepoints per sample pooled. The pooled samples were then centrifuged to remove contaminating cells at 1500 rpm for 3 min. Samples were concentrated by dialysis using VivaFlow50 ultra-filtration 1MDa cartridges (Sartorius) as per manufacturers protocol. The ultrafiltration was driven by a peristaltic pump and any particles smaller than 1MDa passed through the membrane and into the waste container. The ultrafiltration was stopped when the final volume of concentrated virus was less than 15 mL. 5 mL PBS was then flushed through the cartridge to recover virions remaining in the cassette.

#### *Preparation of Gradients*

Continuous gradients were formed using a SG50 gradient maker (Hoefer). By loading the Gradient 'Heavy' and 'Light' solutions into the two linked chambers the solutions were allowed to gradually mix before exiting the gradient maker through one single outlet tube. A peristaltic pump (Pump P1, Pharmacia Fine Chemicals) was used to draw the mixed solution through the tubing to an Ultra-clear centrifuge tube. The tubing was constantly manipulated to ensure careful formation of the gradient from the bottom of the centrifuge tube to the top. This allowed for the lower region of the gradient to be mostly 'heavy' solution up to the 'light' solution in the upper regions of the gradient.

#### *Isolating Virions*

Around 5 mL of concentrated virus was carefully loaded onto the top of the gradient. All gradients were balanced by the careful addition of PBS to the top of the sample if necessary, before ultra-centrifugation for 45 mins at 23,000 rpm. After centrifugation, clear bands could be found containing purified virions, NIEPS, cellular debris and dense bodies. The desired purified virion band was recovered by inserting a 20 G needle and syringe into the ultra-clear tube just below the band, angling the needle bevel upwards and taking the entire virion band. Recovered purified virions were then washed by dilution in excess NaPH buffer to remove gradient solution, and ultra-centrifuged at



23,000 rpm for 1 hr to pellet the virions. The virion pellet was resuspended in PBS and stored at -80 °C.

## **2.4 Molecular Biology Techniques**

### **2.4.1 In-silico Analysis and Oligonucleotide Design**

All primer and oligonucleotide design, sequencing analysis and HCMV genome comparisons were performed using CLC MAIN 6 software (CLC Bio). Melting temperature and other parameters of primers and oligonucleotide were determined using Oligo Explorer 1.2 (GeneLink) and Oligo Analyser (GeneLink) software packages. Primers were designed as to avoid secondary structures, self-annealing regions or primer-dimer formation. Melting temperature of forward and reverse primers were between 60-65°C and similar to each other. All primers were ordered from Eurofins MWG as lyophilized primers, which when received were reconstituted immediately with ddH<sub>2</sub>O to 100 µM and stored at -20°C. For all primer sequences see appendix 1.

### **2.4.2 Polymerase Chain Reaction (PCR)**

PCR reactions were set up as 50 µL reactions on ice in thin-walled RNase and DNase-free tubes (ELKay). Reactions consisted of 40 µL ddH<sub>2</sub>O, 5 µL HIFI buffer 2 (Expand High fidelity; HIFI, 11732641001, Roche), 1.5 µL DMSO, 1 µL of deoxynucleotides (dNTPs) (NEB), 1 µL of template DNA, 1 µM forward and reverse primers 0.5 µL of HIFI polymerase (HIFI, 11732641001, Roche). All PCR reactions included a negative control containing 1 µL ddH<sub>2</sub>O in place of DNA template. A T3000 Thermocycler (Biometra) was used with the following two programs (see tables 5 and 6). Programs were only modified to change the extension time depending on the length of the template to be amplified and to change the annealing temperature depending on the primer melting temperatures.

*Table 8 - LONG PCR programme*

LONG PCR program stages	Temperature (°C)	Time	Cycle
Pre-heating	99	2 min	-
Initial denaturation	95	2 min	1
Denaturation	95	30 s	33
Annealing	55	30 s	
Extension	68	4 min 30 s	
Final extension	68	15 min	1
Hold	4	∞	-

*Table 9 - HIFI PCR programme*

HIFI PCR program stages	Temperature (°C)	Time	Cycle
Pre-heating	99	2 min	-
Initial denaturation	94	2 min	1
Denaturation	94	15 s	34
Annealing	55	30 s	
Extension	72	3 min	
Final extension	72	7 min	1
Hold	4	∞	-

### **2.4.3 DNA Gel Electrophoresis**

Agarose gels were prepared by dissolving 1% (w/v) Hi-Res Standard Agarose (AGTC Bioproducts) in TAE buffer (see section 2.1.1) by microwaving until the agar dissolved. Once cooled sufficiently, 0.5 µg/mL of ethidium bromide (Sigma) was added to the solution and mixed. The agarose solution was poured into gel casts and left to solidify at RT. Once set, 6x DNA loading buffer (see section 2.1.1) was added to DNA samples at a final 1x concentration, and the DNA mixture loaded into the gel wells. Every gel included 10 µL of HighRanger Plus 100 bp DNA Ladder (Norgen biotek). The electrophoresis was run at 100 Volts for 1-2 hours in TAE buffer until bands were sufficiently separated. DNA bands were visualized using UV illumination on a GeneSys xx6 gel doc system.

### **2.4.4 DNA Gel Extraction and Purification**

The desired DNA fragments were cut from the gel whilst being visualised on a UV transilluminator (Spectroline TVC-312A) briefly, taking care not to extend exposure times unnecessarily as to prevent DNA damage. Isolated fragments were weighed in

clean 1.5 mL Eppendorf tubes (Fisher Scientific) and DNA purified using a GeneFlow Q-Spin gel extraction/PCR purification kit as per manufacturers protocol. Briefly, sufficient binding buffer was added to the gel fragments and dissolved at 60 °C until a homogenous solution formed. The DNA gel solution was then centrifuged through DNA binding columns to collect the DNA on the column membrane. The membrane was washed twice by discarding flow-through and adding supplied wash buffer, centrifuging the column and repeating. Residual wash buffer was removed by a final centrifugation after discarding flow-through. DNA was eluted by placing the column in a clean 1.5 mL Eppendorf tube, adding 30 µL of ddH<sub>2</sub>O and centrifuging a final time.

#### **2.4.5 Measuring DNA Concentration**

DNA concentration was measured using a (Nanodrop). The Nanodrop was equilibrated with 2 µL ddH<sub>2</sub>O before loading 2 µL of sample. The sample purity was monitored by checking that the 280/260 reading was ~ 1.8 or within 0.1 of this as per manufacturers guidelines.

#### **2.4.6 Recombineering**

Recombineering processes were carried out as previously described (203).

##### *Theory*

Desired Merlin variants were obtained through recombination mediated genetic engineering (Recombineering) which allows for desired sequences or genes to be modified, inserted or deleted from bacterial artificial chromosome (BAC) cloned HCMV genomes. Recombineering was performed in SW102 *E.coli* containing phage lambda red genes that are expressed from a temperature sensitive promoter. These genes mediate homologous recombination of short stretches of DNA (221). Manipulating the temperature of the bacteria allows for bacterial growth and BAC production without recombination at 32°C and induction of the recombination genes at 42°C. Two successive rounds of transformation are required to manipulate the BAC-cloned HCMV genome. In the first transformation round, the desired DNA region to be modified was replaced with the RpsI cassette, a selectable cassette encoding both positive (Kanamycin resistance) and negative (streptomycin sensitivity) selectable markers (see section 2.4.6.4). In a first round, cells that had successfully inserted the cassette were selected

on the basis of kanamycin resistance. In a second round the cassette was replaced with a desired sequence, and correct recombinants selected based on resistance to streptomycin. The cassette also included *lacZ*A for blue/white screening, as an additional marker. The region of manipulation in the BAC genome was sequenced prior to propagation of a single clone.

#### *DNA Sequence Design and Preparation*

Two sets of primers (~100bp each) were required for recombineering. One set is needed to amplify and insert the *RpsI* cassette into the target region. These were designed with ~80bp of homology to regions flanking the target insertion site in the BAC-cloned genome as well as ~20bp at the 3' end with homology to 5' of the *RpsI* cassette itself. The *RpsI* cassette was amplified with the primers found in appendix 1. The second set of primers were engineered to amplify the desired sequence and replace the *RpsI* cassette. These were designed with both homology to the regions flanking the target sequence and the desired sequence. Again, the desired sequence was amplified as described in section 2.3.1 or smaller modifications were possible with just the two overlapping primers. PCR products were separated on an agarose gel, then the appropriate band cut out and DNA purified.

#### *Production of Competent SW102 E. coli and Transfection of DNA*

SW102 *E. coli* were cultured in LB broth overnight in a shaking incubator (200 rpm at 32°C, thus restricting the expression of recombineering genes). All bacteria containing BACs were cultured with chloramphenicol (12.5 µg/mL). This culture was then used to inoculate (0.5 mL) 25 mL fresh LB broth and the SW102 *E. coli* were cultured to high concentration whilst remaining in log-phase of replication. Cultures were monitored by UV spectrophotometry (Pharmacia Ultraspec 3000) and when a culture density of 0.6 OD units was reached, the phage-lambda red proteins were induced by shifting the culture to 42°C in a water bath for 15 mins with frequent mixing. All further replication was then arrested by cooling to 0°C. Transformation competent cells were then washed three times by centrifuging for 5 mins at 3345 x g at 0°C and then washing with ddH<sub>2</sub>O 0°C. After the final wash, cells were re-suspended in ~400 µL ddH<sub>2</sub>O 0°C and distributed as 25 µL aliquots to pre-cooled 1.5 mL Eppendorfs ready for the addition of 4 µL of purified PCR product. In the first round the *RpsI* cassette was inserted, in the second

round it was replaced to leave the resulting desired sequence (amplified desired DNA sequences from section 2.3.8.2). Once thoroughly mixed the aliquot is transferred to a Geneflow 2mm electroporation cuvette (Cell Projects) and chilled on ice for 5 mins. The samples are then electroporated in a Micropulser electroporation unit (BioRad) using program EC3 delivering a voltage of 2.5 KV. The cells are then allowed to recover in 5 mL LB broth in a shaking incubator for 1 hr (200 RPM at 32°C) in which time homologous recombination of the DNA segment and the BAC occur. Recovered cultures are then plated out onto either positive or negative selection LB agar plates for first or second round transformations respectively. The plates are incubated for 48 hr at 32°C.

#### *Positive and Negative Selection of Transformants*

After recovery of the first round transformation, cultures were plated onto LB agar plates supplemented with 12.5 µg/mL Chloramphenicol, 200 µM IPTG, 80 µg/ml X-gal and 25 µg/ml kanamycin for positive selection of *E.coli* containing BACs which have successfully inserted the Rpsl cassette. *E.coli* containing BACs with inserted Rpsl cassette will also contain the LacZ gene which when plated on IPTG and X-gal allows for an additional check in the form of blue-white screening. Blue colonies that grow on positive plates are selected and overnight cultures grown for small scale DNA purification (see section 2.4.7.5) and genome analysis in the form of a restriction digest.

Second round transformants are plated onto LB agar plates supplemented with 12.5 µg/mL Chloramphenicol, 200 µM IPTG, 80 µg/ml X-gal and 200 µg/ml streptomycin for negative selection of *E.coli* containing BACs which have successfully replaced the Rpsl cassette with the desired sequence and are therefore now streptomycin resistant and kanamycin sensitive. White colonies are selected from negative selection plates as the LacZ gene from the Rpsl cassette is now missing and the X-gal will remain colourless. Similarly, to the first round, overnight cultures of the selected white colonies are set up for small scale DNA purification and restriction digest.

#### *Small Scale BAC DNA Extraction and Purification*

BAC DNA isolation was performed using buffers from the QIAGEN Spin Miniprep Kit (27016) from a 5 mL overnight culture (200 RPM at 32°C) of the SW102 *E. coli* colony containing the desired BAC supplemented with 12.5 µg/ml chloramphenicol. Cells were

pelleted by centrifugation at 4,000 rpm for 5 min at 4 °C and the supernatant discarded. 250 µL of P1 buffer with RNase A was used to resuspend cells before incubating with 250 µL P2 buffer for 5 min at RT to lyse cells. The cell lysis solution is then neutralised with the addition of 250 µL N3 buffer before the resulting flocculate is separated by centrifugation at 13,000 rpm for 10 min. The supernatant containing BAC DNA is then transferred into new 1.5ml Eppendorf tubes (Fisher Scientific) and precipitated by the addition of 750 µL of isopropanol (Fisher) and centrifuged for 10 min at 4 °C. The DNA pellet was then washed by addition of 500 µL of 70% ethanol and centrifuged at 13,000 rpm for 10 min at RT, before being left to dry at 37 °C to remove any residual ethanol. The DNA pellet was then re-suspended in 30 µL of ddH<sub>2</sub>O and the DNA stored at -20 °C.

#### *Restriction Digest*

Restriction digests were performed with the enzyme HindIII to analyse digestion patterns of the BAC genomes from selected transformant colonies from positive and negative selection plates to ensure that no gross rearrangements of the BAC had occurred. Reactions were set up with 8 µL of sample DNA (generated from section 2.4.6.5), 1 µL HindIII enzyme and 1 µL NE 2.1 buffer (New England Biolabs) and incubated at 37 °C for 1 hour. The resulting DNA fragments were visualised by DNA gel electrophoresis (see section 2.4.4) and compared with a predicted pattern generated on CLC Main of the HCMV BAC genome to serve as a positive control of HCMV genome integrity.

#### *Sequencing BACs*

Once a successful BAC was generated sequencing was used to check the region that was modified for any errors. The manipulated region of the BAC was first PCR amplified and gel purified. A Mix2Seq kit (Eurofins Genomics) was used to set up sequencing reactions as per manufacturers protocol. Two µL of either forward or reverse 10 µM sequencing primers were mixed with 15 µL gel purified BAC DNA and sent away to be sequenced in Mix2Seq tubes supplied. Once the sequence of the BAC was confirmed to be correct a 15% glycerol (v/v) stock was made of the SW102 culture containing the BAC, aliquoted and stored at -80 °C.

### *Large Scale BAC DNA Extraction and Purification of DNA*

Isolation of tissue culture transfection grade BAC DNA was performed by large scale overnight culture of the desired SW102 *E. coli* BAC and plasmid DNA purification using a NucleoBond BAC100 kit (Macherey-Nagel) to manufacturers protocol for low-copy number plasmid purification. In brief, 500ml overnight cultures were subjected to alkaline lysis resulting in the precipitation of cellular debris in a flocculate. The flocculate was separated out by pouring the lysate over fine filter paper supplied in the kit. The DNA is isolated by passing the flow-through through a BAC 100 column. The captured DNA in the column is then washed with supplied buffers repeatedly until finally the DNA was recovered with prewarmed elution buffer (supplied with kit). Isopropanol is added to precipitate the eluted DNA before centrifugation at 15000 x g for 30 mins at 4°C. The precipitated DNA is then washed with RT 70% (v/v) ethanol and a further centrifugation at 15000 x g for 10mins RT. The resulting DNA pellet is then air-dried and resuspended in TAE buffer. All purified BAC DNA is stored at 4°C for several months and used for transfection into HFFF Tet cells to generate viral stocks (see section 2.3.1).



## 2.5 Functional Assays

### 2.5.1 Co-Cultures

Separate co-cultures were performed with both adherent (HF-tert and Arpe19) and non-adherent (DCs and LCs) target cells.

#### *Fibroblast -Fibroblast Co-Cultures*

For adherent co-cultures, HF-terts were infected with virus at a MOI of 8 and incubated until co-culture at around 7 days post infection. Infected HF tert cells were trypsinised, counted and approximately 60 infected cells were co-cultured with uninfected target cells (either HF-terts or ARPE19s plated out the day before), in the presence of a range of concentrations of Cytotect, a purified human anti-CMV IgG (Biotest (0mg/ml, 0.5mg/ml, 0.1mg/ml and 0.02mg/ml)), which was replaced every 2 days. At multiple time points images were taken of plaques formed in the target cells on a Leica DMIRBE Microscope. Plaque size was then measured using Fiji, as pixels<sup>2</sup>.

#### *Fibroblast -DC/LC Co-Cultures*

For non-adherent cells, DCs and LCs were incubated either with or without IFN $\alpha$  (6,000 units/ml) overnight before co-culture. Cells were then washed and counted before being added directly to wells 1:1 with infected HF-terts (4 days post infection, MOI of 8). If cells had been cultured in IFN $\alpha$  it was maintained throughout the co-culture. The DCs and LCs were pipetted off the co-culture at 48hr and incubated in fresh wells. At 72hrs post co-culture, cells were stained with BD Horizon Fixable viability stain 570 according to manufacturer's instructions and fixed in 2% paraformaldehyde (PFA) before analysis on a BD Accuri C6 cytometer.

#### *Cell Free DC/LC Infections*

DCs and LCs were incubated with TB40/E at a MOI of 50 for 2hrs on a rocker at 37°C and 5% CO<sub>2</sub>. Supernatant was removed and washed from the cells by centrifugation at 1500 rpm for 3 min. 10% FBS media was added to cells which were left 72hrs before plating onto a 96-well flat bottom plate coated with poly-d-lysine. Cells were fixed with acetone methanol and stained with a primary anti-IE1 antibody, washed with PBS and then

secondary Anti-Mouse IgG added (see table 6). Cells were washed and imaged on a Leica DMIRBE Microscope. Images were analysed with Fiji software.

## 2.5.2 Flowcytometry

### *Accuri C6 Flow Cytometer*

Fluorescence was measured by running samples in 4% PFA through an Accuri C6 flow cytometer. Gating strategies practiced were performed by differentiating different cellular populations based on forward scatter (FSC) relative to the cell size and side scatter (SSC) which is proportional to the cell's granularity. When cells were stained, an unstained sample was used as a negative control to help define the gating strategy. All analyses were performed using Flowjo software (TreeStar Inc., USA).

*Table 10 - Stains and antibodies used for flow cytometry and surface staining*

Immunogen	Company	Catalogue number	Species	Dilution	Conjugate
IE1	Merck Millipore	MAB810R	Mouse	1:500	
Mouse IgG (H+L)	Life Technologies	A11020	Goat	1:500	AlexaFluor594
Mouse IgG (H+L)	Life Technologies	A-21235	Goat	1:500	AlexaFluor647
Human IgG (H+L)	Life Technologies	A-21445	Goat	1:500	Alexafluor647
gB	Virusys	CA005	Mouse	1:200	
MHC I (W632)	Biolegend	311414	Mouse	1:200	
CD107	Biolegend	328606	Mouse	1:333	FITC
CD3	Biolegend	317334	Mouse	1:250	Pe/Cy7
CD56	Beckman Coulter	A07788	Mouse	1:250	PE

### *RL13-Fc Binding Analysis*

HF CARs were seeded in T25s in DMEM10%. The following day, cells were infected at a MOI of 10 under conditions previously described (see section 2.3.3) except in DMEM10%. At 72 hr PI, cells were trypsinised and aliquoted into a 96-well V-bottomed plate (ThermoFisher) in duplicate between the different conditions; no stain, secondary only stain, 100 µL/mL, 10 µL/mL and 1 µL/mL. Cells were pelleted and washed twice by centrifugation at 1500 rpm for 3 min and resuspension in excess PBS. Seronegative Human IgG was added to the appropriate conditions at a concentration of 1-100 µL/mL

and incubated for 30 mins. Seronegative IgG was removed and cells washed twice as before. Cells were resuspended in secondary (Anti-human Alexafluor647) (see table 9) in PBS and incubated for a further 30 mins before pelleting and removing. Cells were washed a further two times as described previously and fixed in 4% PFA for 15 mins. Samples were run and fluorescence quantified as previously described (see section 2.5.2.1).

#### *Cell Surface Glycoprotein Expression Analysis*

72hr post infection (PI) HFFF Tert cells were trypsinised and pelleted. Cells were resuspended in DMEM 10% and 50 µl put into a 96 well plate in triplicate. On ice, cells were washed twice with PBS. Human serum was then added 1/50 to block Fc-receptor interactions, followed by primary antibodies (in individual wells) and then secondary antibody all for 30 min at 4°C with a PBS wash and resuspension in-between each step (for antibodies see table 9). After fixing with 4% PFA, samples were analysed on a BD Accuri C6.

### **2.5.3 Antibody-Dependent Cellular Cytotoxicity (ADCC) Assay**

HFFF Terts were infected as previously described at a MOI of 5. The following day infections were monitored and if satisfactory, PBMCs were isolated as described in section 2.2.3.1 and cultured with 1:6000 IFNα for 24 hrs. The next day, HFFF Terts (48 hr post infection) were exposed in duplicate to the prepared PBMCs, with either CMV positive or negative serum (1/10), and CD107 antibody for 1hr (37°C, 5% CO<sub>2</sub>) before a 5hr incubation with (1/1000) Golgi stop (Biolegend, 317334) at 37°C, 5% CO<sub>2</sub>. Cells were then harvested and washed with PBS twice at 4°C. On ice, cells were stained with anti-CD3 and anti-CD56 (each 1/250 in PBS) before another PBS wash. Cells were then fixed in 4% PFA and run and analysed as previously described (see section 2.5.2.1) (see table 9 for antibodies).

### **2.5.4 SiRNA Knockdown of Cellular Proteins**

siRNA to cellular proteins was used for short term knockdown during viral infection. siRNAs came as 4 sequences per target. The siRNA sequence with the most efficient knockdown was chosen during optimisation. HFFF terts were seeded in 12-well plates in DMEM10% without any antibiotics. The following day, culture medium was replaced

with 1 mL Optimem (ThermoFisher) ready for siRNA transfection. Transfection of siRNA was performed using lipofectamine (ThermoFisher) as per manufacturers instruction for either a forward or reverse transfection in a 12 well plate. Lipofectamine and siRNA diluted in 200  $\mu$ L Optimem were incubated for 20 min to allow for complexation. The lipofectamine and siRNA solution was then added to the cells and left for 48 hrs. siRNA controls were included in every assay, a positive control siRNA to ensure the transfection had been successful and a negative control siRNA as well as an untransfected well, both to ensure no non-specific changes in protein expression had occurred.

*Table 11 - siRNAs used in this study*

Target	Other names	Qiagen Flexitube GeneSolution Catalogue number
TMEM16C	ANO3	GS63982
SERCA	ATP2A1 and ATP2A2	GS487 and GS488 respectively
GRP78	HSPA5	GS3309
DNAJB11	ERdj3	GS51726
Calnexin	CANX	GS821
ERp57	PDIA3, GRP58	GS2923
ABI1	Positive control	55338
AllStars Negative control	Negative Control	1027281

### *Optimisation*

Three different conditions were tested for optimisation in a forward transfection; 1  $\mu$ L lipofectamine with 12 pmol siRNA, 2  $\mu$ L lipofectamine with 24 pmol siRNA and 3  $\mu$ L lipofectamine with 48 pmol siRNA. 48 hr post transfection with siRNA, cell lysates were taken as previously described 2.3.5.3 and siRNA efficiency analysed by expression of protein found by western blot (see section 2.5.5). The siRNA sequence with the most efficient knockdown per target was carried through to the knockdown assays.

### *Knockdown Co-Culture Assay*

HFFF terts were seeded in 12-well plates in DMEM0% without any antibiotics the day before and then infected with GFP expressing virus at a MOI of 8. The following day a reverse transfection was performed as per ThermoFisher protocol in a 48-well plate. 6 pmol of siRNA was diluted in 40  $\mu$ L Optimem in the wells to which 0.5  $\mu$ L lipofectamine

was added and incubated for 20 mins at RT. The infected HFFF terts were trypsinised, resuspended in Optimem and counted. Infected cells were seeded as 200  $\mu$ L aliquots in the 48-well plate containing siRNA so that they would reach 50-70% confluency. The plate is gently rocked to ensure thorough mixing and then incubated for 48 hr. In the meantime, the following day, HFFF terts were seeded in 48-well plates in DMEM0% which will serve as the recipient cells in the co-culture. The following day the co-culture is performed, the recipient cells were washed with PBS and stained by addition of 100  $\mu$ L of DDAO (7-hydroxy-9H(1,3-dichloro-9,9-dimethylacridin-2-one)) diluted in PBS 1:2500 for 15 mins before a further wash in PBS to remove residual stain. The transfected infected cells, which will serve as the donor cells in the co-culture, are trypsinised and counted. The donor cells are added to the stained recipient cells in a series of dilutions; 1:3, 1:5, 1:15. 72 hr post co-culture cells are trypsinised and fixed in 4% PFA and run as previously described (see section 2.5.2.1) on the Accuri C6 Flowcytometer analysing efficiency of viral transfer during knockdown. The fluorescence of recipient infected cells was analysed by gating for DDAO+ (FL4 channel) GFP+ cells.

### **2.5.5 Western Blotting**

Samples were prepared as described in section 2.3.5.3. Samples were loaded as 10  $\mu$ L aliquots to a 10% pre-cast Bis-Tris SDS-Page gel with 10  $\mu$ L Novex Sharp Pre-Stained protein standard (Invitrogen) as a reference ladder. The gel was run in 1x MOPS buffer for 45min at 200 V. During this time the PVDF membrane could be prepared by soaking in Methanol for 10 mins before soaking in transfer buffer with thick blotting paper. Proteins were transferred to PVDF membrane by semi-dry transfer for 2 hr at 10 V in transfer buffer. The membrane was then washed with ddH<sub>2</sub>O and left to air dry to allow for all methanol to evaporate and prevent any further binding of proteins. The PVDF membrane was then rewetted in PBST for 2-4 hr until sufficiently saturated. Primary antibody was added in immunoblotting block buffer and left overnight at 4°C on a rocker. The following morning the primary antibody was removed and washed 3 times with PBST for 5 min. Secondary antibody could then be added in immunoblotting block buffer and left for 1 hr on a rocker before 3x5 min washes in PBST. If high background was an issue, the membrane would be left in an extended wash in PBST for 1 hr on a

rocker. Supersignal West Pico (Thermo Fisher scientific, 10481755) was added as per manufacturer's instructions before imaging using a GeneSys GelDoc (Syngene).

*Table 12 - Antibodies used in Western Blotting*

Immunogen	Company/ Catalogue #	Dilution	Secondary	Company	Dilution
IE1	Millipore MAB810R	1:2000	HRP anti- Mouse	Bio-Rad 170- 6516	1:2000
gB	Abcam ab6499	1:2000			
pp28	Abcam ab6502	1:2000			
pp65	Virusys CA003-100	1:2000			
pp44	Virusys P1202-2	1:2000			
SERCA (ATP2A1, ATP2A2)	Santa Cruz sc- 271669	1:2000			
CNX (Calnexin)	Millipore	1:1000			
ABI 1 (positive control)	gifted	1:200			
Human beta actin	Sigma A- 2066	1:2000	HRP anti- Rabbit	Bio-Rad 170- 6515	1:2000
DNAJB11 (ERdj3)	Santa Cruz sc- 99208	1:2000			
ERp57 (PDIA3/GRP58)	Santa Cruz sc- 28823	1:2000			
TMEM16C (ANO3)	Abcam ab82781	1:2000			
HSPA5 (GRP78)	Santa Cruz sc- 1050	1:2000	HRP anti- Goat	Santa Cruz Biotechnology Sc-2056	1:2000

## 2.5.6 Quantitative PCR (qPCR)

Viral DNA and primers to HCMV gB were used to set up qPCR reactions against serial 10-fold dilutions of BAC DNA (see section 2.4.6.5) and DNA extracted from HFFF Tet cells (see section 2.3.5.1) were used to generate standard curves. Triplicate samples were set up consisting of 200 nM primers, sample diluted to be within the standards range and 1× iQ™ SYBR® Green Supermix (BioRad). Virus genomes were quantified using primers gB F and gB R, while an endogenous control was generated using primers GAPDH F and GAPDH R (for primer sequences see Appendix 1) Reactions were run under the thermocycling conditions described in section 2.5.5.2 on a QuantStudio 12K Flex Real-

Time PCR system. To ensure only the desired sequence was bound by SYBR green, the melt curve of each reaction was carefully analysed.

*Table 13 - qPCR Thermocycling program*

	Hold stage	PCR stage (x40 cycles)		Melt curve stage		
Temperature	95 °C	95 °C	60 °C	95 °C	60 °C	95 °C
Time (min)	03:00	00:15	01:00	00:15	01:00	00:15
Step	1	1	2	1	2	3
Data collection			X			X

## 2.5.7 Infectivity vs Particle Numbers

To compare the particle numbers and infectivity between samples, supernatant timecourses in 12-well plates were set up as previously described (see section 2.3.4.2). HFFF Terts were infected at a MOI of 8. Every day, the supernatant was taken centrifuged at 1500 rpm for 3 min to remove any cellular contamination, and divided between the infectivity analysis and the particle number analysis. Samples were either progressed with fresh or frozen until needed.

### *Infectivity Analysis*

To measure Infectivity, the half aliquot of supernatant sample was subjected to a plaque assay as previously described in section 2.3.2.2.

### *Particle Number Analysis by qPCR*

To quantify particle numbers, the half aliquot of supernatant sample was subjected to DNA extraction with DNase treatment (see section 2.3.5.1) and then qPCR (see section 2.5.6) to quantify viral genomes. As samples were from supernatants, no cellular endogenous control could be used.

### *Particle Number Analysis by NanoSight*

Another method to quantify viral particle numbers was using a NanoSight (NanoSight NS300). Samples prepared as described in section 2.3.6. and diluted to give a concentration of  $10^8$  particles when running. The standard measurements used were 5 x 60 second captures under a flowrate of 50. Analysis of particles was performed on the NanoSight NTA 3.2 software (NanoSight). A detection threshold of 5 was used and a camera level of 13. Particles within the range of 100nm-350nm were considered virions.

## **2.6 Microscopy**

### **2.6.1 Zeiss Microscope for Immunofluorescence**

The Zeiss microscope (Axio Observer Z1) was used for immunofluorescent imaging. Using the Zen2 Pro (Zeiss) software, entire wells could be imaged and the images stitched together to make plaque size measurements and counting more reliable. Exposure time for fluorescent samples was determined by using the auto-exposure function and then ensuring that there was no risk of photobleaching of the samples.

### **2.6.2 Transmission Electron Microscopy (TEM)**

HFFF Terts were plated in DMEM0% in T25s. The following day, cells were infected at a MOI of 5. The cells were fixed, processed and imaged 96hr PI by Dr Hobot as previously described (222).



## **2.7 Statistical Analysis**

GraphPad Prism 6 software (GraphPad Software, Inc., CA, USA) was used for all statistical analyses. Data sets with multiple samples were analysed by either one-way ANOVA or two-way ANOVA tests with Tukey's post-hoc analysis. All data was plotted as mean  $\pm$  standard error mean (SEM) unless otherwise stated. Differences were considered and displayed as significant in figures and tables as follows; \* $p < 0.05$ ; \*\* $p < 0.01$ ; \*\*\* $p < 0.001$  and \*\*\*\* $p < 0.0001$ .

# **CHAPTER 3. GENETIC MANIPULATION AND ANAYLSIS OF RL13**

The RL13 ORF is dispensable for viral growth *in vitro* and has been shown to actively impede viral propagation. This unusual effect is not unique to RL13 as the UL128L is also detrimental for growth in fibroblasts. However, a great deal is known about the role of the UL128L in production of the pentameric complex and providing an expanded HCMV tropism (see Intro Section 1.3.1.3). Not much is known about RL13 and in order to investigate the function of RL13, several new viruses were constructed. New reporter viruses, HCMV RL13 genotypes and non-human CMV RL13 variants were created by recombineering (see Table 14). As the presence of an intact UL128L also restricted viral growth, it was important to distinguish any effects of RL13 expression from UL128 expression. Therefore, where possible, experiments were performed with viruses lacking the expression of the functional proteins ( $\Delta$ RL13 and/or  $\Delta$ UL128) as well as viruses with the expression of both functional RL13 and UL128 (WT) (see table 14).

All viruses containing wildtype sequences of RL13 and/or UL128 carried the risk that mutations would be selected. Therefore, a repression system was used when propagating these viruses. Transcription of the two genes, RL13 and UL128, is repressed by inserting a Tet-operator (TetO) upstream of the TATA box. The virus is then grown up in HFFF Tet cells which express the Tet-repressor (TetR). TetR binds to Tet, repressing gene expression, and therefore removing the selective advantage of genomes carrying mutations in either gene. This therefore allowed for the growth of viruses containing wildtype sequence without risk of mutants being selected for (203).

Using the Tet-repression system as well as being vigilant in checking experiments for signs of RL13 mutations (such as dramatically increased plaque size or efficient viral growth) is vital to ensure reliable research is performed. Stocks thought to be WT in sequence have previously been reported to contain 50/50 mixes of WT and  $\Delta$ RL13 virions. This was not seen for other ORFs showing that strong active selection that favours RL13 mutants is a real concern during prolonged research and replication in fibroblasts (3).

**Table 14 – Viruses used and created for this study.**

Name <sup>1</sup>	pAL number	CMV Backbone strain	RL13	UL128	GFP
$\Delta$ RL13/ $\Delta$ UL128	1111	Merlin	Mutated	Mutated	None
	<b>2079</b>	Merlin	Mutated	Mutated	Fused to IE2
	<b>2159</b>	Merlin	Mutated	Mutated	IE2-P2A-GFP
Wildtype (WT)	1502	Merlin	Tet repressed	Tet repressed	None
	1511	Merlin	Tet repressed +V5 tag	Tet repressed	None
	<b>2081</b>	Merlin	Tet repressed	Tet repressed	Fused to IE2
	<b>2157</b>	Merlin	Tet repressed	Tet repressed	IE2-P2A-GFP
	<b>2176</b>	Merlin	Tet repressed	Tet repressed	IE1-P2A-GFP
$\Delta$ UL128	1516	Merlin	Tet repressed	Mutated	None
	<b>2082</b>	Merlin	Tet repressed	Mutated	Fused to IE2
	<b>2160</b>	Merlin	Tet repressed	Mutated	IE2-P2A-GFP
$\Delta$ RL13	1778	Merlin	Mutated	Tet repressed	None
	<b>1938</b>	Merlin	Mutated	Tet repressed	Fused to IE2
	<b>2167</b>	Merlin	Mutated	Tet repressed	IE2-P2A-GFP
TR RL13	<b>2524</b>	Merlin	From HCMV strain TR	Tet repressed	None
	<b>2526</b>	Merlin	From HCMV strain TR	Tet repressed	IE2-P2A-GFP
TR RL13/ $\Delta$ UL128	<b>2525</b>	Merlin	From HCMV strain TR	Mutated	None
	<b>2527</b>	Merlin	From HCMV strain TR	Mutated	IE2-P2A-GFP
Rh13.1/ $\Delta$ UL128	<b>2574</b>	Merlin	Rh13.1 from RhCMV	Mutated	IE2-P2A-GFP
TB40E		TB40E	TB40E	TB40E	

<sup>1</sup> Often referred to as the genetic background of the virus/group of viruses.

pAL numbers in Bold were created by recombineering for this project, others were created previously by Dr Stanton. Viruses highlighted in any shade of green express GFP.

### **3.1 Generation of HCMV Reporter Viruses to Aid Investigation into RL13 Function**

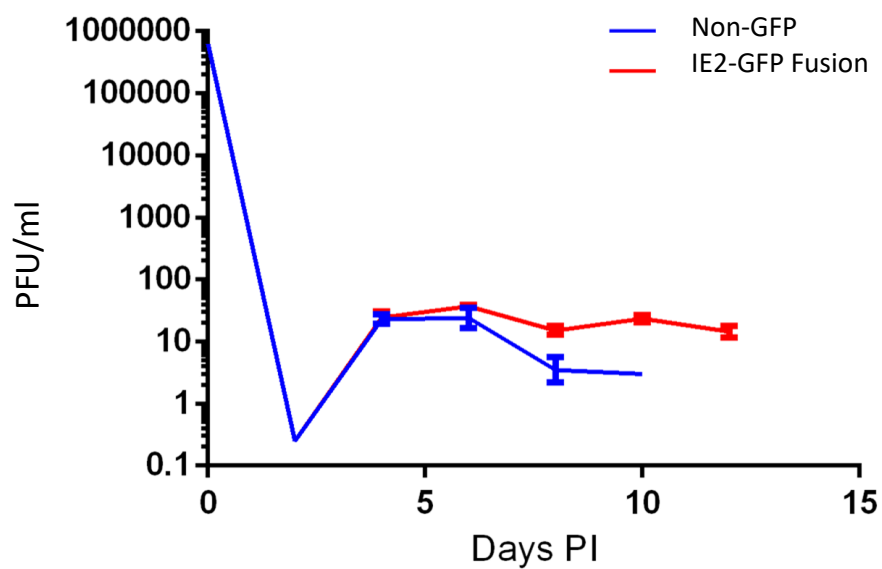
A series of HCMV reporter viruses had previously been constructed in the laboratory that encoded GFP fused to the IE2 ORF by a flexible linker sequence (Table 14). While such constructs were useful, they were not ideal. GFP was detectable in cells infected with these strains by 48h p.i. (data not shown) whereas ppIE1 can be detected as early 2-6h by immunohistochemistry. Moreover, the IE2-GFP fusion virus displayed prolonged growth and slightly higher titres when compared to its non-GFP counterpart (Fig. 8), a result that implies that direct C-terminal tagging of ppIE2 impacted on its function and expression. A new set of reporter viruses was needed that did not display any altered growth properties and that ideally expressed GFP at an earlier timepoint.

#### **3.1.1 Generation of Novel Reporter Viruses by Recombineering**

In order to improve on the previous reporter system, GFP was inserted downstream of IE1 with a P2A peptide rather than a direct fusion between the ORFs, the strategy is outlined in Figure 9. The first aim was to exchange the existing linker for a self-cleaving P2A peptide. The second was to insert the P2A-GFP after IE1, rather than IE2. This required two distinct steps; one to insert the P2A sequence between IE2 and GFP in a previously created virus and the second to clone the new p2A-GFP sequence into the desired BAC after IE1. This process created novel IE2-P2A-GFP viruses as an intermediate from the first step as well as the planned IE1-P2A-GFP viruses. The P2A peptide should minimise any effect on expression of IE1/IE2 due to co-translational cleavage of the linked proteins. The P2A peptide was favoured over an internal ribosome entry site (IRES) as an IRES often results in reduced translational efficiency of the gene placed after the IRES site, and the sequence itself is fairly large at approximately 600bp which makes recombineering less efficient (223, 224).

IE1-P2A-GFP viruses could only be successfully recombineered in the WT and  $\Delta$ UL128 backgrounds despite numerous attempts. After transfection of the BAC DNA, recovery of virus following transfection of the BAC DNA proved unusually problematic. Although the IE1-P2A-GFP sequence could be inserted into the  $\Delta$ UL128 background by recombineering, viral stocks were never produced as recovery of virus after transfection

of the BAC DNA never proved successful. When growing up stocks of WT, the virus spread through the cell monolayer incredibly slowly taking nearly 4 weeks to completely infect a T150, compared to the usual 7-10 days for Merlin HCMV. The highest titre of virus stocks ( $3 \times 10^5$  PFU/mL) achieved with this construct was not sufficient to allow for experimentation. From this we concluded that manipulating the HCMV genome at the C-terminus of the IE1 ORF inhibited virus growth.



*Figure 8 - IE2-GFP fusion virus shows altered growth properties. Infections were set up in HFFF-primary cells (MOI 5) and the supernatant was titred in plaque assays every 2 days to generate this growth curve of  $\Delta$ RL13 viruses. The IE2-GFP fusion virus (red) shows slightly prolonged growth and higher titres compared to the Non-GFP counterpart (blue). Graph courtesy of Dr Stanton (unpublished data).*

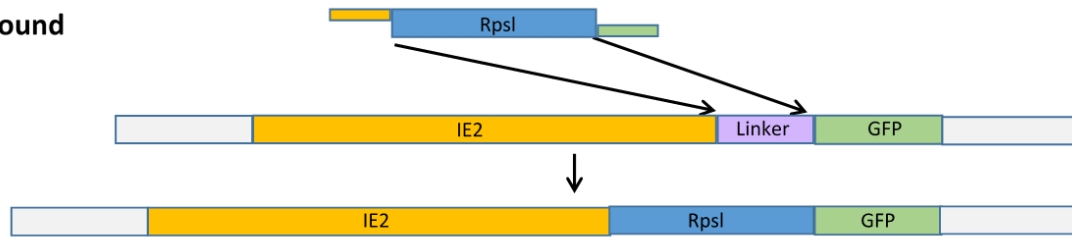
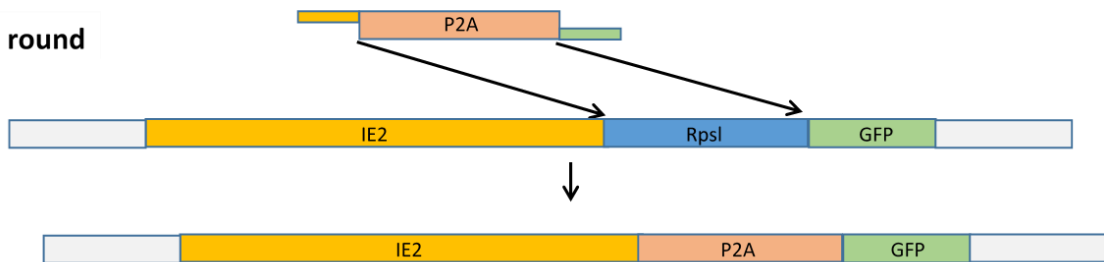
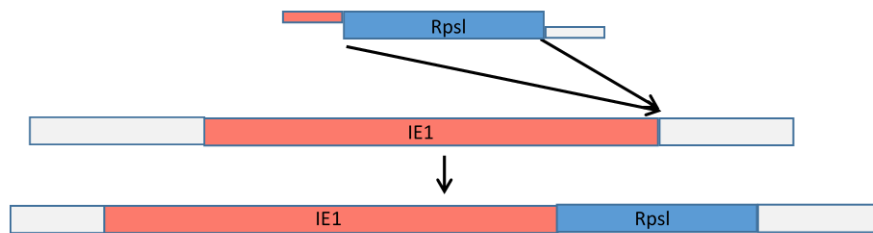
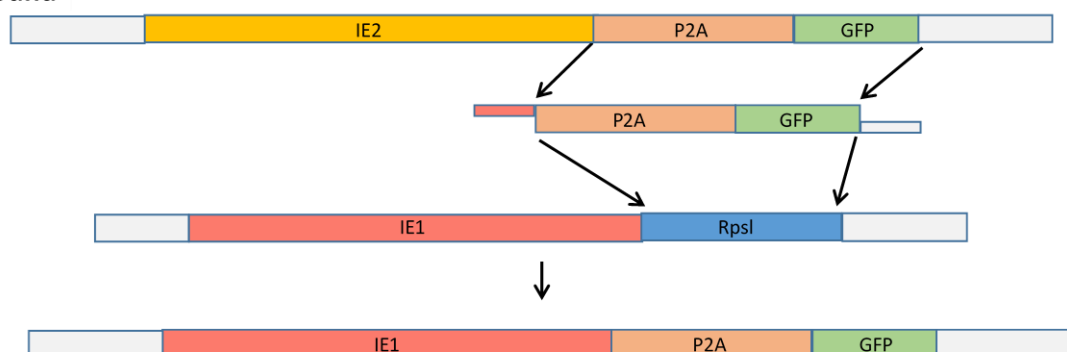
**A****1<sup>st</sup> round****2<sup>nd</sup> round****B****1<sup>st</sup> round****2<sup>nd</sup> round**

Figure 9 - Recombineering of a Novel reporter virus. Original plan to construct IE1-P2A-GFP reporter viruses. (A) IE2-P2A-GFP construct plan to insert the RpsI cassette between the IE2 and GFP ORFs during the first round. The RpsI cassette is then replaced with the P2A sequence in the second round. (B) IE1-P2A-GFP construct plan. First round to insert the RpsI cassette after the IE1 ORF which is replaced in the second round with the P2A-GFP sequence created in (A).



### **3.1.2 Growth characterisation of modified virus by Plaque Assay**

Plaque assays were used to determine if the modifications from recombineering altered any growth kinetics of the virus when compared with an unmodified (non-GFP) virus. Figure 10 shows the effect of inserting a P2A-GFP sequence after the IE1 or IE2 ORFs. As only the WT genetic background of the IE1-P2A-GFP viruses had been successfully made, this was the genetic background used for the comparison. The IE2-GFP fusion viruses, which has already been observed to exhibit impaired growth, were included in this analysis to determine whether the new constructs were an improvement. The IE2-GFP fusion virus showed slightly reduced plaque sizes, although this did not reach statistical significance (Fig. 10). Consistent with the problems experienced when attempting to propagate the virus, the IE1-P2A-GFP virus showed significantly smaller plaque sizes when compared to the non-GFP control. However, the IE2-P2A-GFP virus showed plaque sizes similar of those from the non-GFP viruses. Therefore, due to minimal or no effect on growth properties, only the IE2-GFP fusion and the IE2-P2A-GFP viruses were used for experimentation and the recombineering of the rest of the IE1-P2A-GFP viruses were not pursued.

### **3.1.3 Brighter GFP Expression Observed from IE2-P2A-GFP Virus by Flow Cytometry Assessment**

To determine whether the translational efficiency of the P2A peptide provided an advantage to the brightness of the GFP compared to the directly-fused GFP. Flow cytometry assessment was performed on cells infected with the newly created IE2-P2A-GFP reporter viruses to determine at what timepoint GFP was expressed.

GFP expression of cells infected with two of the genetic backgrounds was assessed at two timepoints (Fig. 11). The IE2-P2A-GFP viruses exhibited a very slight trend of brighter GFP expression however significance could not be calculated due to lack of replicates. All viruses showed brighter GFP at 72 hrs compared with 48 hrs.

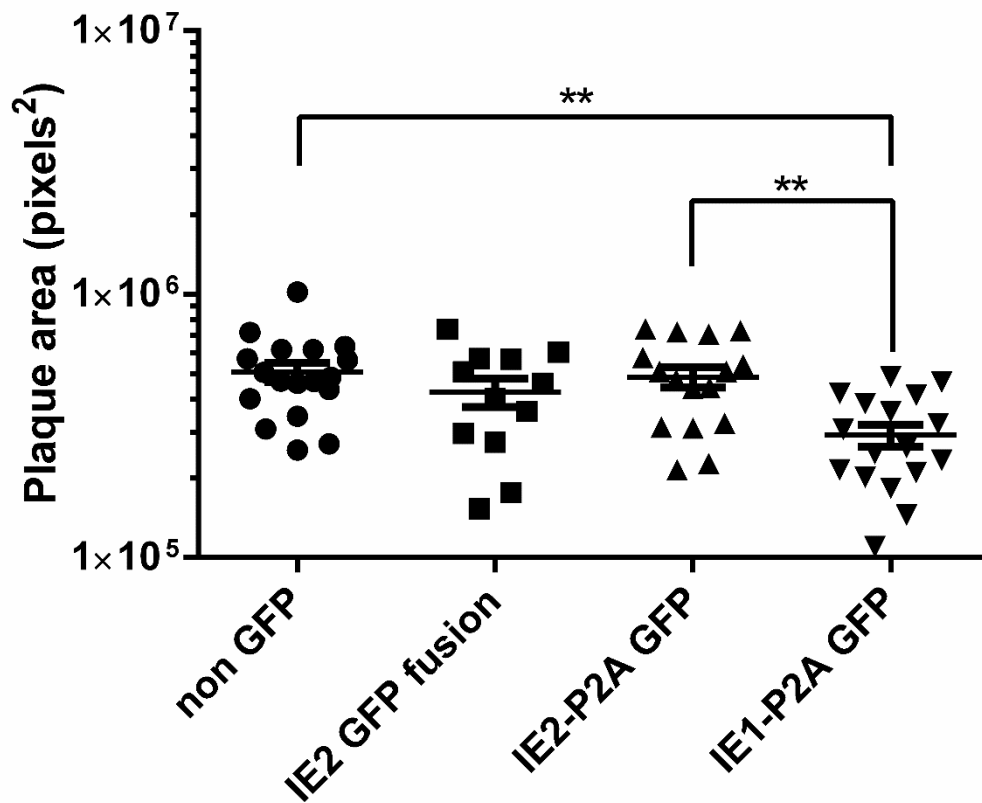


Figure 10 - Comparison of plaque sizes of current and novel reporter viruses. Plaque assays showed that IE1-P2A-GFP virus displays altered growth properties as reduced plaque size. HFFF Primary cells were infected with 40 pfu of each virus (in a WT genetic background), and covered with 2x DMEM and Avicel. 3 weeks PI overlay was removed, cells washed, plaques were IE1-stained and imaged on the Zeiss fluorescent microscope. Plaques were measured using Fiji ImageJ software. Results were subject to a one-way ANOVA with Tukey post-hoc analysis (\*\*= $P < 0.01$ ) Error bars display SEM.

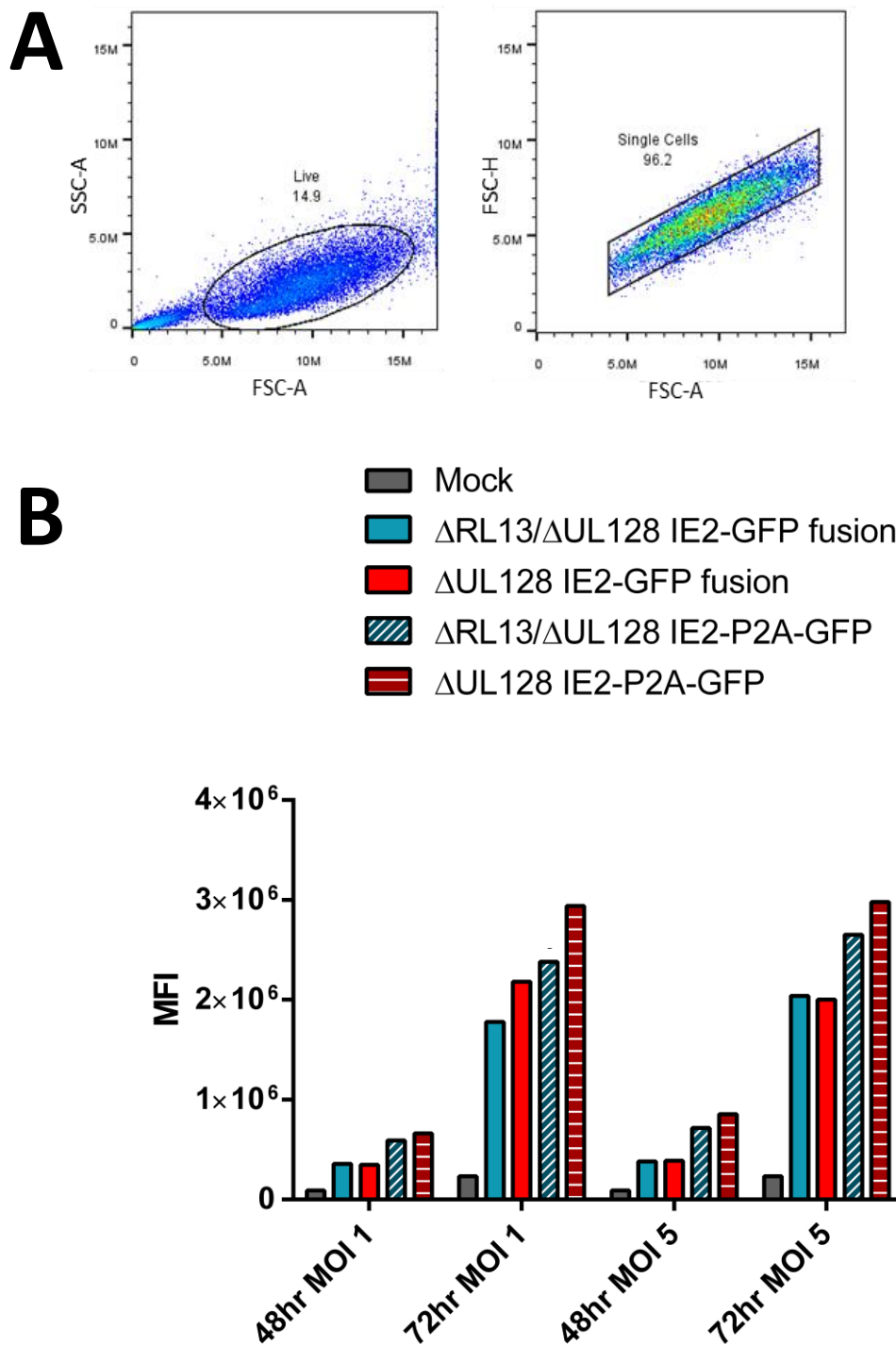


Figure 11 – Novel reporter viruses show brighter GFP expression than IE2-GFP fusion counter parts. HFFF terts were infected at an MOI of 5 with  $\Delta$ RL13/ $\Delta$ UL128 and  $\Delta$ UL128. At the two timepoints shown (48 and 72 hr) cells were trypsinised, fixed with 4% PFA and run on a BD Accuri flow cytometer. (A) The gating strategy used discriminated against dead cells and multiple cells. (B) Comparison of GFP expression from IE2-P2A-GFP and IE2-GFP viruses with and without RL13 expression. Comparisons were made at two MOI (1 and 5) and at two timepoints (48 hr and 72 hr). GFP expression was brightest at 72hrs compared to 48hr from both reporter viruses. Statistical analysis could not be performed due to lack of replicates.

## 3.2 Genetic Analysis of RL13

### 3.2.1 RL13 is a Hypervariable Gene

Passaging of HCMV in cell culture allows for the emergence and selection of mutants adapted for growth in an environment distinctly different to the natural setting that HCMV would encounter (193). Because of this, many of the HCMV strains used in today's research have multiple deletions, mutations and rearrangements within their genomes (225). Not only are the strains used genetically different to clinical virus but their biological properties have become distorted between stocks confirming the existence of strain genetic divergence and variance which has considerable impact on experimental studies (195). Although inhibitory *in vitro*, RL13 is conserved in-vivo suggesting that the gene is important for the survival of HCMV (37). RL13 is also known to be hypervariable (175). To investigate how variable the RL13 ORF is between clinical isolates, the sequences of 96 clinical strains with low *in vitro* passaging were obtained from NCBI (3) and CLC Main software used to align the RL13 ORFs of these sequences.

#### *Analysis of RL13 ORFs*

All 96 sequences were aligned as both the nucleotide and the protein sequences. Both the nucleotide sequences of the RL13 ORFs and the amino acid sequences amongst the 96 isolates displayed variation with the 3' and N terminus displaying the highest degree of conservation (Fig. 12A&B). Previously, the overall selective pressure on HCMV genes was investigated on these 96 sequences by calculating the  $dN/dS$  ratio (3). This compares the number of synonymous or silent (dS) and nonsynonymous or amino acid-changing (dN) substitution rates within a gene alignment. A ratio of 1 suggests a neutral amino acid substitution, whereas a ratio lower than 1 indicates purifying or stabilising selection. If the substitution provides a selective advantage the ratio is greater than 1 (226). Of all HCMV genes, 96%, including RL13, had a ratio of <0.5 (3). RL13 appeared to be under relatively strong evolutionary constraint despite its diversity, with a ratio of 0.321. For comparison, they calculated the ratio of gB (UL55), a glycoprotein found in abundance in the virus envelope and considered to be one of the most conserved human herpesvirus glycoproteins, to be 0.116 (3).

Considering RL13 seemed to be under stabilising selection we wanted to determine whether the RL13 ORFs could be grouped into distinct clades. Using the RL13 ORF sequences obtained, a Phylogram was created (Fig. 13). The Phylogram indeed exhibited distinct clades of RL13 ORFs variants. Some of these clades contain many of the RL13 ORFs suggesting that this particular variant sequence is quite frequent among clinical isolates. Thus, RL13 was hypervariable, however out of 96 clinical isolates, the levels of variation of RL13 ORF DNA sequence are relatively low as only 9 rough clades were generated. This may indicate that the gene is not actively evolving in current populations. Instead, genotypes are relatively fixed, and thus may be advantageous in certain patients or situations *in vivo*.

Consensus protein sequences were generated for each clade to understand the level of variation between clades (Fig. 14). Overall the transmembrane region and YxxL motif showed the highest conservation between clades, whereas the cytoplasmic region proved to be moderately conserved between clades. The signal peptide and Ig-like domain, which is the domain responsible for RL13's Fc binding capabilities, showed the greatest variation of the domains identified between clades.

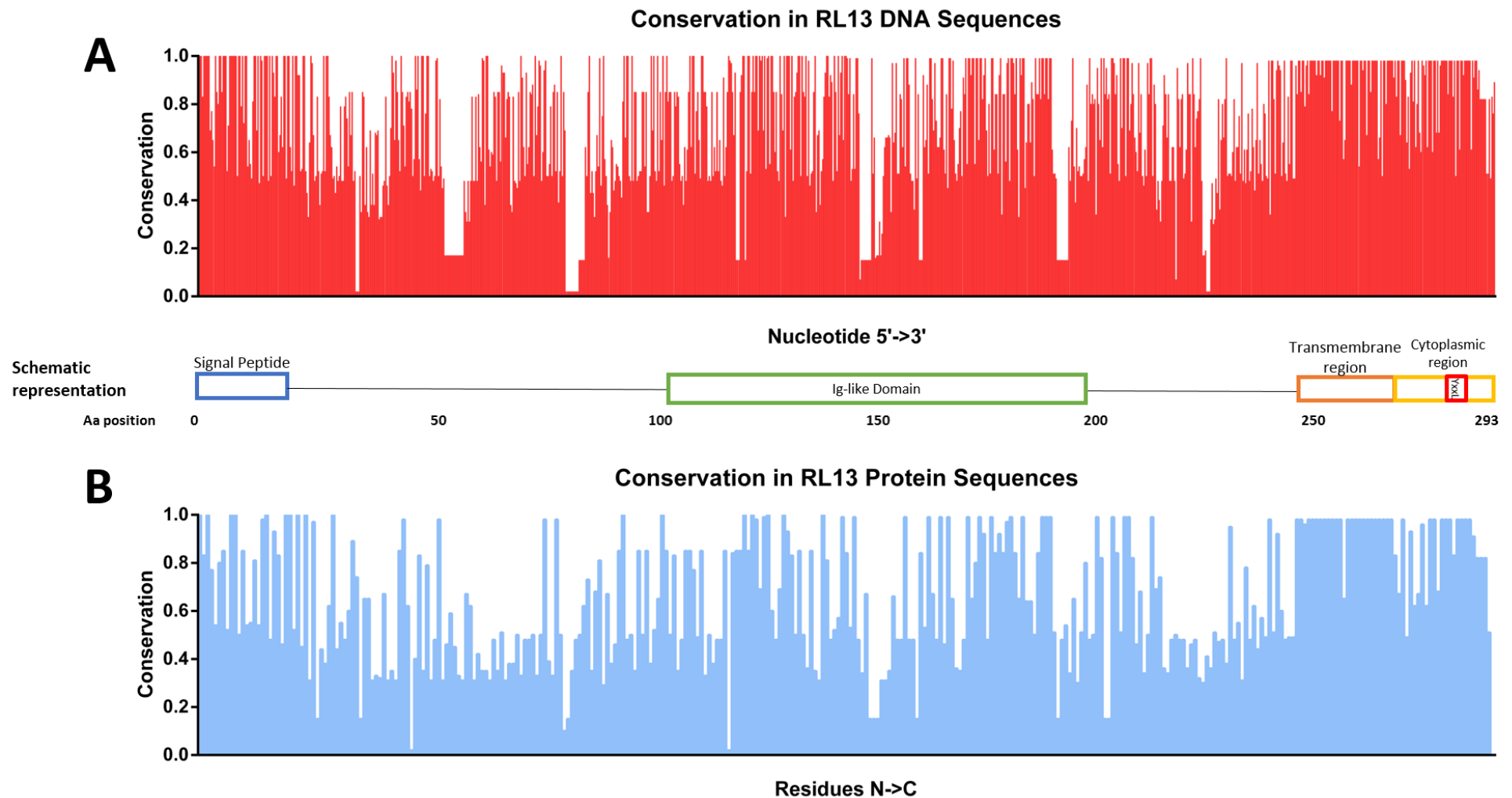


Figure 12 – Conservation of RL13 Nucleotide and Protein sequences with a schematic representation. Conservation of RL13 sequences between HCMV clinical strains with minimal passaging. Sequences obtained from (3) were aligned and processed using CLC Main software. (A) Conservation of nucleotide sequence. (B) Conservation of amino acid sequence. Schematic representation based on the Merlin sequence showing the signal peptide, Ig-like domain, transmembrane region, Cytoplasmic region and YxxL motif.

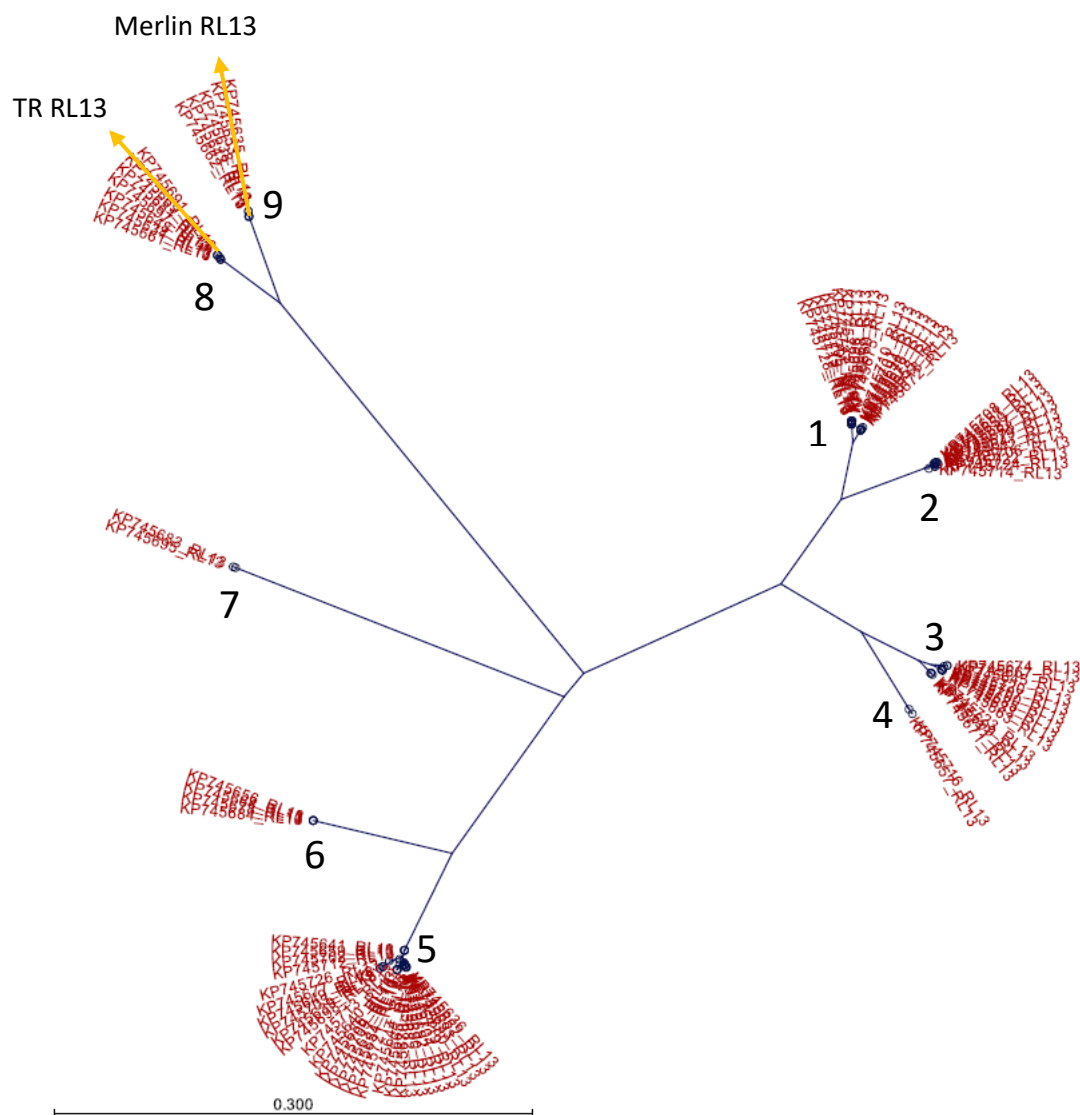


Figure 13 – RL13 ORFs cluster into distinct clades. Radial neighbour-joining tree illustrating the clustering of RL13 ORFs into 9 clades based on similarity of DNA sequence from clinical HCMV with minimal passaging. Sequences were obtained from (3) with the exception of Merlin (GenBank: GU179001.1) and TR (GenBank: AC146906.1) and the phylogram was created using CLC Main software. Scale bar shows divergence as substitutions per amino acid site. Clades are numbered 1-9 clockwise.



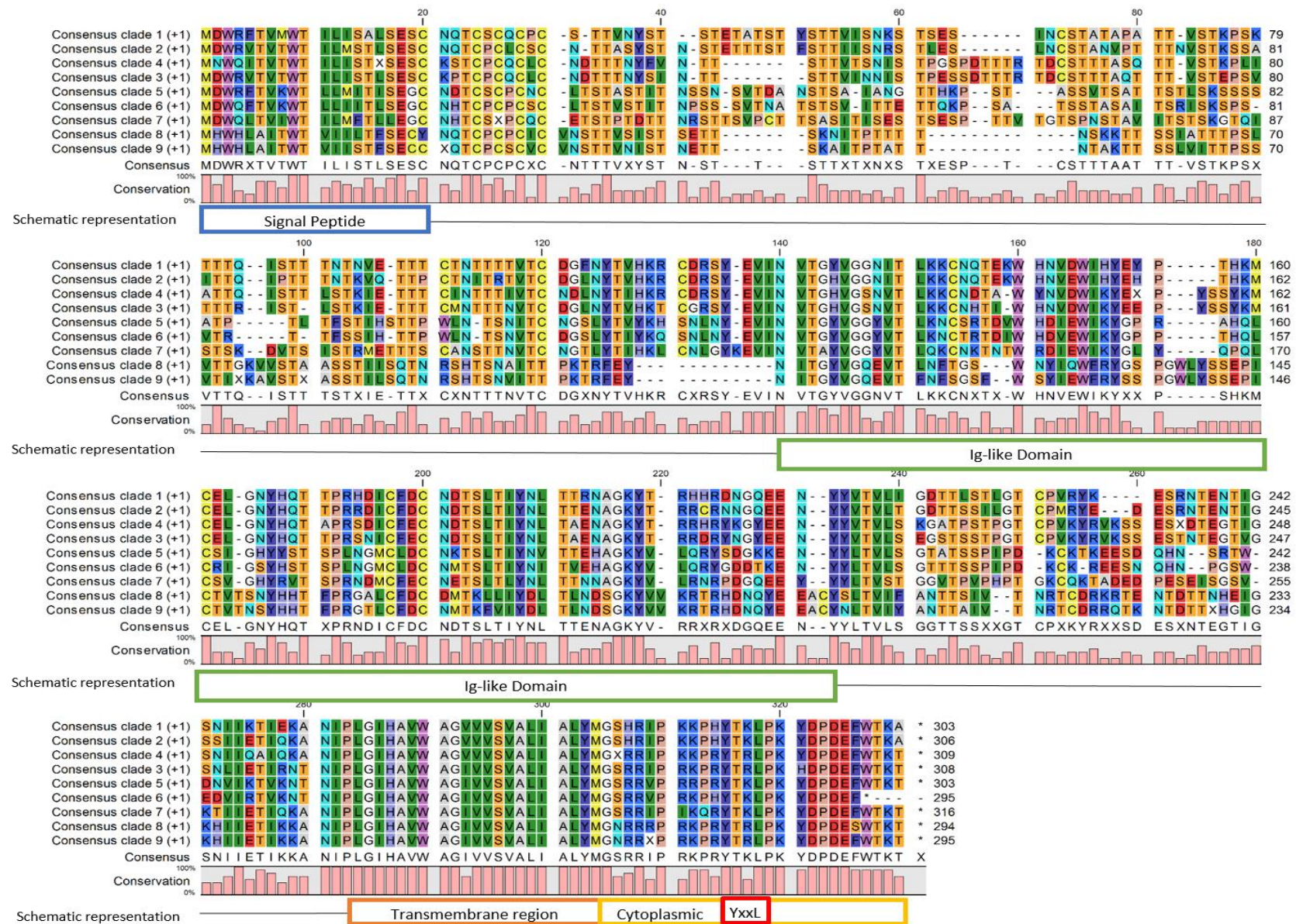


Figure 14 – Consensus sequences between clades display variation. Consensus protein sequences from each clade from figure 12 were generated using CLC Main software and aligned to determine whether any hotspots of variation could be determined between clades. The transmembrane region and YxxL motif showed the high conservation between clades, the cytoplasmic region showed moderate conservation whereas the signal peptide and Ig-like domain showed greatest variation. Schematic representation based on the Merlin sequence.



### 3.2.2 Insertion of TR RL13 into the Merlin BAC

#### *Generation of TR RL13 Merlin BAC Viruses by Recombineering*

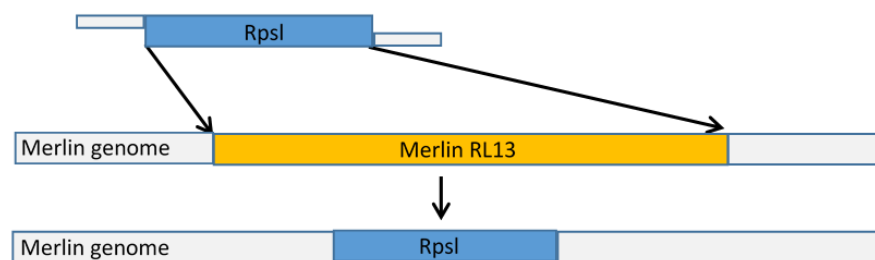
As RL13 is a hypervariable gene, the question arises as to whether all RL13 genotypes exhibit the same ability to repress virus growth. A construct was therefore designed in which the sequence of RL13 in Merlin was replaced with RL13 from another strain. The strain TR was chosen as the genome is readily available and TR RL13 is interesting in that it does not mutate during *in vitro* passage of the TR virus (208). Figure 15 shows the plan that was followed to insert TR RL13 into the Merlin genome in the place of Merlin RL13. The viruses created were TR RL13/ $\Delta$ UL128 and TR RL13, in both IE2-P2A-GFP reporter and a conventional virus (non-GFP) backgrounds. The Tet operator inserted upstream of Merlin RL13 was not removed, nor was it assessed to see if it still conditionally repressed TR RL13. As the viruses were tested directly from transfection there was no need to optimise the Tet operators for use with TR RL13.

#### *The Effect of Inserting TR RL13 into the Merlin BAC on Plaque Size*

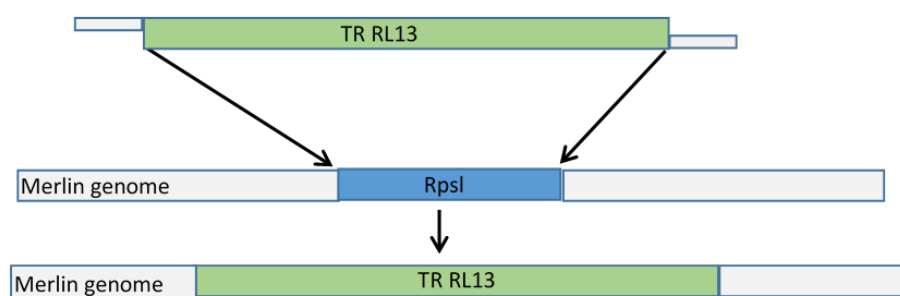
As RL13 significantly inhibits cell-free titres of virus and slows viral spread through the monolayer (203), by monitoring plaque size of the various viruses the effect of the specific RL13 genotype can be analysed. IE2-P2A-GFP viruses were used for ease of measuring plaques on the fluorescent microscope. Both TR RL13 and TR RL13/ $\Delta$ UL128 genetic backgrounds were compared to their Merlin RL13 counterparts. As TR RL13 remains intact during *in vitro* propagation of the TR virus, it is possible that the ORF does not inhibit virus growth, or is not well expressed (208). If this were the case +TR RL13 virus should produce plaques considerably larger than +RL13 Merlin virus.

All viruses expressing either Merlin RL13 and/or UL128 displayed smaller plaques than those of the  $\Delta$ RL13/ $\Delta$ UL128 virus (Fig. 16). The presence of TR RL13 in the virus produced plaques that were comparable to the size of those of the Merlin RL13 counterparts. Viruses expressing both UL128 and either TR RL13 or Merlin RL13 displayed the smallest plaques.

**1<sup>st</sup> round**



**2<sup>nd</sup> round**



*Figure 15 - Recombineering plan to create TR RL13 Merlin BAC. Plan to construct TR RL13 in Merlin. 1<sup>st</sup> round to insert the RpsI cassette in the place of Merlin RL13. During the 2<sup>nd</sup> round the RpsI cassette is then replaced with the TR RL13 sequence.*

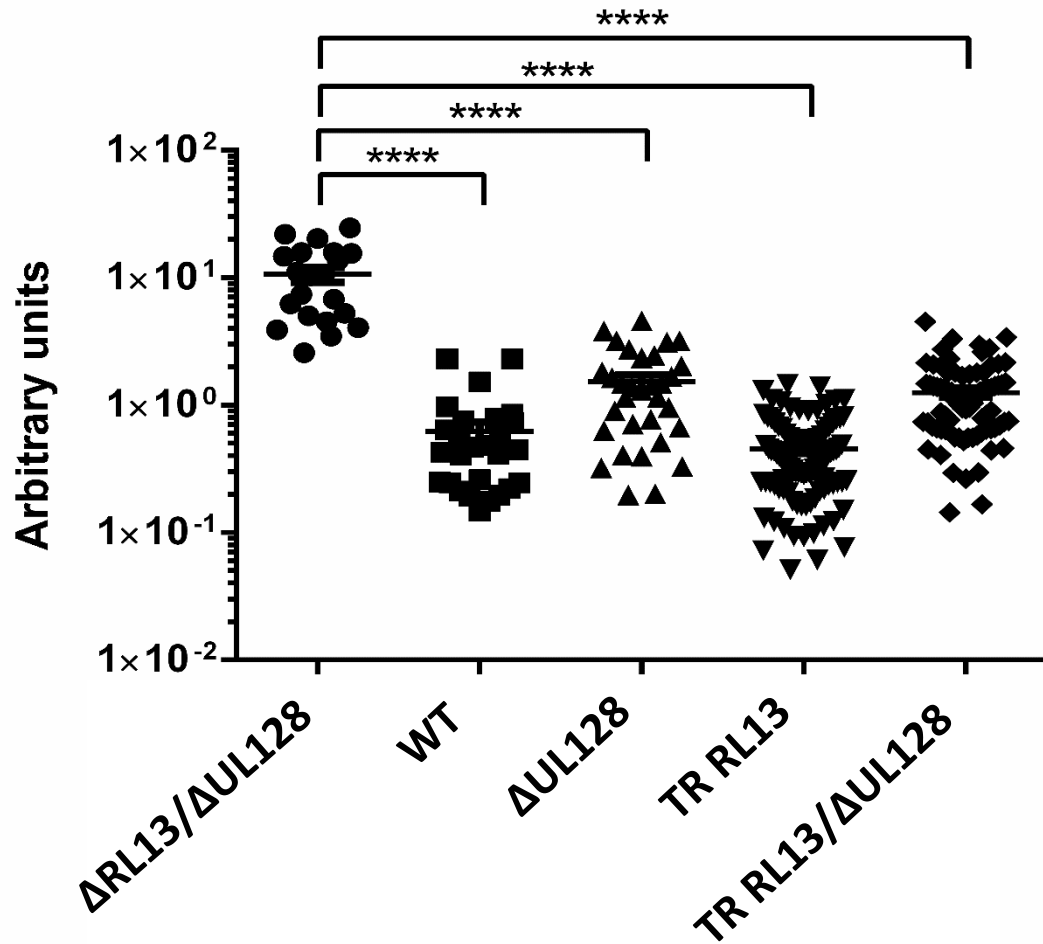


Figure 16 – TR RL13 displays the same phenotype as Merlin RL13 as similar sized plaques. Plaque assay to analyse the effect of TR RL13 on the growth properties of Merlin HCMV. HFFF Primary cells were transfected with  $2\mu\text{g}$  IE2-P2A-GFP BAC DNA, seeded and left in DMEM 10% for 24 hr to recover. The next day cells were overlaid with 2x DMEM and Avicel. 2-3 weeks PI overlay was removed, cells washed and plaques imaged on the Zeiss fluorescent microscope. Plaques were measured using Fiji ImageJ software. Results were subjected to one-way ANOVA with Tukey post-hoc analysis (\*\*\*\*=  $P < 0.0001$ ). Error bars display SEM.

### *TR RL13 Sequence Variation*

To determine whether the TR RL13 sequence, which is different to Merlin RL13, had mutated during *in vitro* passaging of the TR virus, a BLAST nucleotide search was performed. The search revealed 10 hits with 100% identity to TR RL13 (shown in table 15). The 10<sup>th</sup> hit (shown in table 15 in bold italics) is the TR BAC itself (Fig. 15). The remaining 9 sequences are all clinical HCMV isolates and passaged minimally or not at all. This includes the clinical TR isolate sequenced after several passages in fibroblasts. Since the HCMV strain TR RL13 ORF has an identical amino sequence to that in multiple circulating HCMV clinical strains, it is likely that the gene has not been modified during cell culture passaging.

**Table 15 – TR RL13 sequence similarity search.**

<b>Name</b>	<b>Identity to TR RL13</b>	<b>NCBI Accession number</b>	<b>Origin</b>
Human betaherpesvirus 5 strain PAV31, complete genome	100%	KY490061.1	Plasma from transplant patient. Sequenced directly from clinical material.
Human herpesvirus 5 strain JER5550, complete genome	100%	KR534212.1	Amniotic fluid. Sequenced directly from clinical material.
Human herpesvirus 5 strain NANU, complete genome	100%	KU550090.1	Neonatal urine. Sequenced directly from clinical material.
Human herpesvirus 5 strain HAN40, complete genome	100%	KJ361958.1	Bronchoalveolar lavage. Passaged twice before sequencing.
Human herpesvirus 5 strain 2CEN15, complete genome	100%	KJ361948.1	Bronchoalveolar lavage. Passaged once on human fibroblasts prior to sequencing.
Human herpesvirus 5 strain BE/22/2011, complete genome	100%	KP745653.1	Urine. Passaged twice on human fibroblasts prior to sequencing.
Human herpesvirus 5 strain BE/5/2012, complete genome	100%	KP745635.1	Urine. Passaged twice on human fibroblasts prior to sequencing.
Human herpesvirus 5 strain TR, complete genome	100%	KF021605.1	Isolated from a vitreous tumour from the eye of HIV-positive male. Passaged several times before sequencing.
Human herpesvirus 5 strain HAN13, complete genome	100%	GQ221973.1	Bronchoalveolar lavage. Passaged once on human fibroblasts prior to sequencing.
<b><i>Human Herpesvirus 5 TR-BAC isolate, complete sequence</i></b>	<b>100%</b>	<b><i>AC146906.1</i></b>	<b><i>TR BAC derived from the TR clinical ocular isolate. Passaged in fibroblasts.</i></b>

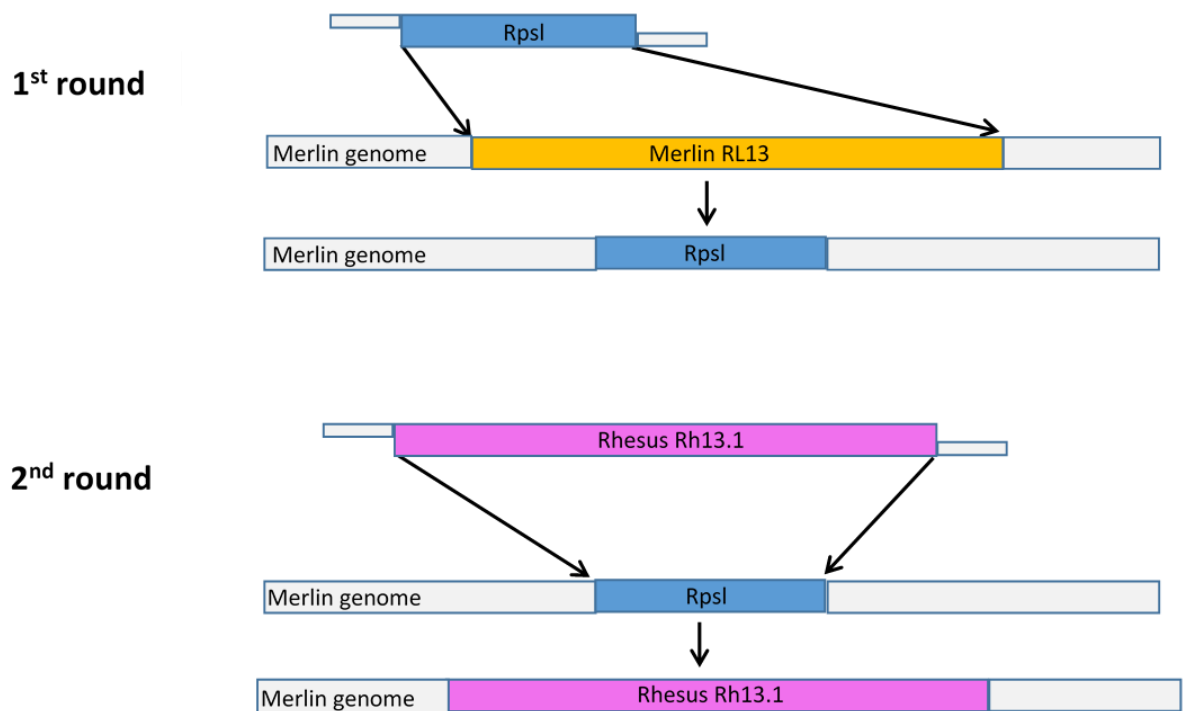
### 3.2.3 Insertion of Rhesus CMV RL13.1 into the Merlin BAC

#### *Recombineering*

Given that two divergent RL13 sequences had the same phenotype in the context of the Merlin genome, we wondered whether the ability to repress viral replication extended to RL13 sequences from CMV that infect different species. Therefore, the Rhesus Macaque CMV (RhCMV) RL13 homolog was used to replace Merlin RL13. RhCMV Rh13.1 is the closest known homolog for HCMV RL13 within the RhCMV genome (218). Rh13.1 exhibits significant homology in both sequence and length to HCMV RL13 (218), and displays a similar phenotype of inhibited viral growth when the ORF is expressed in RhCMV (Früh, personal communication). Figure 17 shows the plan to insert Rh13.1 in the place of Merlin RL13. This time, the first round BAC created in figure 15 (Rpsl in the place of Merlin RL13) could be used and the recombineering process was now to simply swap the Rpsl cassette with Rh13.1. Initially, the genetic backgrounds Rh13.1/ $\Delta$ UL128 and Rh13.1 were to be created as IE2-P2A-GFP and non-GFP viruses. However only the Rh13.1/ $\Delta$ UL128 IE2-P2A-GFP virus was successfully created in time. Like previously with the TR RL13 viruses, the Merlin RL13 Tet operator inserted upstream of the newly inserted Rh13.1 was not removed, checked or optimised for Rh13.1 expression as the viruses were simply intended for plaque assays following transfection.

#### *Plaque Assay*

A plaque assay was set up with the Rh13.1/ $\Delta$ UL128 virus created alongside the Merlin  $\Delta$ UL128 counterpart and a  $\Delta$ RL13/ $\Delta$ UL128 control (both IE2-P2A-GFP viruses). Plaques were measured on the fluorescent microscope, and relative sizes measured using Fiji Software. Unfortunately, the  $\Delta$ RL13/ $\Delta$ UL128 control transfection failed and therefore no plaques were present for measurements. The mean  $\Delta$ RL13/ $\Delta$ UL128 plaque size, generated from a previous experiment (Fig. 15) is included in figure 18 for reference only. Plaque sizes of the  $\Delta$ UL128 virus were small, as expected. The presence of Rh13.1 in the genome showed a slight increase in plaque size however this was not statistically significant, suggesting that Rh13.1 is also able to inhibit spread when expressed from the HCMV genome. However, this must be interpreted with caution as Rh13.1/ $\Delta$ UL128 plaques also show a fairly large range of sizes and the  $\Delta$ RL13/ $\Delta$ UL128 transfection used as a positive control for large plaques was absent.



*Figure 17 - Recombineering plan to create Rh13.1 in Merlin. Construct plan to insert Rh13.1 into Merlin. Only the 2<sup>nd</sup> round step was necessary as the RpsI cassette had previously been inserted into the Merlin BAC genome in place of RL13. The cassette was replaced with the Rh13.1 sequence.*

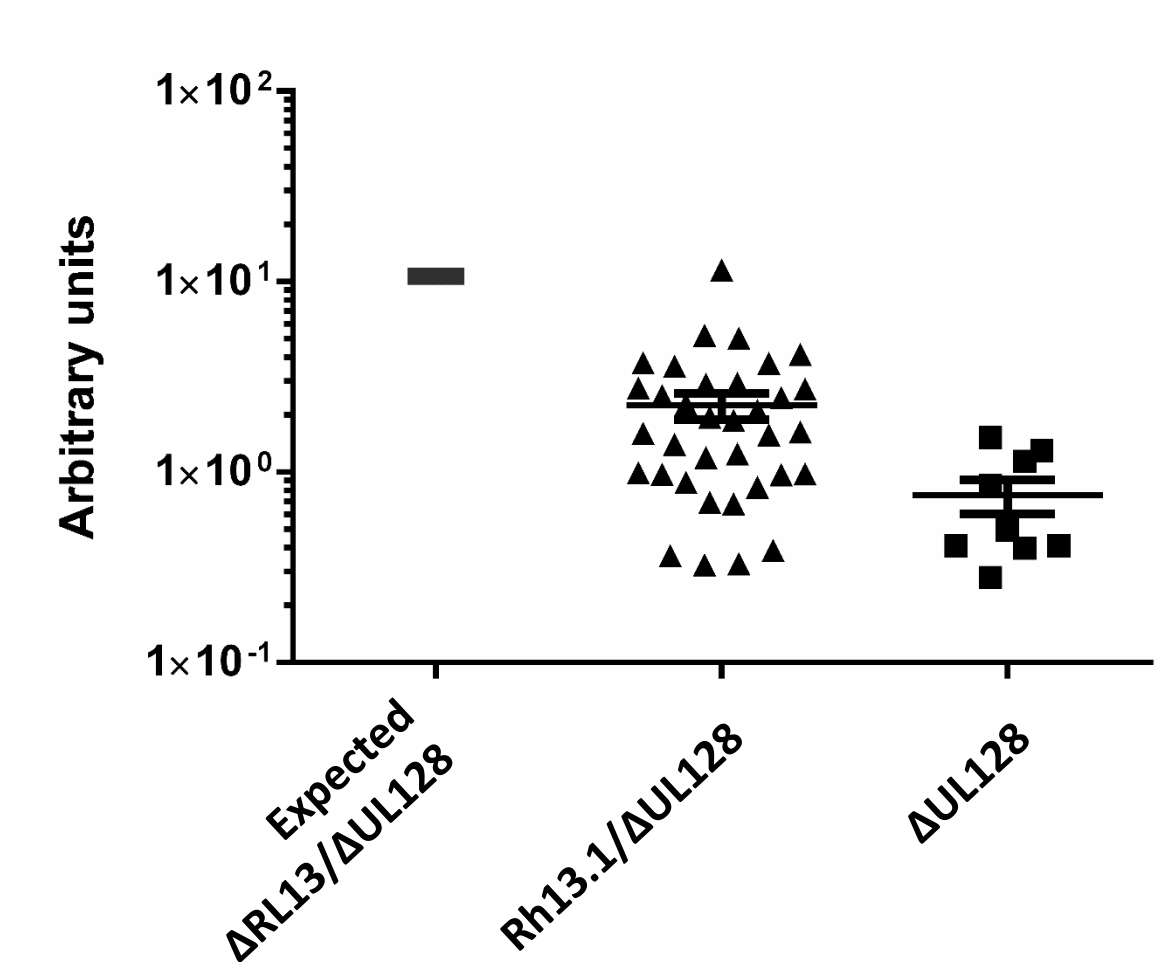


Figure 18 – The effect of Rh13.1 in the Merlin BAC on plaque size. Plaque assay to analyse the effect of Rh13.1 on the growth properties of Merlin HCMV. Although not significant, a trend of slightly larger plaque sizes is seen in the Rh13.1/ $\Delta UL128$  virus compared to  $\Delta UL128$ . The expected average plaque size of the  $\Delta RL13/\Delta UL128$  control is seen displayed as a grey line.  $2\mu\text{g}$  IE2-P2A-GFP BAC DNA was transfected into HFFF Primary cells, seeded and left in DMEM 10% for 24 hr to recover. The following day cells were overlaid with 2x DMEM and Avicel. Overlay was removed 2 weeks PI, cells washed and plaques imaged on the Zeiss fluorescent microscope. Plaques were measured using Fiji ImageJ software. Results were subjected to one-way ANOVA with Tukey post-hoc analysis but no significance found. Error bars display SEM.



### 3.3 Chapter Summary

Multiple viruses were generated in this project, some as novel reporter viruses and others to look at different variants of HCMV RL13 and their effect on the growth phenotype observed for Merlin RL13. The generation of reporter viruses expressing GFP downstream of IE1 resulting in an earlier reporter virus was not achieved in this project due to problems during recombineering, transfection and growth of the viruses.

Recombineering in the four genetic backgrounds resulted in only the WT and  $\Delta$ UL128 backgrounds successfully accepting the construct despite numerous attempts. However, when attempting to propagate the virus in fibroblasts only the WT, albeit relatively poorly, produced infectious viral progeny. Although likely due to chance, this seemed counterintuitive as this background should be the worst to propagate virus from.

However, improved novel reporter viruses (IE2-P2A-GFP backgrounds) that did not show altered growth properties were successfully created. The sequences of these new HCMV reporter viruses were confirmed by sequencing, and will aid future experimentation. The IE2-P2A-GFP viruses displayed GFP expression at 48 hr at a slight increased trend in intensity (although not significant) compared to the previous GFP-fusion viruses. These reporter viruses will be useful for investigating the function of RL13. It would be informative to repeat the analysis of GFP expression from the new IE2-P2A-GFP constructs at earlier timepoints to see whether GFP expression could be achieved at 24hrs.

The transfer of TR RL13 was successfully inserted into the Merlin BAC and the resulting viruses (TR RL13, TR RL13/ $\Delta$ UL128) produced. Plaque assays with these viruses demonstrated that TR RL13 inhibits virus growth in the same way as Merlin RL13, when encoded in the Merlin genome. This transfer of phenotype occurred despite the considerable sequence differences between TR and Merlin and the fact TR RL13 is shown to remain genetically intact *in vitro* (208). Therefore, it is possible that factors elsewhere in the TR genome are responsible for maintaining intact TR RL13. It could be valuable to assess whether Merlin RL13 would be tolerated in the TR BAC. Although I did not explicitly check that the TR RL13 ORF is expressed in the context of the Merlin genomes, the fact that its presence repressed plaque size indicates that it was

expressed. The TR RL13 ORF sequence had 100% identity in many other clinical isolates, indicating that the TR RL13 sequence is not a product of *in vitro* passage.

An IE2-P2A-GFP virus containing Rh13.1 in the place of RL13 was also successfully created and used in a plaque assay to determine the phenotype of Rh13.1 in Merlin. The presence of Rh13.1 in the Merlin genome resulted in slightly larger plaques than those of the Merlin RL13 counterpart, although not statistically significant or to the extent as is usually observed for a virus lacking RL13. Thus, Rh13.1 may have a partial ability to inhibit virus spread in HCMV, although the experiment will need repeating with appropriate controls.

In this project only the RL13 ORFs from TR and RhCMV were analysed in the context of the Merlin genome. It would be interesting to analyse the growth phenotype of more RL13 HCMV variants that come from differing clades in the context of the Merlin genome in future experiments.

RL13 has been designated a hypervariable gene. Genetic analysis of multiple clinical HCMV RL13 ORFs in this project suggests that it may be more appropriate to describe RL13 as having multiple conserved genotypes. When sorted into a Phylogram the RL13 ORFs exhibited distinct clades that could represent multiple conserved genotypes. This could suggest an evolutionary purpose for each clade, such as immune evasion function. The consensus protein sequences of these 9 genotypes were aligned to assess whether each clade varied considerably from one another in specific regions of the protein sequence. Considerable variation was identified in the Ig-like domain and the signal peptide which could suggest that some clades don't share the Fc binding properties of clades 8 and 9 that TR and Merlin are found in, or that the difference in signal peptide could affect the efficiency of protein trafficking or even affect the protein translocation. More conservation was found between clades in the transmembrane domain, YxxL motif and to some extent the cytoplasmic region.

Overall the genetic analysis of RL13 improved our understanding of the variability of the gene and the generation of novel reporter viruses greatly helped the next steps investigating at which point RL13 acted upon the viral lifecycle (see Chapter 4) and analysing the functional effects of RL13 (see Chapter 5).

# **CHAPTER 4. THE EFFECTS OF RL13 ON THE VIRAL LIFECYCLE**

RL13 expression during *in vitro* Merlin infection dramatically reduces cell-free titres of virus and slows viral spread through the monolayer (203). To gain insights into how RL13 expression causes this remarkable phenotype, it was important to determine whether RL13 acted at a particular stage of the viral life cycle.

## 4.1 Replication

### 4.1.1 RL13 Expression has no Effect on Viral Genome Replication

#### *qPCR of Viral Genomes*

It was hypothesised that RL13 may affect the growth properties of Merlin *in vitro* by inhibiting replication of the virus genome. During this study it was also reported that RL13 interacted with host cell nucleoside diphosphate linked moiety X (nudix)-type motif 14 (NUDT14), a UDP-glucose pyrophosphatase, to affect viral DNA replication (227). Therefore, infections were set up with the four genetic backgrounds of viruses and DNA extracted from cells daily. qPCR was performed to measure the copy number of virus genomes in infected cells, and thus determine whether the expression of RL13 inhibited viral DNA replication over a 6-day timecourse. Amplification of UL55 (encodes gB) was measured relative to genomic control (GAPDH) for each sample. Over 6 days, there was no significant difference between any samples found (Fig. 19).

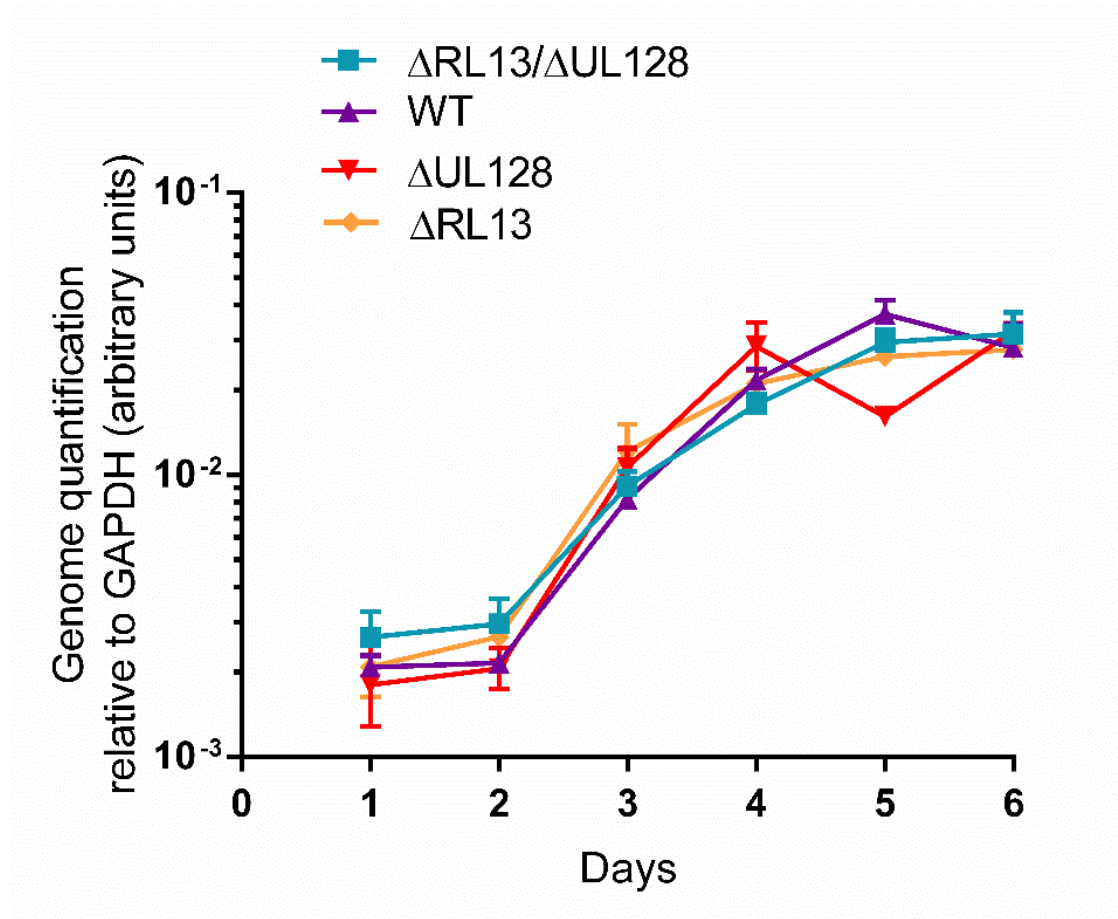
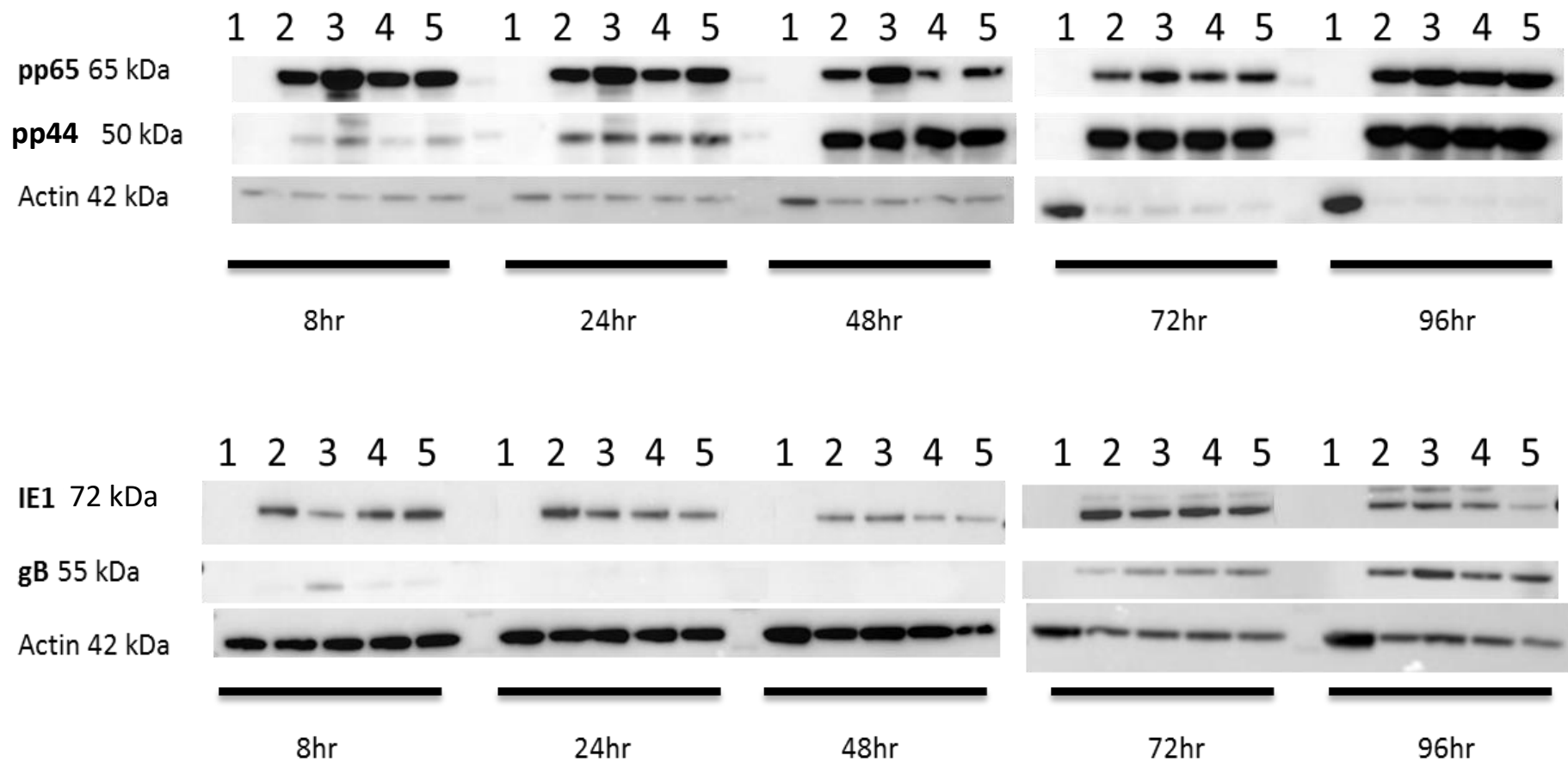


Figure 19 – RL13 expression does not affect viral genome replication. A qPCR was performed using primers to UL55 (gB gene) and endogenous control GAPDH on DNA produced from infected HFFF tert cells over a 6-day viral timecourse using the non-GFP viruses (MOI of 2). No statistically significant difference was found between samples at any timepoint. Data were subject to two-way ANOVA with Tukey post-hoc analysis. Error bars represent SEM.

#### **4.1.2 RL13 Expression has no Effect on Viral Protein Expression**

##### *Western Blot Analysis of the Temporal Protein Expression Cascade*

Since RL13 expression did not affect the efficiency of viral DNA replication, it was hypothesised that RL13 could be impairing the efficiency of virus-encoded protein expression. Infections were therefore performed with all four genetic backgrounds of virus at an MOI of 1 and analysed by western blotting. Immediate-early (IE1), early (pp44) and late (pp65 and gB) protein expression was analysed at 8, 24, 48, 72, and 96 hours. As expected, the levels of Actin in the uninfected control increased overtime. The expression of functional RL13 did not result in major or consistent differences in the temporal cascade of viral protein expression (Fig. 20).



*Figure 20 - Western blots showing temporal viral protein expression. Lanes: 1. Mock, 2.  $\Delta RL13/\Delta UL128$ , 3. WT, 4.  $\Delta UL128$ , 5.  $\Delta RL13$ . Fibroblasts were infected at an MOI of 1 with the non-GFP viruses and cell samples were taken at each timepoint in reducing buffer and subjected to western blotting. No obvious difference was found in the expression of immediate-early (IE1), early (pp44) or late (pp65 and gB) time points with regards to RL13 expression.*



### *Analysis of Early Viral Protein Expression*

The expression of some viral proteins did not follow the anticipated kinetics (210). The expression of gB, a late protein, was unusual in that faint expression was present at 8hrs, and not again until stronger expression present at 72 and 96 hr. pp44 is not expressed until 48 hrs, however there was faint expression present at 8 and 24hr. The late protein pp65 was expected from 72hrs onwards, yet it is seen throughout the timecourse. It seemed likely that protein present at earlier times represents protein from the initial input virus.

To investigate this, infections were repeated with the  $\Delta$ RL13/ $\Delta$ UL128 virus at an MOI of 1 and cell extracts prepared at 8 and 24 hr (Fig. 21). Cells were incubated with the protein synthesis inhibitor Cycloheximide before, during and post infection to determine whether proteins seen at the early timepoints were de novo expressed or not. The major IE protein (IE1) was detectable at 8hr and 24hrs post infection only when cycloheximide was absent. Therefore, the IE1 protein seen is synthesised at 8hrs and 24hrs and not due to input virus. The pp44 blot detected the protein in the 8hr samples with and without cycloheximide and again faintly with and without cycloheximide at 24hrs. pp44 expression was reduced by the presence of cycloheximide, which suggests that some of the protein seen at 8 and 24 is due to input virus. gB and pp65 were present with and without cycloheximide treatment, implying that the early bands seen were indeed delivered by the input virions. Infections were performed with (10%) and without (0%) FBS to determine whether this effected cycloheximide treatment results. Expression of all proteins, but especially gB, was stronger in the absence of FBS. This suggests that infection efficiency is increased in the absence of FBS which has been noticed before (Stanton, personal communication).

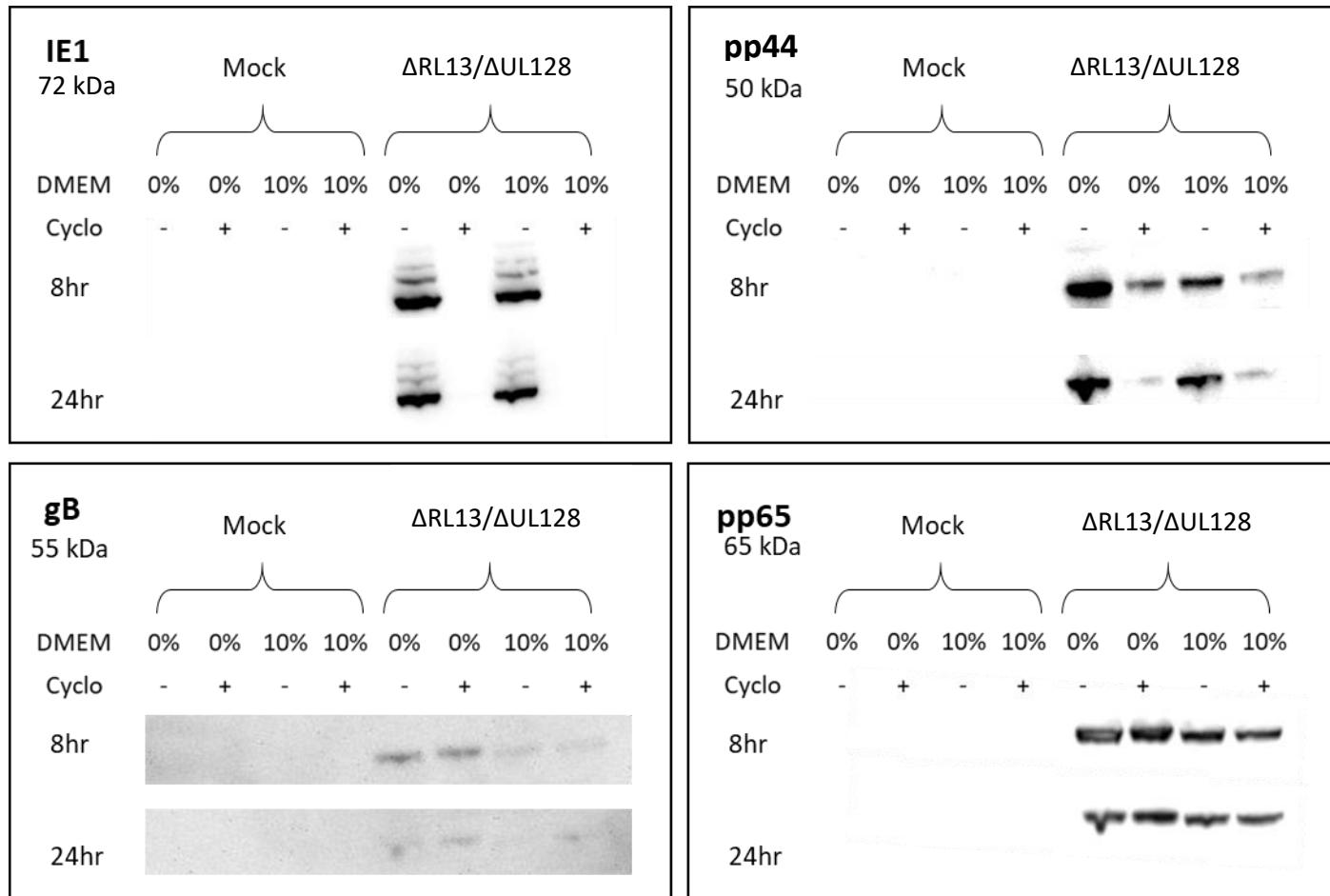


Figure 21 –Early detection of viral proteins attributable to input virions. Infections were set up with  $\Delta$ RL13/ $\Delta$ UL128 non-GFP virus (MOI 1) and Mock with/without cycloheximide. Infections were performed in both DMEM 0% and DMEM 10%. Blots confirmed that IE1 expression seen was de novo expressed, unanticipated pp44 expression was due to input virus. gB and pp65 unexpected expression is solely due to input virus.

## 4.2 Maturation

### 4.2.1 Particle Formation Analysis

#### *Transmission Electron Microscopy analysis of HCMV infected cells.*

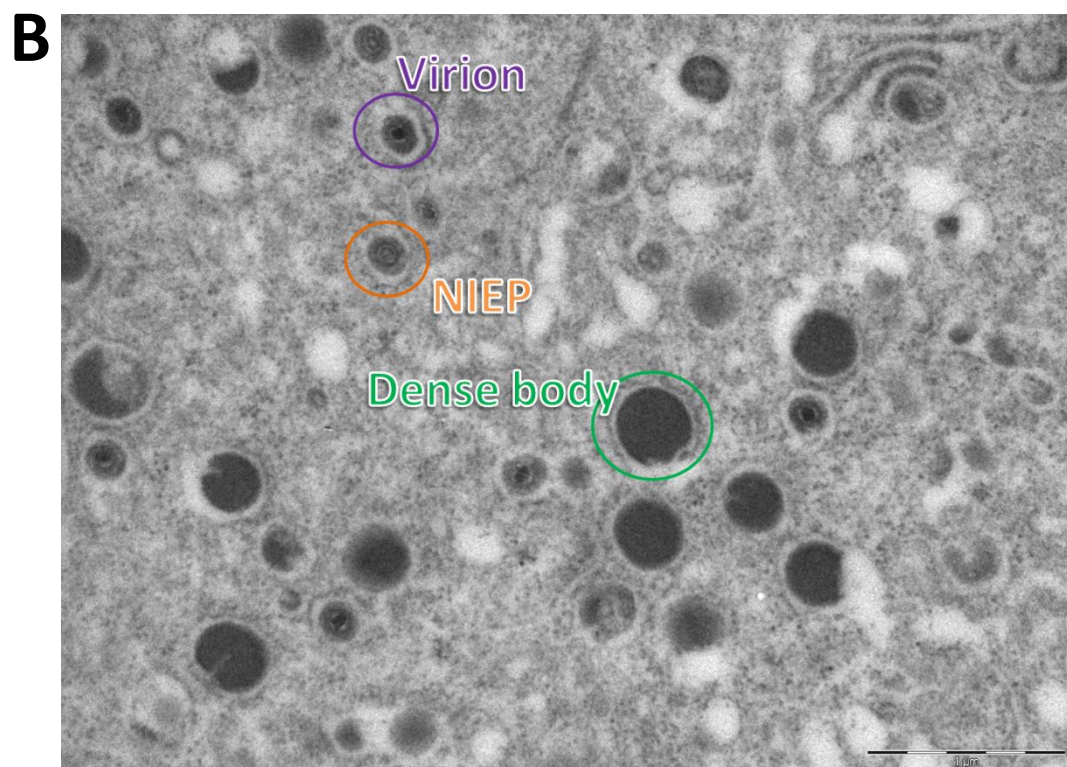
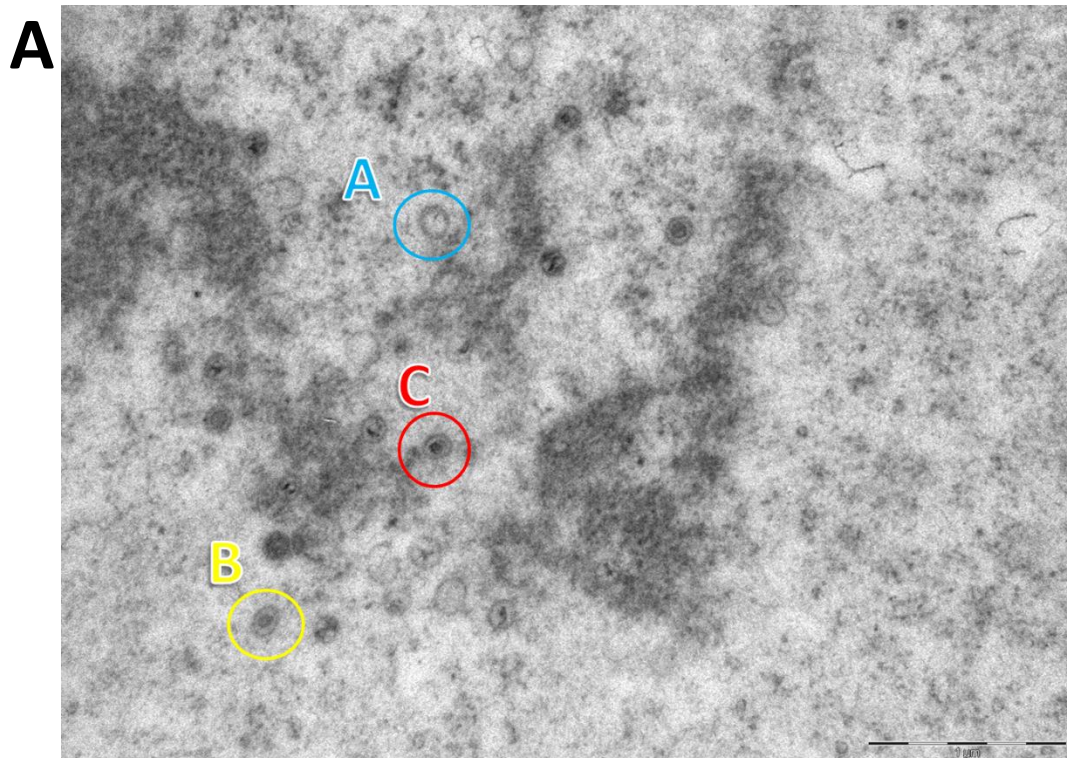
As RL13 expression reduced cell free titres (203), we next proposed that this could be due to a reduction in the number of infectious viral particles generated during infection. We wanted to look at the various particles that are assembled and matured in the infected cell before viral release. Transmission electron microscopy (TEM) was performed to determine the relative numbers of different particle types present during virion formation and maturation as detailed in the Introduction (Section 1.3) and Table 16. Infections with the four genetic backgrounds of virus were set up and 3 days post infection, samples were processed and multiple images taken of the nucleus (where capsids form), and the assembly compartment (AC) within the cytoplasm, where viral particles mature (7). An example of the structure of each type of virus particle quantified is illustrated in Figure 22 and described in Table 16.

#### *RL13 Expression had Minimal Effect on the Number of Viral Particles Formed*

Particles were identified and counted from 20 images from each compartment in each sample. The average particle ratios were calculated from the total particle counts for each compartment in each sample (Fig. 23). When RL13 is expressed there was an increase in the number of C-capsids produced, however this difference was not seen in the numbers of virions produced (Fig. 24), nor would the magnitude of this difference account for the >10-fold reduction in cell-free titres when RL13 is expressed. There was also no difference in average particle ratios in either compartment between the four viruses that reached statistical significance.

**Table 16 - Viral Particles to analyse within the Nucleus and Assembly compartment.** Adapted from (7).

LOCATION	NUCLEUS			ASSEMBLY COMPARTMENT		
PARTICLE	A-capsids	B-capsids	C-capsids	Dense bodies	NIEPs	Virions
DESCRIPTION	Thought to be the result of failed viral DNA encapsidation and lacking both viral DNA and a scaffold.	Likely to have resulted from failed capsid formation as they contain a scaffold but lack viral DNA.	Likely nucleocapsids during maturation, containing viral DNA and lacking scaffold.	Non-infectious enveloped particles lacking capsids and composed mainly of pp65.	Non-infectious enveloped particles (NIEPs) resulting from envelopment of B-capsids.	The only infectious particle containing viral DNA resulting from envelopment of C-capsids.



*Figure 22 - TEM images of the nucleus and the AC of cells infected with  $\Delta$ RL13/ $\Delta$ UL128. Cells were processed 96 hr post infection and sections cut and viewed by TEM by Dr Hobot. Both images show a scale bar of 1  $\mu$ m. (A) Nucleus with A- capsid (blue), B- capsid (yellow) and C- capsid (red) highlighted. (B) AC with Virion, NIEP and dense body highlighted.*

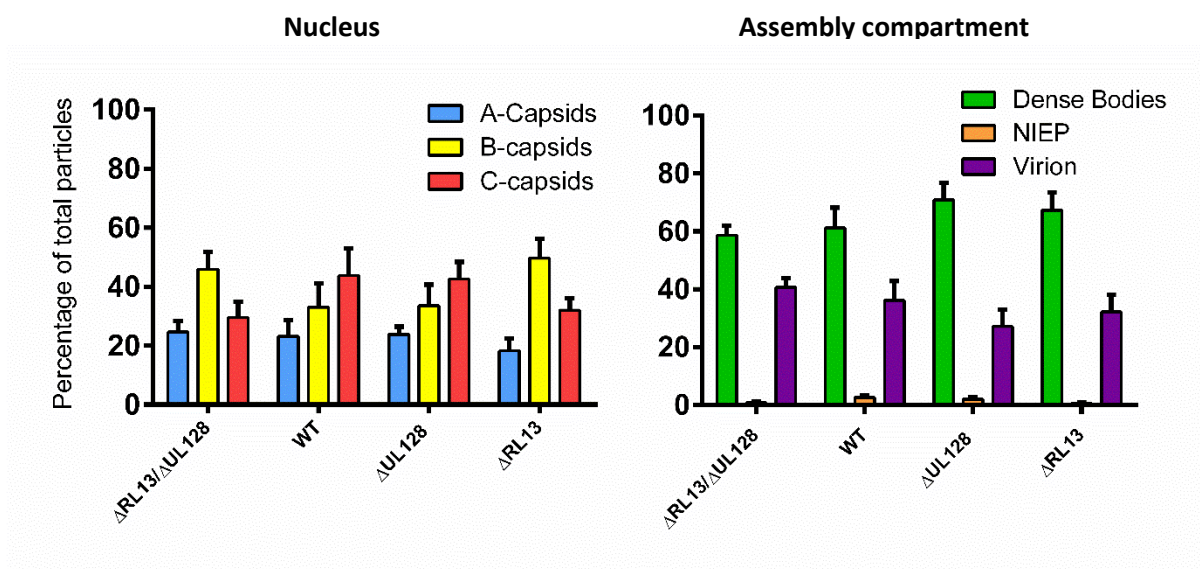


Figure 23 – Expression of RL13 shows no significant difference in the proportions of developing viral particles within either the nucleus or AC. 96 hr post infection cells were processed by Dr Hobot and sections cut and viewed by TEM. Particles were counted and average particle ratios calculated. No significant difference was found when comparing each particle ratio between viruses in either compartment when analysed by two-way ANOVA with Tukey post-hoc analysis. Error bars display SEM.

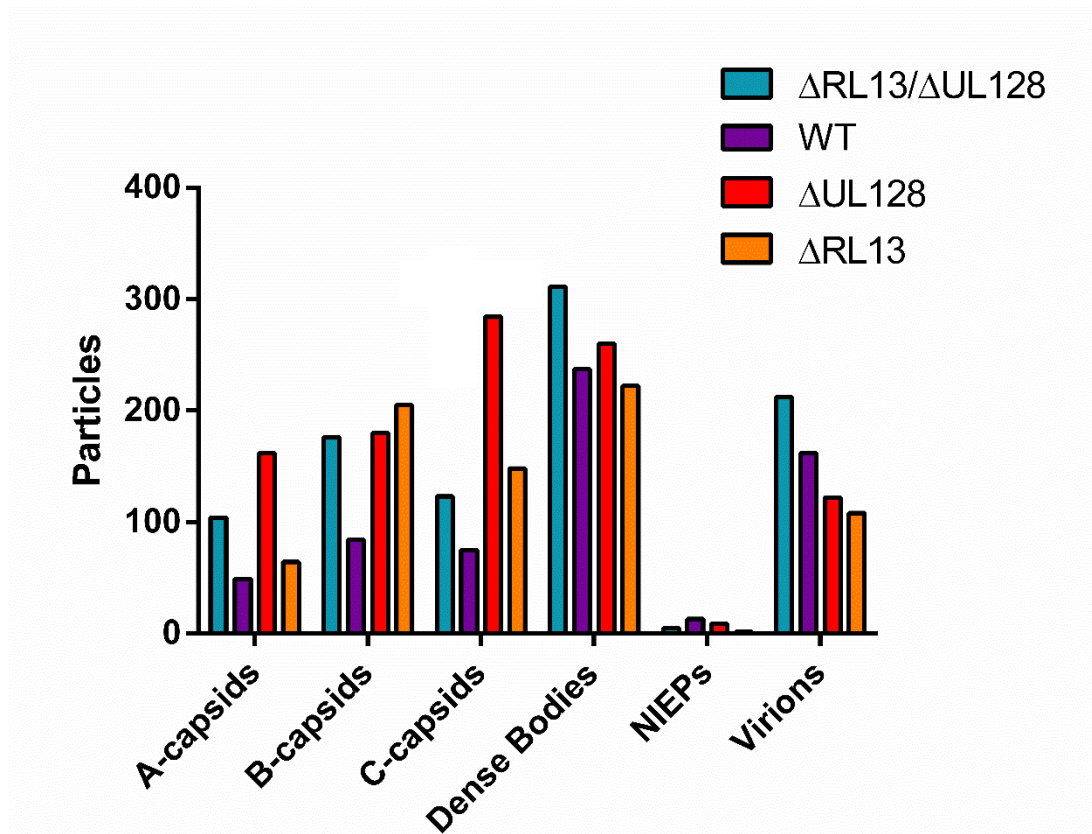


Figure 24 –  $\Delta UL128$  infection produced the greatest total number of C-capsids in the nucleus, however this did not affect the number of virions that mature. 96 hr post infection cells were processed by Dr Hobot and sections cut and viewed by TEM. Particles were counted and total particle numbers calculated. Total C-capsid numbers increased when only RL13 and not UL128 is expressed. No other great difference in total particle numbers was found between each virus. As data is total particle numbers counted, statistical analysis could not be performed due to lack of replicates.

## 4.3 Virion Release

### 4.3.1 Supernatant Virion Particle Numbers VS Infectivity

The difference found between the viruses in the types or numbers of virion particles present in the infected cell was not great enough to explain the >10-fold reduction seen in infectious titres of virus expressing RL13 and/or UL128. It was therefore hypothesised that either the infectivity of viral particles or the number of viral particles successfully released from a productive infection could be altered following RL13 expression.

#### *Analysis by qPCR and Titration Assay*

Cells were infected with the four genetic backgrounds of viruses. Supernatants were collected daily for 10 days and split between a titration assay to determine the infectious titre of the sample, and qPCR to determine the viral genomes (and therefore the viral particle numbers) present. This experiment was repeated numerous times as results varied between repeats. Results that are in line with the majority of findings are represented in figure 25.

The HCMV genome copy numbers detected in infected cell supernatants followed the same trend over time for all of viruses tested (Fig. 25A). The high viral genome copy numbers detected initially that were markedly reduced by day 3 must be due to residual input virus, even though the initial inoculum was washed off. Genome copy numbers then proceeded to increase steadily to their highest numbers at days 5-6. The increase in genomes then reduced gradually until the end of the timecourse. Although there was variation between the viruses at certain timepoints, these differences were neither large nor consistent, nor did they correlate with expression of RL13.

The viral timecourse generated numerous samples needing to be titred. To reduce the number of HF Primary cells used, small scale IE1 immuno-fluorescence titration assays were set up. Biological titres were calculated as fluorescent focus units (FFU) per mL of each virus at each time point. Similarly, to the particle numbers, the four viral titres also followed a very similar trend (Fig. 25B). Again, input virus was seen initially for most viruses which dropped at day 2. Titres began to rise at around days 3-5 and peaked around day 7 before tapering off.  $\Delta$ RL13/ $\Delta$ UL128 had the highest titre throughout the



timecourse as expected. Both UL128 and RL13 independently reduced biological titres, although expression of UL128 led to a greater reduction than RL13. Expression of both led to even lower titres.

Genome/FFU ratios were calculated for each sample at each timepoint (Fig. 25C). A low genome/FFU ratio would mean a virus is efficient at infecting cells. Expression of both intact UL128 or intact RL13 caused higher genome/FFU ratios, however the effect was more pronounced with UL128.

#### *Analysis by NanoSight and Titration Assay*

The results from the qPCR assays varied slightly between experiments. Unfortunately, there was no reasonable cellular DNA control to quantify genomes against for the supernatant samples, especially as samples were DNase treated to remove free DNA prior to extracting encapsidated DNA. Therefore, the experiment was repeated using a NanoSight to quantify particles directly. The NanoSight uses light and Brownian motion to detect, measure and quantify particles on a nanoscale (228), allowing for the quantification of HCMV virions. Samples were collected every other day during a 10-day infectious timecourse, then pooled and concentrated before titration, then further purified on glycerol-tartrate gradients before particle quantification on the NanoSight. As the viral timecourse sample numbers were reduced due to pooling of samples, titration by plaque assay was possible.

Mature HCMV virions range from 150-200nm (45, 74) to 200-300 nm (1) in diameter. Therefore, we focused on particles within a diameter range of 100-350 nm to ensure that all possible virions were recorded (Fig. 26). All viruses showed a similar pattern of particle size distribution between the sizes of 100-350 nm. The double mutant ( $\Delta$ RL13/ $\Delta$ UL128) displayed the greatest total particle numbers over 10 days (Fig. 27A). Viruses expressing UL128 showed only a very slight reduction in particle numbers, whereas viruses expressing RL13 showed approximately 10-fold lower total particle numbers, similar to the levels of the WT virus. This suggests that the expression of intact RL13 inhibits virion particle release. The total virion infectious titres over the 10-day infection displayed a similar pattern to the previous timecourse in that the expression of either RL13 or UL128 reduced total titres from the level of the double mutant (Fig. 27B), with an additive effect when both are expressed together. Genome/PFU ratios over the

10-days (Fig. 27C) were similar to those seen in the previous experiment (Fig. 24C). The double mutant ( $\Delta$ RL13/ $\Delta$ UL128) proved again to be the most efficient virus with the lowest genome/PFU ratio. Expression of UL128 gave a clear increase in genome/PFU ratio. Expression of RL13 also led to an increase in genome/PFU ratio, although this was not as dramatic as UL128 (Fig. 27C).

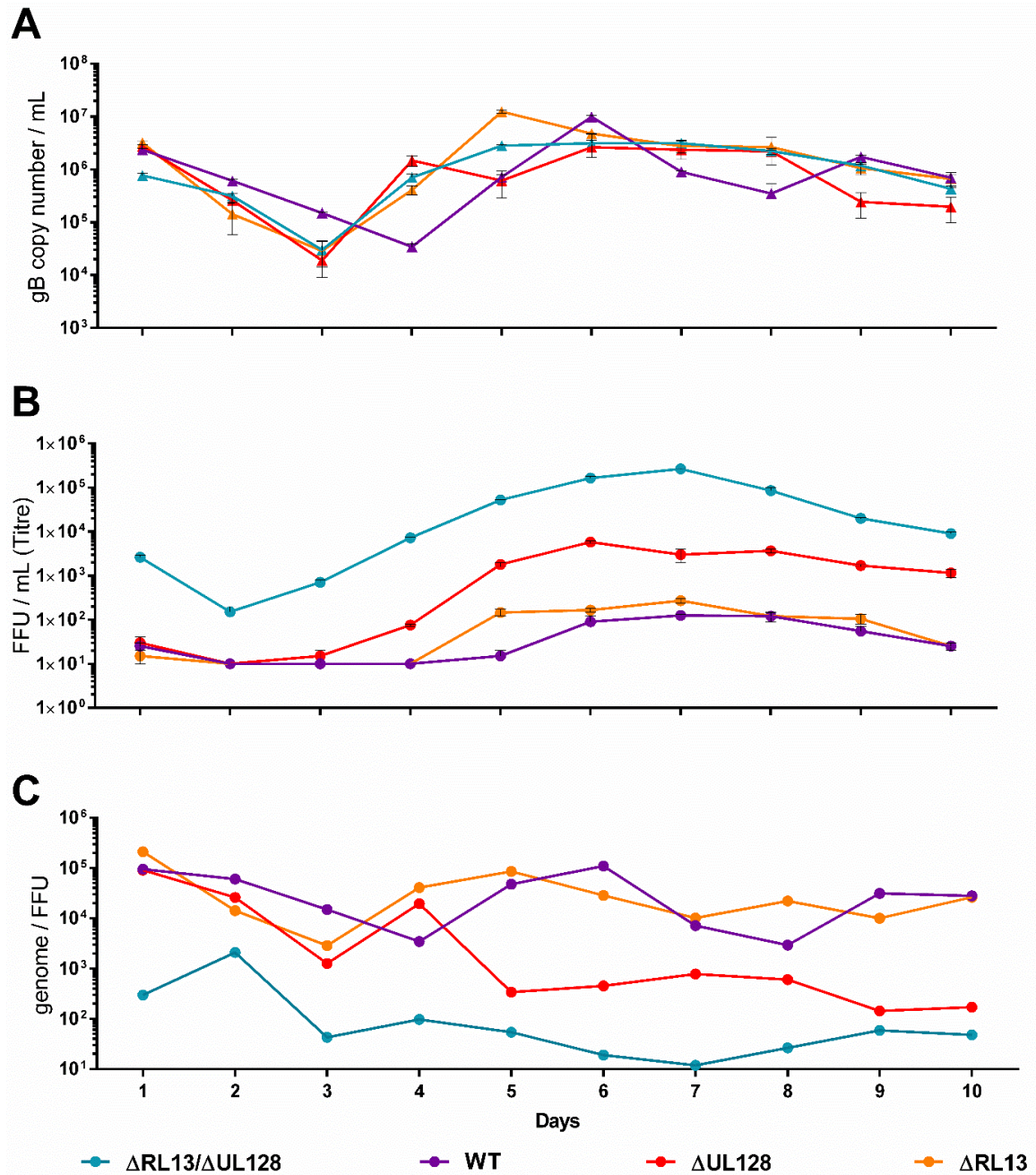
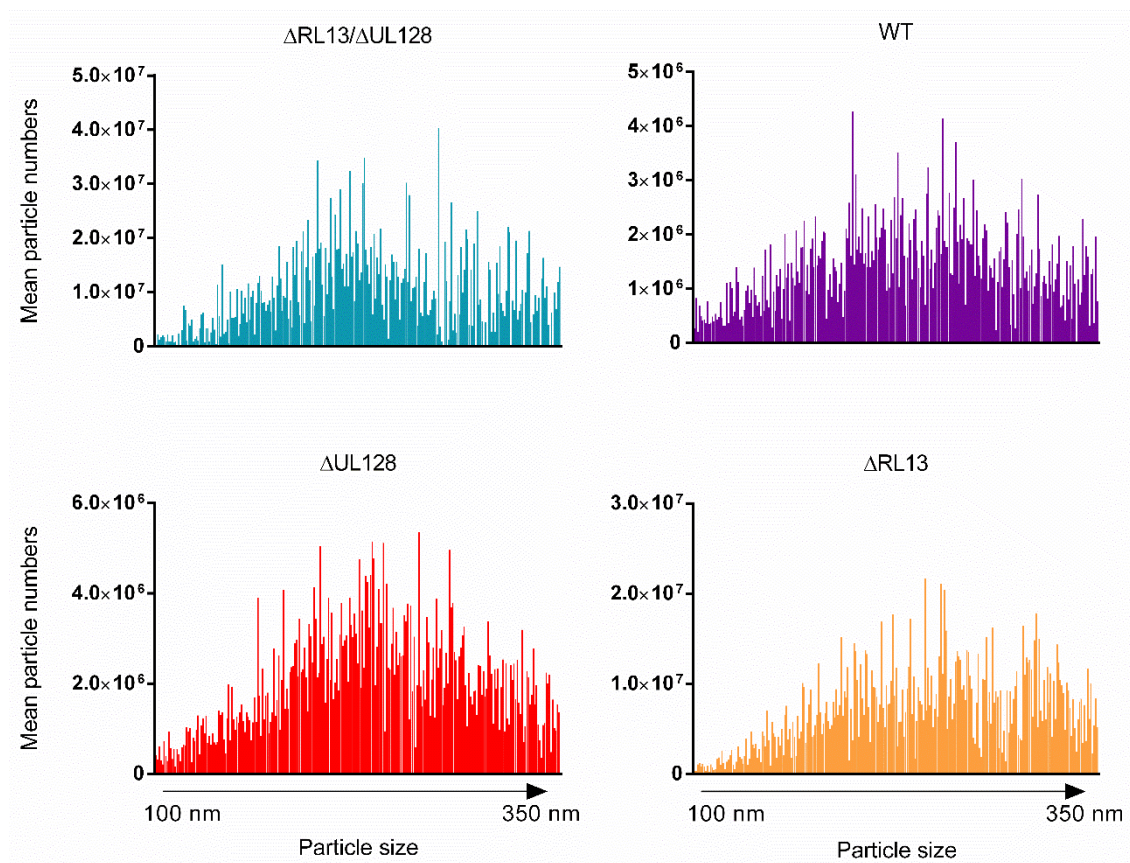


Figure 25 - RL13 expression does not affect genome copy numbers but does affect titre over a timecourse of 10 days. Cells were infected at an MOI of 8 with non-GFP viruses of all four genetic backgrounds. Supernatant was collected every day and split between a plaque assay and DNase treatment before qPCR. (A) Genome copy number quantified by qPCR showed no consistent significant differences between viral samples. (B) Titre of supernatant was measured by IE1-stained titration assay and calculated as FFU. A drastic reduction in titre was seen when RL13 is expressed. (C) Genome/FFU ratio of each virus. Data were analysed by Two-way ANOVA and all samples found to be significantly different to each other ( $p < 0.0001$ ) at each timepoint for both genome copy/ $\mu$ L (A) and titre (B). Genome/FFU ratios (C) between viruses were analysed by Two-way ANOVA and found to be statistically significant ( $p < 0.01$ ) from one another. Error bars display SEM.



*Figure 26 – Particle size distribution of viruses between 100-350 nm. Cells were infected at an MOI of 8 with non-GFP viruses of all four genetic backgrounds. Supernatant was collected, pooled and concentrated from a 10-day timecourse and split between a titration assay (Figure 23B) and NanoSight analysis of particle numbers. Particles were quantified within a 100-350 nm range and although particle numbers differed between viruses the size distribution of particles between 100-350 nm displayed a similar pattern.*



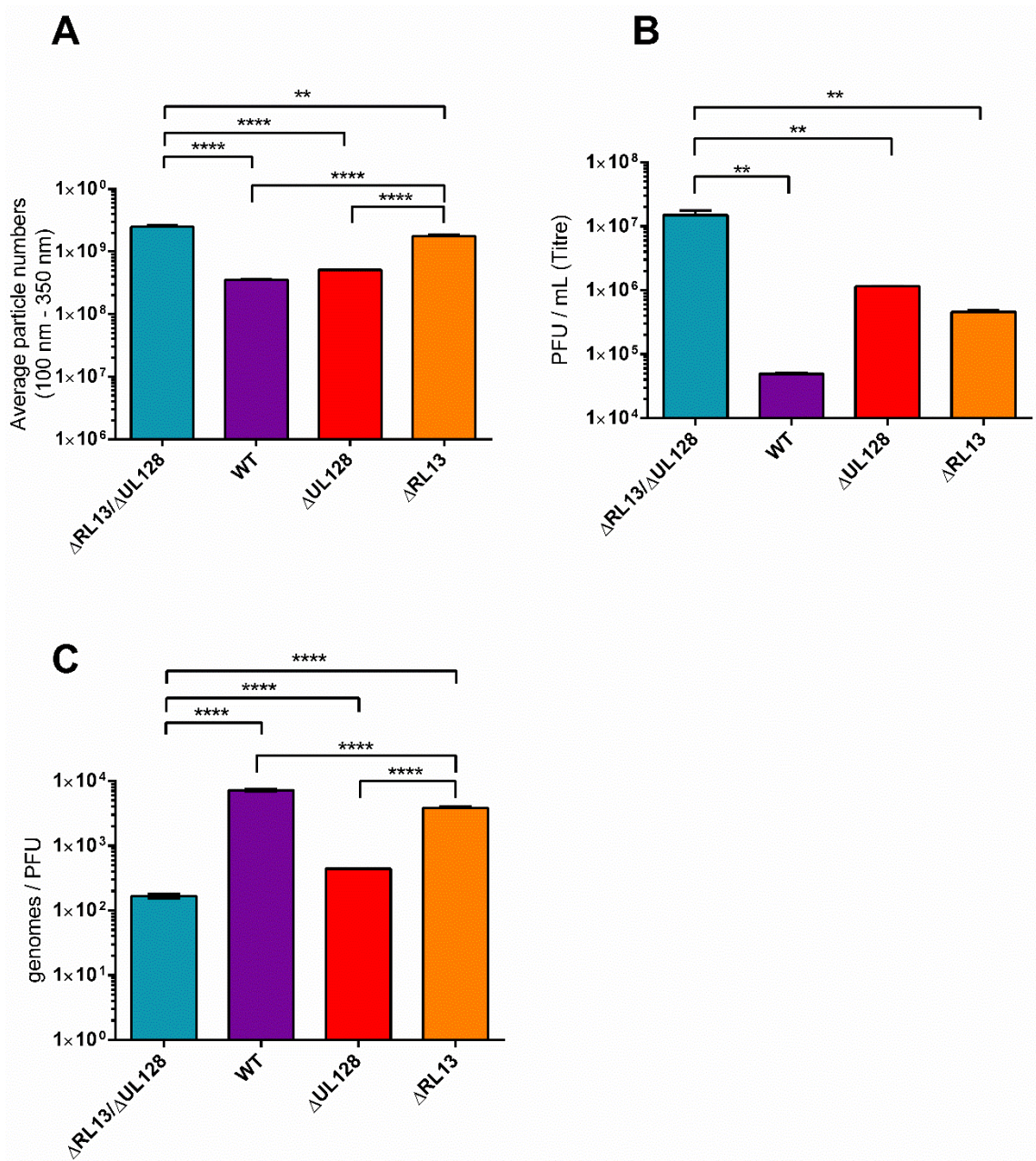


Figure 27 – RL13 expression results in a relatively low genome/PFU ratio despite reducing particle numbers and viral titre. Cells were infected at an MOI of 8 with non-GFP viruses of all four genetic backgrounds. Supernatant was collected, pooled and concentrated from a 10-day timecourse and split between NanoSight analysis of particle numbers (A) and a titration assay (B). Particles were quantified within a 100-350 nm range and results showed that expression of either RL13 and/or UL128 reduced particle numbers and viral titre. Genome/PFU ratios (C) were calculated and results showed that expression of UL128 causes a higher genome/PFU ratio. One-way ANOVAs were performed with Tukey post-hoc analysis (\*\*=  $P < 0.01$ , \*\*\*\*=  $P < 0.0001$ .) Error bars display SEM.

## 4.4 Chapter Summary

RL13 expression has been shown to dramatically reduce cell-free titres of virus and slow viral spread through the monolayer during *in vitro* Merlin infection (203). It was important to investigate each step of the viral lifecycle to gain more of an understanding of how RL13 expression could promote this phenotype.

When assessing the first few stages of viral progeny production no significant difference was found in viral genome quantification and so it was concluded that RL13 expression did not cause reduced cell-free titres and inhibited growth *in vitro* by inhibiting viral genome replication. The expression of RL13 also had little effect on the temporal protein expression cascade when looking at selected viral proteins from different kinetic classes, over a timecourse of 96 hrs. The expression of some of these proteins however was unusual and further steps were taken that showed the presence of early and late phase viral protein at the earliest timepoints could be attributed to input virions. For example, pp65 was found to appear much earlier than predicted but when infections were performed in the presence of cycloheximide conclusions could be made that this unusually early expression was due to input virions. Previous work has reported pp65 remaining in cells for hours which supports this conclusion. Pp65 has been found intracellularly 16hrs after infection (229) and has been found to remain on the cell surface up to 24hrs after infection (210). For greater insight this could be repeated with a greater selection of viral proteins from the kinetic classes.

When looking at the effect of RL13 expression on particle formation and maturation the expression of RL13 showed to minimally effect the proportions of developing viral particles within infected cells. However no significant differences were found between the average particle ratios of the viral samples within either compartment.

Finally, the effect of RL13 expression on viral particle release and infectivity of those particles was assessed. Analysis of particle numbers using the qPCR approach produced somewhat variable results. Despite this, there was no experiment in which expression of RL13 resulted in a difference in genome copy number that would account for the >10-fold reduction seen in infectious titres. Particle infectivity was reduced by expression of RL13.

Due to variability in the qPCR assays, the experiment was repeated, but the qPCR assay was replaced with a NanoSight assay to determine particle numbers directly. The results showed that the expression of intact RL13 reduced both the infectivity of particles and the quantity of particles released. Interestingly it was expression of intact UL128 had a greater effect on genome/PFU ratios than RL13. RL13 expressing virus had the genome/PFU ratio most similar to that of the double mutant. However, it should be noted that the NanoSight experiment was only performed once and required pooling of timepoints as well as more significant levels of processing than the QPCR experiment, potentially accounting for the slightly different results. As the Genome/FFU and Genome/PFU ratios relied on the particle number analysis of both experiments the limitations of each assay extended to this data too.

Taken together, RL13 clearly acts to reduce particle infectivity, however more work is needed to determine whether there is a significant and consistent effect on particles released. This finding led the investigation to analyse gpRL13, as it is present in the virion envelope and comes into contact with cells during entry. Next I investigated whether the gpRL13 present on the virions had any functional consequences leading to this reduced infectivity, or whether it provided an immunological advantage for WT HCMV during *in vivo* infection.

## **CHAPTER 5. THE FUNCTIONAL EFFECTS OF RL13**



GpRL13 is not just a non-essential protein, its presence markedly inhibits virus replication *in vitro*. The incorporation of gpRL13 in to virions is a feature its shares with members of the UL128L. In the case of the three proteins encoded by UL128L, there is experimental evidence they impair virus infection of fibroblast by their effect on virion receptor recognition, through displacing the interaction between gO and gH/gL (Intro section 1.3.1.3). It is therefore important to consider the functional consequences of gpRL13 in the virions themselves. Values for HCMV titres could be reduced if gpRL13 were to affect how the virions are released, transmitted between cells or interact with cell-surface receptors during entry. In addition, previous work has shown involvement of RL13 with aspects of the immune system (173).

Therefore, the effects of RL13 on the virion, host cell and immune system were explored to determine whether any effects seen could be responsible for the loss in viral titre seen when RL13 is expressed. The published work stating RL13s role in immune evasion was also replicated with Merlin.

## 5.1 Effects of RL13 on the Virus

### 5.1.1 Analysis of Viral Infection Spread by Co-Culture

A consequence of RL13 and UL128L expression by clinical HCMV strains is that the virus is extremely cell-associated and must be transmitted primarily by direct cell-to-cell spread (103, 104). Interestingly, direct cell-cell infections in retroviruses has been shown to more readily overcome immune restriction factors as compared to cell-free infections (230). As RL13 forces HCMV to be transmitted directly from cell-to-cell rather than cell-free spread (203), Co-culture experiments were used to investigate whether RL13 enabled the virus to better overcome innate and intrinsic anti-viral host immunity. This was performed in multiple cell types that the virus would encounter during infection and also in the presence of IFN or neutralising antibodies. Understanding how HCMV spreads through tissues and immune cells such as fibroblasts, epithelial cells, DCs and LCs could greatly aid the design of vaccines and therapeutics to protect these cells during infection.

#### *DC/LC Co-Culture*

DCs are antigen-presenting cells and are thought to be some of the first immune cells to come into contact with HCMV during infection and aid viral dissemination and even reactivation from latency (231). As messengers between the innate and the adaptive immune systems, DCs establish themselves deep within mucosae and skin (231) whilst LCs are a tissue-resident DC uniquely found in the epithelium (232). In cell culture, immature LCs are resistant to cell-free infection with HCMV (233, 234), whilst monocyte-derived DCs are fully permissive to HCMV infection (231). Infection of LCs with Merlin lacking RL13 was likewise heavily restricted by the cell-free route, however infection by the cell-cell route was more efficient, indicating that cell-cell spread could more readily overcome innate immune responses (235).

Interferons (IFN) are a group of cytokine mediators that are released in response to a pathogenic threat and are a part of the innate immune response. Once bound to an IFN receptor an excess of Interferon stimulated genes are expressed in attempt to restrict and control the infection. IFN alpha (IFN $\alpha$ ) is a type I IFN also known as viral IFNs that are

induced by viral infections. IFN $\alpha$  is synthesized by most cell types when infected with virus (236).

Co-cultures between infected HF Terts and DCs/LCs were set up to investigate whether RL13 expression provided an advantage to the virus during infection in DCs and LCs enabling the virus to overcome IFN-induced antiviral factors. Experiments were conducted using all four genetic backgrounds of the IE2-GFP fusion viruses enabling the transmission of virus to be tracked by flow cytometry. HF-terts were infected and co-cultured 1:1 with either uninfected DCs or LCs, with or without IFN $\alpha$ . DC/LC were removed from the co-culture at 48hrs and percentage infection determined at 72hrs by the presence of GFP using Flow cytometry. Direct cell-cell spread of HCMV to monocyte-derived DCs and LCs was dependent on UL128 expression (Fig. 28A). The assay was repeated with viruses expressing functional UL128 and with or without IFN $\alpha$  (Fig. 28B). There was efficient cell-cell spread in all samples compared to  $\Delta$ UL128, although the addition of IFN $\alpha$  slightly reduced infection efficiency in both LCs and DCs. The effect of RL13 expression on cell-cell infection efficiency was comparatively small, but a significant reduction in infection efficiency could be attributed to RL13 (Fig. 28A and 28B). A cell-free control was set up with the HCMV virus TB40-BAC4, to test whether cell-free entry was restricted as previously reported (Fig. 28C). Both LC and DC cell-free infections were less efficient compared to cell-cell spread, and the addition of IFN $\alpha$  restricted infection further, as was seen previously with a virus lacking RL13 (Stanton, unpublished). Therefore cell-cell spread of virus in DCs and LCs proved to be more efficient than cell-free spread in the presence of IFN $\alpha$ , however this was independent of RL13 expression.

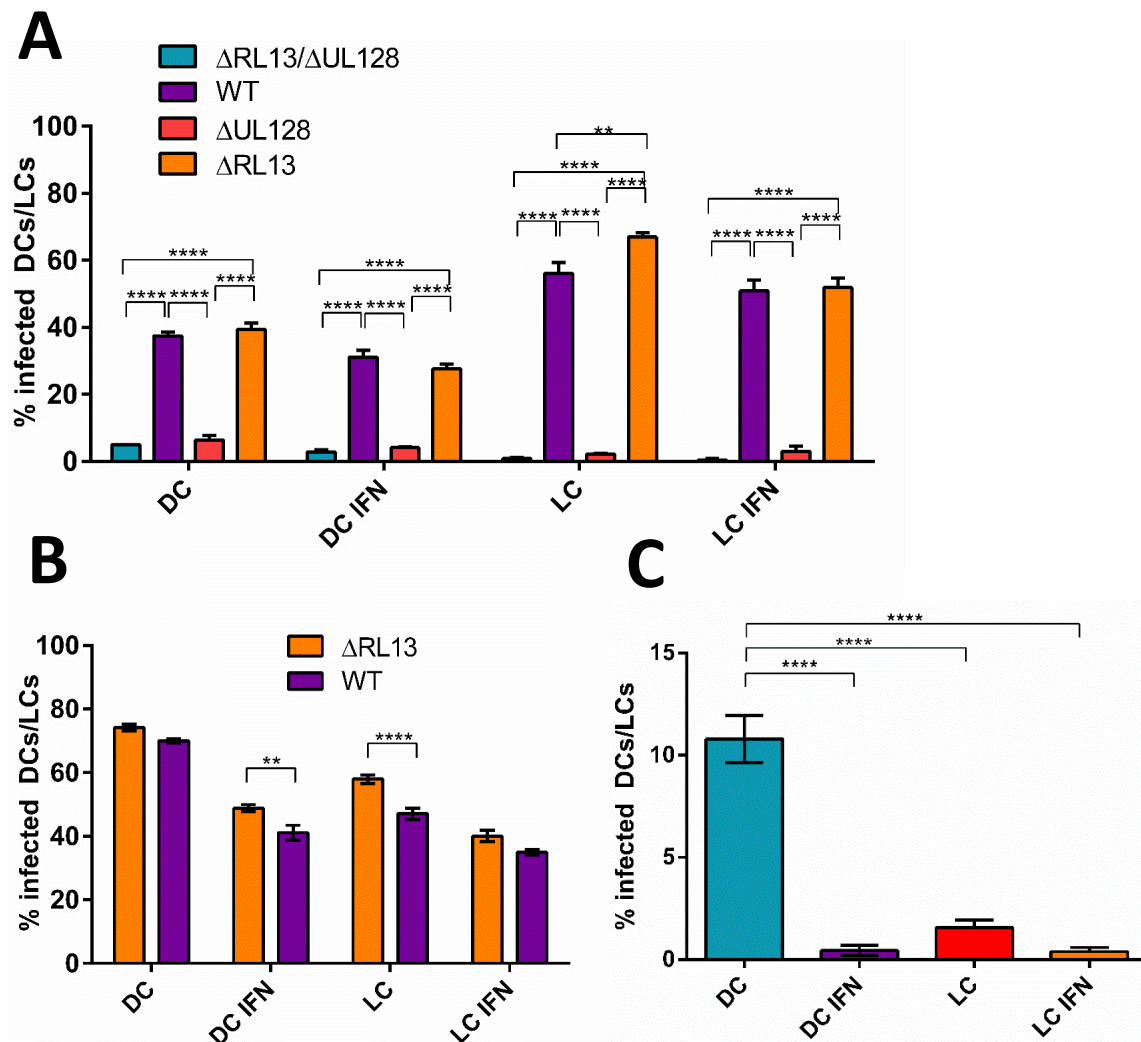


Figure 28 - Cell-cell spread is dependent on UL128 expression, however RL13 expression provides no advantage to cell-cell spread. DCs and LCs were co-cultured with HF terts infected with GFP expressing viruses. Non-adherent cells were removed and at 72hr post co-culture, percentage infection was determined by flow cytometry. (A) All four genetic backgrounds of virus were used with and without the treatment with IFN $\alpha$ . (B) Only viruses expressing UL128 were used for a repeat experiment. (C) Cell-free infections were set up as a control to ensure that restriction of cell-free infection occurred as previously reported. DCs and LCs with or without IFN $\alpha$  were infected with cell-free virus TB40 ( $\Delta$ RL13 reduced expression) for 72hrs after which cells were washed, fixed and stained for IE1 and DAPI. Fluorescent microscopy was used to take images and % infected DCs/LCs per field of view was calculated using Fiji. Data were analysed by two-way ANOVA with Tukey post-hoc analysis. Error bars display SEM.

### *HFFF Tert Co-Culture*

Retrovirus spreading via the cell-cell route is able to avoid the humoral immune response, unlike cell-free infections (237). As RL13 causes HCMV to remain highly cell-associated (203), it was important to determine whether RL13 affected sensitivity to neutralising antibodies. The effect of RL13 on cell-cell spread was investigated by performing co-cultures in the presence of Cytotect, a purified human IgG containing high titre HCMV-neutralising antibody. Approximately 60 infected HF terts were plated onto uninfected HFFF terts (Fig. 29), plaques were then allowed to form and sizes measured at various timepoints.

In HFFF tert–HFFF tert co-cultures (Fig. 29), plaque sizes of virus lacking both UL128 and RL13 were significantly larger compared to all other viruses. Virus expressing both RL13 and UL128 had even smaller plaque sizes than that of the single mutant viruses, showing that these genes have an additive effect on plaque size. Plaque sizes of virus lacking both UL128 and RL13 were inhibited by Cytotect in a dose-dependent manner. However, when either RL13 or UL128 were expressed, plaque sizes were unaffected by Cytotect. Thus, expression of either RL13 or the UL128L provided resistance to neutralising antibodies in HFFF.

### *ARPE19 Co-Culture*

The same co-cultures were set up with infected HFFF terts plated on ARPE19s (adult retinal pigmented epithelials) (Fig. 30) with a wider range of cytotect concentrations to determine if the same effect of RL13 expression was seen in another adherent cell type. Infections were set up only with virus expressing UL128, as viral entry and spread in epithelial cells is dependent on the pentameric complex. Plaque sizes from the virus containing RL13 were comparable across the different Cytotect concentrations. Virus expressing RL13 proved to be affected by neutralising antibody. Low levels of Cytotect resulted in enhanced infection as a slight increase in plaque size was observed. Although, these differences were only seen at the low cytotect concentrations, and were relatively small in magnitude. Overall, neither virus was inhibited by neutralising antibodies in ARPE19 cells regardless of the expression of RL13.

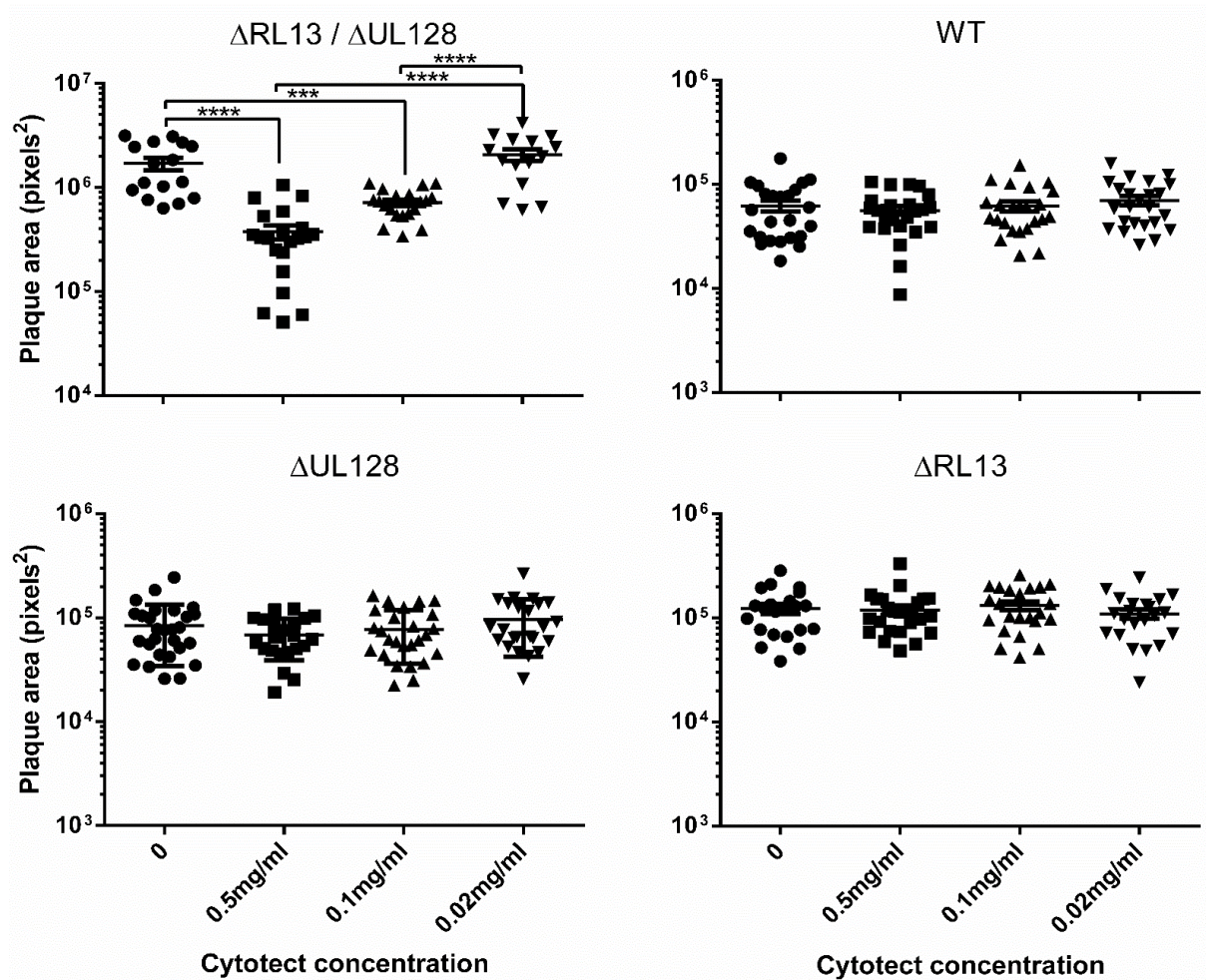


Figure 29 - Cell-cell spread of virus expressing RL13 and/or UL128 shows resistance to neutralising antibodies in HFFF Terts. HFFF terts were infected with GFP expressing viruses of all four genetic backgrounds with a varying concentration range of Cytotect and plated onto HFFF terts. Fluorescent images of viral plaques were captured and then measured. Plaques sizes displayed were measured at 10 days post infection. One-way ANOVAs were performed with Tukey post-hoc analysis (\*=  $P < 0.05$ , \*\*=  $P < 0.01$ , \*\*\*=  $P < 0.001$ , \*\*\*\*=  $P < 0.0001$ .) Error bars display SEM.

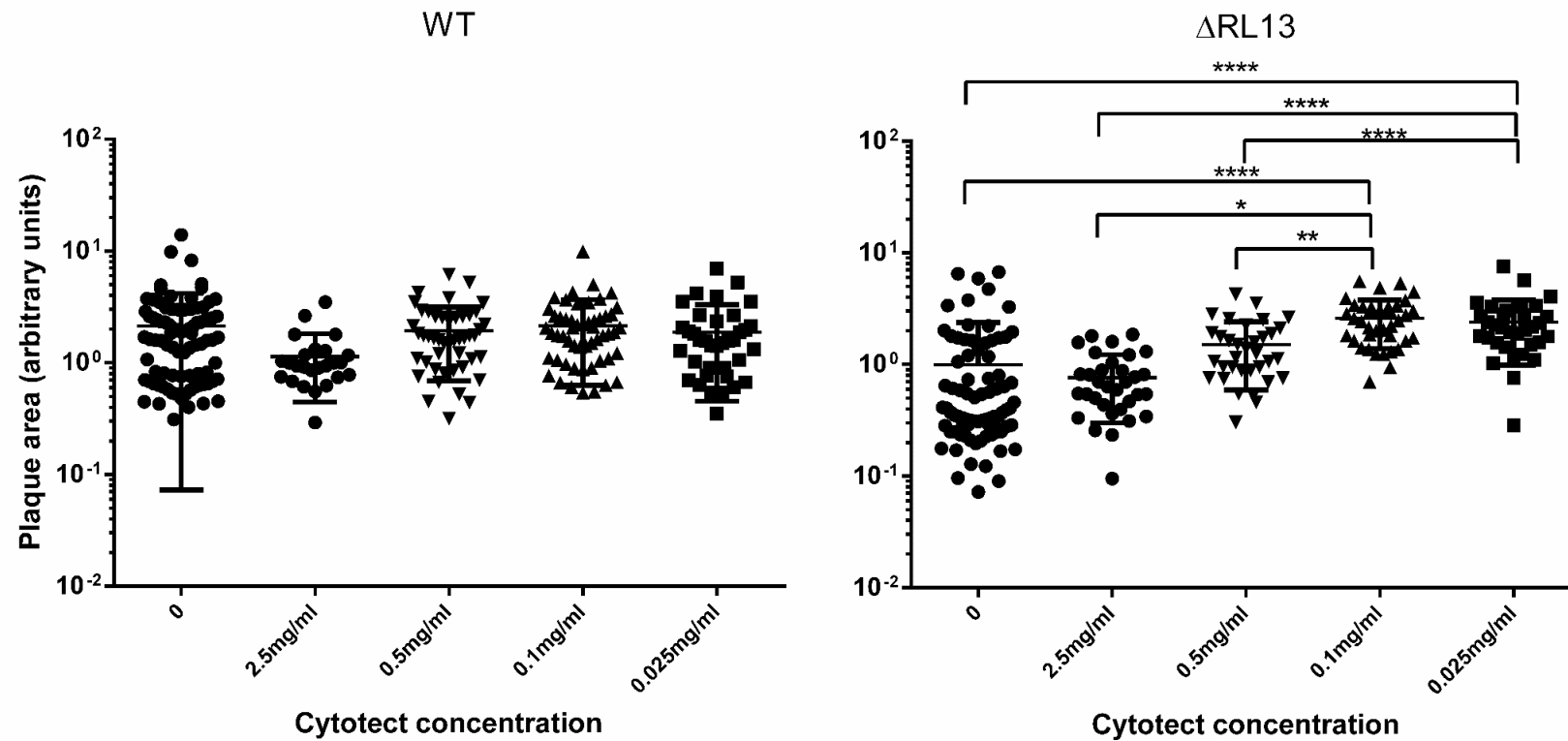


Figure 30 - Cell-cell spread of virus expressing UL128 shows resistance to neutralising antibodies in ARPE19s. HFFF terts were infected with  $\Delta$ RL13 or  $\Delta$ RL13 GFP expressing viruses with a varying concentration range of Cytotect and plated onto ARPE19s. As UL128 is needed for infection of epithelial cells its presence may mask any effect that RL13 expression has on cell-cell spread. Fluorescent images of viral plaques were captured and then measured. Plaques displayed were at 10 days post infection. One-way ANOVAs were performed (\*=  $P < 0.05$ , \*\*=  $P < 0.01$ , \*\*\*\*=  $P < 0.0001$ . Error bars display SEM.

### 5.1.2 Analysis of RL13 Expression Effect on Virion Composition

As RL13 affects virion infectivity (Chapter 4), it was important to determine whether these effects were due to its expression altering the virion proteome, and thus influencing virion binding and/or entry. Previously produced mass spectrometry (MS) data comparing WT and  $\Delta$ RL13 virions and WT and  $\Delta$ RL13/ $\Delta$ UL128 virions were analysed (Data produced by Isa Murrell). The viruses were cultured in HFFF tert cells grown in SILAC media before concentrating the viral preparations by centrifugation as previously described for growing up viral stocks (see section 2.3.1). Virions were purified by layering the concentrated virus preparations on glycerol tartrate gradients to separate virions from cellular debris and other virus particles as they migrate through the gradient at different rates. Further steps were taken to remove salts derived from the gradient and the virions were pelleted and resuspended ready for quantitative SILAC-MS (Isa Murrell, personal communication). In this manner, the relative amounts of each protein could be compared between viruses.

#### *Analysis of Virion Composition*

For this project the MS data was used to identify statistically significant enrichment or loss of protein in the virions lacking or containing RL13. The relative abundance of each protein between the samples was normalised to the capsid protein UL86, then analysed by significance B, using Perseus software. First, the WT and  $\Delta$ RL13 virion comparison was analysed. Both Human and HCMV proteins were identified in the virions (Fig. 31). Generally, most proteins identified were shifted towards enrichment in the WT virions, however this enrichment was not significant. In the WT virions, 6 proteins were significantly reduced ( $p < 0.00000000001$ ) and 9 proteins were significantly reduced but to a lower degree of significance ( $p < 0.00001$ ) (Displayed in table 17). A further 83 proteins were reduced, and 7 proteins enriched, to an even lower degree of significance ( $p < 0.05$ ) but were too numerous to include in table 17. No viral proteins (other than RL13) were reduced or enriched in this comparison. The majority of the proteins that were identified with highly significant reduction in WT virions, were human proteins involved in the immune response. Many were components of Igs or potential Ig Fc receptors, involved in Ig internalisation or binding. This could suggest manipulation of the immune response and a strategy to avoid Ig detection.



To validate the identification of these proteins another comparison was analysed (WT compared to  $\Delta$ RL13/ $\Delta$ UL128 virions) to ensure that these hits could be identified again (Fig. 32). All proteins identified in the first comparison in table 17 were also found to be reduced in the WT virions in the second comparison and so are more likely to be true differences. A viral protein, UL48 the large tegument protein, was found to be significantly enriched ( $p < 0.00001$ ) in the  $\Delta$ RL13/ $\Delta$ UL128 virions. This was not found in the first comparison and so this difference is assumed to be due to UL128 and not RL13.

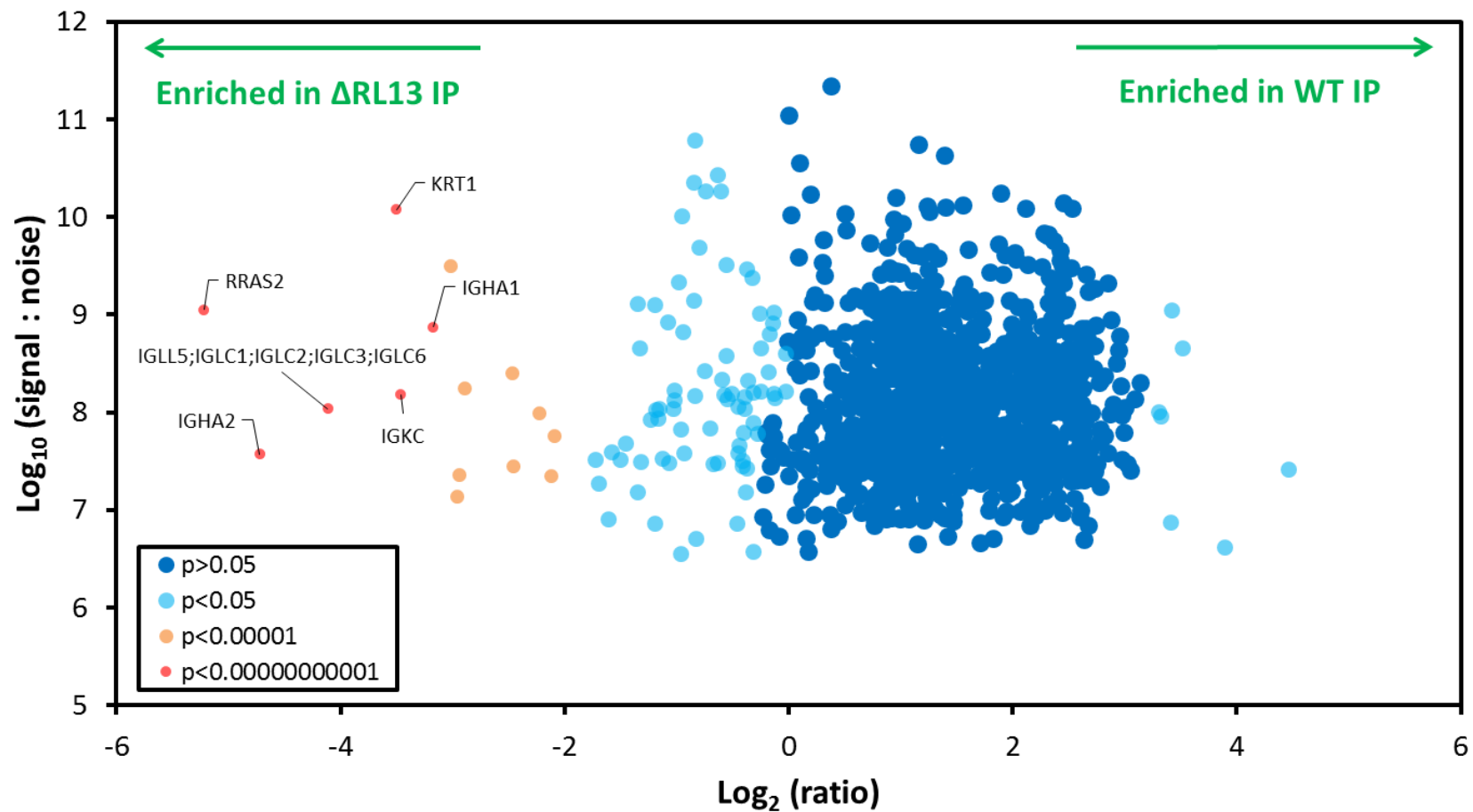


Figure 31 – RL13 expression results in significant loss of proteins within the virion. SILAC-MS comparison of WT and  $\Delta$ RL13 virions, which identified both Human and HCMV proteins present in the virion. Data were analysed using Perseus software. 13 proteins were found to be highly significantly ( $p < 0.00000000001$  or  $p < 0.00001$ ) reduced significantly in the virion when RL13 was expressed.

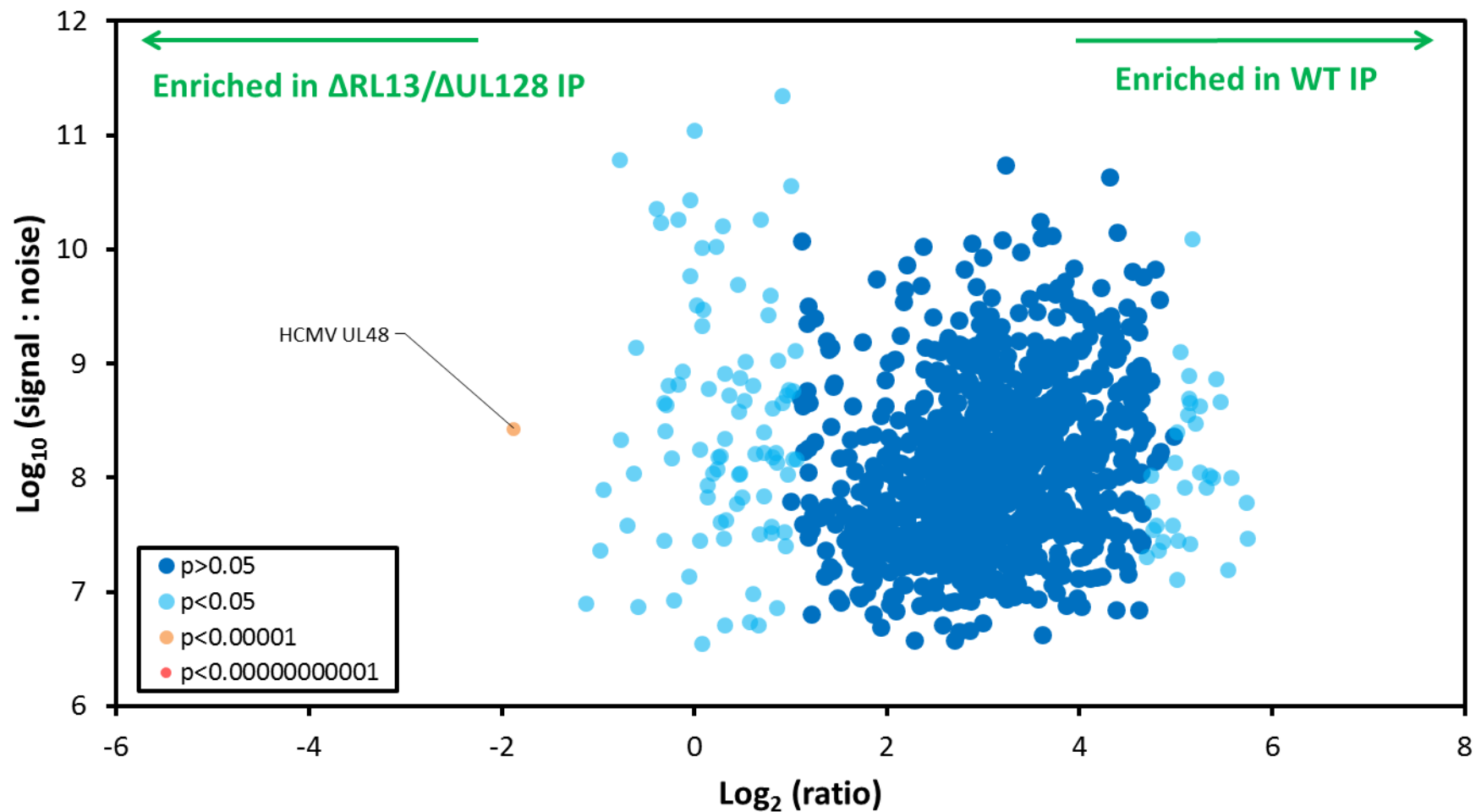


Figure 32 – Second virion composition comparison to verify first analysis. SILAC-MS comparison of WT and  $\Delta\text{RL13}/\Delta\text{UL128}$  virions, which identified both Human and HCMV proteins present in the virion. Data were analysed using Perseus software. 1 protein was found to be highly significantly ( $p < 0.00001$ ) reduced in the virion when RL13 and UL128 is expressed.

Table 17 – Proteins identified that were highly significantly reduced in the virion when RL13 was expressed.

Protein Identified	Full Protein name	Protein description
<b><math>p &lt; 0.00000000001</math></b>		
RRAS2	Ras-related protein R-Ras2	A GTP-binding protein with GTPase activity found in the plasma membrane (238). Has displayed transforming properties similar to those of the Ras subfamily of proteins (239).
KRT1	Keratin 1, a type II keratin	Structural protein expressed in Keratinocytes in the epidermis (240). <i>(Likely contamination)</i>
IGHA1	Ig alpha-1 chain C region	Constant domain isotype of immunoglobulin A heavy chain. Constant domains specify effector function, for example binding Fc receptors (241).
IGKC	Ig kappa chain C region	The constant domain of immunoglobulin light $\kappa$ chain. Constant domains specify effector function, for example binding Fc receptors (241).
IGLC3;IGLL5; IGLC1;IGLC2; IGLC6	Ig lambda constant 3; Ig lambda like polypeptide 5; Ig lambda constant 1; Ig lambda constant 2; Ig lambda constant 6	Various constant domains of immunoglobulin light $\lambda$ chain. Constant domains specify effector function, for example binding Fc receptors (241).
IGHA2	Ig alpha-2 chain C region	Constant domain isotype of immunoglobulin A heavy chain. Constant domains specify effector function, for example binding Fc receptors (241).
<b><math>p &lt; 0.00001</math></b>		
IGJ	Immunoglobulin J chain	A small polypeptide that links two monomers of IgA or IgM and is important in secretory immunity (242).
MAP2K1;MAP 2K2	Dual specificity mitogen-activated protein kinase 1 and 2	an essential protein kinase and component of the MAP kinase pathway required for cell survival and proliferation (243).
S100A8	Protein S100-A8	A member of the Myeloid-related Proteins (MRP). A small zinc- and calcium-binding protein highly expressed in neutrophils, monocytes, activated macrophages and some epithelial and activated endothelial cells. It is mainly found as calprotectin (S100A8/A9) which can enhance the migration of monocytes across endothelial cells. S100A8 is important in the immune response, the regulation of inflammatory processes and can induce adhesion and chemotaxis of neutrophils (244).
S100A9	Protein S100-A9	A member of the Myeloid-related Proteins (MRP). A small zinc- and calcium-binding protein highly expressed in neutrophils, monocytes, activated macrophages and some epithelial and activated endothelial cells. It is mainly found as calprotectin (S100A8/A9) which can enhance the migration of monocytes across endothelial cells. S100A9 is important in the immune response, the

		regulation of inflammatory processes and can induce adhesion and chemotaxis of neutrophils (244).
NDUFS2	NADH dehydrogenase [ubiquinone] iron-sulfur protein 2	A subunit of Complex I, also known as the mitochondrial membrane respiratory chain NADH dehydrogenase (245).
LTF	Lactotransferrin	Also known as Lactoferrin, is a multifunctional protein with iron-binding, antibacterial and anti-viral properties. It is localised in neutrophil granules and found in various exocrine fluids such as tears, saliva and breast milk (246).
PIGR	Polymeric immunoglobulin receptor	Binds polymeric IgM and IgA on the epithelial cell basolateral surface. The protein complex is then taken into the cell, transported and secreted at the epithelial apical surface (247).
F10	Coagulation factor X/Activated factor Xa	An important enzyme of the coagulation cascade. This vitamin K-dependent glycoprotein acts by cleaving prothrombin to create thrombin during blood clotting (248).
KRT2	Keratin, type II cytoskeletal 2 epidermal	Protein expressed in the epidermis and is associated with the activation and proliferation of keratinocyte and keratinization (240, 249). ( <i>Likely contamination</i> )

### 5.1.3 HCMV Virion Stability

RL13 expression causes a reduction in cell-free titres and may also reduce virion particles released (Chapter 4). HCMV is an enveloped virus that is known to be sensitive to low pH, fat solvents and even extreme physical conditions such as temperature (250). As gpRL13 is expressed on the virion envelope it was hypothesised that RL13 could affect the stability of the virions after egress from infected cells relative to the RL13 mutant virions resulting in the reduction in cell-free titres.

#### *Titration of Virus Over Time*

To investigate whether RL13 had an effect on virion stability, cells were infected with all four genetic backgrounds (non-GFP), then supernatants removed at 3 days post-infection. Supernatants were incubated at room temperature in a clean upright T25, then aliquots removed and used to infect fresh cells at certain timepoints. These fresh cell infections were then titrated by IE1 staining (Fig. 33). Consistent with previous findings,  $\Delta$ RL13/ $\Delta$ UL128 showed the highest titres, however after 72 hrs storage its titre had declined by nearly 100-fold and were within a much closer range to the titres of virus containing UL128 and/or RL13. While the WT virus had the lowest starting titre, it remained stable over the course of 72 hrs. The viruses lacking RL13 or UL128 alone exhibited approximately a 10-fold loss in titre over 72 hrs. These results imply that rather than destabilising HCMV virions, RL13 and an intact UL128L provided some resistance to virion degradation, and this effect was enhanced when both were expressed together.

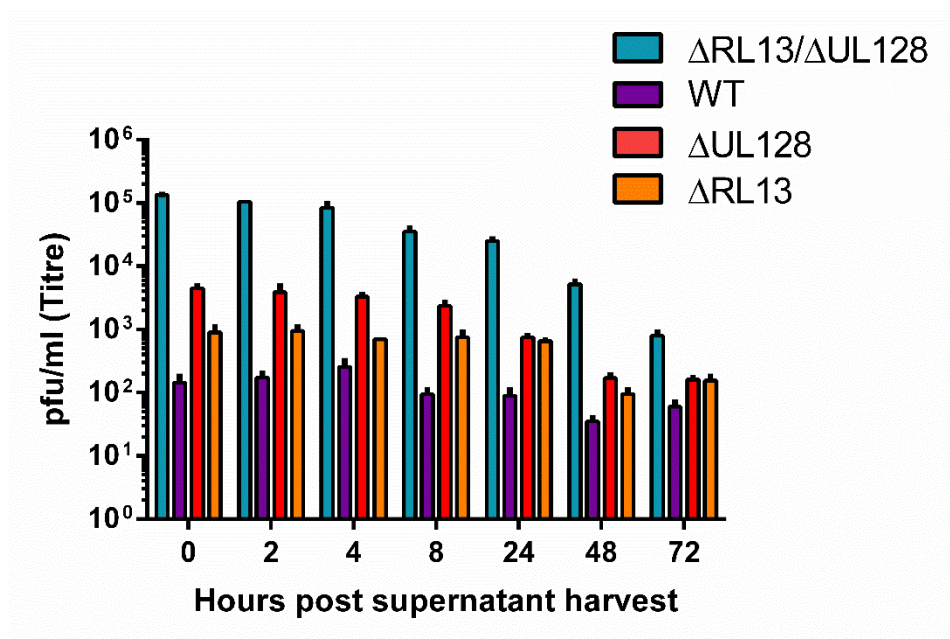


Figure 33 – Virus expressing RL13 and UL128 display virion degradation resistance. Viral supernatant from all four genetic backgrounds was left for 0-72hr and titred. Results showed that the presence of both RL13 and UL128 provided resistance to viral degradation over time when compared to the  $\Delta RL13/\Delta UL128$  virus. Titres are in duplicate and therefore statistics could not be performed.

### *Titration of Virus at Different Temperatures Over Time*

Although the  $\Delta$ RL13/ $\Delta$ UL128 virus showed the greatest loss of titre in the previous experiment, the titre was never reduced to the titre of the viruses containing UL128 and RL13 at that time point. It was therefore possible that the titre reduced the most because it started off higher. This experiment was therefore repeated with a longer timecourse, from 0-144hrs. Virion stability was tested at 3 different temperatures; 37 °C (Fig. 34A), room temperature (RT) (Fig. 34B) and 4 °C (Fig. 34C). Titres for the  $\Delta$ RL13/ $\Delta$ UL128 incubated at 37 °C showed a similar pattern of degradation to the previous experiment. However, unlike the previous experiment, viruses expressing RL13 and/or UL128 exhibited virion degradation across all temperature conditions over the timecourse. The 4 °C timecourse exhibited the most dramatic loss in titre for all four genetic backgrounds with no titre detectable after 48 hrs (Fig. 34C). HCMV Merlin appears to be very sensitive to storage at 4°C, more so than at RT. Titres observed at RT dropped more suddenly over 8-24 hr compared to 37 °C but remained detectable for slightly longer. This important information could aid future experimentation using Merlin as the virus should clearly never be exposed to 4°C for extended periods of time. Overall, RL13 and/or UL128 expression did not appear to provide an advantage to virion stability.



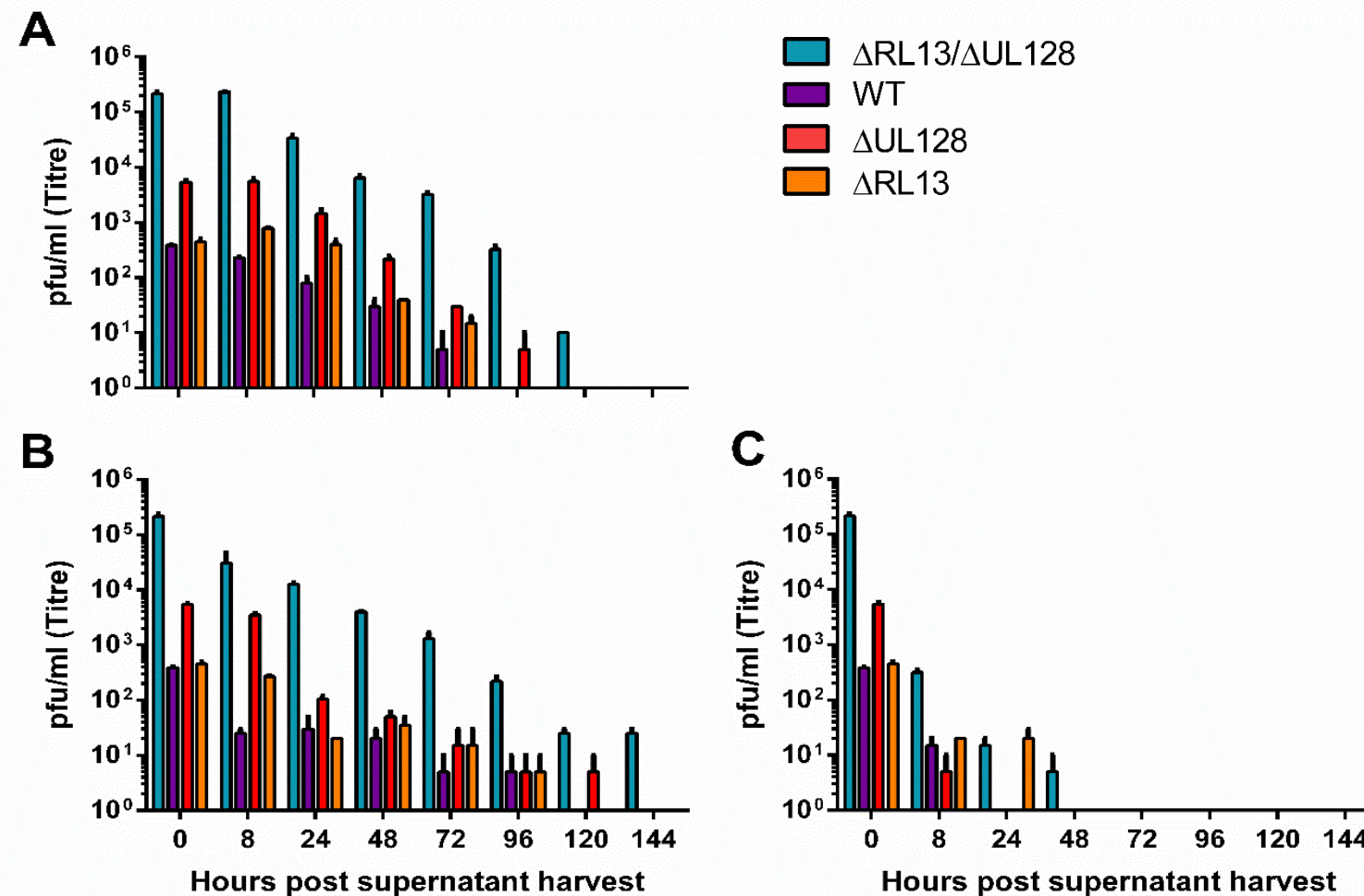


Figure 34 – Virion degradation over 144 hrs in different temperature conditions. Viral supernatant from all four genetic backgrounds was left for 0-144 hr at either (A) 37 °C, (B) RT or (C) 4 °C and titred. Results varied compared to the previous experiment, with all viruses regardless of genetic background displaying susceptibility to virion degradation over time. The 4 °C temperature conditions caused the fastest and most dramatic virion degradation across all samples. Titres are in duplicate and therefore statistics could not be performed.

## **5.2 Effects of RL13 on the Host Cell**

### **5.2.1 Cell Surface Glycoprotein Expression**

#### *Flow Cytometry*

Previously, cell-surface proteomics on cells infected in parallel with HCMV WT and  $\Delta$ RL13/ $\Delta$ UL128 showed there was a reduction in cell-surface expression of certain virus-encoded glycoproteins (most notably gB) when both RL13 and the UL128L were intact (Stanton, unpublished). To determine whether this difference was a result of RL13 or UL128 expression, FACs was performed on infected cells infected with the four genetic backgrounds. Gating of cells discriminated against dead cells and other debris (Fig. 35A). The efficiency of HCMV infection was determined by monitoring cell surface MHC-I downregulation (data not shown). As first observed in the proteomics experiment, expression levels of gB were reduced in WT virus compared to  $\Delta$ RL13/ $\Delta$ UL128 virus. However analysis of the individual RL13 or UL128 mutant viruses, showed that the reduced expression was most likely due to the presence of intact UL128 and not RL13 expression (Fig. 35B).

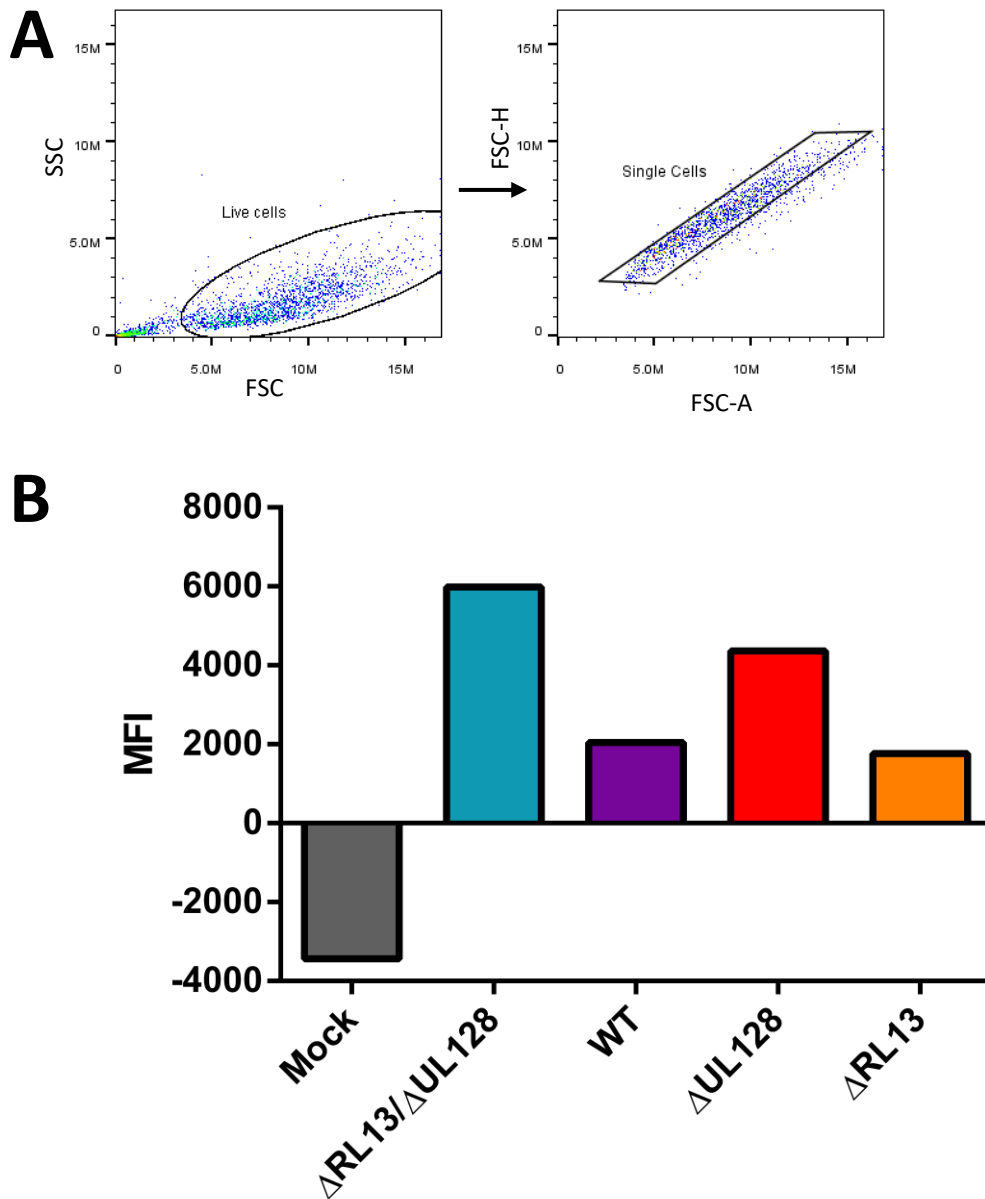


Figure 35 - RL13 expression does not affect gB cell-surface expression on infected cells. HF- terts were infected at an MOI of 5 and stained for gB at 72 hr PI. Efficient infection was determined by MHC I staining and background fluorescence determined by IgG staining. Results show a reduced expression pattern of gB in WT virus and  $\Delta$ RL13 virus when compared to the double mutant, but not in  $\Delta$ UL128 virus. (A) Gating strategy used to discriminate against cellular debris and then select for single cells. (B) Mean fluorescence intensity (MFI) of each sample. Statistical analysis could not be performed due to lack of replicates.

## 5.2.2 Identifying Functionally Relevant RL13: Protein Interactions

### *RL13: Host Cell Protein Complexes Highlighted by SILAC Immunoprecipitation (IP)*

An antibody specific for a V5 epitope tag fused to gpRL13 tagged immunoprecipitated a set of host cell proteins (see Table 18) from HCMV infected cells in a SILAC-IP experiment (Stanton, unpublished). These proteins were then identified by Mass spectrometry and a number were found to be chaperons (ERp57, CNX, DNAJB11, GRP78) that may be involved in the folding of gpRL13, and TREM16C and SERCA control ion channels. Out of these proteins, ERp57, DNAJB11, SERCA and to some extent HSPA5 co-localised with gpRL13 to the AC in the cytoplasm (Stanton, unpublished, see figures S1 and S2). As the majority of these proteins are found within the ER their expression in the cytoplasm is expected. However, their presence in the assembly compartment is less predictable. It was therefore important to determine whether these interactions with gpRL13 during productive HCMV infection were responsible for the inhibitory phenotype and restriction of cell-free virus released. By knocking down said host protein and testing for the ability of RL13 to inhibit efficient viral transfer between infected and uninfected cells.

### *Analysis of V5-Tagged RL13 by Plaque Assay*

The SILAC-IP was performed using a WT virus in which the RL13 ORF was V5-tagged (+RL13 V5/+UL128). It was therefore important to determine whether the V5-tag affected the growth or infection properties of the virus compared to the non-V5-tagged counterpart. The plaque size of WT virus was not affected significantly by the V5 tag yet reassuringly both had significantly smaller plaques than that of the control virus,  $\Delta$ RL13 (Fig. 36). Incorporating the epitope tag on the C-terminus of gpRL13 did not alter its capacity to impair growth of HCMV plaques.

### *Optimisation of siRNA Co-Cultures*

Four siRNA to each of the 6 host target proteins were tested for their ability to knock down the relevant protein. SERCA is encoded by 3 genes (SERCA1, 2, and 3) which give rise to the 3 isotypes ATP2A1, ATP2A2 and ATP2A3 (251). siRNA to ATP2A1 and ATP2A2 were available and so 4 siRNA to each were tested. Cells were transfected with siRNA

and western blotting used to determine whether the target protein had been sufficiently knocked down. Toxicity to cells was also considered when selecting siRNAs. If multiple siRNAs proved efficient both were selected for optimisation, for example both siRNAs GRP58 5 and GRP58 6 were equally efficient for ERp57 knockdown (see figure 37). All siRNA to TMEM16C failed to efficiently knockdown the target protein and so no further investigation was performed with this host cell target protein.

Three different optimisation conditions were assessed for all siRNAs chosen; 12pmol siRNA with 1µl lipofectamine (Optimisation 1), 24pmol siRNA with 2µl lipofectamine (Optimisation 2) and 48pmol siRNA with 3µl lipofectamine (Optimisation 3). Western blotting was again used to assess which optimisation condition was best for each siRNA. Figure 87 shows the optimisation of the chosen siRNAs selected from figure 37.

Optimisation condition 1 showed to be the most effective across the board. One siRNA for each target protein was selected with the exception of two siRNAs chosen for DNAJB11. Neither of the two siRNAs optimised for DNAJB11 proved to as efficient as the other protein siRNAs or was one more superior than the other and so, both siRNAs were chosen at the optimisation level that was most successful for the other protein targets.

#### *Analysis of RL13: Protein Interactions on Infection Capacity by Si-RNA Co-Culture Assay*

Once the most efficient siRNAs were chosen and optimised for each target protein, siRNA co-culture assays were performed to assess which protein: RL13 interactions were necessary for viral infection efficiency. HFFF were infected with IE2-GFP-fusion virus of either  $\Delta$ UL128 or  $\Delta$ RL13/ $\Delta$ UL128 background. The following day cells were transfected with siRNA. At 72h post-infection, cells were stained with a far-red dye (DDAO), and co-cultured with uninfected HFFF. Donor and recipient cells were distinguished by DDAO staining.

RL13 expression is inhibitory to cell free viral spread. Therefore, if the host protein is relevant to the RL13 phenotype, knocking it down should either abrogate RL13-mediated inhibition of virus spread in the  $\Delta$ UL128 virus, or mimic the RL13 phenotype in the  $\Delta$ RL13/ $\Delta$ UL128 virus. Co-cultures were performed multiple times with multiple donor: recipient cell ratios and at 48hr and 72hr post-co-culture. The results illustrated in figure 39 are representative of multiple experiments. In line with previous data,

transfer of virus between donor and recipient cells was significantly more efficient in the virus lacking RL13, compared to the virus containing RL13. No difference in infection efficiency was observed with any of the siRNA when using virus  $\Delta$ UL128. Cells infected with  $\Delta$ RL13/ $\Delta$ UL128 and transfected with GRP78, ERp57 or CANX siRNA showed a slight reduction in infection efficiency compared to scramble. This effect was more prominent in the 1:5 co-culture ratio. This suggested that these interactions with RL13 could have some importance in promoting infection and not inhibiting as hypothesised, although results were variable between experiments, and were relatively small. Interestingly, DNAJB11 knockdown tended to increase infection efficiency slightly compared to scramble in both viral conditions, suggesting that this proteins expression hinders infection regardless of the presence of gpRL13. Result trends from the 48-hr co-culture were replicated in the 72 hr results but with greater GFP positivity.

*Table 18 – Host cell proteins identified in a SILAC-IP to bind RL13 during infection.*

<b>Protein Name</b>	<b>Full name</b>	<b>Function</b>	<b>Co-localisation?<sup>1</sup></b>
ERp57	Endoplasmic reticulum p57	A component of the calnexin/calreticulin chaperone system that promotes folding and quality control of newly synthesised glycoproteins in the ER (252).	Yes
TMEM16C	Transmembrane protein 16C, also known as ANO3 (anoctamin 3)	May act as a potassium channel regulator and could inhibit pain signalling (253).	Unknown
CANX	Calnexin	ER chaperone protein involved in coordinating newly synthesised glycoprotein folding (254, 255).	No
DNAJB11	DnaJ heat shock protein family (Hsp40) member B11	Co-chaperone protein that is involved in synthesis and secretion of proteins by stimulating Hsp 70 chaperones (256).	Yes
SERCA	Sarcoplasmic/endoplasmic reticulum calcium ATPase 1+2	Calcium pump found in the sarcoplasmic or endoplasmic reticulum. Catalyses hydrolysis of ATP to transport Ca <sup>2+</sup> (257).	Yes
HSPA5	Heat shock protein family A (Hsp70) member 5 or 78 kDa glucose-regulated protein GRP78 or BiP	ER Chaperone protein involved in the transportation, folding and assembly of proteins. Also targets misfolded proteins for degradation (258).	Yes/No

<sup>1</sup>*Stanton, unpublished. See Figures S1 and S2.*

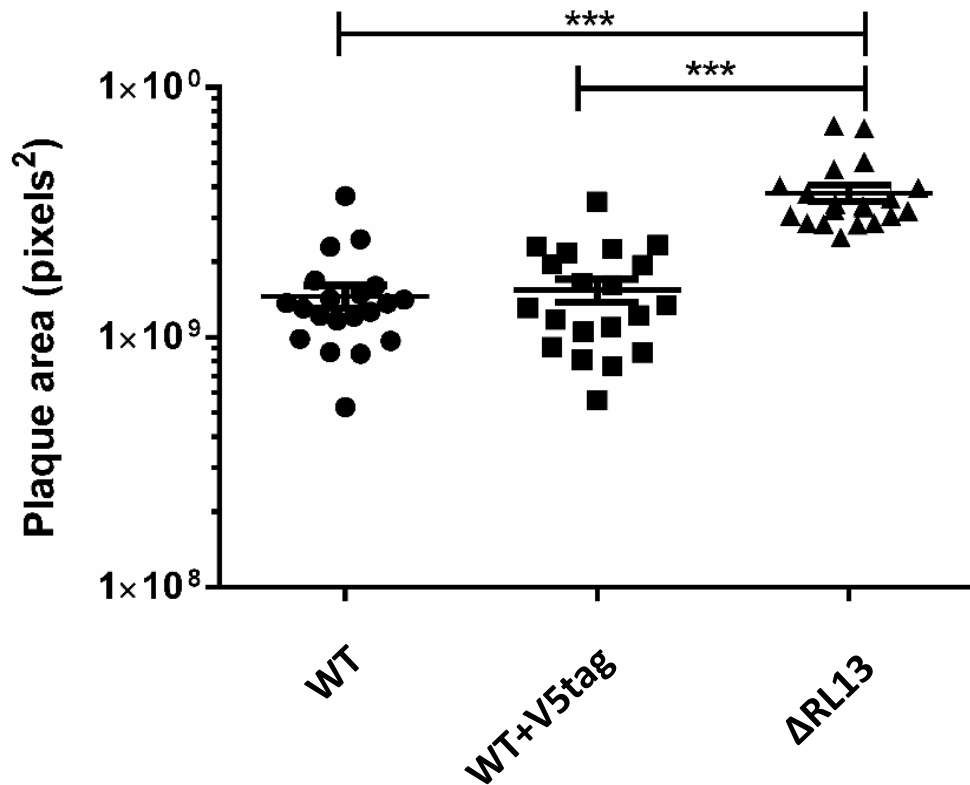
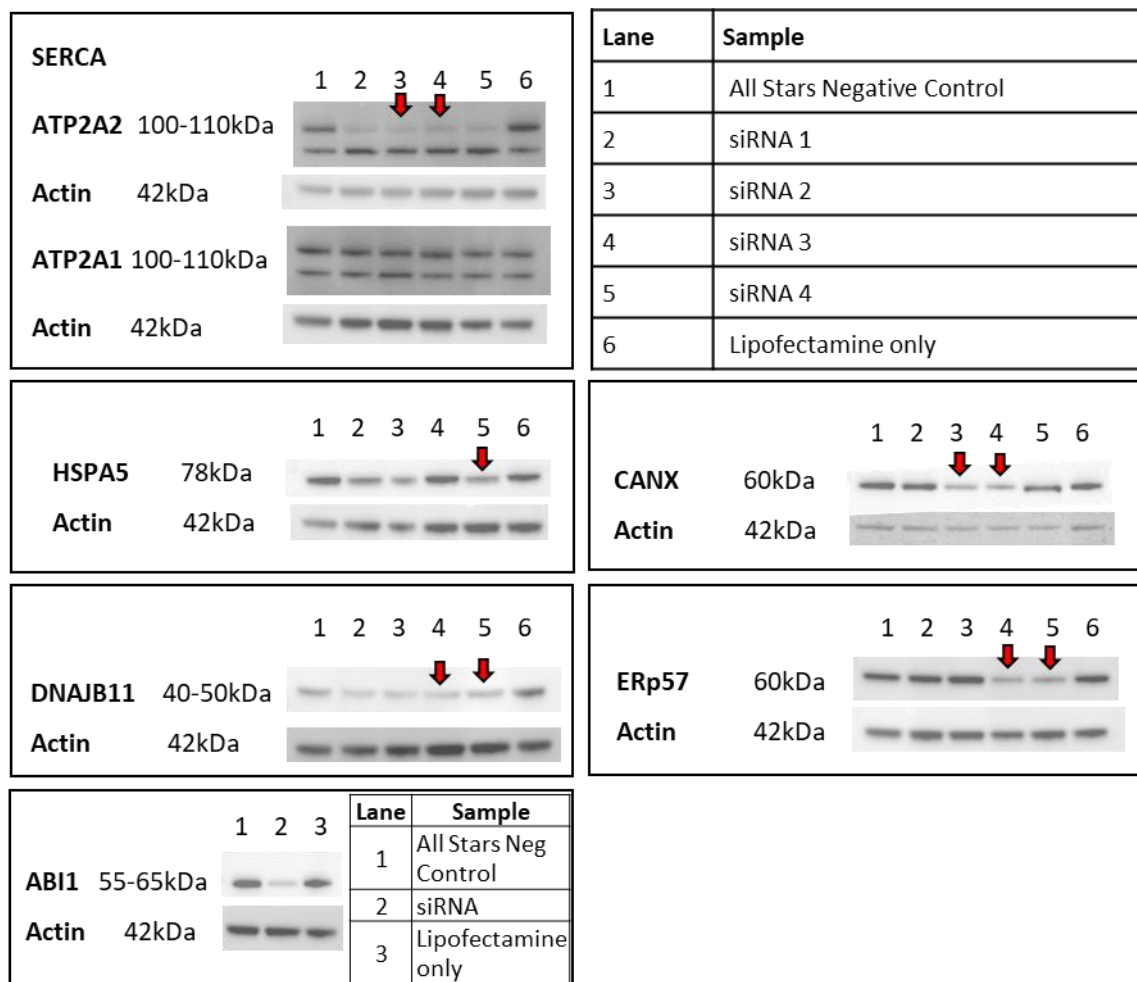
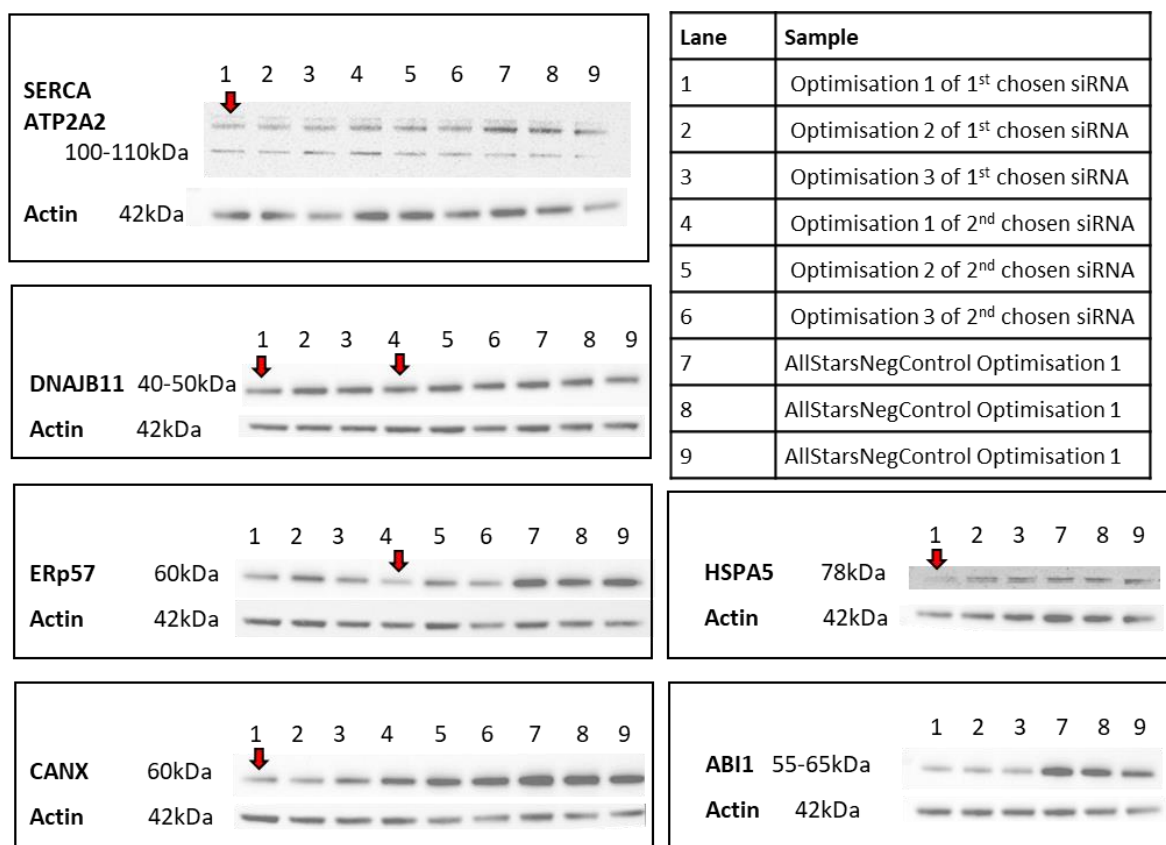


Figure 36 - The V5-tag does not affect RL13 expression. A plaque assay with +RL13 V5/+UL128 and two controls, WT and  $\Delta$ RL13, was set up in duplicate. 2 weeks post-infection the relative area was measured between 20 plaques per virus at 200 pfu. The V5 tag does not significantly affect the growth properties of the virus and therefore does not affect the expression of RL13. Analysis was performed by one-way ANOVA and Bonferroni post-test, \*\*\* =  $p < 0.001$ . Error bars display SEM.





*Figure 37 -Selection of siRNA to target proteins. All western blotting performed at 48 hr post transfection of siRNA. siRNAs for each target protein were chosen on the basis that they were the most efficient or least toxic to cells. The siRNAs that were selected are indicated by the red arrows. TMEM16C was not pursued further as neither the antibody staining nor the siRNA knockdown proved to be efficient.*



*Figure 38 - Optimisation of chosen siRNA to target proteins. siRNA was chosen to each of the 5 target proteins and ABI1 (the positive control, known to efficient knockdown its target). Three Optimisation condition 1 proved to be the most efficient for knockdown of all target proteins. When knockdown was comparable between optimisation conditions the decision was made based on the toxicity to cells. Chosen optimisation conditions are indicated by the red arrows. Samples in lanes are described in the table seen above. HSPA5 and ABI1 only had one chosen siRNA to optimise and therefore lanes 4-6 are absent.*

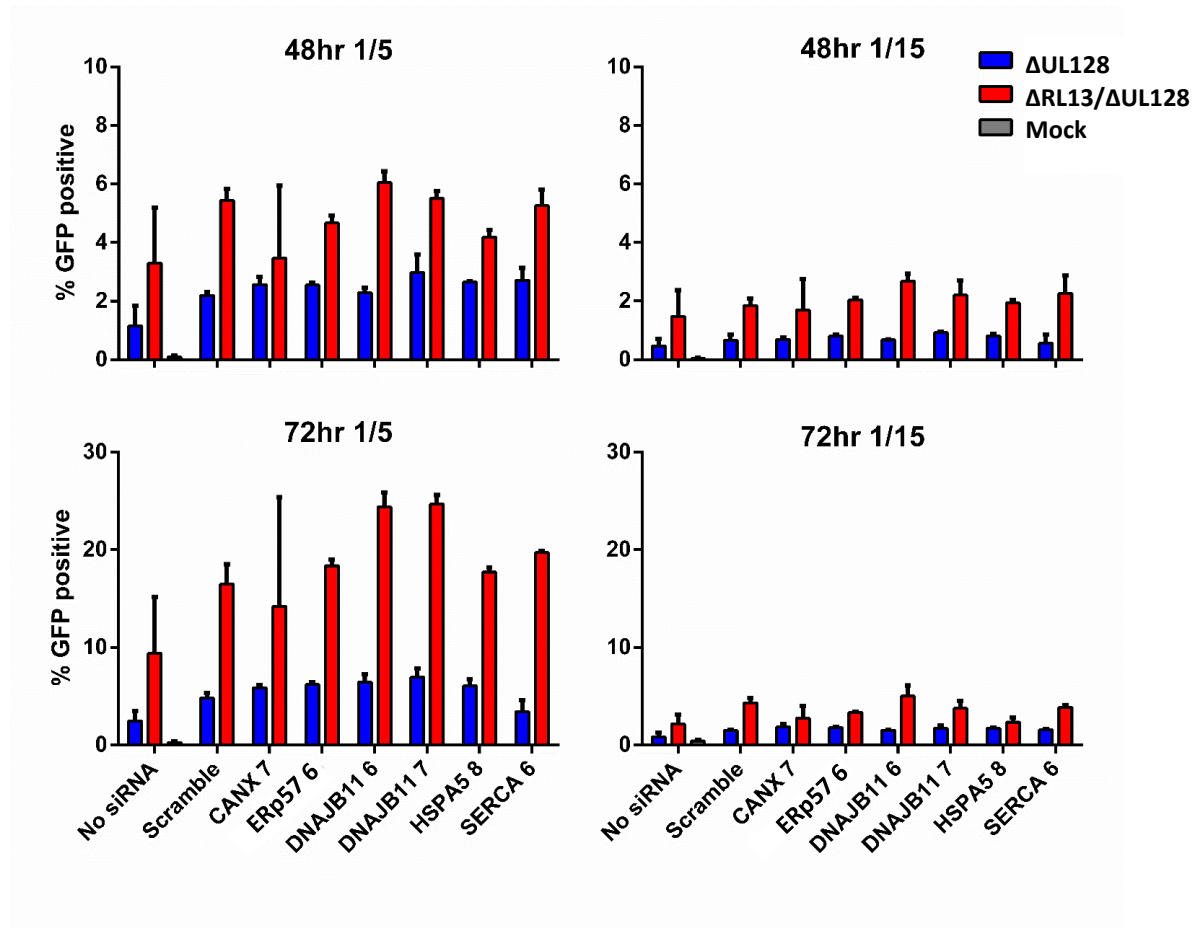


Figure 39 – An example siRNA Co-culture assay at 48 hr and 72 hr. Co-cultures were performed at 48 hr and 72 hr at a 1:5 and a 1:15 ratio, with the greatest clarity of results in the 1:5 ratio 72 hr co-culture. Greatest infection efficiency was seen in cells infected with  $\Delta RL13/\Delta UL128$ .  $\Delta UL128$  samples showed little difference in infection efficiency between target knockdowns and scramble control.

## 5.3 Effects of RL13 on the Host Immune System

### 5.3.1 RL13 is an Fc-Binding Protein

#### *Flow Cytometry*

During this study RL13 was described as a Fc binding protein (see Intro section 1.5.3) with immune evasion potential. Recombinant glycoprotein RL13 obtained from TR or Merlin trafficked to the cell membrane and bound and internalized exogenous IgG or IgG constant fragment. A tyrosine-based motif (YxxL) that functions to intracellularly target transmembrane proteins was identified in the C-terminal cytoplasmic domain of RL13 (173). Genome comparisons demonstrated that the endocytic YxxL motif was 100% conserved among the 96 clinical isolates (3), suggesting this function is an important immune evasion strategy *in vivo*. This conservation of motif could explain why functional differences in Fc binding between TR and Merlin RL13 were not identified despite the ORF sequence differences (173). Other RL11 family members such as RL11 and RL12 was identified as an IgG-Fc binding glycoprotein which can manipulate the host humoral immune response (173, 174).

Although it is unlikely that Fc-binding could be responsible for the growth phenotype displayed by virus expressing RL13, it was a potential function of RL13 that merited investigation. The conclusion was also not reached using systems permitting robust expression of RL13 in all cells (173), and so it was also important to determine if the results could be replicated.

Cells were infected with replication deficient recombinant adenovirus (RAd) encoding RL13, RL11, UL119 or a control vector. Cells were incubated with either a purified seronegative serum from a single donor, or a purified pooled seronegative human IgG at varying concentrations from 1µg/mL - 100µg/mL 72 hr p.i, and then a fluorescent anti-human secondary antibody. Cells were gated to discriminate against cellular debris and then selected for single cells (Fig. 40A). Background levels of fluorescence were determined with no stain samples and secondary stain only samples on the Mock sample of each infection and condition (Fig. 40B). RL13 did not show substantial binding of human IgG at lower IgG concentrations, whereas UL119 showed binding at all concentrations. However, at the higher IgG concentrations, RL13 bound IgG to a similar

extent as, and in some conditions more than, RL11 (Fig. 40C). Some cytotoxicity associated with RL11 resulted in lower cell counts. Not much difference was seen in the results between the two different human IgG sources except that RL13 bound 10ug/mL pooled greater than 10ug/mL D58.

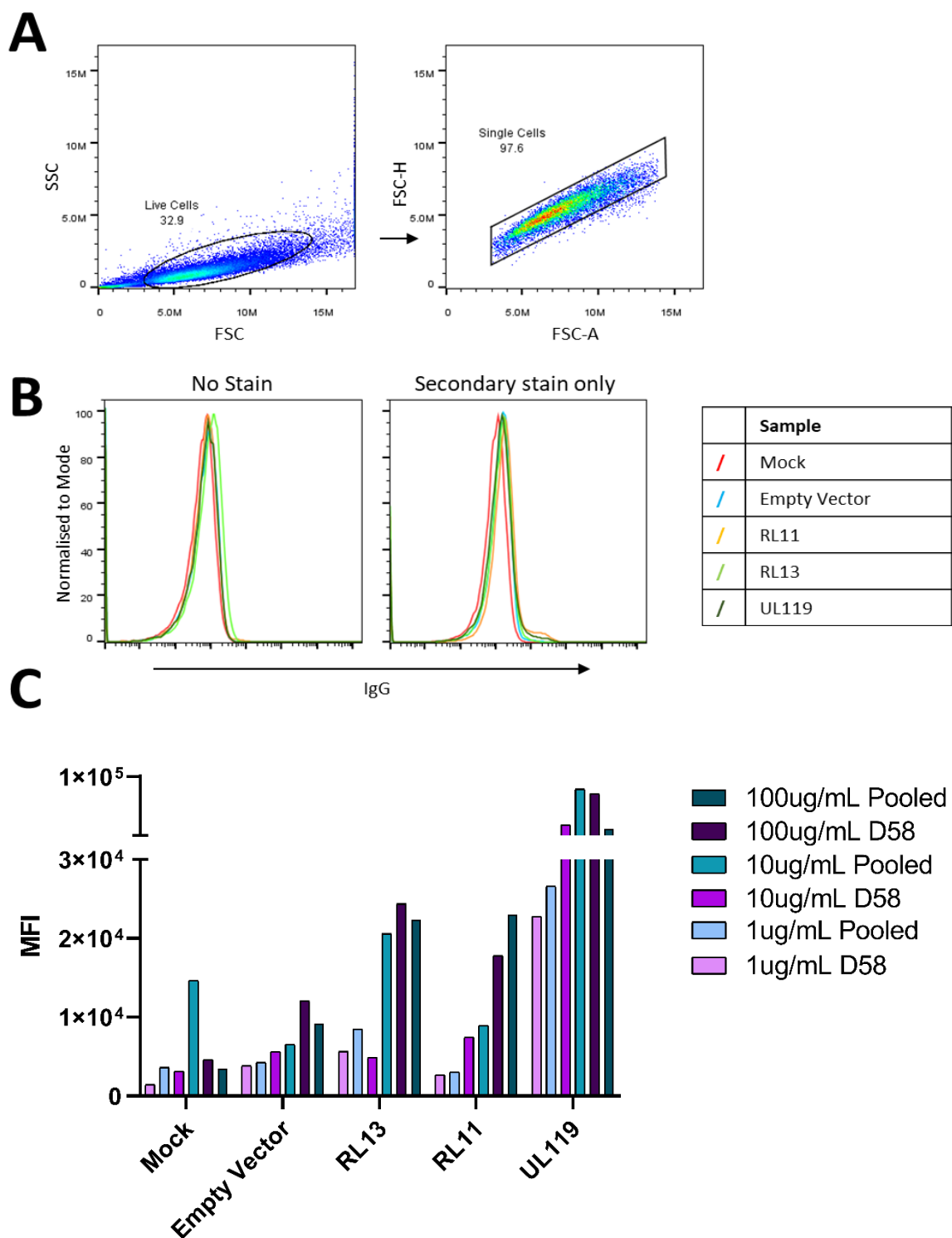


Figure 40 – RL13 binds Fc at higher IgG concentrations. Cells were infected with Rads expressing either RL13, RL11, UL119, an empty control Rad (empty vector) or left as mock. 72 hr PI cells were incubated with Human IgG at varying concentrations and then a fluorescent anti-human secondary Ab. Cells were run on a Flow cytometer and fluorescence quantified between samples. (A) Gating strategy used to discriminate against cellular debris and then sort for single cells. (B) No stain and secondary only stain to determine background levels of fluorescence. (C) Mean fluorescence intensity (MFI) of each sample. Results showed that RL13 bound human IgG more than the empty vector and to the same extent if not more efficiently than RL11. Statistical analysis could not be performed due to lack of replicates.

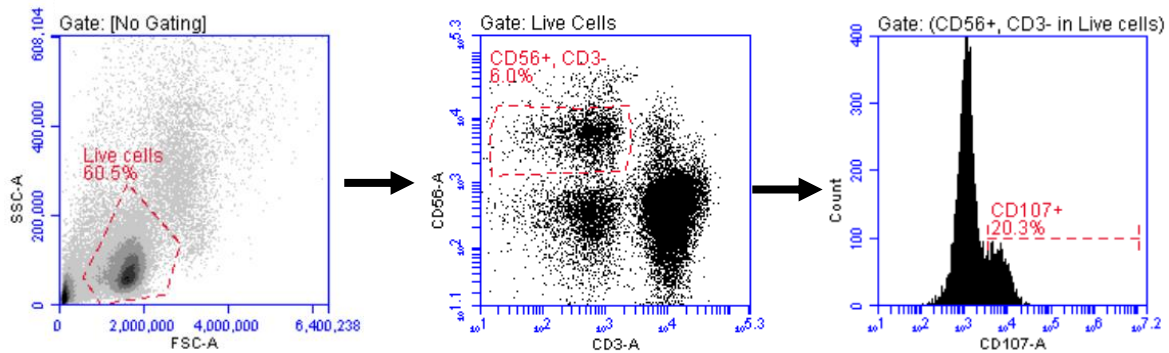
### 5.3.2 NK Cell Degranulation

#### *Antibody Dependent Cellular Cytotoxicity*

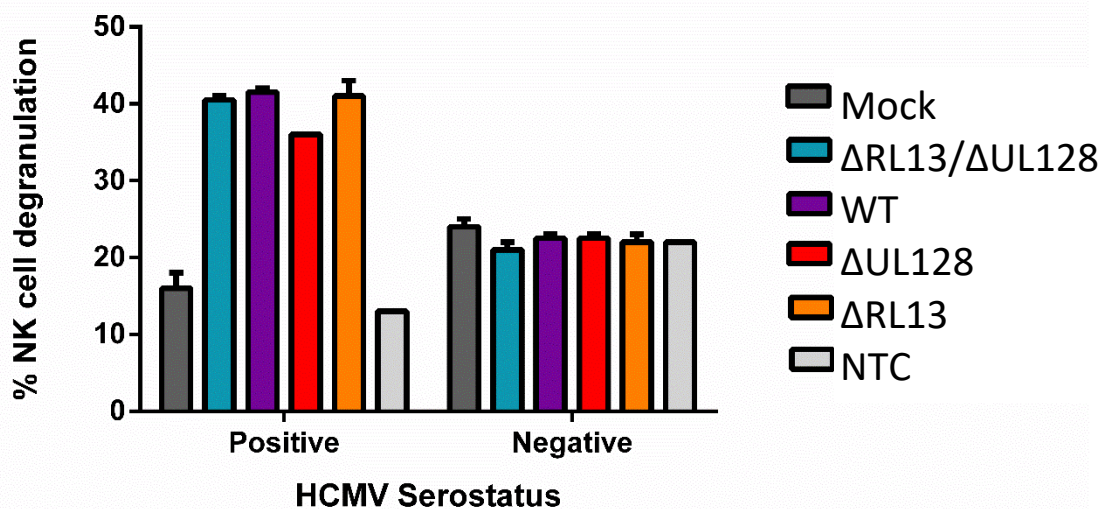
Previous work (Stanton, unpublished) showed that infections with WT virus resulted in reduced NK cell degranulation against target cells compared to  $\Delta$ RL13/ $\Delta$ UL128 when assays were performed in the presence of anti-CMV antibody (ADCC assays). As RL13 proved to be an Fc binding protein (173) which was replicated in this project, it is possible that RL13 could function as an immune evasion gene. By binding the Fc portion of the cell-surface bound antibody gpRL13 could protect cells from ADCC through antibody bipolar bridging (see Intro section 1.5.3). It could therefore be likely that the effect seen previously was due to RL13 and not UL128 expression. Thus, ADCC CD107 assays were performed with the four different genetic background viruses to test this.

Cells infected with the four genetic backgrounds of virus were used as target cells with PBMCs (source of seropositive NK cells) used as effector cells. CD107a expression measured by flow cytometry was used as a surrogate marker for the identification of NK cell activity on target cells. All samples were gated as shown (Figures 41A and 42A) to discriminate against cellular debris and then to select for CD56<sup>+</sup>, CD3<sup>-</sup> cells (NK cells). On this occasion, NK cell degranulation was not affected by RL13 expression (figure 41B). It was hypothesized that this differing result was due to the human serum used, and so the assay was repeated using multiple serums (Figure 42B). Different serums did show varying levels of degranulation, however, serum did not consistently affect the level of degranulation in response to viruses either lacking or containing intact RL13.

**A**



**B**



*Figure 41 - RL13 expression does not affect NK cell degranulation against infected target cells. An ADCC CD107 assay was performed with Target cells infected with all four genetic backgrounds (MOI of 5. Mock infected target cells (Mock) and no target control (NTC) were used as controls. Target cells were exposed to effector cells (PBMCs) 48 hr infection. (A) Gating strategies to discriminated against cellular debris and to sort CD56+, CD3- NK cells. (B) Results show no significant difference of percentage NK cell degranulation between viruses. (NTC: No target control). Data were analysed by two-way ANOVA with Tukey post-hoc analysis. Error bars display SEM.*



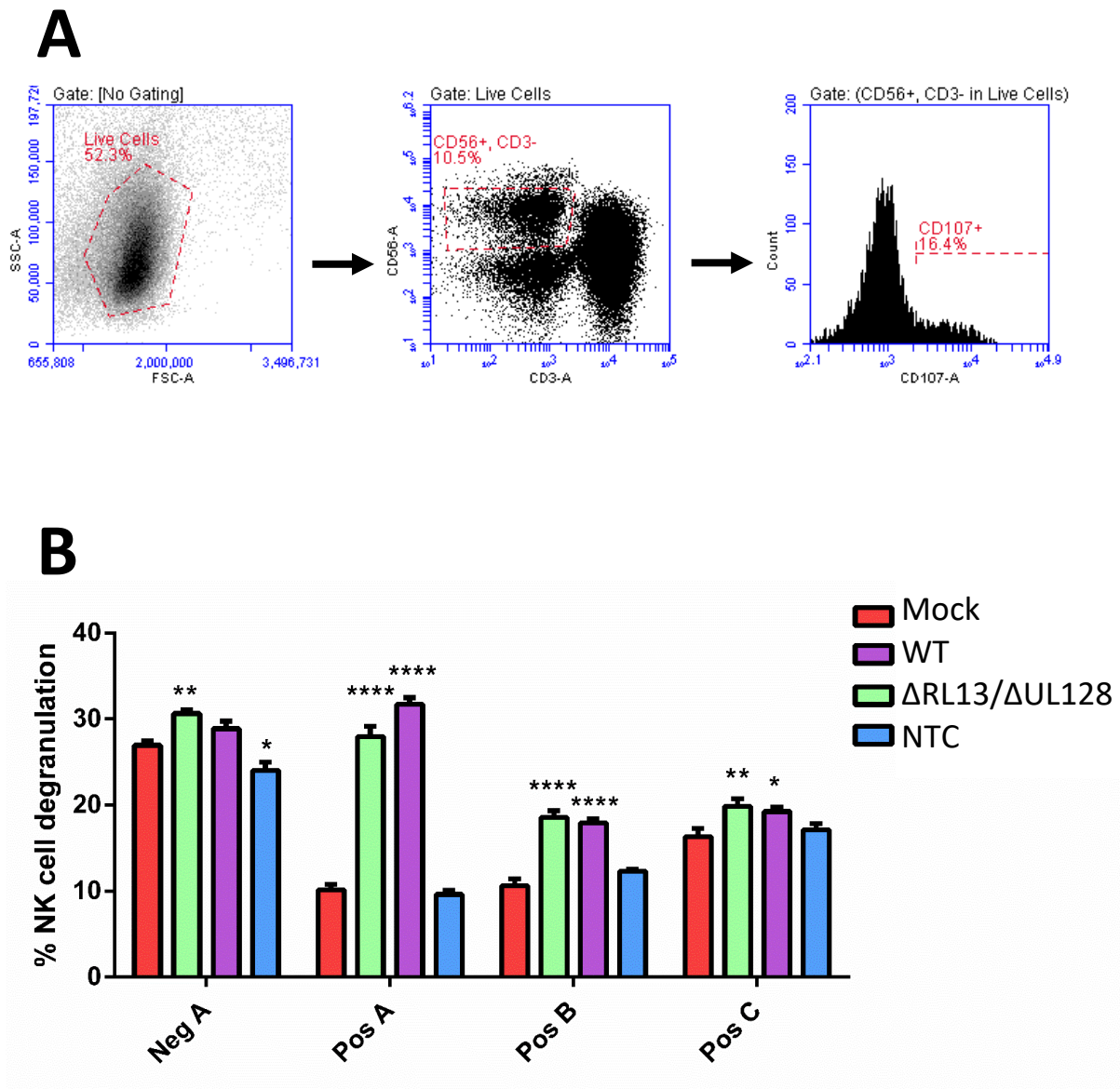


Figure 42 - ADCC varies with different donor's serum. Another ADCC CD107 assay was performed using 3 positive human serum and 1 negative human serum. Target cells were infected with ΔRL13/ΔUL128 and WT viruses (MOI of 5). Mock infected target cells (Mock) and no target control (NTC) were used as controls. (A) Gating strategies to discriminate against cellular debris and to sort CD56+, CD3- NK cells. (B) 48hr PI NK cell degranulation was measured and results show varying amounts of degranulation between serum samples. Data were analysed by two-way ANOVA with Tukey post-hoc analysis compared to the Mock of each serum (\*=  $P < 0.05$ , \*\*=  $P < 0.01$ , \*\*\*=  $P < 0.001$ , \*\*\*\*=  $P < 0.0001$ .) Error bars display SEM.

## 5.4 Chapter Summary

It was important to consider the functional consequences of gpRL13 in the virion envelope and to determine whether this had any implications or advantages for HCMV infection.

As RL13 expression forces the virus to spread cell-to-cell rather than cell-free co-cultures were set up with adherent and non-adherent cell types to determine whether this viral spread mechanism could prove advantageous. Cytotect, a purified polyclonal human anti-CMV IgG, was included in co-cultures at varying concentrations to determine whether viral transmission by cell-cell spread could evade neutralising antibodies. In adherent cell types such as fibroblasts and epithelials, the expression of RL13 or UL128 alone, or in combination, provided significant resistance to neutralising antibody in fibroblasts. Although RL13 and UL128 expression both independently provide resistance to neutralising antibodies, it can only be confirmed that RL13 provides this advantage in fibroblasts as UL128 is required for entry into epithelials and so the effect of RL13 alone could not be measured.

As important immune cells, DCs and LCs are likely to be among the first antigen presenting cells to come into contact with HCMV during the acute phase of a primary infection where they are thought to contribute to viral dissemination and important for reactivation of HCMV from latency. It was therefore important to determine whether RL13 affected infection of these cell types and whether using HCMV strains lacking WT RL13 for research would potentially affect the interpretation of results. RL13 expression provided no advantage to the virus to overcome anti-viral restriction in DCs and LCs, although again this could only be investigated in the presence of UL128. Thus, RL13 may have effects on virus spread, but these effects are masked when UL128 is present. More co-cultures in clinically relevant cell types and live cell imaging of infections with fluorescent virions in future work will provide valuable information regarding the mechanism by which HCMV spreads cell-cell.

The expression of RL13 proved to affect the composition of the virion as 15 host proteins were identified as being lost from the virion when RL13 was expressed. These proteins were identified again in a second comparison (WT compared to  $\Delta$ RL13/ $\Delta$ UL128 virions), thus giving more confidence that these were true differences. It is not immediately

obvious how these proteins could affect virion infectivity to the levels that the WT virions do. Many of these proteins identified are Ig fragments or Fc receptors and so it is unclear at how they are present in the sample especially as the virions were gradient purified. However, these changes in composition could affect the virions in other ways.

MAP2K1 and MAP2K2 are involved in the MAPK/ERK signalling pathway, required for not only the proliferation and survival of hematopoietic cells but also for the differentiation of monocytes *in vitro* (259). As myeloid cell differentiation leads to the reactivation of the HCMV lytic lifecycle (32, 134) (See section 1.4.3), WT virions could be more likely to promote a latent state as virions lack the MAP2K1 and MAP2K2 kinases that participate in this monocyte differentiation signalling cascade.

Ras-2 is a GTP-binding protein found in the plasma membrane (238). Small GTP-binding proteins have been implicated in HIV-1 intracellular trafficking, budding and release of virions (260). Additionally, RhoB GTPase is required for productive infection of HCMV and is implicated in virion egress. Knockdown of RhoB resulted in significantly reduced viral titre (261). It could be possible that the GTPase Rras-2 assists HCMV virion egress and in doing so becomes incorporated into the  $\Delta$ RL13 virion partially explaining the significant increase seen in NanoSight quantified extracellular virions when RL13 was mutated (with increased presence of Rras-2 in the virion). R-Ras2 also interacts with T and B cell receptors which is essential for cell survival. R-Ras2 knockout mice displayed a 30% decrease in the number of T cells (262). T cells are valuable in the cellular immune response against HCMV. Although R-Ras2 expression is tightly regulated it could be possible that R-Ras2 present in the virion envelope binds T cell and B cell receptors. This data could possibly suggest that the WT RL13 virions with significantly reduced presence of Rras-2 results in a loss of this tonic signalling of T and B cells leading to slightly impaired cellular immune response. Although just speculation and much more work would be needed to investigate whether this would provide an advantage to the +RL13 clinical strains.

Lactoferrin was significantly reduced in the virion when RL13 was expressed. Lactoferrin prevents HCMV entry into cells (263) most likely by competing with the glycoproteins gB, gM and gN for heparan sulphate (264). Its incorporation into the virion seems unusual given its antiviral properties, especially considering that its production is mainly

from mucosal epithelial cells (265). Lactoferrin is found in serum and as human and bovine forms exhibit high homology it is possible that its presence is due to the use of FBS during cell culture. Lactoferrin could be incorporated into the virion during viral replication or it could directly interact with the WT virions extracellularly much like how bovine lactoferrin binds structural polypeptides of adenovirus particles (266).

Coagulation factor X/Xa (FX/FXa) cannot be a contaminant from FBS as FBS is depleted of cells, fibrin and clotting factors. Although the liver is the major site of FX production, human primary fibroblasts have been shown to express FX (267). Interestingly, not only is the procoagulant phospholipid, phosphatidylserine, found in the virion envelope (268), but HCMV has been demonstrated to have endogenous mechanisms to activate FX to FXa on the envelope surface (269). Therefore, thrombogenic activity can be stimulated in the absence of tissue damage providing an explanation as to why HCMV can be associated with a vascular pathology and the acceleration of a number of vascular diseases. In this thesis phosphatidylserine was also identified with no significant difference in abundance between the virion samples. It is thought that phosphatidylserine is incorporated into the envelope during particle formation of AD169 whereas FX binds extracellularly (269). FX/FXa however was significantly enriched on virions lacking RL13 in this thesis. Ad169 contains a frameshift mutation in RL13 (191, 225), possibly suggesting that only expression of WT RL13 could inhibit binding of FX/FXa.

Some proteins that were significantly reduced in the virion when RL13 was expressed did not provide an obvious advantage or disadvantage to the virus. The myeloid proteins, S100A8 and S100A9, and the A100A8/A9 complex, calprotectin have multiple extracellular functions during infection specifically related to inflammation (270). However, these proteins do not have a transmembrane region and so it remains unclear what advantage the reduction of these two proteins or complex would bring to the WT HCMV virions when incorporated into the tegument. The gene product of NDUFS2 is located in the mitochondrion inner membrane and was found to be significantly reduced when RL13 was present in the virion. NDUFS2 is part of the first complex of the mitochondrial respiratory chain, NADH-dehydrogenase (245). It is unclear why HCMV would possess this protein in the virion and why its incorporation is RL13-dependent.

Apart from gpRL13, all HCMV-encoded proteins were present in similar abundance in  $\Delta$ RL13 and WT virions, except for the large tegument protein UL48. UL48 was reduced in the WT virions compared to the  $\Delta$ RL13/ $\Delta$ UL128 and so it's important to bear in mind this difference could be UL128-dependent. The large tegument protein is likely to be important in viral capsid transport and stabilisation and envelopment (110). Loss of UL48 expression leads to the failure of the AC to form (271). If the reduction of UL48 in the virion suggested reduced expression of UL48 leading to reduced capsid transport, stabilisation, envelopment and abrogated AC formation, this could contribute to the reduction in viral particles numbers seen from the WT virions. However, if this were the case, these results would have been confirmed by a difference in the TEM of particles forming and maturing and reduced stability from WT virions which were not.

It was then hypothesised that the stability of virions once released from the cells could be affected by the change in virion composition and therefore could account for the loss in viral titre. Yet, the presence of RL13 did not reduce the stability of virions. In fact, when first analysed at 37 °C, RL13 provided a substantial advantage to maintaining virion titre when left for long periods of time before titration. The same effect was seen with the UL128L expressing virus and the WT virus. However, when repeated at various temperatures and for a longer timecourse all viruses showed substantial titre loss and no consistent advantage could be attributed to RL13. Although the  $\Delta$ RL13/ $\Delta$ UL128 virus showed the greatest reduction in titre, it was also the virus with the greatest titre to begin with. It is possible that agglutination in the high titre virus could be responsible for this, however this could only be determined if the starting titres (timepoint 0hr after supernatant collection) were comparable between viruses. This assay could be improved by quantifying virion numbers as well as titre at each timepoint and by dispersing potential virion aggregates by either vigorous vortexing or pipetting.

Due to previous data (Stanton, unpublished) suggesting that WT virion infection led to a reduction in cell-surface viral glycoproteins such as gB when compared with  $\Delta$ RL13/ $\Delta$ UL128 infection. In this project however, RL13 was found to have no discernible effect on cell-surface gB expression. The reduction in gB observed previously is here shown to be dependent on restoring UL128 expression. gB is a highly conserved virion envelope glycoprotein that is recognised by the immune system in many different ways

including CD4+ T cells, anti-HCMV antibodies and TLR2 (see Intro 1.5.3). The results here could suggest that the expression of intact UL128L provides a mechanism for immune evasion for the virus and would therefore be an important hypothesis to follow up.

Specific host proteins were previously shown to interact with and, some, co-localise with RL13. These interactions were investigated by knocking down said proteins and the capability of infection analysed by co-culture and flow cytometry. DNAJB11 knockdown resulted in slightly increased infection of recipient cells indicating its expression could hinder infection regardless of RL13. It is likely that knockdown of the chaperone host proteins could interfere with infection as result of protein interactions elsewhere within the viral genome. As results varied between co-culture assays, and differences were relatively small, it was not possible to draw convincing conclusions as to which cellular proteins are responsible for the RL13 phenotype. It seems likely that knockdown of target proteins was not efficient enough, or was not maintained throughout the duration of the assay. Due to the short lifespan of siRNA it was difficult to use within a HCMV assay without the risk of either ending the experiment too early for a quantifiable transfer of virus or too late and risk the efficiency of siRNA. The possibility of using CRISPR instead of siRNA for complete long-term knockdown of target cells could be investigated in the future. This alternate approach could assist in the investigation into TMEM16C which was unsuccessful using siRNA. The use of CRISPR would also eliminate the risk that transfection of siRNA can induce the IFN response which could affect viral replication of subsequent cells (272). Despite variation, the results that were obtained indicate that none of the proteins tested were required for RL13-mediated suppression of infection and that the critical interaction with RL13 to result in this phenotype is yet to be determined.

Recently RL13 was shown to bind Fc (173). It was important to determine whether we too could replicate this finding with Merlin RL13. A few issues arose with the Fc binding assay, such as toxicity leading to low cell counts in the RL11 RAd infected samples. Another caveat is that the empty vector control showed an increase in fluorescence compared to Mock at the highest concentration of IgG, and this background could have masked low levels of binding by the HCMV proteins. Increased fluorescence was seen in the 10ug/mL pooled IgG Mock sample, which could mean that fluorescence levels in the

10ug/mL samples are exaggerated. This experiment was only performed with n=1 and so it would be beneficial to repeat it. Nevertheless, RL11 bound human IgG to a similar extent as RL13, indicating that RL13 can act as a Fc binding protein at higher IgG concentrations.

As RL13 binds Fc it was possible that the expression of RL13 could also inhibit ADCC. Previous work also hinted that infections with WT HCMV resulted in reduced ADCC compared to  $\Delta$ RL13/ $\Delta$ UL128 (Stanton, unpublished). However, in this project, RL13 expression did not consistently affect NK cell degranulation. This was performed with multiple donor serums and results suggested that the difference in ADCC seen previously was due to serum donor differences.

Overall, the presence of gpRL13 did prove to have an effect on the virion. gpRL13 influenced the method of viral transmission, the composition of the virion, and showed evidence of Fc-binding capabilities all of which furthers our understanding of the function of the RL13 gene in *in vivo* infection.

## **CHAPTER 6. DISCUSSION**



Work in this thesis has furthered the understanding of the function of the HCMV gene RL13 and has provided insights into how and why its expression is so inhibitory to viral propagation *in vitro*. In my opinion this work has resulted in 3 main findings; the importance of working with HCMV strains that express functional RL13, RL13 has multiple conserved phenotypes and that the restrictive phenotype of RL13 *in vitro* can be explained in part by a reduction in virion infectivity. These findings will be discussed further below.

## 6.1 The Importance of RL13

The expression of RL13 is strongly inhibitory to HCMV propagation in cell culture with disruptive mutations appearing in RL13 rapidly upon culture in fibroblasts (203). High-throughput analysis of HCMV genome diversity found that only 3.9% of clinical isolates sequenced contained an ORF disrupting mutation in RL13. These clinical isolates were passaged on average 2-3 times on fibroblasts before sequencing (3), thus these mutations could be a result of adaptation to fibroblasts. In either case, RL13 is intact in the majority of clinical strains. Given this, it must be advantageous for the virus in the human host. If *in vitro* studies are to recapitulate the *in vivo* situation, it is therefore vital to work *in vitro* with strains that represent the full genetic potential of HCMV, and data in this thesis demonstrates this.

A large majority of HCMV research to date has been performed using RL13 mutant viruses, because it was not possible to grow RL13 intact viruses *in vitro*. The Tet-repression system used in the Merlin BAC solved this problem, making working with genetically intact RL13 (WT HCMV) possible for the first time (203). However, this required *in vitro* acquired mutations to be repaired, and Tet-repression elements to be added to a BAC clone of the virus. Recently an alternative method of WT HCMV propagation whilst keeping RL13 genetically intact has been proposed (273), suggested as a possible method for deriving BAC clones from clinical isolates without the risk of mutation. They reported that serial passage (>p20) of a clinical isolate in fibroblasts was achieved without mutation in RL13 or the UL128L by culturing in the presence of anti-HCMV hyperimmunoglobulin. The clinical isolate also retained the ability to infect epithelial cells (273). The presence of HCMV-hyperimmunoglobulin in the cell culture medium was thought to force the virus to replicate by cell-cell spread much like *in vivo*, by neutralising cell-free virions. This alleviates the selective pressures that promote RL13 and UL128L mutation which result in the release of cell-free virions (203, 273). The stocks propagated by this method, although enabling growth of RL13-intact genomes without needing to BAC clone, only reach titres of  $10^4$ - $10^5$  pfu/mL which are unlikely to be sufficient for many aspects of HCMV research. Using the Tet-repression system, sufficient titres are achieved by propagating RL13+ strains whilst translationally repressing the ORF. This not only ensures that RL13 remains genetically intact, but also

relieves any inhibition that gpRL13 places on viral propagation. Therefore, the Tet-repression system has advantages for propagating WT HCMV *in vitro*, and so improved novel reporter viruses expressing Tet-regulated RL13 were needed for this study. An ideal reporter gene for this project would be expressed to high levels, early in infection. IE1 seemed like an ideal candidate as expression levels are highest immediately after infection (210). Unfortunately, the proposed construct of IE1-P2A-GFP was unsuccessful. Despite this, a successful reporter virus expressing GFP fused to the C-terminal of IE1 has previously been created in AD169 (274). The MIE gene has multiple splice variants and is complex (see Intro section 1.4.1). Insertion of a substantial sequence such as GFP could potentially impact the functioning of the gene products (IE1 or IE2) required for efficient viral propagation, and/or the efficiency of splicing that results in expression of both gene products. Our constructs contained the P2A peptide that results in co-translational cleavage of the IE gene and GFP, and theoretically should have been less likely to have interfered with the IE1 gene products to the same extent as a fusion construct (as was used in the AD169 background) would have. It is possible that the reason the construct in IE1 in this thesis failed was due to strain-specific differences between Merlin and AD169. The IE2-P2A-GFP viruses on the other hand were recovered successfully and provided key tools for progressing this project. It seems likely that although the P2A sequence was used in both the IE1 and IE2 constructs, fusing to IE1 impacted on effects on splicing that were inhibitory for efficient viral replication. IE2 levels are recognised to increase dramatically at 48-72h (210), which is when GFP became detectable, suggesting that expression levels were simply insufficient at earlier timepoints.

As the glycoprotein encoded by RL13 is expressed in the virion envelope (203) and traffics to the cell surface where it is exposed at least transiently (173), RL13 could potentially modulate the tropism of the virus as well as function to aid immune evasion or virulence. These potential attributes of the expression of RL13 demonstrate the importance of using clinically relevant HCMV strains in HCMV research. During this thesis RL13 was described as a Fc binding protein with immune evasion potential (173). Recombinant glycoprotein RL13 obtained from TR and Merlin trafficked to the cell membrane and bound and internalized exogenous IgG or IgG constant fragment. A

tyrosine-based motif (YxxL) that functions to intracellularly target transmembrane proteins was identified in the C-terminal cytoplasmic domain of RL13 (173). Genome comparisons demonstrated that the endocytic YxxL motif was 100% conserved among the 96 clinical isolates (3), suggesting this motif is advantageous to HCMV *in vivo*. Using flow cytometry this function of RL13 was supported in this thesis but only at the higher IgG levels tested. The lowest concentration of IgG that Fc-binding of RL13 was seen was at 10µg/mL, however this is around 700-fold lower than serum IgG levels in the healthy population (275), suggesting that in immunocompetent hosts with much higher serum IgG levels than tested, RL13 could successfully function to bind Fc. Having proven that RL13 was an Fc-binding protein, it was hypothesised that it may potentially inhibit ADCC as well along with many other HCMV encoded NK evasion genes. The IgG subtypes of IgG1 and IgG3 are good mediators of ADCC (276) and RL13 was shown to selectively bind IgG1 and IgG2 subtypes (173). However, there was no evidence that RL13 expression resulted in a significantly decreased NK degranulation response in the assays in this thesis, suggesting that it is unlikely that RL13 functions as an NK evasion gene to inhibit ADCC. However, these NK assays were performed in the context of HCMV meaning that other Fc-binding proteins such as UL119 and RL11 were present and could mask any effect of RL13. The Ig-like domain showed great variation in protein sequence between the 9 clades observed when analysing the 96 clinical RL13 ORFs. It could be possible that a clade with great variation compared to clades 8 and 9 (containing TR and Merlin respectively) has evolved the ability to inhibit ADCC. Nevertheless, it is clear that RL13 does not enhance the ADCC-avoidance properties of UL119 and RL11, in the context of *in vitro* infection.

Anti-CMV vaccines generally aim to induce immune responses such as neutralising antibodies (277). Most HCMV vaccine research is performed using highly passaged strains lacking expression of WT RL13 and UL128, and therefore produce high titres of cell-free virions. Clinical HCMV contains RL13 and UL128, and is therefore mainly found in a cell-associated form (103), which affects sensitivity to neutralising antibodies in other viruses. It was therefore important to investigate the effect of neutralising antibodies on HCMV expressing RL13 and UL128. RL13 and UL128 both independently

provided viral resistance to neutralising antibody in fibroblasts. However, plaque size consistently remained smaller than  $\Delta$ RL13/ $\Delta$ UL128 virus, even under high antibody concentrations, suggesting that in this context, no actual growth advantage is achieved when these genes are expressed.

The UL128L encoded envelope proteins are together the major target of neutralising antibody response (278), thus the loss of the pentameric complex from the virion envelope should result in reduced sensitivity to neutralising antibody. However data from this thesis, which contributed to recently published work (235), showed that expression of UL128, and equally RL13, forces the virus to spread cell-cell; a mechanism that is resistant to neutralising antibodies (235). Additionally, the fact that the majority of WT HCMV *in vivo* is cell-associated (103), clinical isolates in cell culture also remain mostly cell-associated (200, 279) and the infrequent release of cell-free virus detected in blood *in vivo* (280), support a cell-cell spread mechanism that is utilised throughout the majority of infection *in vivo*. The cell-cell method of viral spread has been exploited by other viruses, such as HIV (281). Cell-cell spread of HIV virions still requires the assembly and maturation of fully formed enveloped virions (282). Although it is not yet determined whether HCMV utilises the same mechanism as HIV to spread cell-cell, it is probable that HCMV also needs fully formed enveloped virions for productive cell-cell infection as many envelope proteins are required for plaque formation, and some tegument proteins are involved with initiating viral replication (1). It has been reported that loss of UL99, which results in capsids being unable to acquire envelope, can still spread cell-to-cell, however this spread is much more inefficient than enveloped particles, indicating that it is not the dominant route of natural spread (283).

No difference in the numbers of matured virions in the assembly complex between WT and mutant HCMVs were detected by TEM in this thesis despite the restriction of cell-free virion titres by RL13. Viral replication kinetics are enhanced during cell-cell spread of HIV (281, 284, 285) likely due to the fact that many infectious virions are transferred simultaneously during cell-cell spread of virus (286). It is possible that the reduction in cell-free virions caused by RL13 is due to multiple virions being transferred to neighbouring cells instead of being released into the supernatant. In addition, enhanced

replication kinetics were not seen when comparing genome replication, temporal protein cascade or particle maturation and formation of HCMV in this thesis between WT and HCMV RL13 mutants.

DCs and LCs have been shown to participate in primary infection of HCMV in very different ways. Immature DCs are fully permissive to cell-free infection whilst immature LCs are not (231, 233). However, only UL128 was necessary for cell-cell spread in these cells, with RL13 not providing an advantage in any of the conditions tested. Interestingly, immature LCs were readily infected when infection was by the cell-cell route (irrespective of RL13). Furthermore, cell-cell infection of these cells was only slightly inhibited in the presence of IFN $\alpha$ , whereas cell-free infections performed in parallel were strongly affected by the disruptive effects of IFN $\alpha$ . Thus, suggesting again that the survival of WT HCMV during *in vivo* infection is more likely ensured by cell-cell spread. The data in this thesis has demonstrated the advantages and importantly the differences of WT HCMV driven cell-cell spread compared to cell-free spread seen with laboratory HCMV strains. The cell-cell transmission of HCMV enabled by UL128 expression allows for the expansion of host cell tropism to include LCs as well as DCs. Cell-cell spread also provides a higher resistance to IFN $\alpha$ , as well as resistance to neutralising antibodies during infection.

The favoured model of HCMV particle assembly requires that virion envelope glycoproteins are first transported to and thus transiently exposed on the cell surface before being endocytosed to become components of the virion envelope (85). Glycoproteins exposed on the cell surface are potential targets for the immune system. It was considered that RL13 could act as an immune evasion function by downregulating gB cell surface expression, however, RL13 proved to have no effect on the cell-surface gB expression. The effect on gB cell-surface expression was in fact found to be UL128L-dependent. gB is highly immunogenic and both binding and neutralising anti-gB antibodies are found in almost all seropositive individuals (1). As gB is a major target of the humoral immune system, reducing its cell-surface expression through this undetermined UL128-dependent mechanism could provide an advantage to UL128+

HCMV strains. Of course, this preliminary data would need to be investigated further to confirm this assumption but nevertheless, this demonstrates the importance of working with WT HCMV strains as not only functions of RL13 will be absent, but other clinically relevant genes such as UL128 as well.

Other advantages of RL13-containing strains could be overlooked when designing therapeutics with laboratory HCMV strains. As RL13 was shown to bind Fc in isolation, the presence of gpRL13 in the virion envelope could potentially provide Fc-binding capabilities to cell-free virions providing the virus with advantageous immune evasion mechanisms. Furthermore, virions lacking RL13 had other alterations in composition compared to the WT virus, with  $\Delta$ RL13 virions lacking 15 host proteins. The majority of these seem likely to be contamination, with several being components of immunoglobulins or potential Ig Fc receptors, involved in Ig internalisation or binding. It is surprising that the Ig fragments are present in the samples as samples were gradient purified and previously cultured with FBS, meaning any Ig proteins present could possibly be bovine and misidentified as human. Aside from these potential contaminants, a number of additional proteins were reduced in the virion when RL13 was expressed (see table 17). Although none provide an obvious explanation for why RL13 intact virions have reduced infectivity, or why their abundance is altered following RL13 expression, some have the potential to alter the activity of HCMV virions and therefore highlight advantages of using WT HCMV in research (Discussed in section 5.4).

As with all the proteins found to be altered between the WT and  $\Delta$ RL13 virions it is uncertain whether their RL13-dependent virion incorporation is due to their increased abundance caused by downstream effects of RL13 expression or due to direct interaction with gpRL13 during virion particle formation. However, the SILAC-IP performed on cell infections previously (Stanton, unpublished) did not identify the proteins discussed above indicating that the RL13-dependent virion composition alterations are unlikely to be due to direct interaction with gpRL13. All that is certain is that the expression of RL13 changes the composition of the virion. Further work could involve CRISPR/siRNA knockdown of these proteins to determine the importance of the compositional changes to the virion with gpRL13 incorporated.

## 6.2 Is RL13 Hypervariable?

RL13 has been described as part of a defined set of hypervariable genes (175). The majority of HCMV genes have highly conserved sequences, however, some genes have substantial genetic variation between strains and are designated hypervariable. Many of these genes encode for proteins that are either confirmed or predicted to be membrane-associated or secreted and therefore likely to interact with the host immune system.

Other hypervariable genes in this discrete group include UL146 and UL139 (194). UL146 encodes a chemokine designated vCXC-1 and displays variability throughout the sequence length (196, 287). Remarkably, the UL146 sequences of strains have been grouped into one of 14 defined genotypes (175, 194). The alignment of the RL13 ORFs obtained from 96 clinical isolates along with the RL13 ORF from Merlin, TR and AD169 in this thesis resulted in tightly delimited clusters encompassing 9 RL13 genotypes.

Genotype analysis has been performed for RL13 before, identifying 8 genotypes.

However, when identifying clusters, the pruning procedure was to identify a maximum of 8 genotypes in order to proceed with their statistical analysis of their dataset (288).

This method could easily underestimate the true number of unrestricted genotypes.

Whereas the majority of the HCMV genome undergoes a high-frequency of recombination, RL13 was found to be a region in high linkage disequilibrium which is consistent with locally reduced recombination, whereby genotypes are sufficiently divergent from one another to prevent recombination between them (288).

As genetic variation is prevalent in clinical HCMV strains, it has been hypothesised that HCMV strain variation could affect the outcome of infection, which poses problems for disease management and vaccine research (289). To date, the association of a particular genotype with a particular clinical disease outcome has been evaluated in many studies, some reporting inconclusive or contradictory results (194). Others however have found evidence of a relationship between genetic variant and pathogenic potential in the polymorphisms of several genes (mainly glycoproteins) including UL146 and UL147 (3). An increased risk of CNS damage was associated with the G1 UL146 genotype, whilst an increased risk of pneumonia was associated with the G7 genotype (290). The RL13



variants have diverged for a reason therefore it is likely that the different clades observed provide the virus with different pathogenic potential. Multiple virus genotypes can be found within patients (291, 292). It is possible that infection with multiple RL13 genotypes could complement each other. It is also possible that the different RL13 genotypes provide advantages in certain hosts, and that host genetics also play a role in the success of HCMV pathogenesis. Further insight into the immunological purpose of these RL13 genotypes could be gathered from investigating whether the amino acid sequence variation affects the chemical or structural properties of the protein.

The groupings of the RL13 ORFs was interesting. The Merlin RL13 was grouped into a fairly small clade. TR, which may be functionally different from Merlin RL13 as its sequence does not mutate *in vitro* (208), was found on the adjoining branch suggesting that compared to the other clades, TR and Merlin are more alike than first thought. Fc binding potential were described for Merlin RL13 and TR RL13 (173), as these strains are found on adjoining arms it seems logical that they possess the same or similar functions. Whether or not this function is specific to these closely divergent arms in the phylogenetic tree is yet to be determined, however it was found that the Ig-like domain that is responsible for the Fc binding capabilities showed considerable variation between the 9 clades. It would be interesting to determine whether neighbouring clades had evolved this function and/or were also able to inhibit ADCC. In this thesis RL13 did not affect NK cell degranulation significantly enough to confidently call it an NK evasion gene. However only RL13 from Merlin was analysed.

It would be interesting to determine whether other isolates found within the clade TR was in also genetically retain their RL13 ORF during cell culture as their sequences are so similar. Interestingly, when TR RL13 was inserted into the Merlin genome, it inhibited virus growth in the same way as Merlin RL13. This indicates that factors elsewhere in the TR genome could be responsible for maintaining intact RL13 in the TR genome, or potentially that factors outside the immediate RL13 ORF, such as epigenetics, differ between the genotypes.

This analysis of phenotype transfer was also performed with a RL13 homologue from RhCMV, Rh13.1, which (although it needs repeating) suggested that Rh13.1 expressed in the HCMV genome is also able to inhibit spread to some degree. The fact that this

phenotype of restricted viral spread is retained by RL13 despite considerable sequence differences indicates that it is an important biological function.

Previous analysis of polymorphic HCMV gene protein sequences, including the genotypes of gB and gH, has shown that significant sequence variation is seen at the N terminus and limited variability shown at the C terminus (289). This is consistent with the amino acid sequence analysis of RL13 in this thesis as the vast majority of sequence variation is observed at the N terminus of the protein which encompasses the signal peptide and Ig-like domain. The transmembrane region of RL13 was almost completely conserved amongst the clinical isolates retaining the ability of RL13 to be expressed in the cell membrane and virion envelope. Interestingly the YxxL motif required for the ligand-dependent internalisation of the RL13-Fc complex is located in the C-terminal tail of RL13 (173). This YxxL motif is 100% conserved in clinical isolates sequenced (3) and therefore this internalisation function is likely to be important to the functioning to all RL13 genotypes.

In summary, one question that arises from this data is whether the hypervariable tag often associated with RL13 is fitting or whether polymorphic is more appropriate.

### **6.3 Investigating the Restrictive Phenotype of RL13 in *in vitro* HCMV infection**

An aim of this thesis was to investigate why expression of RL13 *in vitro* results in >10-fold reduction of infectious titres of cell-free virus and inhibited viral spread. I hypothesised that RL13 could interact with or affect a particular stage of the HCMV lifecycle to result in this phenotype.

First, the viral DNA replication stage was investigated. During this study it was reported that RL13 interacted with host cell nucleoside diphosphate linked moiety X (nudix)-type motif 14 (NUDT14), a UDP-glucose pyrophosphatase, to affect viral DNA replication (227). Using fluorescence confocal microscopy, gpRL13 co-localised with NUDT14 in the cell membrane and cytoplasm. siRNA knockdown of NUDT14 resulted in an increase of viral DNA in infected cells (227). The qPCR data measuring viral genomic replication in this thesis did not corroborate this result and showed no evidence a difference in genome replication between strains expressing/not expressing RL13. The study by Wang et al (2016) was performed using an N terminal GFP tag on RL13 of HCMV strain Han. The N terminal GFP tag has the potential to disrupt the signal peptide of RL13 greatly effecting the results seen. In reverse transfection assays N-terminal tagging with GFP adversely affects protein localization with over 50% of N-terminal fusion proteins localising incorrectly likely due to masked signal peptides (293).

Similarly to the analysis of viral genome replication, analysis of viral temporal protein expression and viral particle formation and maturation showed no inhibitory effect that could be reasonably attributed to the expression of RL13 to explain the reduced cell-free titres and viral replication inhibition associated with WT HCMV. Moving forward it was considered that expression of RL13 could reduce cell-free virus and be inhibitory to replication by interfering with either the release of virions from infected cells or the infectivity of those virions released, or even both. Although the infectivity and particle numbers of virions measured by NanoSight and plaque assay was only performed once, taken with the results from the qPCR assays these experiments indicated that RL13 and UL128 expression reduced viral infectivity both individually and together. Since RL13 changes the composition of the virion, it has the potential to affect viral infectivity.

However, no obvious reason for the infectivity of virions to change was apparent in the virion composition comparisons. Equally, no apparent reason for a difference in infectivity was identified from the SILAC-IP of host cell proteins found to bind RL13 during infection as the majority of proteins were chaperone proteins involved in protein folding.

Unfortunately, a confident conclusion could not be reached when analysing virion particle numbers as the data were inconsistent between the qPCR and NanoSight assays, no appropriate internal controls were available, and the NanoSight experiment was only performed once. The qPCR assay, was performed numerous times and over multiple timepoints and so is the most reliable data at present. RL13 expression did not lead to a significant or consistent reduction in cell-free virions released into the supernatant over a 10-day period. In support of this qPCR data, RL13 induced restriction of cell-free virions does not originate at the DNA or protein stage of viral replication and there was also no evidence in the TEM data of different numbers of virions produced or of an accumulation of virions in the AC of the samples containing RL13, and so it seems unlikely that there would be a difference in the number of RL13-containing virions released. Therefore, it is possible that the reduction in RL13-containing cell-free virions occurs after virion egress. As HCMV is an enveloped virus it is sensitive to low pH, fat solvents and even extreme physical conditions such as temperature (250). Reduced virion stability caused by a difference in an envelope protein has been observed before in Hepatitis B virus. The mutation in the S envelope protein of Hepatitis B resulted in a reduced stability phenotype when treated with NP40 compared to the wildtype control (294). Therefore, it was hypothesised that virions with intact RL13 in the envelope could have reduced stability once leaving the cell compared to the RL13 mutant virions and this susceptibility to virion degradation was the cause of the drastic drop in viral titre. However, the expression of RL13 and/or UL128 did not appear to provide a significant advantage to virion stability over long periods of time. Although the  $\Delta$ RL13/ $\Delta$ UL128 virus showed the greatest reduction in titre, it was also the virus with the greatest titre to begin with. More so at higher temperatures, high concentrations of viral particles can induce aggregation (295). Aggregation of virions will result in an underestimation of the actual titre, as a viral aggregate will result in an individual plaque forming instead of the

dispersion of those virions making up that aggregate initiating multiple plaques. Therefore, the  $\Delta$ RL13/ $\Delta$ UL128 could appear to have the greatest titre drop but in fact the virions aggregate during the incubation times. In cell culture propagation of vaccinia virus, 69-90% was found to be aggregates of anywhere from 2-150 virions. When these viral preps were treated with sonic waves the viral titre increased and the dispersed virus was found to be 2-3 fold more efficient at initiating viral plaque formation (296). Many viruses have been found to form aggregates including adenovirus, poliovirus and influenza. Although viral aggregation has been found to increase survival in certain environments and even provide resistance to some disinfectants (295) the large size of aggregates could attract unwanted attention from the immune system as protein aggregates elicit an enhanced immune response (297). Thus, lower titres of HCMV (Such as those seen in RL13+ and UL128+ samples) that don't aggregate as much would be beneficial during *in vivo* infection. Although it should be noted that aggregation of virions was not seen during NanoSight analysis of virion particles. Regardless of genetic background all viruses were most labile at 4°C, which has been reported for HCMV many times before (250). Remarkable stability of HCMV at RT and 37°C was seen, which is all the more surprising given that the lipid envelope of HCMV is known to be fragile (250). The WT virus retained ~100-50% of its starting titre in 48hrs at both RT and 37°C. These temperatures would be biologically relevant for viral transmission via body fluids such as urine. Although referred to as virion stability, the mechanism for the reduction in titre was not investigated. The loss in titre could have been due to a reduction in infectivity or the number of virions remaining.

Some host cell proteins were previously demonstrated in a SILAC-IP to interact with and some shown to co-localise or recruit RL13. In this thesis these host proteins were investigated further by siRNA knockdown to try to determine whether any of these interactions with RL13 could result in the inhibitory phenotype and restriction of cell-free virus associated with expression of RL13. The results exhibited variation and whether efficient knockdown was achieved for the duration of the experiment was questionable. Although the data identified some proteins that could possibly be important during HCMV infection these affected viruses independently of RL13

expression. As many of the proteins were chaperone proteins involved in protein folding and secretion it is possible that their interaction with RL13 was during protein synthesis and formation. The fact that several of the proteins (SERCA, DNAJB11, ERp57) were shown to be recruited with RL13 to the AC (Stanton, unpublished) suggests that this could be an important interaction. One protein, ERp57, forms part of the peptide loading complex involved in antigen presentation by MHC (298). This could suggest that RL13, like other HCMV proteins, is in some way involved in the inhibition of Tcell recognition and Tcell mediated killing. Although this proposed theory would be unlikely to result in reduced cell-free titres of virus and inhibited viral propagation, further work exploring the possibility of inhibited Tcell recognition of HCMV infected cells could help determine whether RL13 provides an advantage to the virus *in vivo* through this interaction. Therefore, the results in this thesis suggest that the critical interaction with RL13 is still yet to be defined with further work.

During this thesis it was discovered that deletion of UL74 (gO) results in a very similar phenotype to that of the one RL13 expression promotes (299). In fibroblasts UL74 promotes increased plaque sizes and neutralising antibody-sensitive cell-free spread, but only in the absence of UL128 expression. When RL13 expression was downregulated in this context the viral spread capacity was significantly enhanced (299). It is tempting to speculate that there may be a link between UL74 and RL13/UL128L induced viral spread mechanisms. We know from data in this thesis that expression of the UL74 gene product gO on the virion was not manipulated by RL13 expression and that RL13 did not immunoprecipitate with UL74 during infection in fibroblasts. UL74 is more likely to be affected by UL128L expression as the gene products of UL128L and UL74 compete for gH/gL when forming the pentamer and trimer respectively (88) (see Intro section 1.3.1.3).

Co-cultures performed in this thesis and published work (235) demonstrate that RL13 and UL128 can both independently induce cell-cell spread of virus in fibroblasts. The co-cultures in epithelials however showed that cell-cell spread was driven by UL128 regardless of RL13 expression. It seems redundant for two genes to give rise to the same phenotype, however as only UL128L forced the virus to move cell-cell in epithelials, DCs

and LCs, two genes with the same function but relevant in different cell types seems more purposeful. Release of HCMV virions with different compositions and tropisms has been reported to be cell-type induced (146) (see Intro section 1.5.2). The HCMV homolog of UL74, m74, was necessary for establishing infection *in vivo* of diverse tissues but found to be nonessential during intra-host cell-cell dissemination of virus within the organ tissues (300). In humans, cell-free HCMV is detected in breast milk and urine (38) and yet once isolated and propagated *in vitro* the clinical virus is cell-associated (200). Epithelial cells, which can be found in the breast tissue and kidneys, are prime candidates for shedding of cell-free infectious virions enabling interhost transmission. Whereas efficient viral proliferation is associated with the infection of ubiquitous cell types such as fibroblasts (138). It is tempting to speculate on the role of RL13 during natural infection given this information: Cell-free spread promoted by the trimer (gH/gL/gO) is required for host-host transmission of the virus in bodily fluids, whereas during intra-host dissemination of virus via the immunologically covert cell-associated mechanism of viral spread is promoted by not one but two genes, RL13 and UL128, independently of each other but dependent on cell type. UL128 is known to be involved in tropism, whereas RL13 has the potential to modulate tropism but as of yet, this tropism is unknown. Whether these genes (UL74, UL128L, RL13) do interact/compete/mediate one another to result in this viral spread switch which seems beneficial to the different stages of HCMV pathogenesis is unknown.

## 6.4 Future Directions and Concluding Remarks

This thesis aimed to investigate the function of the HCMV gene RL13 and to determine how and why its expression is so inhibitory to viral propagation *in vitro*. Although the *in vivo* purpose and mechanism by which RL13 acts was not determined, data described in this thesis provides significant insight into this elusive HCMV gene that is so problematic to work with in cell culture. Work described here should help advance the field of HCMV research and will aid in future investigations into the role of RL13 in HCMV pathogenesis.

RL13 was proposed (173) and confirmed in this thesis to bind Fc in isolation. It would be useful to see if this interaction remains true in the context of HCMV infection, however the presence of other recognised efficient HCMV Fc-binding proteins (UL119 and RL11) make it hard to see how RL13 could add to their effects. The Fc-binding property of RL13 does not explain the ability of RL13 to inhibit replication and suggests that there is another distinct interaction/effect by which gpRL13 impacts the HCMV life cycle. The retention of this effect in multiple genotypes and even across species, suggests that it may be the bonafide function of RL13. Further work investigating the proteins identified to bind and co-localise with RL13 with CRISPR could help identify any important interactions.

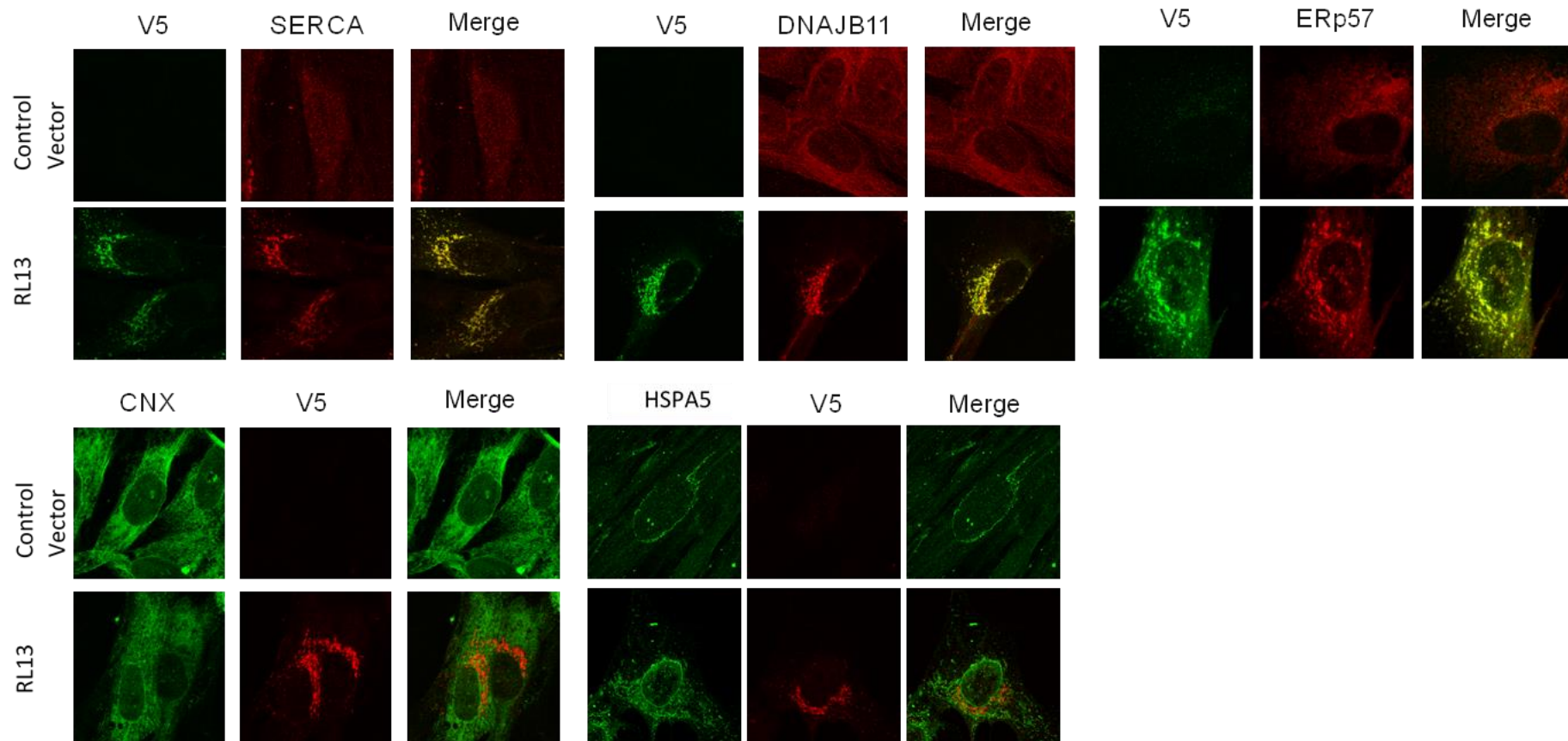
Alternatively, the restrictive phenotype and subsequent selection of RL13 mutants in cell culture may be an artefact of cell culture. However, with the data demonstrating the cell-cell spread method forced by RL13 and/or UL128L in fibroblasts in this thesis and the fact that clinical HCMV is often cell-associated, it seems possible that this restrictive phenotype is beneficial to the survival of the virus in *in vivo* infections. The fact that two genes in the HCMV genome result in this phenotype may seem redundant, although each protein may function under different circumstances, or by different methods. Further co-culture assays in more clinically relevant cell types could help investigate the potential role of RL13 in tropism. In addition, the presence of RL13 in the virion envelope has the potential to interact with additional cell surface receptors during entry. This aspect of RL13 function was not investigated during this thesis, but the production of soluble RL13 would be an interesting way to probe it.



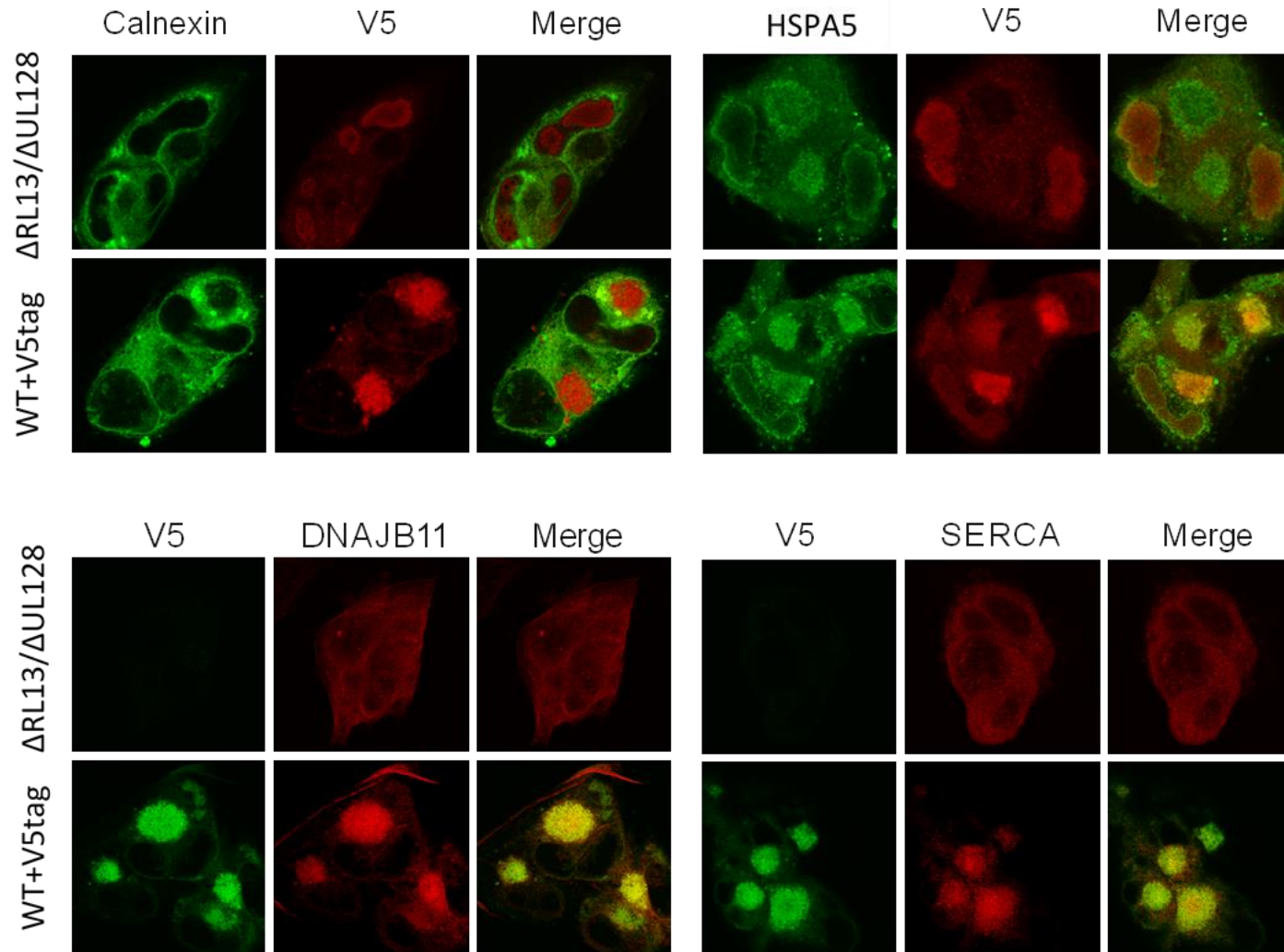
Although I can only comment for the 96 clinical strains, Merlin and TR, only 9 clades were identified for RL13. To my knowledge, this is the first evidence of genotypes for RL13 using an unrestricted pruning approach. Although more clinical strains would need to be sequenced to add confidence to this proposal, maybe the term hypervariable is misleading and RL13 is in fact a polymorphic HCMV gene with multiple conserved genotypes. Current efforts in HCMV vaccine development should therefore consider not only the genetic differences between laboratory strains and clinical isolates but also the different genetic variants between clinical isolates. This adds further implications for achieving therapeutics and vaccines active against all variants of HCMV and maybe implies that although variation between clinical isolates should be considered during design, that highly conserved genes would be a more likely choice for providing broad-spectrum immunity to HCMV.

Overall, this data demonstrates the importance of not only working with HCMV strains that contain and express the RL13 ORF fully intact, but also the consideration of other commonly mutated ORFs such as UL128, which effects not only the tropism of the virus but impacts how the virus spreads especially in the presence of neutralising antibodies and the expression of cell-surface glycoproteins which are major targets for the humoral immune system. RL13 expression reduced the expression of many host proteins within the virion which could potentially result in advantages for the +RL13 HCMV strains. RL13 also forced the virus to spread cell-cell in fibroblasts in the presence of neutralising antibodies, reduced infectivity of released viral particles and could potentially provide immune evasion through antibody-bipolar bridging as gpRL13 binds Fc. All these effects of RL13 expression could be valuable to bear in mind during vaccine design and would be missed when working with highly passaged, mutated lab strains of HCMV.

## **CHAPTER 7. APPENDIX**



**Figure S1 – RL13 recruits some host cell proteins to the AC.** Cells were infected with Rads expressing either RL13-V5 or an empty control Rad. 72 hr PI cells were fixed with PFA, permeabilised with 0.5% NP40, and incubated with antibodies to each of the host cell proteins. Secondary antibodies to each of the host cell proteins and V5 were then incubated with the samples. Samples were washed and imaged on a Leica SP5 confocal microscope. Proteins DNAJB11, SERCA and ERp57 are localised with RL13 to the AC. (Stanton, unpublished)



**Figure S2 – RL13 recruits some host cell proteins to the AC.** Cells were infected with  $\Delta$ RL13/ $\Delta$ UL128 or WT with RL13 V5-tagged. 72 hr PI cells were fixed with PFA, permeabilised with 0.5% NP40 and incubated with antibodies to each of the host cell proteins. Secondary antibodies to each of the host cell proteins and V5 were then incubated with the samples. Samples were washed and imaged on a Leica SP5 confocal microscope. Proteins DNAJB11, SERCA and to some degree HSPA5 are localised with RL13 to the AC. (Stanton, unpublished)

*Supplementary Table 1 – Primer sequences used in this project*

Project	Primer Name	Sequence	
qPCR	gB	F	CTGCGTGATATGAACGTGAAGG
		R	ACTGCACGTACGAGCTGTTGG
	GAPDH	F	CCTCTGACTTCAACAGCGACAC
		R	TGTCATACCAGGAAATGAGCTTGA
IE1/2-P2A-GFP	Rpsl R into Link	R	TGTGGCCGTTTACGTCGCCGTCCAGCTCGACCAGGATGGGCACCACCCCGGTGAACAGCTCCTCGCCCTTGCTCACCATCTGAGGTTCTTATG GCTCTTG
	Rpsl F into Link	F	GAGACCCCTCCCGAAGACCTGGACACCCTGAGCCTGGCCATCGAGGCAGCCATCCAGGACCTGAGGAACAAATCTCAGCCTGTGACGGAAGATCACTTCG
	Insert P2A-R	R	ACCAGGATGGGCACCACCCCGGTGAACAGCTCCTCGCCCTTGCTCACCATGGGGCCTGGATTCTCTTCGACATCCCGGCCTGCTTCAGCAGAGAGAAGT
	Insert P2A-F	F	TGAGCCTGGCCATCGAGGCAGCCATCCAGGACCTGAGGAACAAATCTCAGAGCGGCTCCGGTGCCACCAACTTCTCTCTGCTGAAGCAGGCCGGGGATGT
	Rpsl R after IE1	R	GAGTATAACATAGAGTATAATATAGAGTATACAATAGTGACGTGGGATCCATAACAGTAACTGATATATATACAATAGTCTGAGGTTCTTATG GCTCTTG
	Rpsl F after IE1	F	GATGGTGCTGAGGAACCCACCGCCTCTGGAGGCAAGAGCACCCACCCTATGGTGACTAGAAAGCAAGGCTGACCAGTAACCTGTGACGGAAGATCACTTCG
	P2AGFP after IE1 F		AGGAAGAGGAGGATGGTGCTGAGGAACCCACCGCCTCTGGAGGCAAGAGCACCCACCCTATGGTGACTAGAAAGCAAGGCTGACCAGAGCGGCTCCGGTGTC
	P2AGFP after IE1 R		GTATAACATAGAGTATAATATAGAGTATACAATAGTGACGTGGGATCCATAACAGTAACTGATATATATACAATAGTTTACTTGTACAGCTCGTCCATGC
	Seq R	R	GAACAGTGATCAGGAAGAAAGTGAA

	Seq F	F	ATTGACAGCCTGGGCGA
TR/Rhes us into Merlin	Rpsl into RL13 R	R	CGACTTATAAGTGATTAACCTCAGAATAAACACACCCCAAACATTAATGACTAAAGATAAAAAATTTATTGATGTGCATACTGAGGTTCTTATGG CTCTTG
	Rpsl into RL13 F	F	ACACATGAAATTAAGTAACATATCTACCATGAAATACAGCAAAGATATACTAATGTCTATCCATCCAATAGCGGTACCCCTGTGACGGAAGATC ACTTCG
	TRRL13 in Rpsl F	F	ACGCAACACATGAAATTAAGTAACATATCTACCATGAAATACAGCAAAGATATACTAATGTCTATCCATCCAATAGCGGTACCATGCACTGGCA TCTTGC
	TRRL13 in Rpsl R	R	GACTTATAAGTGATTAACCTCAGAATAAACACACCCCAAACATTAATGACTAAAGATAAAAAATTTATTGATGTGCATATCAGGTTTTAGTCCAA AACTCA
	RhRL13 into Rpsl FOR	F	ATGAAATTAAGTAACATATCTACCATGAAATACAGCAAAGATATACTAATGTCTATCCATCCAATAGCGGTACCATGACTAAGTATACGTGCTT CAGATC
	RhRL13 into Rpsl REV	R	TTATAAGTGATTAACCTCAGAATAAACACACCCCAAACATTAATGACTAAAGATAAAAAATTTATTGATGTGCATACTAGGAAAACATTGACTTC ACAGCG
	Seq	R	GTT CGC AGT TAT TGT GAT TCC A
	Seq	F	CAA ACG CCA ACG TAT CAA CA

*F – Forward primer, R – Reverse primer*

## **CHAPTER 8. REFERENCES**

1. Mocarski SM, Shenk T, Griffiths PD, Pass FP. Cytomegaloviruses. *Fields Virology*. 6th ed. Philadelphia: Lippincott Williams & Wilkins; 2013. p. 1960-2014.
2. Gibson W, Bogner E. Morphogenesis of the cytomegalovirus virion and subviral particles. In: Reddehase M, editor. *Cytomegaloviruses* 2013. p. 230-47.
3. Sijmons S, Thys K, Mbong Ngwese M, Van Damme E, Dvorak J, Van Loock M, et al. High-throughput analysis of human cytomegalovirus genome diversity highlights the widespread occurrence of gene-disrupting mutations and pervasive recombination. *J Virol*. 2015.
4. Wilkie GS, Davison AJ, Kerr K, Stidworthy MF, Redrobe S, Steinbach F, et al. First fatality associated with elephant endotheliotropic herpesvirus 5 in an Asian elephant: pathological findings and complete viral genome sequence. *Sci Rep*. 2014;4:6299.
5. Crough T, Khanna R. Immunobiology of human cytomegalovirus: from bench to bedside. *Clin Microbiol Rev*. 22. United States 2009. p. 76-98, Table of Contents.
6. Das S, Vasanji A, Pellett PE. Three-dimensional structure of the human cytomegalovirus cytoplasmic virion assembly complex includes a reoriented secretory apparatus. *J Virol*. 2007;81(21):11861-9.
7. Tandon R, Mocarski ES. Viral and host control of cytomegalovirus maturation. *Trends Microbiol*. 2012;20(8):392-401.
8. Stratton K, Durch J, Lawrence R. *Vaccines for the 21st Century: A Tool for Decision making*. Washington DC: National Academies Press; 2000.
9. Davison AJ, Eberle R, Ehlers B, Hayward GS, McGeoch DJ, Minson AC, et al. The order Herpesvirales. *Arch Virol*. 2009;154(1):171-7.
10. Roizmann B, Desrosiers RC, Fleckenstein B, Lopez C, Minson AC, Studdert MJ. The family Herpesviridae: an update. The Herpesvirus Study Group of the International Committee on Taxonomy of Viruses. *Arch Virol*. 1992;123(3-4):425-49.
11. Murphy E, Shenk T. Human cytomegalovirus genome. *Curr Top Microbiol Immunol*. 2008;325:1-19.
12. Reddehase MJ. Margaret Gladys Smith, mother of cytomegalovirus: 60th anniversary of cytomegalovirus isolation. *Medical microbiology and immunology*. 2015;204(3):239-41.
13. Reddehase MJ, Lemmermann N. Preface: from protozoan to proteomics. In: *Cytomegaloviruses: molecular biology and immunology*. Caister Academic Press, Norfolk, UK 2006.
14. Jesionek AKB. Über einen Befund von Protozoenartigen gebildet in den Organen eines hereditärluetischen Fetus. *Munch Med Wochenschr*. 1904;51:1905-7.
15. Ribbert H. Ueber protozoenartige Zellen in der Niere eines syphilitischen Neugeborenen und in der Parotis von Kindern. *Zentralbl Allg Pathol*. 1904;15:945-8.
16. Vonglahn WC, Pappenheimer AM. Intranuclear Inclusions in Visceral Disease. *Am J Pathol*. 1925;1(5):445-66.3.



17. Minder W. Die Aetiologie der Cytomegalia infantum. *Schweizer Med Wochenschr.* 1953;83:1180-2.
18. Wyatt JP, Saxton J. Generalized cytomegalic inclusion disease. *J Pediatr.* 1950;36(3):271-94, illust.
19. Rowe WP, Hartley JW, Waterman S, Turner HC, Huebner RJ. Cytopathogenic agent resembling human salivary gland virus recovered from tissue cultures of human adenoids. *Proc Soc Exp Biol Med.* 1956;92(2):418-24.
20. Smith MG. Propagation in Tissue Cultures of a Cytopathogenic Virus from Human Salivary Gland Virus (Sgv) Disease. *Proceedings of the Society for Experimental Biology and Medicine.* 1956;92(2):424-30.
21. Weller TH, Macauley JC, Craig JM, Wirth P. Isolation of intranuclear inclusion producing agents from infants with illnesses resembling cytomegalic inclusion disease. *Proc Soc Exp Biol Med.* 1957;94(1):4-12.
22. Ho M. The history of cytomegalovirus and its diseases. *Med Microbiol Immunol.* 2008;197(2):65-73.
23. Weller TH, Hanshaw JB, Scott DE. Serologic differentiation of viruses responsible for cytomegalic inclusion disease. *Virology.* 1960;12:130-2.
24. Staras SA, Dollard SC, Radford KW, Flanders WD, Pass RF, Cannon MJ. Seroprevalence of cytomegalovirus infection in the United States, 1988-1994. *Clin Infect Dis.* 2006;43(9):1143-51.
25. Kenneson A, Cannon MJ. Review and meta-analysis of the epidemiology of congenital cytomegalovirus (CMV) infection. *Rev Med Virol.* 2007;17(4):253-76.
26. Bate SL, Dollard SC, Cannon MJ. Cytomegalovirus seroprevalence in the United States: the national health and nutrition examination surveys, 1988-2004. *Clin Infect Dis.* 2010;50(11):1439-47.
27. Zuhair M, Smit GSA, Wallis G, Jabbar F, Smith C, Devleeschauwer B, et al. Estimation of the worldwide seroprevalence of cytomegalovirus: A systematic review and meta-analysis. *Rev Med Virol.* 2019:e2034.
28. Sia IG, Patel R. New strategies for prevention and therapy of cytomegalovirus infection and disease in solid-organ transplant recipients. *Clin Microbiol Rev.* 2000;13(1):83-121, table of contents.
29. Britt W. Virus entry into host, establishment of infection, spread in host, mechanisms of tissue damage. *Human Herpesviruses: Biology, Therapy, and Immunoprophylaxis: Cambridge university Press; 2007.*
30. Stowell JD, Forlin-Passoni D, Din E, Radford K, Brown D, White A, et al. Cytomegalovirus survival on common environmental surfaces: opportunities for viral transmission. *J Infect Dis.* 2012;205(2):211-4.
31. Goodrum F, Caviness K, Zagallo P. Human cytomegalovirus persistence. *Cell Microbiol.* 2012;14(5):644-55.
32. Reeves MB. Chromatin-mediated regulation of cytomegalovirus gene expression. *Virus Res.* 2011;157(2):134-43.

33. Conboy TJ, Pass RF, Stagno S, Alford CA, Myers GJ, Britt WJ, et al. Early clinical manifestations and intellectual outcome in children with symptomatic congenital cytomegalovirus infection. *The Journal of pediatrics*. 1987;111(3):343-8.
34. Boppana SB, Fowler KB, Britt WJ, Stagno S, Pass RF. Symptomatic congenital cytomegalovirus infection in infants born to mothers with preexisting immunity to cytomegalovirus. *Pediatrics*. 1999;104(1 Pt 1):55-60.
35. Nichols WG, Boeckh M, Carter RA, Wald A, Corey L. Transferred herpes simplex virus immunity after stem-cell transplantation: clinical implications. *J Infect Dis*. 2003;187(5):801-8.
36. Cunha BA. Cytomegalovirus pneumonia: community-acquired pneumonia in immunocompetent hosts. *Infect Dis Clin North Am*. 2010;24(1):147-58.
37. Boeckh M, Geballe AP. Cytomegalovirus: pathogen, paradigm, and puzzle. *J Clin Invest*. 2011;121(5):1673-80.
38. Stagno S, Pass RF, Cloud G, Britt WJ, Henderson RE, Walton PD, et al. Primary cytomegalovirus infection in pregnancy. Incidence, transmission to fetus, and clinical outcome. *JAMA*. 1986;256(14):1904-8.
39. Dollard SC, Grosse SD, Ross DS. New estimates of the prevalence of neurological and sensory sequelae and mortality associated with congenital cytomegalovirus infection. *Rev Med Virol*. 2007;17(5):355-63.
40. Fowler KB, Stagno S, Pass RF, Britt WJ, Boll TJ, Alford CA. The outcome of congenital cytomegalovirus infection in relation to maternal antibody status. *N Engl J Med*. 1992;326(10):663-7.
41. Pass RF, Fowler KB, Boppana SB, Britt WJ, Stagno S. Congenital cytomegalovirus infection following first trimester maternal infection: symptoms at birth and outcome. *J Clin Virol*. 2006;35(2):216-20.
42. Ahlfors K, Ivarsson SA. Cytomegalovirus in breast milk of Swedish milk donors. *Scand J Infect Dis*. 1985;17(1):11-3.
43. Emery VC. Investigation of CMV disease in immunocompromised patients. *J Clin Pathol*. 2001;54(2):84-8.
44. Griffiths PD. CMV as a cofactor enhancing progression of AIDS. *J Clin Virol*. 2006;35(4):489-92.
45. Schottstedt V, Blümel J, Burger R, Drosten C, Gröner A, Gürtler L, et al. Human Cytomegalovirus (HCMV) - Revised. *Transfusion medicine and hemotherapy : offizielles Organ der Deutschen Gesellschaft für Transfusionsmedizin und Immunhamatologie*. 2010;37(6):365-75.
46. Kempen JH, Jabs DA, Wilson LA, Dunn JP, West SK, Tonascia J. Mortality risk for patients with cytomegalovirus retinitis and acquired immune deficiency syndrome. *Clin Infect Dis*. 2003;37(10):1365-73.
47. Arthurs SK, Eid AJ, Pedersen RA, Kremers WK, Cosio FG, Patel R, et al. Delayed-onset primary cytomegalovirus disease and the risk of allograft failure and mortality after kidney transplantation. *Clin Infect Dis*. 2008;46(6):840-6.

48. Cantoni N, Hirsch HH, Khanna N, Gerull S, Buser A, Bucher C, et al. Evidence for a bidirectional relationship between cytomegalovirus replication and acute graft-versus-host disease. *Biol Blood Marrow Transplant*. 2010;16(9):1309-14.
49. Mitchell DA, Xie W, Schmittling R, Learn C, Friedman A, McLendon RE, et al. Sensitive detection of human cytomegalovirus in tumors and peripheral blood of patients diagnosed with glioblastoma. *Neuro Oncol*. 2008;10(1):10-8.
50. Scheurer ME, Bondy ML, Aldape KD, Albrecht T, El-Zein R. Detection of human cytomegalovirus in different histological types of gliomas. *Acta Neuropathol*. 2008;116(1):79-86.
51. Hjelmessaeth J, Sagedal S, Hartmann A, Rollag H, Egeland T, Hagen M, et al. Asymptomatic cytomegalovirus infection is associated with increased risk of new-onset diabetes mellitus and impaired insulin release after renal transplantation. *Diabetologia*. 2004;47(9):1550-6.
52. Lawlor G, Moss AC. Cytomegalovirus in inflammatory bowel disease: pathogen or innocent bystander? *Inflamm Bowel Dis*. 2010;16(9):1620-7.
53. Caposio P, Orloff SL, Streblow DN. The role of cytomegalovirus in angiogenesis. *Virus Res*. 2011;157(2):204-11.
54. Pawelec G, Akbar A, Beverley P, Caruso C, Derhovanessian E, Fülöp T, et al. Immunosenescence and Cytomegalovirus: where do we stand after a decade? *Immun Ageing*. 2010;7:13.
55. Vadlapudi AD, Vadlapatla RK, Mitra AK. Current and emerging antivirals for the treatment of cytomegalovirus (CMV) retinitis: an update on recent patents. *Recent Pat Antiinfect Drug Discov*. 2012;7(1):8-18.
56. Anderholm KM, Bierle CJ, Schleiss MR. Cytomegalovirus Vaccines: Current Status and Future Prospects. *Drugs*. 2016;76(17):1625-45.
57. Biron KK. Antiviral drugs for cytomegalovirus diseases. *Antiviral research*. 71. Netherlands2006. p. 154-63.
58. Erice A. Resistance of human cytomegalovirus to antiviral drugs. *Clin Microbiol Rev*. 1999;12(2):286-97.
59. Sullivan V, Talarico CL, Stanat SC, Davis M, Coen DM, Biron KK. A protein kinase homologue controls phosphorylation of ganciclovir in human cytomegalovirus-infected cells. *Nature*. 1992;358(6382):162-4.
60. Fishman JA. Infection in solid-organ transplant recipients. *N Engl J Med*. 2007;357(25):2601-14.
61. Plotkin SA, Furukawa T, Zygraich N, Huygelen C. Candidate cytomegalovirus strain for human vaccination. *Infect Immun*. 1975;12(3):521-7.
62. Plotkin SA, Smiley ML, Friedman HM, Starr SE, Fleisher GR, Wlodaver C, et al. Towne-vaccine-induced prevention of cytomegalovirus disease after renal transplants. *Lancet*. 1984;1(8376):528-30.

63. Pass RF, Duliege AM, Boppana S, Sekulovich R, Percell S, Britt W, et al. A subunit cytomegalovirus vaccine based on recombinant envelope glycoprotein B and a new adjuvant. *J Infect Dis.* 1999;180(4):970-5.
64. Frey SE, Harrison C, Pass RF, Yang E, Boken D, Sekulovich RE, et al. Effects of antigen dose and immunization regimens on antibody responses to a cytomegalovirus glycoprotein B subunit vaccine. *J Infect Dis.* 1999;180(5):1700-3.
65. Li F, Freed DC, Tang A, Rustandi RR, Troutman MC, Espeseth AS, et al. Complement enhances in vitro neutralizing potency of antibodies to human cytomegalovirus glycoprotein B (gB) and immune sera induced by gB/MF59 vaccination. *NPJ Vaccines.* 2017;2:36.
66. Pass RF, Zhang C, Evans A, Simpson T, Andrews W, Huang ML, et al. Vaccine prevention of maternal cytomegalovirus infection. *N Engl J Med.* 2009;360(12):1191-9.
67. Bernstein DI, Munoz FM, Callahan ST, Rupp R, Wootton SH, Edwards KM, et al. Safety and efficacy of a cytomegalovirus glycoprotein B (gB) vaccine in adolescent girls: A randomized clinical trial. *Vaccine.* 2016;34(3):313-9.
68. Griffiths PD, Stanton A, McCarrell E, Smith C, Osman M, Harber M, et al. Cytomegalovirus glycoprotein-B vaccine with MF59 adjuvant in transplant recipients: a phase 2 randomised placebo-controlled trial. *Lancet.* 2011;377(9773):1256-63.
69. Baraniak I, Kropff B, Ambrose L, McIntosh M, McLean GR, Pichon S, et al. Protection from cytomegalovirus viremia following glycoprotein B vaccination is not dependent on neutralizing antibodies. *Proc Natl Acad Sci U S A.* 2018;115(24):6273-8.
70. Nelson CS, Huffman T, Jenks JA, Cisneros de la Rosa E, Xie G, Vandergrift N, et al. HCMV glycoprotein B subunit vaccine efficacy mediated by nonneutralizing antibody effector functions. *Proc Natl Acad Sci U S A.* 2018;115(24):6267-72.
71. Kharfan-Dabaja MA, Boeckh M, Wilck MB, Langston AA, Chu AH, Wloch MK, et al. A novel therapeutic cytomegalovirus DNA vaccine in allogeneic haemopoietic stem-cell transplantation: a randomised, double-blind, placebo-controlled, phase 2 trial. *Lancet Infect Dis.* 2012;12(4):290-9.
72. Adler SP, Plotkin SA, Gonczol E, Cadoz M, Meric C, Wang JB, et al. A canarypox vector expressing cytomegalovirus (CMV) glycoprotein B primes for antibody responses to a live attenuated CMV vaccine (Towne). *J Infect Dis.* 1999;180(3):843-6.
73. Berencsi K, Gyulai Z, Gönczöl E, Pincus S, Cox WI, Michelson S, et al. A canarypox vector-expressing cytomegalovirus (CMV) phosphoprotein 65 induces long-lasting cytotoxic T cell responses in human CMV-seronegative subjects. *J Infect Dis.* 2001;183(8):1171-9.
74. Baldick CJ, Shenk T. Proteins associated with purified human cytomegalovirus particles. *J Virol.* 1996;70(9):6097-105.
75. Varum SM, Streblow DN, Monroe ME, Smith P, Auberry KJ, Pasa-Tolic L, et al. Identification of proteins in human cytomegalovirus (HCMV) particles: the HCMV proteome. *J Virol.* 2004;78(20):10960-6.
76. Brown JC, Newcomb WW. Herpesvirus capsid assembly: insights from structural analysis. *Curr Opin Virol.* 2011;1(2):142-9.

77. Gibson W. Structure and formation of the cytomegalovirus virion. *Curr Top Microbiol Immunol.* 2008;325:187-204.
  78. Mocarski Jr E. Betaherpes viral genes and their functions. In: Arvin A, Campadelli-Fiume G, Mocarski E, Moore PS, Roizman B, Whitley R, et al., editors. *Human Herpesviruses: Biology, Therapy, and Immunoprophylaxis.* Cambridge: Cambridge University Press
- Copyright (c) Cambridge University Press 2007.; 2007.
79. Newcomb WW, Cockrell SK, Homa FL, Brown JC. Polarized DNA ejection from the herpesvirus capsid. *J Mol Biol.* 2009;392(4):885-94.
  80. Borst EM, Mathys S, Wagner M, Muranyi W, Messerle M. Genetic evidence of an essential role for cytomegalovirus small capsid protein in viral growth. *J Virol.* 2001;75(3):1450-8.
  81. Chen DH, Jiang H, Lee M, Liu F, Zhou ZH. Three-dimensional visualization of tegument/capsid interactions in the intact human cytomegalovirus. *Virology.* 1999;260(1):10-6.
  82. Irmieri A, Gibson W. Isolation and characterization of a noninfectious virion-like particle released from cells infected with human strains of cytomegalovirus. *Virology.* 1983;130(1):118-33.
  83. Schauflinger M, Fischer D, Schreiber A, Chevillotte M, Walther P, Mertens T, et al. The tegument protein UL71 of human cytomegalovirus is involved in late envelopment and affects multivesicular bodies. *J Virol.* 2011;85(8):3821-32.
  84. Dunn W, Chou C, Li H, Hai R, Patterson D, Stolc V, et al. Functional profiling of a human cytomegalovirus genome. *Proc Natl Acad Sci U S A.* 2003;100(24):14223-8.
  85. Britt B. Maturation and egress. In: Arvin A, Campadelli-Fiume G, Mocarski E, Moore PS, Roizman B, Whitley R, et al., editors. *Human Herpesviruses: Biology, Therapy, and Immunoprophylaxis.* Cambridge: Cambridge University Press
- Copyright (c) Cambridge University Press 2007.; 2007.
86. Sprague ER, Reinhard H, Cheung EJ, Farley AH, Trujillo RD, Hengel H, et al. The human cytomegalovirus Fc receptor gp68 binds the Fc CH2-CH3 interface of immunoglobulin G. *J Virol.* 2008;82(7):3490-9.
  87. Isaacson MK, Juckem LK, Compton T. Virus entry and innate immune activation. *Curr Top Microbiol Immunol.* 2008;325:85-100.
  88. Kabanova A, Marcandalli J, Zhou T, Bianchi S, Baxa U, Tsybovsky Y, et al. Platelet-derived growth factor-alpha receptor is the cellular receptor for human cytomegalovirus gHgLgO trimer. *Nat Microbiol.* 2016;1(8):16082.
  89. Ryckman BJ, Chase MC, Johnson DC. HCMV gH/gL/UL128-131 interferes with virus entry into epithelial cells: evidence for cell type-specific receptors. *Proc Natl Acad Sci U S A.* 2008;105(37):14118-23.
  90. Ryckman BJ, Rainish BL, Chase MC, Borton JA, Nelson JA, Jarvis MA, et al. Characterization of the human cytomegalovirus gH/gL/UL128-131 complex that mediates entry into epithelial and endothelial cells. *J Virol.* 2008;82(1):60-70.

91. Martinez-Martin N, Marcandalli J, Huang CS, Arthur CP, Perotti M, Foglierini M, et al. An Unbiased Screen for Human Cytomegalovirus Identifies Neuropilin-2 as a Central Viral Receptor. *Cell*. 2018;174(5):1158-71.e19.
92. Revello MG, Gerna G. Human cytomegalovirus tropism for endothelial/epithelial cells: scientific background and clinical implications. *Rev Med Virol*. 2010;20(3):136-55.
93. Gibson W, Roizman B. Proteins specified by herpes simplex virus. 8. Characterization and composition of multiple capsid forms of subtypes 1 and 2. *J Virol*. 1972;10(5):1044-52.
94. Gibson W. Structure and assembly of the virion. *Intervirology*. 1996;39(5-6):389-400.
95. Liu F, Zhou H. Comparative virion structures of human herpesviruses. In: Arvin AC-F, G.Mocarski, E.Moore, P.Roizman, B.Whitley, R.Yamanishi, K., style="page-break-before:always bca, /> m-b-ts-b, editors. *Human Herpesviruses: Biology, Therapy, and Immunoprophylaxis*: Cambridge University Press; 2007.
96. Pepperl S, Münster J, Mach M, Harris JR, Plachter B. Dense bodies of human cytomegalovirus induce both humoral and cellular immune responses in the absence of viral gene expression. *J Virol*. 2000;74(13):6132-46.
97. Isaacson MK, Compton T. Human cytomegalovirus glycoprotein B is required for virus entry and cell-to-cell spread but not for virion attachment, assembly, or egress. *J Virol*. 2009;83(8):3891-903.
98. Hobom U, Brune W, Messerle M, Hahn G, Koszinowski UH. Fast screening procedures for random transposon libraries of cloned herpesvirus genomes: mutational analysis of human cytomegalovirus envelope glycoprotein genes. *J Virol*. 2000;74(17):7720-9.
99. Evers DL, Wang X, Huang ES. Cellular stress and signal transduction responses to human cytomegalovirus infection. *Microbes Infect*. 2004;6(12):1084-93.
100. Compton T, Nepomuceno RR, Nowlin DM. Human cytomegalovirus penetrates host cells by pH-independent fusion at the cell surface. *Virology*. 1992;191(1):387-95.
101. Ryckman BJ, Jarvis MA, Drummond DD, Nelson JA, Johnson DC. Human cytomegalovirus entry into epithelial and endothelial cells depends on genes UL128 to UL150 and occurs by endocytosis and low-pH fusion. *Journal of virology*. 2006;80(2):710-22.
102. Haspot F, Lavault A, Sinzger C, Laib Sampaio K, Stierhof YD, Pilet P, et al. Human cytomegalovirus entry into dendritic cells occurs via a macropinocytosis-like pathway in a pH-independent and cholesterol-dependent manner. *PLoS One*. 2012;7(4):e34795.
103. Ziemann M, Hennig H. Prevention of Transfusion-Transmitted Cytomegalovirus Infections: Which is the Optimal Strategy? *Transfus Med Hemother*. 2014;41(1):40-4.
104. Roenhorst HW, Kallenberg CG, The TH. The cellular immune response to cell-associated and cell-free cytomegalovirus (CMV) antigens after primary CMV-infection in non-immunocompromised hosts: development and maintenance of CMV-latency and its influence on immunocompetence. *Clinical and experimental immunology*. 1988;74(3):326-32.
105. Gerna G, Percivalle E, Baldanti F, Sozzani S, Lanzarini P, Genini E, et al. Human cytomegalovirus replicates abortively in polymorphonuclear leukocytes after transfer from infected endothelial cells via transient microfusion events. *J Virol*. 2000;74(12):5629-38.

106. Kinzler ER, Compton T. Characterization of human cytomegalovirus glycoprotein-induced cell-cell fusion. *J Virol.* 2005;79(12):7827-37.
107. Yu Y, Clippinger AJ, Alwine JC. Viral effects on metabolism: changes in glucose and glutamine utilization during human cytomegalovirus infection. *Trends Microbiol.* 2011;19(7):360-7.
108. Yurochko AD. Human cytomegalovirus modulation of signal transduction. *Curr Top Microbiol Immunol.* 2008;325:205-20.
109. Jean Beltran PM, Cristea IM. The life cycle and pathogenesis of human cytomegalovirus infection: lessons from proteomics. *Expert Rev Proteomics.* 2014;11(6):697-711.
110. Kim YE, Oh SE, Kwon KM, Lee CH, Ahn JH. Involvement of the N-Terminal Deubiquitinating Protease Domain of Human Cytomegalovirus UL48 Tegument Protein in Autoubiquitination, Virion Stability, and Virus Entry. *J Virol.* 2016;90(6):3229-42.
111. Kalejta RF. Functions of human cytomegalovirus tegument proteins prior to immediate early gene expression. *Curr Top Microbiol Immunol.* 2008;325:101-15.
112. Saffert RT, Kalejta RF. Inactivating a cellular intrinsic immune defense mediated by Daxx is the mechanism through which the human cytomegalovirus pp71 protein stimulates viral immediate-early gene expression. *J Virol.* 2006;80(8):3863-71.
113. Wilkinson GW, Akrigg A, Greenaway PJ. Transcription of the immediate early genes of human cytomegalovirus strain AD169. *Virus Res.* 1984;1(2):101-6.
114. Stenberg RM, Depto AS, Fortney J, Nelson JA. Regulated expression of early and late RNAs and proteins from the human cytomegalovirus immediate-early gene region. *J Virol.* 1989;63(6):2699-708.
115. Wilkinson GW, Kelly C, Sinclair JH, Rickards C. Disruption of PML-associated nuclear bodies mediated by the human cytomegalovirus major immediate early gene product. *J Gen Virol.* 1998;79 ( Pt 5):1233-45.
116. Spector DJ, Tevethia MJ. Protein-protein interactions between human cytomegalovirus IE2-580aa and pUL84 in lytically infected cells. *J Virol.* 1994;68(11):7549-53.
117. McVoy MA, Adler SP. Human cytomegalovirus DNA replicates after early circularization by concatemer formation, and inversion occurs within the concatemer. *J Virol.* 1994;68(2):1040-51.
118. Heming JD, Conway JF, Homa FL. Herpesvirus Capsid Assembly and DNA Packaging. *Adv Anat Embryol Cell Biol.* 2017;223:119-42.
119. Wang JB, McVoy MA. A 128-base-pair sequence containing the pac1 and a presumed cryptic pac2 sequence includes cis elements sufficient to mediate efficient genome maturation of human cytomegalovirus. *J Virol.* 2011;85(9):4432-9.
120. Bogner E. Human cytomegalovirus terminase as a target for antiviral chemotherapy. *Rev Med Virol.* 2002;12(2):115-27.
121. Stinski MF, Petrik DT. Functional roles of the human cytomegalovirus essential IE86 protein. *Curr Top Microbiol Immunol.* 2008;325:133-52.

122. Muranyi W, Haas J, Wagner M, Krohne G, Koszinowski UH. Cytomegalovirus recruitment of cellular kinases to dissolve the nuclear lamina. *Science*. 2002;297(5582):854-7.
123. Leelawong M, Guo D, Smith GA. A physical link between the pseudorabies virus capsid and the nuclear egress complex. *J Virol*. 2011;85(22):11675-84.
124. Schierling K, Buser C, Mertens T, Winkler M. Human cytomegalovirus tegument protein ppUL35 is important for viral replication and particle formation. *J Virol*. 2005;79(5):3084-96.
125. Ahlqvist J, Mocarski E. Cytomegalovirus UL103 controls virion and dense body egress. *J Virol*. 2011;85(10):5125-35.
126. Cepeda V, Esteban M, Fraile-Ramos A. Human cytomegalovirus final envelopment on membranes containing both trans-Golgi network and endosomal markers. *Cell Microbiol*. 2010;12(3):386-404.
127. Mendelson M, Monard S, Sissons P, Sinclair J. Detection of endogenous human cytomegalovirus in CD34+ bone marrow progenitors. *J Gen Virol*. 1996;77 ( Pt 12):3099-102.
128. Hahn G, Jores R, Mocarski ES. Cytomegalovirus remains latent in a common precursor of dendritic and myeloid cells. *Proc Natl Acad Sci U S A*. 1998;95(7):3937-42.
129. Sinclair J, Sissons P. Latency and reactivation of human cytomegalovirus. *J Gen Virol*. 2006;87(Pt 7):1763-79.
130. Meier JL, Stinski MF. Regulation of human cytomegalovirus immediate-early gene expression. *Intervirology*. 1996;39(5-6):331-42.
131. Bain M, Mendelson M, Sinclair J. Ets-2 Repressor Factor (ERF) mediates repression of the human cytomegalovirus major immediate-early promoter in undifferentiated non-permissive cells. *J Gen Virol*. 2003;84(Pt 1):41-9.
132. Rauwel B, Jang SM, Cassano M, Kapopoulou A, Barde I, Trono D. Release of human cytomegalovirus from latency by a KAP1/TRIM28 phosphorylation switch. *Elife*. 2015;4.
133. Saffert RT, Penkert RR, Kalejta RF. Cellular and viral control over the initial events of human cytomegalovirus experimental latency in CD34+ cells. *J Virol*. 2010;84(11):5594-604.
134. Reeves MB, Sinclair JH. Circulating dendritic cells isolated from healthy seropositive donors are sites of human cytomegalovirus reactivation in vivo. *J Virol*. 2013;87(19):10660-7.
135. Reeves MB, Lehner PJ, Sissons JG, Sinclair JH. An in vitro model for the regulation of human cytomegalovirus latency and reactivation in dendritic cells by chromatin remodelling. *J Gen Virol*. 2005;86(Pt 11):2949-54.
136. Jackson JW, Sparer T. There Is Always Another Way! Cytomegalovirus' Multifaceted Dissemination Schemes. *Viruses*. 2018;10(7).
137. Sinzger C, Jahn G. Human cytomegalovirus cell tropism and pathogenesis. *Intervirology*. 1996;39(5-6):302-19.
138. Sinzger C, Digel M, Jahn G. Cytomegalovirus cell tropism. *Curr Top Microbiol Immunol*. 2008;325:63-83.
139. Farrell HE, Lawler C, Tan CS, MacDonald K, Bruce K, Mach M, et al. Murine Cytomegalovirus Exploits Olfaction To Enter New Hosts. *MBio*. 2016;7(2):e00251-16.



140. Grefte A, van der Giessen M, van Son W, The TH. Circulating cytomegalovirus (CMV)-infected endothelial cells in patients with an active CMV infection. *J Infect Dis.* 1993;167(2):270-7.
141. Sweet C. The pathogenicity of cytomegalovirus. *FEMS Microbiol Rev.* 1999;23(4):457-82.
142. Daley-Bauer LP, Roback LJ, Wynn GM, Mocarski ES. Cytomegalovirus hijacks CX3CR1(hi) patrolling monocytes as immune-privileged vehicles for dissemination in mice. *Cell Host Microbe.* 2014;15(3):351-62.
143. Taylor-Wiedeman J, Sissons JG, Borysiewicz LK, Sinclair JH. Monocytes are a major site of persistence of human cytomegalovirus in peripheral blood mononuclear cells. *J Gen Virol.* 1991;72 ( Pt 9):2059-64.
144. Parish T, Smith DA, Kendall S, Casali N, Bancroft GJ, Stoker NG. Deletion of two-component regulatory systems increases the virulence of *Mycobacterium tuberculosis*. *Infect Immun.* 2003;71(3):1134-40.
145. Cunningham ML, Titus RG, Turco SJ, Beverley SM. Regulation of differentiation to the infective stage of the protozoan parasite *Leishmania major* by tetrahydrobiopterin. *Science.* 2001;292(5515):285-7.
146. Scrivano L, Sinzger C, Nitschko H, Koszinowski UH, Adler B. HCMV spread and cell tropism are determined by distinct virus populations. *PLoS Pathog.* 2011;7(1):e1001256.
147. van de Berg PJ, Heutinck KM, Raabe R, Minnee RC, Young SL, van Donselaar-van der Pant KA, et al. Human cytomegalovirus induces systemic immune activation characterized by a type 1 cytokine signature. *J Infect Dis.* 2010;202(5):690-9.
148. Thompson MR, Kaminski JJ, Kurt-Jones EA, Fitzgerald KA. Pattern recognition receptors and the innate immune response to viral infection. *Viruses.* 2011;3(6):920-40.
149. Neefjes J, Jongsma ML, Paul P, Bakke O. Towards a systems understanding of MHC class I and MHC class II antigen presentation. *Nat Rev Immunol.* 2011;11(12):823-36.
150. Petersen JL, Morris CR, Solheim JC. Virus evasion of MHC class I molecule presentation. *J Immunol.* 2003;171(9):4473-8.
151. Noris M, Remuzzi G. Overview of complement activation and regulation. *Semin Nephrol.* 2013;33(6):479-92.
152. Spiller OB, Hanna SM, Devine DV, Tufaro F. Neutralization of cytomegalovirus virions: the role of complement. *J Infect Dis.* 1997;176(2):339-47.
153. Gafa V, Manches O, Pastor A, Drouet E, Ambroise-Thomas P, Grillot R, et al. Human cytomegalovirus downregulates complement receptors (CR3, CR4) and decreases phagocytosis by macrophages. *J Med Virol.* 2005;76(3):361-6.
154. Akira S, Uematsu S, Takeuchi O. Pathogen recognition and innate immunity. *Cell.* 2006;124(4):783-801.
155. Boehme KW, Guerrero M, Compton T. Human cytomegalovirus envelope glycoproteins B and H are necessary for TLR2 activation in permissive cells. *J Immunol.* 2006;177(10):7094-102.
156. Biron CA, Byron KS, Sullivan JL. Severe herpesvirus infections in an adolescent without natural killer cells. *N Engl J Med.* 1989;320(26):1731-5.

157. Iversen AC, Norris PS, Ware CF, Benedict CA. Human NK cells inhibit cytomegalovirus replication through a noncytolytic mechanism involving lymphotoxin-dependent induction of IFN-beta. *J Immunol.* 2005;175(11):7568-74.
158. Wilkinson GW, Tomasec P, Stanton RJ, Armstrong M, Prod'homme V, Aicheler R, et al. Modulation of natural killer cells by human cytomegalovirus. *J Clin Virol.* 2008;41(3):206-12.
159. Patel M, Vlahava VM, Forbes SK, Fielding CA, Stanton RJ, Wang ECY. HCMV-Encoded NK Modulators: Lessons From in vitro and in vivo Genetic Variation. *Front Immunol.* 2018;9:2214.
160. Fielding CA, Aicheler R, Stanton RJ, Wang EC, Han S, Seirafian S, et al. Two novel human cytomegalovirus NK cell evasion functions target MICA for lysosomal degradation. *PLoS Pathog.* 2014;10(5):e1004058.
161. La Rosa C, Diamond DJ. The immune response to human CMV. *Future Virol.* 2012;7(3):279-93.
162. Sylwester AW, Mitchell BL, Edgar JB, Taormina C, Pelte C, Ruchti F, et al. Broadly targeted human cytomegalovirus-specific CD4+ and CD8+ T cells dominate the memory compartments of exposed subjects. *J Exp Med.* 2005;202(5):673-85.
163. Hanley PJ, Bollard CM. Controlling cytomegalovirus: helping the immune system take the lead. *Viruses.* 2014;6(6):2242-58.
164. Sester U, Gartner BC, Wilkens H, Schwaab B, Wossner R, Kindermann I, et al. Differences in CMV-specific T-cell levels and long-term susceptibility to CMV infection after kidney, heart and lung transplantation. *Am J Transplant.* 2005;5(6):1483-9.
165. Shanley JD, Jordan MC, Stevens JG. Modification by adoptive humoral immunity of murine cytomegalovirus infection. *J Infect Dis.* 1981;143(2):231-7.
166. Jonjic S, Pavic I, Polic B, Crnkovic I, Lucin P, Koszinowski UH. Antibodies are not essential for the resolution of primary cytomegalovirus infection but limit dissemination of recurrent virus. *J Exp Med.* 1994;179(5):1713-7.
167. Klenovsek K, Weisel F, Schneider A, Appelt U, Jonjic S, Messerle M, et al. Protection from CMV infection in immunodeficient hosts by adoptive transfer of memory B cells. *Blood.* 2007;110(9):3472-9.
168. Dauby N, Kummert C, Lecomte S, Liesnard C, Delforge ML, Donner C, et al. Primary human cytomegalovirus infection induces the expansion of virus-specific activated and atypical memory B cells. *J Infect Dis.* 2014;210(8):1275-85.
169. Britt WJ, Vugler L, Butfiloski EJ, Stephens EB. Cell surface expression of human cytomegalovirus (HCMV) gp55-116 (gB): use of HCMV-recombinant vaccinia virus-infected cells in analysis of the human neutralizing antibody response. *J Virol.* 1990;64(3):1079-85.
170. Urban M, Klein M, Britt WJ, Hassfurth E, Mach M. Glycoprotein H of human cytomegalovirus is a major antigen for the neutralizing humoral immune response. *J Gen Virol.* 1996;77 ( Pt 7):1537-47.
171. Shimamura M, Mach M, Britt WJ. Human cytomegalovirus infection elicits a glycoprotein M (gM)/gN-specific virus-neutralizing antibody response. *J Virol.* 2006;80(9):4591-600.

172. Fouts AE, Chan P, Stephan JP, Vandlen R, Feierbach B. Antibodies against the gH/gL/UL128/UL130/UL131 complex comprise the majority of the anti-cytomegalovirus (anti-CMV) neutralizing antibody response in CMV hyperimmune globulin. *J Virol.* 2012;86(13):7444-7.
173. Cortese M, Calò S, D'Aurizio R, Lilja A, Pacchiani N, Merola M. Recombinant human cytomegalovirus (HCMV) RL13 binds human immunoglobulin G Fc. *PLoS one.* 2012;7(11):e50166.
174. Atalay R, Zimmermann A, Wagner M, Borst E, Benz C, Messerle M, et al. Identification and expression of human cytomegalovirus transcription units coding for two distinct Fcγ receptor homologs. *J Virol.* 2002;76(17):8596-608.
175. Dolan A, Cunningham C, Hector RD, Hassan-Walker AF, Lee L, Addison C, et al. Genetic content of wild-type human cytomegalovirus. *J Gen Virol.* 2004;85(Pt 5):1301-12.
176. Davison A. Chapter 2 Comparative analysis of the genomes. *Human Herpesviruses: Biology, Therapy, and Immunoprophylaxis.* Cambridge: Cambridge University Press; 2007.
177. Chee MS, Bankier AT, Beck S, Bohni R, Brown CM, Cerny R, et al. Analysis of the protein-coding content of the sequence of human cytomegalovirus strain AD169. *Curr Top Microbiol Immunol.* 1990;154:125-69.
178. Davison AJ, Dolan A, Akter P, Addison C, Dargan DJ, Alcendor DJ, et al. The human cytomegalovirus genome revisited: comparison with the chimpanzee cytomegalovirus genome. *J Gen Virol.* 2003;84(Pt 1):17-28.
179. Stern-Ginossar N, Weisburd B, Michalski A, Le VT, Hein MY, Huang SX, et al. Decoding human cytomegalovirus. *Science.* 2012;338(6110):1088-93.
180. Nightingale K, Lin KM, Ravenhill BJ, Davies C, Nobre L, Fielding CA, et al. High-Definition Analysis of Host Protein Stability during Human Cytomegalovirus Infection Reveals Antiviral Factors and Viral Evasion Mechanisms. *Cell Host Microbe.* 2018;24(3):447-60.e11.
181. Grey F, Tirabassi R, Meyers H, Wu G, McWeeney S, Hook L, et al. A viral microRNA down-regulates multiple cell cycle genes through mRNA 5'UTRs. *PLoS Pathog.* 2010;6(6):e1000967.
182. Pfeffer S, Sewer A, Lagos-Quintana M, Sheridan R, Sander C, Grasser FA, et al. Identification of microRNAs of the herpesvirus family. *Nat Methods.* 2005;2(4):269-76.
183. Dunn W, Trang P, Zhong Q, Yang E, van Belle C, Liu F. Human cytomegalovirus expresses novel microRNAs during productive viral infection. *Cell Microbiol.* 2005;7(11):1684-95.
184. Tuddenham L, Pfeffer S. Roles and regulation of microRNAs in cytomegalovirus infection. *Biochim Biophys Acta.* 2011;1809(11-12):613-22.
185. Stark TJ, Arnold JD, Spector DH, Yeo GW. High-resolution profiling and analysis of viral and host small RNAs during human cytomegalovirus infection. *J Virol.* 2012;86(1):226-35.
186. Gatherer D, Seirafian S, Cunningham C, Holton M, Dargan DJ, Baluchova K, et al. High-resolution human cytomegalovirus transcriptome. *Proc Natl Acad Sci U S A.* 2011;108(49):19755-60.
187. Cha TA, Tom E, Kemble GW, Duke GM, Mocarski ES, Spaete RR. Human cytomegalovirus clinical isolates carry at least 19 genes not found in laboratory strains. *J Virol.* 1996;70(1):78-83.
188. Chou SW. Reactivation and recombination of multiple cytomegalovirus strains from individual organ donors. *J Infect Dis.* 1989;160(1):11-5.

189. Chou SW, Dennison KM. Analysis of interstrain variation in cytomegalovirus glycoprotein B sequences encoding neutralization-related epitopes. *J Infect Dis.* 1991;163(6):1229-34.
190. Lurain NS, Fox AM, Lichy HM, Bhorade SM, Ware CF, Huang DD, et al. Analysis of the human cytomegalovirus genomic region from UL146 through UL147A reveals sequence hypervariability, genotypic stability, and overlapping transcripts. *Virol J.* 2006;3:4.
191. Davison AJ, Akter P, Cunningham C, Dolan A, Addison C, Dargan DJ, et al. Homology between the human cytomegalovirus RL11 gene family and human adenovirus E3 genes. *J Gen Virol.* 2003;84(Pt 3):657-63.
192. Pignatelli S, Dal Monte P, Rossini G, Landini MP. Genetic polymorphisms among human cytomegalovirus (HCMV) wild-type strains. *Rev Med Virol.* 2004;14(6):383-410.
193. Dargan DJ, Douglas E, Cunningham C, Jamieson F, Stanton RJ, Baluchova K, et al. Sequential mutations associated with adaptation of human cytomegalovirus to growth in cell culture. *J Gen Virol.* 2010;91(Pt 6):1535-46.
194. Bradley AJ, Lurain NS, Ghazal P, Trivedi U, Cunningham C, Baluchova K, et al. High-throughput sequence analysis of variants of human cytomegalovirus strains Towne and AD169. *J Gen Virol.* 2009;90(Pt 10):2375-80.
195. Brown JM, Kaneshima H, Mocarski ES. Dramatic interstrain differences in the replication of human cytomegalovirus in SCID-hu mice. *J Infect Dis.* 1995;171(6):1599-603.
196. Penfold ME, Dairaghi DJ, Duke GM, Saederup N, Mocarski ES, Kemble GW, et al. Cytomegalovirus encodes a potent alpha chemokine. *Proc Natl Acad Sci U S A.* 1999;96(17):9839-44.
197. Benedict CA, Butrovich KD, Lurain NS, Corbeil J, Rooney I, Schneider P, et al. Cutting edge: a novel viral TNF receptor superfamily member in virulent strains of human cytomegalovirus. *J Immunol.* 1999;162(12):6967-70.
198. Wills MR, Ashiru O, Reeves MB, Okecha G, Trowsdale J, Tomasec P, et al. Human cytomegalovirus encodes an MHC class I-like molecule (UL142) that functions to inhibit NK cell lysis. *J Immunol.* 2005;175(11):7457-65.
199. Waldman WJ, Roberts WH, Davis DH, Williams MV, Sedmak DD, Stephens RE. Preservation of natural endothelial cytopathogenicity of cytomegalovirus by propagation in endothelial cells. *Arch Virol.* 1991;117(3-4):143-64.
200. Sinzger C, Schmidt K, Knapp J, Kahl M, Beck R, Waldman J, et al. Modification of human cytomegalovirus tropism through propagation in vitro is associated with changes in the viral genome. *J Gen Virol.* 1999;80 ( Pt 11):2867-77.
201. Sinzger C, Knapp J, Plachter B, Schmidt K, Jahn G. Quantification of replication of clinical cytomegalovirus isolates in cultured endothelial cells and fibroblasts by a focus expansion assay. *J Virol Methods.* 1997;63(1-2):103-12.
202. MacCormac LP, Grundy JE. Two clinical isolates and the Toledo strain of cytomegalovirus contain endothelial cell tropic variants that are not present in the AD169, Towne, or Davis strains. *J Med Virol.* 1999;57(3):298-307.

203. Stanton RJ, Baluchova K, Dargan DJ, Cunningham C, Sheehy O, Seirafian S, et al. Reconstruction of the complete human cytomegalovirus genome in a BAC reveals RL13 to be a potent inhibitor of replication. *The Journal of clinical investigation*. 2010;120(9):3191.
204. Cui X, Adler SP, Davison AJ, Smith L, Habib e-S, McVoy MA. Bacterial artificial chromosome clones of viruses comprising the towne cytomegalovirus vaccine. *J Biomed Biotechnol*. 2012;2012:428498.
205. Hahn G, Rose D, Wagner M, Rhie S, McVoy MA. Cloning of the genomes of human cytomegalovirus strains Toledo, TownevarRIT3, and Towne long as BACs and site-directed mutagenesis using a PCR-based technique. *Virology*. 2003;307(1):164-77.
206. Borst EM, Hahn G, Koszinowski UH, Messerle M. Cloning of the human cytomegalovirus (HCMV) genome as an infectious bacterial artificial chromosome in *Escherichia coli*: a new approach for construction of HCMV mutants. *J Virol*. 1999;73(10):8320-9.
207. Sinzger C, Hahn G, Digel M, Katona R, Sampaio KL, Messerle M, et al. Cloning and sequencing of a highly productive, endotheliotropic virus strain derived from human cytomegalovirus TB40/E. *J Gen Virol*. 2008;89(Pt 2):359-68.
208. Murrell I, Tomasec P, Wilkie GS, Dargan DJ, Davison AJ, Stanton RJ. Impact of sequence variation in the UL128 locus on production of human cytomegalovirus in fibroblast and epithelial cells. *J Virol*. 2013;87(19):10489-500.
209. Li M, Ma Y, Ji Y, He R, Qi Y, Sun Z, et al. Human cytomegalovirus RL13 gene transcripts in a clinical strain. *Virus Genes*. 2011;43(3):327-34.
210. Weekes MP, Tomasec P, Huttlin EL, Fielding CA, Nusinow D, Stanton RJ, et al. Quantitative temporal viromics: an approach to investigate host-pathogen interaction. *Cell*. 2014;157(6):1460-72.
211. Van Damme E, Van Loock M. Functional annotation of human cytomegalovirus gene products: an update. *Frontiers in Microbiology*. 2014;5.
212. Murphy E, Yu D, Grimwood J, Schmutz J, Dickson M, Jarvis MA, et al. Coding potential of laboratory and clinical strains of human cytomegalovirus. *Proc Natl Acad Sci U S A*. 2003;100(25):14976-81.
213. Chang CP, Vesole DH, Nelson J, Oldstone MB, Stinski MF. Identification and expression of a human cytomegalovirus early glycoprotein. *J Virol*. 1989;63(8):3330-7.
214. Shikhagaie M, Merce-Maldonado E, Isern E, Muntasell A, Alba MM, Lopez-Botet M, et al. The human cytomegalovirus-specific UL1 gene encodes a late-phase glycoprotein incorporated in the virion envelope. *J Virol*. 2012;86(8):4091-101.
215. Vink C, Beuken E, Bruggeman CA. Complete DNA sequence of the rat cytomegalovirus genome. *J Virol*. 2000;74(16):7656-65.
216. Thale R, Lucin P, Schneider K, Eggers M, Koszinowski UH. Identification and expression of a murine cytomegalovirus early gene coding for an Fc receptor. *J Virol*. 1994;68(12):7757-65.
217. Powers C, Fruh K. Rhesus CMV: an emerging animal model for human CMV. *Med Microbiol Immunol*. 2008;197(2):109-15.

218. Malouli D, Nakayasu ES, Viswanathan K, Camp DG, Chang WL, Barry PA, et al. Reevaluation of the coding potential and proteomic analysis of the BAC-derived rhesus cytomegalovirus strain 68-1. *J Virol*. 2012;86(17):8959-73.
219. Murrell I, Wilkie GS, Davison AJ, Statkute E, Fielding CA, Tomasec P, et al. Genetic Stability of Bacterial Artificial Chromosome-Derived Human Cytomegalovirus during Culture In Vitro. *J Virol*. 2016;90(8):3929-43.
220. Matrosovich M, Matrosovich T, Garten W, Klenk HD. New low-viscosity overlay medium for viral plaque assays. *Virol J*. 2006;3:63.
221. Warming S, Costantino N, Court DL, Jenkins NA, Copeland NG. Simple and highly efficient BAC recombineering using galK selection. *Nucleic Acids Res*. 2005;33(4):e36.
222. Newman GRH, J. A. Resin Microscopy and On-Section Immunocytochemistry. 2nd ed. Heidelberg: Springer; 2001 2001.
223. Kim JH, Lee SR, Li LH, Park HJ, Park JH, Lee KY, et al. High cleavage efficiency of a 2A peptide derived from porcine teschovirus-1 in human cell lines, zebrafish and mice. *PLoS One*. 2011;6(4):e18556.
224. Trichas G, Begbie J, Srinivas S. Use of the viral 2A peptide for bicistronic expression in transgenic mice. *BMC Biol*. 2008;6:40.
225. Akter P, Cunningham C, McSharry BP, Dolan A, Addison C, Dargan DJ, et al. Two novel spliced genes in human cytomegalovirus. *J Gen Virol*. 2003;84(Pt 5):1117-22.
226. Yang Z, Bielawski JP. Statistical methods for detecting molecular adaptation. *Trends Ecol Evol*. 2000;15(12):496-503.
227. Wang G, Ren G, Cui X, Lu Z, Ma Y, Qi Y, et al. Human cytomegalovirus RL13 protein interacts with host NUDT14 protein affecting viral DNA replication. *Mol Med Rep*. 2016;13(3):2167-74.
228. Malloy A, Carr B. Nanoparticle tracking analysis - The Halo (TM) system. *Part Part Syst Char*. 2006;23(2):197-204.
229. Grefte JM, van der Gun BT, Schmolke S, van der Giessen M, van Son WJ, Plachter B, et al. The lower matrix protein pp65 is the principal viral antigen present in peripheral blood leukocytes during an active cytomegalovirus infection. *J Gen Virol*. 1992;73 ( Pt 11):2923-32.
230. Richardson MW, Carroll RG, Stremlau M, Korokhov N, Humeau LM, Silvestri G, et al. Mode of transmission affects the sensitivity of human immunodeficiency virus type 1 to restriction by rhesus TRIM5alpha. *J Virol*. 2008;82(22):11117-28.
231. Hertel L. Human cytomegalovirus tropism for mucosal myeloid dendritic cells. *Rev Med Virol*. 2014;24(6):379-95.
232. Reeves MB, MacAry PA, Lehner PJ, Sissons JG, Sinclair JH. Latency, chromatin remodeling, and reactivation of human cytomegalovirus in the dendritic cells of healthy carriers. *Proc Natl Acad Sci U S A*. 2005;102(11):4140-5.
233. Hertel L, Lacaille VG, Strobl H, Mellins ED, Mocarski ES. Susceptibility of immature and mature Langerhans cell-type dendritic cells to infection and immunomodulation by human cytomegalovirus. *J Virol*. 2003;77(13):7563-74.

234. Huang MM, Kew VG, Jestice K, Wills MR, Reeves MB. Efficient human cytomegalovirus reactivation is maturation dependent in the Langerhans dendritic cell lineage and can be studied using a CD14+ experimental latency model. *Journal of virology*. 2012;86(16):8507-15.
235. Murrell I, Bedford C, Ladell K, Miners KL, Price DA, Tomasec P, et al. The pentameric complex drives immunologically covert cell-cell transmission of wild-type human cytomegalovirus. *Proc Natl Acad Sci U S A*. 2017;114(23):6104-9.
236. Samuel CE. Antiviral actions of interferons. *Clin Microbiol Rev*. 2001;14(4):778-809, table of contents.
237. Morita E, Sundquist WI. Retrovirus budding. *Annu Rev Cell Dev Biol*. 2004;20:395-425.
238. Drivas GT, Shih A, Coutavas E, Rush MG, D'Eustachio P. Characterization of four novel ras-like genes expressed in a human teratocarcinoma cell line. *Mol Cell Biol*. 1990;10(4):1793-8.
239. Graham SM, Cox AD, Drivas G, Rush MG, D'Eustachio P, Der CJ. Aberrant function of the Ras-related protein TC21/R-Ras2 triggers malignant transformation. *Mol Cell Biol*. 1994;14(6):4108-15.
240. Fuchs E. Keratins and the skin. *Annual review of cell and developmental biology*. 1995;11:123-53.
241. Schroeder HW, Cavacini L. Structure and function of immunoglobulins. *The Journal of allergy and clinical immunology*. 2010;125(2 Suppl 2):S41-52.
242. Johansen FE, Braathen R, Brandtzaeg P. Role of J chain in secretory immunoglobulin formation. *Scand J Immunol*. 2000;52(3):240-8.
243. Liu X, Yan S, Zhou TH, Terada Y, Erikson RL. The MAP kinase pathway is required for entry into mitosis and cell survival. *Oncogene*. 2004;23(3):763-76.
244. Ryckman C, Vandal K, Rouleau P, Talbot M, Tessier PA. Proinflammatory activities of S100: proteins S100A8, S100A9, and S100A8/A9 induce neutrophil chemotaxis and adhesion. *Journal of immunology*. 2003;170(6):3233-42.
245. Procaccio V, de Sury R, Martinez P, Depetris D, Rabilloud T, Soularue P, et al. Mapping to 1q23 of the human gene (NDUFS2) encoding the 49-kDa subunit of the mitochondrial respiratory Complex I and immunodetection of the mature protein in mitochondria. *Mamm Genome*. 1998;9(6):482-4.
246. Sanchez L, Calvo M, Brock JH. Biological role of lactoferrin. *Arch Dis Child*. 1992;67(5):657-61.
247. Asano M, Komiyama K. Polymeric immunoglobulin receptor. *J Oral Sci*. 2011;53(2):147-56.
248. Hoffman M, Monroe DM. Coagulation 2006: A modern view of hemostasis. *Hematol Oncol Clin N*. 2007;21(1):1-+.
249. Bloor BK, Tidman N, Leigh IM, Odell E, Dogan B, Wollina U, et al. Expression of keratin K2e in cutaneous and oral lesions: association with keratinocyte activation, proliferation, and keratinization. *Am J Pathol*. 2003;162(3):963-75.
250. Ho M. Chapter 4. Cytomegalovirus: Biology and Infection: Springer Science & Business Media; 2013.

251. Periasamy M, Kalyanasundaram A. SERCA pump isoforms: their role in calcium transport and disease. *Muscle Nerve*. 2007;35(4):430-42.
252. Frickel EM, Frei P, Bouvier M, Stafford WF, Helenius A, Glockshuber R, et al. ERp57 is a multifunctional thiol-disulfide oxidoreductase. *The Journal of biological chemistry*. 2004;279(18):18277-87.
253. Huang F, Wang X, Ostertag EM, Nuwal T, Huang B, Jan YN, et al. TMEM16C facilitates Na(+)-activated K<sup>+</sup> currents in rat sensory neurons and regulates pain processing. *Nat Neurosci*. 2013;16(9):1284-90.
254. Ellgaard L, Molinari M, Helenius A. Setting the standards: quality control in the secretory pathway. *Science*. 1999;286(5446):1882-8.
255. Zapun A, Petrescu SM, Rudd PM, Dwek RA, Thomas DY, Bergeron JJ. Conformation-independent binding of monoglucosylated ribonuclease B to calnexin. *Cell*. 1997;88(1):29-38.
256. Suh WC, Burkholder WF, Lu CZ, Zhao X, Gottesman ME, Gross CA. Interaction of the Hsp70 molecular chaperone, DnaK, with its cochaperone DnaJ. *Proceedings of the National Academy of Sciences of the United States of America*. 1998;95(26):15223-8.
257. Berridge MJ, Bootman MD, Roderick HL. Calcium signalling: dynamics, homeostasis and remodelling. *Nat Rev Mol Cell Biol*. 2003;4(7):517-29.
258. Wang M, Wey S, Zhang Y, Ye R, Lee AS. Role of the unfolded protein response regulator GRP78/BiP in development, cancer, and neurological disorders. *Antioxid Redox Signal*. 2009;11(9):2307-16.
259. Miranda MB, McGuire TF, Johnson DE. Importance of MEK-1/-2 signaling in monocytic and granulocytic differentiation of myeloid cell lines. *Leukemia*. 2002;16(4):683-92.
260. Audoly G, Popoff MR, Gluschkof P. Involvement of a small GTP binding protein in HIV-1 release. *Retrovirology*. 2005;2:48.
261. Goulidaki N, Alarifi S, Alkahtani SH, Al-Qahtani A, Spandidos DA, Stournaras C, et al. RhoB is a component of the human cytomegalovirus assembly complex and is required for efficient viral production. *Cell Cycle*. 2015;14(17):2748-63.
262. Delgado P, Cubelos B, Calleja E, Martinez-Martin N, Cipres A, Merida I, et al. Essential function for the GTPase TC21 in homeostatic antigen receptor signaling. *Nat Immunol*. 2009;10(8):880-8.
263. Harmsen MC, Swart PJ, de Bethune MP, Pauwels R, De Clercq E, The TH, et al. Antiviral effects of plasma and milk proteins: lactoferrin shows potent activity against both human immunodeficiency virus and human cytomegalovirus replication in vitro. *J Infect Dis*. 1995;172(2):380-8.
264. Vanarsdall AL, Johnson DC. Human cytomegalovirus entry into cells. *Curr Opin Virol*. 2012;2(1):37-42.
265. Gonzalez-Chavez SA, Arevalo-Gallegos S, Rascon-Cruz Q. Lactoferrin: structure, function and applications. *Int J Antimicrob Agents*. 2009;33(4):301.e1-8.



266. Pietrantoni A, Di Biase AM, Tinari A, Marchetti M, Valenti P, Seganti L, et al. Bovine lactoferrin inhibits adenovirus infection by interacting with viral structural polypeptides. *Antimicrob Agents Chemother.* 2003;47(8):2688-91.
267. Dashty M, Akbarkhanzadeh V, Zeebregts CJ, Spek CA, Sijbrands EJ, Peppelenbosch MP, et al. Characterization of coagulation factor synthesis in nine human primary cell types. *Sci Rep.* 2012;2:787.
268. Prydzial EL, Wright JF. Prothrombinase assembly on an enveloped virus: evidence that the cytomegalovirus surface contains procoagulant phospholipid. *Blood.* 1994;84(11):3749-57.
269. Sutherland MR, Raynor CM, Leenknecht H, Wright JF, Prydzial EL. Coagulation initiated on herpesviruses. *Proc Natl Acad Sci U S A.* 1997;94(25):13510-4.
270. Wang S, Song R, Wang Z, Jing Z, Ma J. S100A8/A9 in Inflammation. *Front Immunol.* 2018;9:1298.
271. Das S, Ortiz DA, Gurczynski SJ, Khan F, Pellett PE. Identification of human cytomegalovirus genes important for biogenesis of the cytoplasmic virion assembly complex. *J Virol.* 2014;88(16):9086-99.
272. Reynolds A, Anderson EM, Vermeulen A, Fedorov Y, Robinson K, Leake D, et al. Induction of the interferon response by siRNA is cell type- and duplex length-dependent. *Rna.* 2006;12(6):988-93.
273. Ourahmane A, Cui X, He L, Dittmer D, Schleiss M, Hertel L, et al. Inclusion of antibodies to cell culture media preserves the integrity of genes encoding RL13 and the pentameric complex components during fibroblast passage of human cytomegalovirus. 2018.
274. Dimitropoulou P, Caswell RC, McSharry BP, Greaves RF, Spandidos DA, Wilkinson GWG, et al. Differential relocation and stability of PML-body components during productive human cytomegalovirus infection: Detailed characterization by live-cell imaging. 2010.
275. Gonzalez-Quintela A, Alende R, Gude F, Campos J, Rey J, Meijide LM, et al. Serum levels of immunoglobulins (IgG, IgA, IgM) in a general adult population and their relationship with alcohol consumption, smoking and common metabolic abnormalities. *Clin Exp Immunol.* 2008;151(1):42-50.
276. Rozsnyay Z, Sarmay G, Walker M, Maslanka K, Valasek Z, Jefferis R, et al. Distinctive role of IgG1 and IgG3 isotypes in Fc gamma R-mediated functions. *Immunology.* 1989;66(4):491-8.
277. Sung H, Schleiss MR. Update on the current status of cytomegalovirus vaccines. *Expert Rev Vaccines.* 2010;9(11):1303-14.
278. Lilleri D, Kabanova A, Lanzavecchia A, Gerna G. Antibodies against neutralization epitopes of human cytomegalovirus gH/gL/pUL128-130-131 complex and virus spreading may correlate with virus control in vivo. *J Clin Immunol.* 2012;32(6):1324-31.
279. Waldman WJ, Sneddon JM, Stephens RE, Roberts WH. Enhanced endothelial cytopathogenicity induced by a cytomegalovirus strain propagated in endothelial cells. *J Med Virol.* 1989;28(4):223-30.
280. Gerna G, Sarasini A, Patrone M, Percivalle E, Fiorina L, Campanini G, et al. Human cytomegalovirus serum neutralizing antibodies block virus infection of endothelial/epithelial cells, but not fibroblasts, early during primary infection. *J Gen Virol.* 2008;89(Pt 4):853-65.

281. Carr JM, Hocking H, Li P, Burrell CJ. Rapid and efficient cell-to-cell transmission of human immunodeficiency virus infection from monocyte-derived macrophages to peripheral blood lymphocytes. *Virology*. 1999;265(2):319-29.
282. Monel B, Beaumont E, Vendrame D, Schwartz O, Brand D, Mammano F. HIV cell-to-cell transmission requires the production of infectious virus particles and does not proceed through env-mediated fusion pores. *J Virol*. 2012;86(7):3924-33.
283. Silva MC, Schroer J, Shenk T. Human cytomegalovirus cell-to-cell spread in the absence of an essential assembly protein. *Proc Natl Acad Sci U S A*. 2005;102(6):2081-6.
284. Davis AJ, Li P, Burrell CJ. Kinetics of viral RNA synthesis following cell-to-cell transmission of human immunodeficiency virus type 1. *J Gen Virol*. 1997;78 ( Pt 8):1897-906.
285. Sato H, Orenstein J, Dimitrov D, Martin M. Cell-to-cell spread of HIV-1 occurs within minutes and may not involve the participation of virus particles. *Virology*. 1992;186(2):712-24.
286. Del Portillo A, Tripodi J, Najfeld V, Wodarz D, Levy DN, Chen BK. Multiploid inheritance of HIV-1 during cell-to-cell infection. *J Virol*. 2011;85(14):7169-76.
287. Stanton R, Westmoreland D, Fox JD, Davison AJ, Wilkinson GW. Stability of human cytomegalovirus genotypes in persistently infected renal transplant recipients. *J Med Virol*. 2005;75(1):42-6.
288. Lassalle F, Depledge DP, Reeves MB, Brown AC, Christiansen MT, Tutill HJ, et al. Islands of linkage in an ocean of pervasive recombination reveals two-speed evolution of human cytomegalovirus genomes. *Virus Evol*. 2016;2(1):vew017.
289. Rasmussen L, Geissler A, Winters M. Inter- and intragenic variations complicate the molecular epidemiology of human cytomegalovirus. *J Infect Dis*. 2003;187(5):809-19.
290. Paradowska E, Jablonska A, Plociennikowska A, Studzinska M, Suski P, Wisniewska-Ligier M, et al. Cytomegalovirus alpha-chemokine genotypes are associated with clinical manifestations in children with congenital or postnatal infections. *Virology*. 2014;462-463:207-17.
291. Stanton RJ, Westmoreland D, Fox JD, Davison AJ, Wilkinson GW. Stability of human cytomegalovirus genotypes in persistently infected renal transplant recipients. *J Med Virol*. 2005;75(1):42-6.
292. Guo G, Zhang L, Ye S, Hu Y, Li B, Sun X, et al. Polymorphisms and features of cytomegalovirus UL144 and UL146 in congenitally infected neonates with hepatic involvement. *PLoS One*. 2017;12(2):e0171959.
293. Palmer E, Freeman T. Investigation into the use of C- and N-terminal GFP fusion proteins for subcellular localization studies using reverse transfection microarrays. *Comp Funct Genomics*. 2004;5(4):342-53.
294. Kalinina T, Iwanski A, Will H, Sterneck M. Deficiency in virion secretion and decreased stability of the hepatitis B virus immune escape mutant G145R. *Hepatology*. 2003;38(5):1274-81.
295. Gerba CP, Betancourt WQ. Viral Aggregation: Impact on Virus Behavior in the Environment. *Environ Sci Technol*. 2017;51(13):7318-25.

296. Galasso GJ, Sharp J, Sharp DG. THE INFLUENCE OF DEGREE OF AGGREGATION AND VIRUS QUALITY ON THE PLAQUE TITER OF AGGREGATED VACCINIA VIRUS. *J Immunol.* 1964;92:870-8.
297. Rosenberg AS. Effects of protein aggregates: an immunologic perspective. *Aaps j.* 2006;8(3):E501-7.
298. Cresswell P, Ackerman AL, Giodini A, Peaper DR, Wearsch PA. Mechanisms of MHC class I-restricted antigen processing and cross-presentation. *Immunol Rev.* 2005;207:145-57.
299. Laib Sampaio K, Stegmann C, Brizic I, Adler B, Stanton RJ, Sinzger C. The contribution of pUL74 to growth of human cytomegalovirus is masked in the presence of RL13 and UL128 expression. *J Gen Virol.* 2016;97(8):1917-27.
300. Lemmermann NA, Krmpotic A, Podlech J, Brizic I, Prager A, Adler H, et al. Non-redundant and redundant roles of cytomegalovirus gH/gL complexes in host organ entry and intra-tissue spread. *PLoS Pathog.* 2015;11(2):e1004640.